# MEF2C in the Development of the Striatum

This thesis is submitted for the degree of Doctor of Philosophy at Cardiff University

David Quinn

Supervisors:

Professor Anne Rosser

Dr Michael Taylor

February 2020


# Thesis Summary

Understanding the process of normal striatal differentiation is important for gaining insight into diseases affecting this area of the brain, ranging from addiction to neurodegenerative conditions such as Huntington's disease (HD). An Affymetrix screen of mouse striatal development revealed MEF2C to be significantly up-regulated suggesting that could plays a role in striatal development. Recent research has shown that the knockout (KO) of MEF2C impaired neuronal differentiation and maturation, affected hippocampal based learning and memory and directly influenced neuronal development including dendrite morphogenesis and spine density. Then aim of this investigation was to determine what, if any, role MEF2C holds in the development of the mouse striatum.

Chapter 3 established *Mef2c*$^{loxP/loxP}$ mice as a WT control and that heterozygous mice were not significantly different to WT, therefore necessitating the use of a conditional KO model. LacZ and protein expression analysis revealed that Gsx2-Cre is expressed throughout the striatum at both P7 and 3 months, appearing to dramatically reduce the numbers of MEF2C positive MSNs, thus is suitable to serve as the KO model.

Chapter 4 demonstrated that Conditional KO of MEF2C results in fewer DARPP-32 expressing cells at P7, a total cell count reduction at 3 months (most severely with FOXP1 and DARPP-32), with FOXP1 and DARPP-32 counts remaining lower at 12 and 18 months. The conditional KO striatal volume is reduced in all adult ages, but not at P7. Substantial neurogenesis occurs in the P14 striatum but is significantly reduced following loss of MEF2C expression, with proliferation in both genotypes reduced by P24, suggesting that MEF2C lowers total cell counts in adult mice by hindering striatal cell proliferation. Loss of MEF2C is results in an increase in spine density and count in adult mice but does not affect dendrites.

Chapter 5 demonstrated loss of MEF2C has a range of significant effects on cells isolated from the developing E18 striatum and analysed *in vitro*, altering the cellular composition of striatal culture populations both immediately after plate down and following several days of cultures. MEF2C expression is required for normal proliferative activity, apoptotic activity and the *in vitro* differentiation of MSNs.

# Acknowledgements

First, a huge thank you to my supervisors Anne and Mike for their continuous support and guidance over the years. I really couldn't have asked for more approachable and dedicated supervisors, you have provided me with invaluable experience and I will be forever grateful. To colleagues, thank you all for providing a friendly and enjoyable place for me to work and for keeping me going over the years. Thank you, Sus, for your incredible friendship and for being a knee-down inspiration (shame about the rest). Thank you Oly, Kyle and Laura for your continuous ridiculous distractions, semi-destructive games of "ball" and shot Thursdays.

Thank you also to Sophie, Mariah, Ngoc-Nga, Anne-Marie, Rachel and Charlie for your (near) infinite patience with me and my general inconvenience.

A rare yet sincere thank you to my friends who inexplicably stood by me over the years despite my consistent inability to socialise. Ben, Dan, Sam, Jerry, Adam, Zoe, George and even Josh, your unique mixes of camaraderie and abuse kept me stable and made going back to the office seem just that little bit more inviting. I promise you will all be seeing more of me soon!

Soph, you took care of me form the first moment we met and never stopped, I owe you more than I can hope to repay and you are simply incredible, irreplaceable and the best!

Thank you to my parents for constantly looking out for my wellbeing and unwavering support. Not many only get a 13-day warning that their son is getting married yet your support for us both only increased. In return, we forced you to adopt a cat that falls out of windows and periodically raid your home for supplies – which is fair I think! Thank you also to my two brothers Paul and Alan, for always being dependable, for pitying/laughing at my work to poverty ratio and for accepting that being Dr Quinn makes me the best son, so I win.

Last, but for my own safety certainly not least, Lisa. Thank you for always being the rock that I could build everything else around and for making me look better by association. Thank you for putting up with me all this time, you deserve this as much as I do and I can't wait for our next adventure! Я люблю свою жену!

"If I can fathom all mysteries, all knowledge and have a faith that can move mountains, but do not have love, I am nothing."

# Table of Contents

# List of Figures

## Chapter 1



## Chapter 2

## Chapter 3



## Chapter 4

## Chapter 5



**Preliminary experiment 1**



**Preliminary experiment 2**



**Experiment 3**

# List of Tables

# Abbreviations

| | |
|---|---|
| AD | Alzheimer’s disease |
| AIMs | Abnormal involuntary movements |
| ANOVA | Analysis of variance |
| bHLH | Basic helix-loop-helix |
| BrdU | Bromodeoxyuridine / 5-bromo-2'-deoxyuridine |
| BSA | Bovine serum albumin |
| CASPASE-3 | Cysteine-aspartic acid protease 3 |
| CDKL5 | Cyclin-dependent kinase-like 5 |
| CTIP2 | COUP TF1-interacting protein 2 |
| CV | Cresyl violet |
| DARRP-32 | Dopamine and cyclic AMP-regulated phosphoprotein |
| DNA | Deoxyribose nucleic acid |
| DS/VS | Dorsal/Ventral Striatum |
| FOXP1 | Forkhead Transcription Factor 1 |
| E18 | Embryonic day 18 |
| EB | Embryoid Body |
| ERK5 | Extracellular-signal-regulated kinase 5 |
| mEPSCs | Miniature excitatory postsynaptic currents |
| ESC | Embryonic stem cells |
| FBS | Fetal calf serum |
| FEZF2 | Family Zinc Finger 2 |
| FOXG1 | Forkhead box G1 |

| | |
|---|---|
| GABA | γ-Aminobutyric acid |
| GFAP | Glial fibrillary acidic protein |
| GP | Globus Pallidus |
| GSX2 | Genetic-Screened Homeobox 2 |
| HBSS | Hanks Balanced Salt Solution |
| HCL | Hydrochloric acid |
| HD | Huntington’s Disease |
| HDAC | Histone deacetylase |
| HET | Heterozygous |
| KI67 | Antigen KI-67 |
| KO | Knockout |
| KO1 | Knockout variant 1 |
| KO3 | Knockout variant 3 |
| LGE | Lateral ganglionic eminence |
| MAP2 | Microtubule associated protein 2 |
| MAPK | Mitogen-Activated Protein Kinase |
| MECP2 | Methyl CpG binding protein 2 |
| MEF2 | Myocyte Enhancer Factor |
| MEF2A | Myocyte enhancer factor 2a |
| MEF2B | Myocyte enhancer factor 2b |
| MEF2C | Myocyte enhancer factor 2c |
| MEF2D | Myocyte enhancer factor 2d |
| MGE | Medial ganglionic eminence |
| MRI | Magnetic resonance imaging |

| | |
|---|---|
| mRNA | Messenger ribonucleic acid |
| Mutt | Mutant Huntington protein |
| MZ | Mantle zone |
| NEUN | Neuronal nuclei |
| NKX2.1 | NK2 homeobox 1 |
| NPCs | Neural precursor cells |
| NS | Normal Serum |
| NUR77 | Nerve growth factor IB |
| P19 cells | embryonic carcinoma cell line as a model system |
| P7 | Post-natal day 7 |
| PBS | Phosphate-buffered saline |
| PCR | Polymerase chain reaction |
| PD | Parkinson’s disease |
| PFA | Paraformaldehyde |
| PLL | Poly-L-Lysine |
| ROI | Region of interest |
| SN | Substantia nigra |
| SNc | Subcortical nuclei pars compacta |
| SNP | Short nucleotide repeat |
| SNr | Subcortical nuclei pars reticulata |
| STN | Subthalamic nucleus |
| SVZ | Sub-ventricular zone |
| TCF4 | Transcription Factor 4 |
| TBS | Tris-buffered saline |

| | |
|---|---|
| TXTBS | Triton X-100 TBS |
| TM1 | Targeted mutation 1 |
| TM2 | Targeted mutation 2 |
| UV | Ultraviolet |
| TNS | Tris non-Saline |
| VP | Ventral palladium |
| VZ | Ventricular zone |
| WGE | Whole ganglionic eminence |
| WT | Wild-type |

# Chapter 1: Introduction

Understanding the process of normal development of the striatum is important for gaining insight into diseases affecting this area of the brain, ranging from addiction to neurodegenerative conditions such as Huntington's disease (HD). Furthermore, it is essential in attempting to design methodology for the differentiation of pluripotent cells into a striatal cell phenotype. Being able to do this accurately is essential for generating cells for cell replacement therapies (Evans, 2013) and for meaningful disease modelling (i.e. producing cultures of striatal cells). Although a number of protocols describing methods for differentiating striatal cells from pluripotent stem cells have been published (Aubry *et al.*, 2008; Delli Carri *et al.*, 2013; Arber *et al.*, 2015), none have yet generated the proportion of medium spiny striatal neurons (MSNs) that differentiate in the normal striatum. Furthermore, *in vitro* and post-transplantation comparisons of such cells with those derived from the developing striatum have shown them to be functionally inferior, suggesting that the differentiation protocols are sub-optimal (Aubry *et al.*, 2008). An Affymetrix screen of mouse striatal development, conducted by the host lab, revealed expression of the myocyte enhancer factor 2c (*Mef2c*) gene to be significantly up-regulated during striatal development in embryogenesis (*Affymetrix*, 2020). Here I have addressed the question as to whether *Mef2c* is important for striatal development as suggested by this finding.

## 1.1 The Adult Striatum and its Development

The basal ganglia are located in the forebrain and top of the midbrain, consisting of the striatum (caudate and putamen in humans), Globus pallidus (GP), substantia nigra (pars reticula and pars compacta) and subthalamic nucleus. The striatum itself is comprised of the dorsal and ventral striatum: the latter contains the nucleus accumbens, the medial and ventral regions of the caudate and putamen, with the remaining caudate and putamen in the dorsal striatum (Haber and McFarland, 1999).

The basal ganglia have classically been associated with motor co-ordination, however more recent studies have revealed open and closed system loops involving several other regions of the brain, including the cortex, thalamus and cerebellum (Braunlich and Seger, 2013; Hélie, Ell and Ashby, 2015). The striatum is the largest nucleus in the basal ganglia

and has central roles in cognitive ability, movement co-ordination and emotion processing (Gerfen, 1992; Jain *et al.*, 2001; Graybiel, 2005). A coronally sliced adult mouse brain provides clear structural distinction between the cortex and the striatum as shown in Figure 1.01 below.

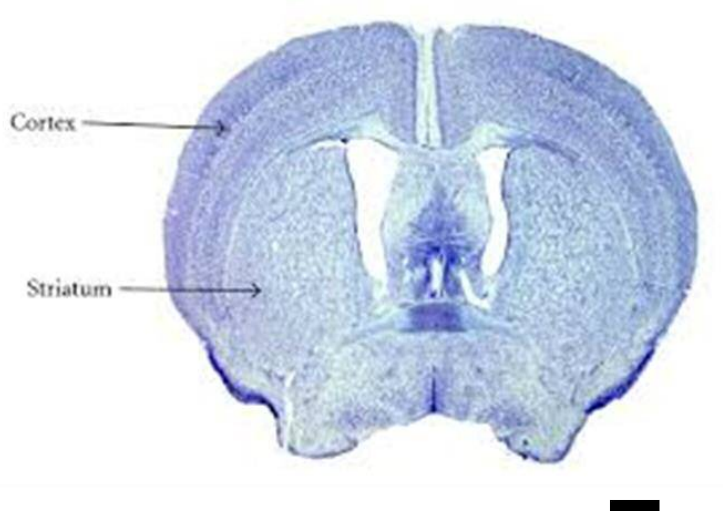


Figure 1.01 Coronal section of mouse brain, illustrating the regional separation of the cortex and the striatum. Scale bar 1000μm.

As illustrated in Figure 1.02, the basal ganglia function in connection with the cortex and thalamus, which is required to actuate deliberate, goal-orientated somatic nervous system motor functions, along with cognitive and limbic system function. Furthermore, the basal ganglia system is responsible for motivation of these actions, along with emotive regulation, and thus is an integral system in reward and subsequent behaviour reinforcement and habit formation (Wise and Rompre, 1989; Nestler, Hope and Widnell, 1993; Schultz, 1997; Koob *et al.*, 2004). The cognitive responsibilities of the basal ganglia system also involve procedural sub-conscious learning and working memory tasks (Miyachi, Hikosaka and Lu, 2002). Broadly speaking, it is the ventral striatum (VS) that is associated with emotion, the caudate nucleus with cognition, and the putamen with sensorimotor function. However, there is no structural boundary between the VS and the caudate nucleus, thus a strict separation of responsibilities cannot be made. As previously described the basal ganglia system is also functionally linked with the frontal cortex, as is the main basal ganglia output (the thalamus), thus it interacts with frontal cortex regions mediating motivation and emotional drive, action-planning and motor actions.

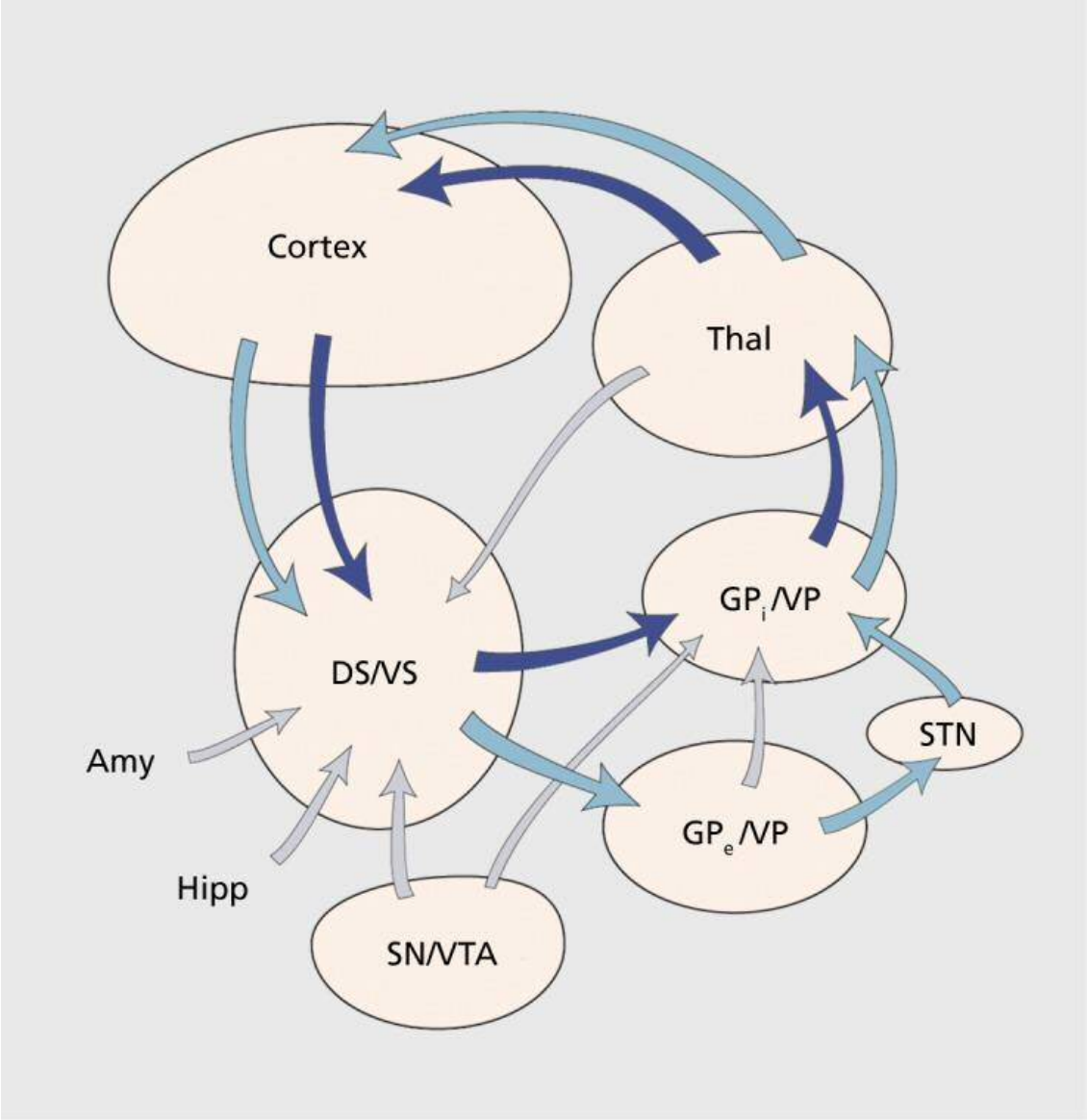


Figure 1.02: Illustration of the interconnectivity of different regions of the cortico-basal ganglia circuit. Thal = Thalamus; DS/VS = Dorsal Striatum/ Ventral Striatum; $GP_i$/VP = Internal Globus Pallidus/Ventral Pallidum; $GP_e$/VP = External Globus Pallidus/Ventral Pallidum; STN = Subthalamic Nucleus, SN/VTA = Substantia Nigra, Ventral Tegmental Area. Adapted from (Haber, 2016)

Afferent striatal projections orientate most prominently from the cerebral cortex, along with the thalamus and from brain stem dopaminergic cells. Cortical inputs are received in a regionally specific manner dependant on their origin, so that the dorsolateral striatum receives sensory-motor area inputs, the ventromedial striatum inputs from limbic areas and the central striatum from a range of associative cortical areas (Selemon and Goldman-Rakic, 1985; Haber *et al.*, 2006). Subsequently, the striatum projects regionally to the Substantia Nigra (SN), pars reticulata (SNr), pars compacta (SNc) and the pallidal complex (comprised of the GPe and GPi of the globus pallidus and the ventral pallidum)

as appropriate (Parent and Hazrati, 1995; Smith, Shink and Sidibé, 1998). Specifically, the GPi and GPe receive inputs from the dorsal striatum (including the caudate nucleus and putamen) and the ventral pallidum (VP) to the VS (Johnston *et al.*, 1990; Lyons *et al.*, 1996). The GPi and SNr output to the thalamus and thereafter back to the cortex, thus completing the direct cortico-basal ganglia circuit.

There are two distinct pathways through which signals may travel in this circuit: the direct and indirect pathways. The indirect pathway is completed through projection from the GPe and VP to the subthalamic nucleus (STN), then back to the GPi. When signals are sent from the cortex to the basal ganglia they follow the direct pathway circuit, leading to silencing of the neurons in the globus pallidus, thereby silencing the inhibiting pathway (Haber, 2016). This signal may then travel to both the putamen and the caudate nucleus. This frees the thalamus from the inhibitory effects of the globus pallidus and allows movement to occur when the transmission is sent back to the motor cortex or other cortical areas. For this intricate system to function properly, the delicate balance between excitatory dopaminergic and inhibitory GABAergic pathways needs to be maintained, which is achieved primarily through the maintenance of healthy, mature MSNs. Loss or damage of these cells may result in a range of abnormalities, including loss of motor control, cognitive and emotional abilities, such as those seen in HD.

### 1.1.1 Striatal development

The embryonic nervous system originates with neural induction and neurulation, which in turn allows for formation of the neural tube. The neural tube is patterned along the anterior-posterior axis, folding into the prosencephalon (forebrain) and an anterior part of the neural tube consisting of the telencephalon from which the striatum is later formed, as well as the mesencephalon (midbrain) diencephalon and rhombencephalon (Rubenstein *et al.*, 1998). The telencephalon divides into the dorsal telencephalon (or pallium) and the ventral telencephalon (or sub-pallium). It is the sub-pallium specifically that later forms the striatum and from which cells that will populate the GP, olfactory bulb and a proportion of cortical cells derive (Jain *et al.*, 2001). The formation of the telencephalon and its subdivisions up to this point are highly conserved among mammals (Rubenstein *et al.*, 1998; Puelles *et al.*, 2000).

Post-mitotic neurons forming from highly proliferative zones within the sub-pallium migrate to form intra-ventricular bulges referred to as the whole ganglionic eminence (WGE), which is comprised of the medial and lateral ganglionic eminences (MGE/LGE) in mice as shown in Figure 1.03 below.

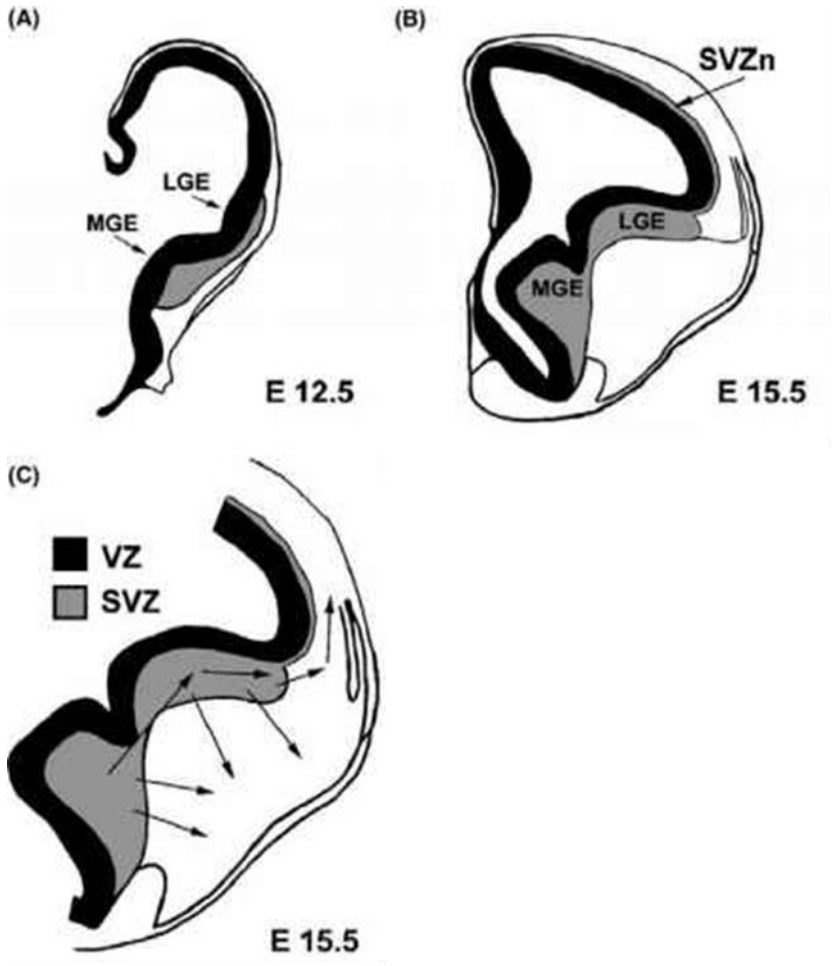


Figure 1.03: Illustration of MGE, LGE, SVZ and VZ in the developing mouse telencephalon at E12.5 and E15.5 and the migratory direction of neurons supplying the developing cortex and striatum. (A) Coronal view of the developing mouse forebrain at E12.5, with the MGE and LGE becoming more prominent at (B) E15.5. (C) Radial migratory directions of MGE and LGE derived cells as they migrate to the striatum, neo-cortex and nucleus accumbens. Adapted from (Lavdas et al., 1999).

The amygdaloid body and GP arise from the MGE with the LGE forming the caudate and putamen within the human striatum (Deacon, Pakzaban and Isacson, 1994), however it should be noted that in the mouse striatum there is no separation of the caudate and putamen. Surrounding the developing telencephalon is the ventricular zone (VZ) located on the lateral ventricles and the subventricular zone (SVZ), which is unique to the telencephalon and extends from the basal region of the VZ. Both of these areas are highly proliferative with projection neurons deriving from within these structures comprising 90% of LGE neurons (Molkentin *et al.*, 1995; Stenman, Toresson and Campbell, 2003).

Olfactory bulb neurons, however, derive mainly from the dorsal LGE (Toresson, Potter and Campbell, 2000), though they also form in the MGE and migrate to these regions (Campbell, Olsson and Björklund, 1995; Stewart A Anderson *et al.*, 1997; Lin *et al.*, 1998). Following proliferation, neurons migrate to the mantle zone (MZ) of the developing striatum, where they then differentiate. Though initial evidence suggested cortical neurons also originated from the LGE (Corbin *et al.*, 2000), more recent investigations have shown that parvalbumin- and somatostatin-positive cortical interneurons form from the MGE (Wonders and Anderson, 2006; Xu, Tam and Anderson, 2008; Miyoshi *et al.*, 2010; Rudy *et al.*, 2011; Hu *et al.*, 2017).

### 1.1.2 Neuronal migration during embryonic development

During embryonic development, neurons from the WGE migrate throughout the telencephalon and into the developing striatum. The prevalent mode of neuronal migration in the mammalian brain is radial migration (see Figure 1.03), which is particularly important in the development of laminar structures such as the neocortex and hippocampus (Rakic, 1972; Brand and Rakic, 1979; Eckenhoff and Rakic, 1984; Selemon and Goldman-Rakic, 1985; Hamasaki *et al.*, 2003a). Post-mitotic neurons have been shown to follow elongated radial glial cells (Rakic, 1972), which develop from the cerebral wall upon the inception of corticogenesis (Brand and Rakic, 1979). Proliferative radial glia may also be neuronal precursors (Noctor *et al.*, 2001), which may suggest a separate generation of neurons provide the radial organisations of the cortex. Similarly, radial glial cells of the E15 developing rat telencephalon project from the LGE to the striatum, suggesting that they provide a route for the outward migration of striatal precursor cells (Halliday and Cepko, 1992; de Carlos, López-Mascaraque and Valverde, 1996; Kakita and Goldman, 1999). However, the striatum of Reeler mice, which have a mutation causing abnormal radial layering of the brain (which therefore particularly affects the cortex), was not found to be abnormally affected, thus a different mechanism likely underlies a significant portion of striatal neuron migration (Schiffmann, 1997; Lambert de Rouvroit and Goffinet, 1998; Hamasaki *et al.*, 2003a).

Tangential migration of neurons as shown in Figure 1.04 below is suggested to occur between the basal telencephalon and the intermediate zone of the developing cortex (DeDiego, Smith Fernández and Fairén, 1994; Tamamaki, Fujimori and Takauji, 1997). Tangential migration from the MGE also supplies the Globus Pallidus and striatum (Shimamura *et al.*, 1995; Meyer *et al.*, 1998; Olsson, Björklund and Campbell, 1998; Lavdas *et al.*, 1999; Sussel *et al.*, 1999; Wichterle *et al.*, 1999; Wonders and Anderson, 2006). Neuronal precursor cells expressing the NK2 homeobox 1 (Nkx2.1)

homeodomain protein have been shown to migrate tangentially from the MGE into the developing striatum, thereafter differentiating into cholinergic interneurons expressing parvalbumin and calretinin markers (Hamasaki *et al.*, 2003a; Wonders and Anderson, 2006). Both the highly conserved homeobox genes Dlx1 and 2, which function as transcription factors in the developing telencephalon (S. A. Anderson *et al.*, 1997; Pleasure *et al.*, 2000; Hamasaki *et al.*, 2003a), and semaphorin 3A/F signals (Marin *et al.*, 2001) have been shown to regulate migration of MGE cells into the striatum, suggesting a network of proteins are required for normal migratory patterns.

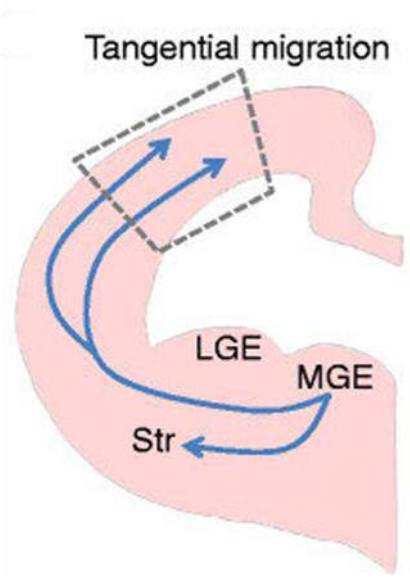


Figure 1.04: Diagram of Tangential Migration of LGE and MGE derived neurons into the striatum and cortex (boxed). Adapted from (Moffat *et al.*, 2015)

In the postnatal striatum, little is known about migratory processes of striatal MSNs, likely due to earlier conclusions of a cessation of striatal neurogenic activity in the early postnatal days (Fentress, Stanfield and Cowan, 1981). The latter chapters of this dissertation will begin to address this issue, in the context of how it relates to postnatal phenotypes of striatal MEF2C knockout (KO).

### 1.1.3 **MSN development**

MSNs are projection neurons that comprise >90% of all striatal neurons (Bolam *et al.*, 2000), with the remaining proportion comprised from interneurons. MSNs can be sub-categorised based on their neurochemical markers, interconnectivity with surrounding neurons and, to a lesser degree, location. Striasomes, or patch neurons, are a mosaic-like organisation of MSNs and comprise between 15-20% of striatal MSNs, with the

remaining 80-85% made up from matrix neurons (Gerfen, 1992). The first MSNs are born between E11-E13 and laterally migrate into the developing striatum before forming into patch or striasome MSNs, with later-derived matrix MSNs (E13-E16) migrating and surrounding patch MSNs (van der Kooy and Fishell, 1987; Krushel, Connolly and van der Kooy, 1989; Song and Harlan, 1994; Hoffarth *et al.*, 1995). At E18.5 it is possible to identify whether an MSN is patch or matrix using factors such as the Dopamine and cyclic AMP-regulated phosphoprotein (DARRP-32) (Foster *et al.*, 1987). However, this method of identification is not entirely accurate and is not thought to persist into postnatal and adult stages, where DARPP-32 is present in both MSN subtypes. Broadly speaking, patch MSNs are highly connected with dopaminergic neurons in the SNc and SNr, with matrix neurons providing input to inhibitory Gamma-amino butyric acid (GABA)ergic neurons (Gerfen, 1984; Gerfen, Baimbridge and Miller, 1985).

GABA is an inhibitory neurotransmitter utilised by cells within the CNS and striatum, as are other neurotransmitters including Dopamine (DA). Dopaminergic afferents from the substantia nigra at E14 allow for further development of striatal patch MSNs and have been shown to persist to E19 (Edley and Herkenham, 1984). MSNs within patch and matrix compartments are believed to remain within their "boundaries" in terms of local axonal collateral and dendrite formation (Gerfen, Baimbridge and Miller, 1985; Kawaguchi, Wilson and Emson, 1989). MSNs may project to the GP, VP and SN (Preston, Bishop and Kitai, 1980; Johnston *et al.*, 1990), or their axonal projections may form inhibitory GABAergic synaptic connections with other MSNs or interneurons within the striatum (Bolam *et al.*, 1986; Pickel and Chan, 1990; Smith, Shink and Sidibé, 1998). The inputs MSNs receive from the cortex and thalamus are mainly glutamatergic, with cortical fibres forming asymmetric (excitatory) terminals on MSN dendritic spines (Somogyi, Bolam and Smith, 1981; Smith *et al.*, 1998). MSNs may also receive inputs from interneurons and other MSNs (Difiglia, 1987; Yung, 1996). Interneurons have been shown to be more responsive to cortical input than MSNs in some instances, suggesting they may play an important role in integrating information from different cortical regions towards MSNs (Mallet *et al.*, 2005).

Basal ganglionic DA neurons are integral in modulating motor control as well as with learning and memory, and are integral to the striatal reward process (Wise and Rompre, 1989; De la Fuente-Fernández *et al.*, 2002; Rice and Cragg, 2004; Zald *et al.*, 2004). Pharmacological and behavioural analyses of DA pathways have shown the nigrostriatal pathways within which they operate to be associated with the encoding of reward and saliency prediction error (De la Fuente-Fernández *et al.*, 2002; Rice and Cragg, 2004; Zald *et al.*, 2004; Joshua, Adler and Bergman, 2009). Two MSN subtypes are

differentiated through their dopamine enrichment properties, defined as D1 and D2, though a number of other genes also contribute to the identity of these two subtypes (Gerfen *et al.*, 1990; Le Moine *et al.*, 1990; Bernard, Normand and Bloch, 1992; Ince, Ciliax and Levey, 1997; Lobo *et al.*, 2006, 2007; Heiman *et al.*, 2008; Lobo and Nestler, 2011). D1 neurons differ in functionality to D2 neurons through their pathway interactions, with D1 classically associated with the direct or excitatory pathway and D2 with the indirect or inhibitory pathway (Gerfen, 1984, 1992; Lobo and Nestler, 2011). D1 dopamine receptors are preferentially expressed in the striato-nigral MSNs of the direct pathway, with D2 in striato-pallidal MSNS of the indirect pathway (Gerfen *et al.*, 1990; Valjent *et al.*, 2009; Bertran-Gonzalez *et al.*, 2010). MSNs are therefore integral in pathways involving numerous brain regions and neurotransmitters and must be tightly regulated, as basal ganglia loops control many aspects including motor control, cognition and reward/motivation (MINK, 1996; Redgrave, Prescott and Gurney, 1999; Schultz, 2002; Bromberg-Martin, Matsumoto and Hikosaka, 2010). MSNs are the main cell type affected in the striatum in HD through degeneration, and are also a critical element of the circuitry that degenerates in Parkinson's Disease (PD) (Albin, Young and Penney, 1989).

### 1.1.4 **Post-natal development and neurogenesis**

MSN neurogenesis in mice begins at E12.5, however this proliferation extends to some days postnatally in murine models (Das and Altman, 1970; Brand and Rakic, 1979; Smart and Sturrock, 1979; Fentress, Stanfield and Cowan, 1981). In the initial few days postnatally there is a turnover of neurons in the striatum, with many neurons dying while others are formed (Fentress, Stanfield and Cowan, 1981). This is evidenced from the presence of newly dividing cells from the SVZ while pyknotic neurons within the striatum degenerate (Fentress, Stanfield and Cowan, 1981). Cell death is an almost ubiquitous feature of vertebrate neurogenesis, although such a turnover of cells is less well established but yet present in the motor columns of the amphibian spinal cord and the dorsal root ganglia of the chick (Hughes, 1961; Hamburger, W and Yip, 1981).

In the adult mice, two brain regions have been identified as capable of substantial ongoing neuronal turnover in the adult brain – the hippocampus and the olfactory bulb (Lemasson *et al.*, 2005; Feliciano and Bordey, 2013), with both regions' neurogenic activity well established. The neurogenic region that produces cells for the olfactory bulb is the subventricular zone immediately adjacent to the striatum, which migrate along the rostral migratory stream to the olfactory bulbs. The extent to which new cells populate the striatum in health and disease is less certain.

## 1.2 *Mef2c* in brain development

MEF2C is detectable in both GABAergic inhibitory interneurons and neuroblasts in the developing mouse forebrain, increasing its expression at E14 in GABAergic interneurons (Cho *et al.*, 2011). Furthermore, MEF2C expression during forebrain development is up-regulated not only in mature ventral GABAergic interneurons, but also in dorsal primary neuroblasts and developing ventral GABAergic interneurons, with this expression found to be reduced in t-box brain protein 1 (Tbr1) null mice during cortical-layer development (Winden *et al.*, 2009; Bedogni *et al.*, 2010; Paciorkowski *et al.*, 2013). Moreover, a role for MEF2C in synaptic maturation has also been suggested (Pfeiffer *et al.*, 2010), highlighting the fact that MEF2C is a key regulatory element in a variety of differing neural processes (Paciorkowski *et al.*, 2013).

### 1.2.1 *Mef2c* during NPC neural differentiation

Expression of *Mef2c* messenger ribonucleic acid (mRNA) is first detected in the ventral portion of the mouse telencephalon at E11.5, with all other myocyte enhancer factor 2 (MEF2) proteins expressed in overlapping yet distinct patterns in the midbrain, frontal cortex, thalamus, hippocampus and hindbrain by E13.5 (G E Lyons *et al.*, 1995) as shown in Figure 1.05 below. MEF2C expression appears to align with temporal and spatial patterns of striatal cell development and maturation in the developing embryo, indicating it may play a role in neuronal differentiation (G E Lyons *et al.*, 1995; Cho *et al.*, 2011).

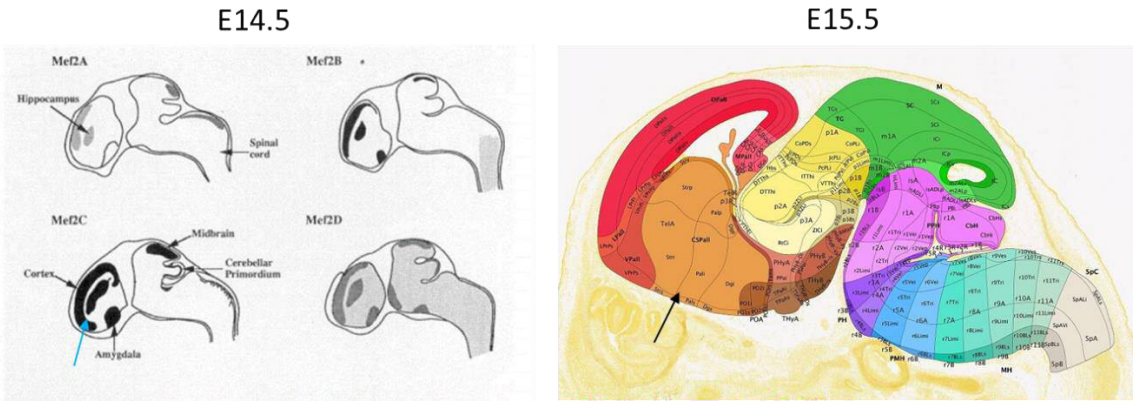


Figure 1.05: (Left) Illustration of expression patterns of MEF2 proteins in the E14.5 mouse embryo showing strong MEF2C expression in the developing WGE (blue arrow), adapted from (G E Lyons *et al.*, 1995). (Right) Image adapted from the Allen Mouse Reference Atlas confirming location of mouse striatum (black arrow) at E15.5.

As previously described, MEF2C is expressed both initially in the telencephalon and midbrain in literature (G E Lyons *et al.*, 1995) and more precisely in the developing striatum (Evans, 2013). *Mef2c* mRNA expression is present from E13.5, increasing steadily until P0, before slightly dropping at postnatal day 7 (P7) (Evans, 2013). mRNA can generally be expected to correlate with protein expression, though it should be noted this is not always the case.

### 1.2.2 *Mef2c* in Human Embryonic Stem Cell Differentiation

Expression levels of MEF2C vary throughout the differentiation process of human embryonic stem cells (hESC)s to mature neurons. MEF2C is initially expressed in low levels in hESCs before gradually increasing as the cells differentiate into neuroprogenitor cells (NPCs), thereafter slightly declining upon initial immature neuron formation, before increasing further throughout neural maturation (Cho *et al.*, 2011). Interestingly, MEF2D expression does not increase until the latter stages of NPC differentiation, but sharply increases during neuronal maturation, with MEF2A expression remaining low throughout, despite it being widely expressed in the brain (Cho *et al.*, 2011). The knockdown of MEF2C prior to the formation of NPCs causes a ~2-fold greater amount of cell death, with smaller than normal neurospheres forming, adding further evidence to the role of MEF2C as a cell survival factor and aid in neurogenesis (Z Mao *et al.*, 1999; S Okamoto *et al.*, 2000; Cho *et al.*, 2011). Constituently activated *Mef2c* has also been shown to increase the number of DA neurons, which when transplanted into Parkinsonian Rats, resulted in improved motor function to a significantly greater degree than non-programmed cells (Cho *et al.*, 2011).

## 1.3 MEF2 Overview

The MEF2 gene family encodes transcription factors with key roles in cell differentiation, proliferation, morphogenesis, survival and apoptosis of a range of cell types, including cardiac, neural and immunity-regulating cells (Kasler and Verdin, 2007; Potthoff and Olson, 2007; Clark *et al.*, 2013). It is a combination of both widely expressed and cell type-specific transcription factors that is required for the interpretation of extracellular signals during the *in vivo* development process, through which the formation of specific and specialised cell-types may be regulated and subsequently integrated into specific tissues. This occurs as a result of the activation of a cascade of regulatory and structural genes such as the MEF2 family (Potthoff and Olson, 2007).

### 1.3.1 MEF2 molecular information

MEF2 is a member of the MADS-box gene family. Its MADS-box forms a deoxyribose nucleic acid (DNA)-binding domain through which DNA sequence motifs are bound (West, Shore and Sharrocks, 1997; Svensson, 2000). MADS-box-containing proteins have a variety of functions in numerous cell types, though are most often associated with muscle or neural development, cell proliferation and differentiation (Shore and Sharrocks, 1995). This domain is located towards the N-terminus of the MEF2 protein and is adjacent to the MEF2 domain. It is the combination of these two domains which characterise the MEF2 family (Ying *et al.*, 2013) and mediate protein dimerization, DNA binding, homodimerization of MEF2 polypeptides and some co-factor interactions (Black and Olson, 1998; Zhang *et al.*, 2002; Potthoff and Olson, 2007; Ying *et al.*, 2013). These domains are conserved in *Mef2a*, b, c and d, though the C-terminus regions in all forms of mammalian MEF2 are highly divergent as shown in Figure 1.06. Alternative splicing occurs in the more divergent transactivation region, with one functional consequence the modulation of transcriptional activity (Martin, Schwarz and Olson, 1993; Molkentin *et al.*, 1996; Potthoff and Olson, 2007; Hakim *et al.*, 2010; Sekiyama, Suzuki and Tsukahara, 2012).

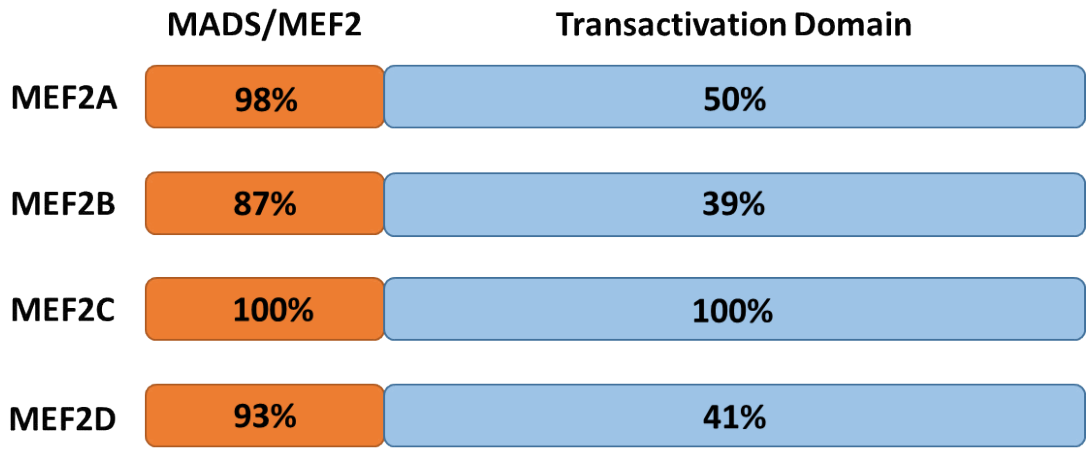


Figure 1.06: Illustration of the amino acid sequence homology between MEF2A, B and D relative to MEF2C, with the highly conserved MADS/MEF2 region (orange) and more variable downstream transactivation domain (blue) independently compared.

### 1.3.2 Regulation of MEF2 Activity

Regulation of MEF2 activity involves a wide range of processes that may occur at various stages including transcription, translation and protein degradation (Okamoto, Li, Ju, Schölzke, *et al.*, 2002; Zhu and Gulick, 2004). MEF2 protein activity is regulated by

mitogen-activated protein kinase signalling pathways (MAPKs) as has been demonstrated in yeast, *Drosophila* and in invertebrates (Dodou and Treisman, 1997; Han *et al.*, 1997; Kato *et al.*, 1997; Potthoff and Olson, 2007). Most MAPKs are involved in an organism's reaction to stress and/or damage, including DNA damage, oxidative stress and infection, with their involvement observed in a range of cell types and processes such as cell mitosis, apoptosis, proliferation and differentiation (Pearson *et al.*, 2001). Whilst different MAPKs have differing characteristics, the majority hold to a "classical" form, where their activation is dependent on two phosphorylation events and similar substrate recognition sites (Coulombe and Meloche, 2007). These MAPKs facilitate the phosphorylation of the transcriptional activation domain within the MEF2 protein, regulating its transcriptional activity. For example, the MAPK Extracellular-signal-regulated kinase 5 (ERK5) is a co-activator of MEF2, interacting through a single-dependant direct association with the transcriptional activation domain (Yang *et al.*, 1998; Potthoff and Olson, 2007). ERK5 activation is signalled in response to developmental cues for the direction of endothelial formation and cardiac morphogenesis, though it is also believed to be involved in neurogenesis (Regan *et al.*, 2002).

MEF2 activity is also influenced in skeletal muscle development at a transcriptional level by the myogenic basic helix-loop-helix (bHLH) transcription factors, which bind to a muscle-specific control region in the *Mef2c* gene (Molkentin *et al.*, 1995; Wang *et al.*, 2001), along with the thyroid hormone response element (Lee *et al.*, 1997; Zhu and Gulick, 2004). bHLH transcription factors are necessary for expression at all stages of muscle development (Zhu and Gulick, 2004). Furthermore, a 3' untranslated region of the *Mef2a* gene transcript was found to act as a repressor at the translation stage (Black, Lu and Olson, 1997), which may contribute to preventing of an over-abundance of MEF2 proteins leading to *N*-methyl-d-aspartate (NMDA) induced apoptosis via dominant-interference (Okamoto, Li, Ju, Schölzke, *et al.*, 2002). This over-abundance is capable of circumventing the neuroprotection normally facilitated by the presence of the MEF2C protein (Okamoto, Li, Ju, Schölzke, *et al.*, 2002). Transcriptional co-regulators including Cyclin D-cdk4 (Lazaro, Bailey and Lassar, 2002), histone acetyltransferase's (HATs) alongside histone deacetylase's (HDACs) (most notably HDAC-4) (Miska *et al.*, 1999; McKinsey, Zhang and Olson, 2001), and p-300 (Youn, Chatila and Liu, 2000; Zhu and Gulick, 2004) are also known to regulate MEF2 activity, with some interactions calcium-dependant (McKinsey, Zhang and Olson, 2002).

## 1.4 Processes involving MEF2

### 1.4.1 MEF2 in Muscle

The discovery of MEF2 as a regulator of muscle gene expression (Gossett et al., 1989) subsequently led to the discovery of its involvement in muscle development. The specific role MEF2 plays in muscle development was investigated extensively in *Drosophila* models, where it was found to be first expressed in early mesoderm tissue and subsequently through various muscle cell lineages and myoblast differentiation (Bour et al., 1995; Lilly et al., 1995; Ranganayakulu et al., 1995; Potthoff and Olson, 2007). MEF2 was further characterised in a later study following the advent of chromatin immunoprecipitation and microarray analysis that covered ~50% of the entire *Drosophila* genome (Sandmann et al., 2006). The bHLH regulation of skeletal muscle at the transcriptional level involves families of transcription factors, which associate and together activate muscle gene expression (Haberland et al., 2007). These myogenic bHLH proteins thereafter form a positive-feedback loop perpetuated by their own expression, with HDAC9 expression required to repress of MEF2 activity. HDAC9, as with other HDACs, bind to the MADS domain of MEF2 via an N-terminal peptide sequence, establishing co-repressor complexes and subsequently preventing MEF2 from activating target genes (McKinsey et al., 2000; McKinsey, Zhang and Olson, 2001; Chang et al., 2006; Haberland et al., 2007). Interestingly, the HAT p300/CBP co-activator family also docks to the MADS domain of MEF2 which given that they are mutually exclusive in their interaction with MEF2, creates a mechanism through which MEF2 target genes may be activated or repressed in a binary fashion (Lu et al., 2000; McKinsey, Zhang and Olson, 2001; Haberland et al., 2007).

### 1.4.2 MEF2 in Immunity

Although MEF2 is best known for its role in muscle, it is also known to be involved in other tissues and systems. In *Drosophila* models it was discovered that MEF2 had a role in immune and metabolic activities, with its mutation causing extensive failures of systemic anabolism and general immune function (Clark et al., 2013). In *Drosophila* the fat body, a loose functional homolog of the mammalian liver and adipose tissue, is responsible both for hormonal immune response and as a site of metabolic stores, with this tissue found to be susceptible to MEF2 knockdown. The increased anabolism occurring as a result of MEF2 knockdown causes a reduction in the overall size of the fat body along with reductions in triglyceride and glycogen levels (Clark et al., 2013).

Furthermore, normal expression of MEF2 is essential for the promotion of many infection-induced antimicrobial peptides and as such, *Drosophila* models without regular MEF2 expression were found to be severely immune-compromised (Clark et al., 2013). In *Drosophila*, the transcription of metabolic and immune target genes is regulated by the phosphorylation of MEF2 at a conserved site. Phosphorylation at this site occurs in healthy *Drosophila* and promotes the transcription of metabolic genes. However, in an infected model the MEF2 becomes dephosphorylated at this site and promotes immune targets through association with the TATA-binding protein, forming a MEF2-TATA compound located within the promoter regions of antimicrobial peptides (Clark et al., 2013). Whilst this does not of course necessarily directly translate to mammalian models, it does highlight the extent to which MEF2 may be involved in diverse vital biological processes.

Thymocytes (T-cells) are lymphocytes in cell-mediated immunity involving multiple signalling cascades that, through the resulting alterations in gene expressions, may direct the T-cell state or function (Potthoff and Olson, 2007). Specifically, calcium signalling was found to play key roles in T-cell receptor (TCR) induced apoptosis along with the nerve growth factor IB (NUR77), a gene whose expression requires two MEF2 sites in the NUR77 promoter region (Woronicz et al., 1995; Youn et al., 1999). MEF2 proteins within T-cells which have not yet been stimulated to undergo TCR-induced apoptosis are associated with co-repressors including HDAC7 and Cabin1, both of which inhibit Nur77 expression (Youn *et al.*, 1999; Youn, Chatila and Liu, 2000; Dequiedt *et al.*, 2003; Potthoff and Olson, 2007). However, through TCR activation the HDAC7 protein may become dissociated from the MEF2 though nucleocytoplasmic shuttling (Potthoff and Olson, 2007), with its subsequent translocation to the cytoplasm facilitating the MEF2 activation (Parra *et al.*, 2005). In this way, the MEF2 protein is in itself regulated through its association with transcriptional repressors and highlights the importance of the MEF2-HDAC relationship, specifically in T-cell development, differentiation and TCR choice (Kasler and Verdin, 2007; Potthoff and Olson, 2007).

It should also be noted that when MEF2 interacts with class IIa histone deacetylases these together form a base from which many epigenetic regulatory mechanisms are influenced and as such, MEF2 may play a key role in the mediation of these mechanisms including chromatin configurations and microRNA modulation (Potthoff and Olson, 2007).

## 1.5 The MEF2 Family and MEF2C

The MEF2 family have been shown to directly influence neuronal development, including dendrite morphogenesis, the differentiation of post-synaptic structures and the excitatory synapse number (Flavell et al., 2006; Shalizi et al., 2006; Potthoff and Olson, 2007). A specific example is the sumoylation of the MEF2A mammalian protein that facilitates the promotion of post-synaptic differentiation of neurons through the resulting repression of negative dendritic regulators including the transcription factor NUR77 (Shalizi et al., 2006; Scheschonka, Tang and Betz, 2007). Moreover, the activity-regulated-cytoskeletal-associate protein (ARC) and the synaptic RAS GTPase-activating protein (syngap1) are responsible for synaptic disassembly, with both activities regulated by dephosphorylation of MEF2 (Vazquez *et al.*, 2004; Flavell *et al.*, 2006; Potthoff and Olson, 2007).

### 1.5.1 Similarities and differences between *Mef2a, b, c* and *d*

In vertebrates there are four *Mef2* genes, *Mef2a, b, c* and *d*. During development the four *Mef2* genes are expressed differently both spatially and temporally from the embryo through to adulthood (Edmondson *et al.*, 1994). *Mef2a, c* and *d* have very similar gene structures and alternative splicing patterns between coding exons, with exon 1 encoding the MADS box and exon 2 encoding the adjacent MEF2 motif (Black and Olson, 1998). The *Mef2b* gene sequence however is dissimilar downstream of the MADS/MEF2 domains and also differs in its expression patterns.

*Mef2a, c* and *d* each contain a mutually exclusive splice sites located in exons α1 and α2, with a skipping alternative splice site in exon β (Figures 1.07-1.08), a combination of which are variably included in mRNAs. However, there are differences between these three *Mef2* genes. For example, *Mef2d* has an additional coding exon at its 3' end, and *Mef2c* has a γ acceptor site in the final coding exon. This γ region is >98% conserved among vertebrates, though no other vertebrate or *Drosophila Mef2* genes share this site (Zhu and Gulick, 2004). *Mef2a* and *Mef2d* encode only 4 possible variants commonly referred to as α1, α1β, α2, or α2β variants. Due to the γ region present within *Mef2c* however, eight variants are possible, referred to as α1, α1β, α1γ, α1βγ α2, α2β, α2γ or α2βγ (Zhu and Gulick, 2004). However, MEF2C variants were recently discovered that contain neither of the α splice sites that had previously been believed to be alternative but required splice acceptor sites (Infantino *et al.*, 2013). In this way, isoforms containing no α but either of the β or γ sites are also possible in addition to the variants listed above (Infantino *et al.*, 2013). By stark contrast, given *Mef2b*'s gene structure dissimilarity to

the other members of the *Mef2* family, only two isoforms exist (termed A and B) each with distinct C-terminal domains (Ying *et al.*, 2013).

### 1.5.2 *Mef2c* exon detail

*Mef2c* consists of 13 exons including three splicing sites labelled α, β and γ as previously described. The β domain comprises the 10th exon with the γ splice acceptor site located at the beginning of the final exon (Sekiyama, Suzuki and Tsukahara, 2012). The β exon is a skipping-type alternative splicing site, with isoforms including or excluding this region dependant on cell type, and is located in the middle of the transcriptional activation domain of the *Mef2c* gene (Hakim *et al.*, 2010). Isoforms with the inclusion of the β exon when fused with Gal4 showed an increase in transcription activation level compared to those without the β exon, suggesting this exon functions as a promoter of transcriptional activity (Zhu and Gulick, 2004; Hakim *et al.*, 2010). Conversely, there is evidence to suggest that inclusion of the γ region may repress transcriptional activity (Zhu and Gulick, 2004). *Mef2c* α1γ variants in a recent investigation were found to be 2.5 fold less active that α1 fragments, with α1β more transcriptionally active than either variant (Black, Lu and Olson, 1997; Zhu and Gulick, 2004; Zhu, Ramachandran and Gulick, 2005; Infantino *et al.*, 2013). Figure 1.07 below illustrates approximate positions of key *Mef2c* exons and splice patterns.


Figure 1.07: Illustration of *Mef2c* exon locations with particular reference to α, β and γ. Adapted from (Sekiyama, Suzuki and Tsukahara, 2012).

### 1.5.3 α Exons

Exons α1 and α2 consist of very short nucleotide sequences. α1 transcripts are present abundantly in neuronal and cardiac cells, whereas α2 transcripts are present in cardiac cells but not in neuronal (Hakim *et al.*, 2010). Whilst it was previously believed that all MEF2C isoforms contained either the α1 or α2 exons, a recent investigation by (Infantino *et al.*, 2013) revealed two transcripts containing neither. Whilst neither transcript contains either α exon, one (VP1) contains exclusively the β exon and the other (VP2) contains exclusively the γ region as shown in Figure 1.08.

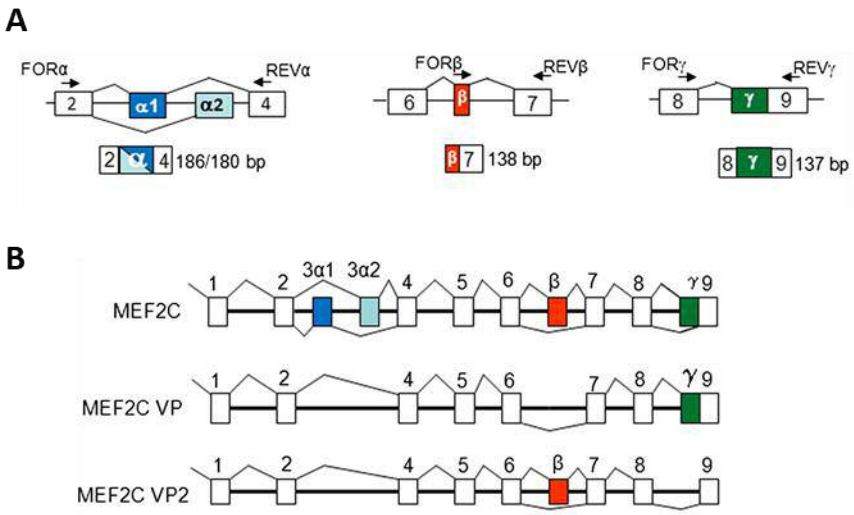


Figure 1.08: Splice patterns of *Mef2c* variants (A) involving α, β and γ sites and (B) the more transcriptionally active MEF2C VP α-excluding variants relative to *Mef2c* α-including variants. Adapted from (Infantino *et al.*, 2013).

Given the relatively new discovery of these variants, little is known about in which cells they are predominantly expressed. However, they have been found to co-localise in the nucleus with other MEF2 variants, indicating that the α exon is not involved in the subcellular localisation process (Infantino *et al.*, 2013). VP variants, which is to say MEF2C variants lacking an α exon, were also found to be considerably more transcriptionally active when compared to the relative transcriptional activity of all other variants containing either α exon. When VP1 (γ), and VP2 (β) activity was compared to that of α1γ and α1β respectively, VP1 demonstrated a 2-fold increase in transcriptional activity with VP2 also demonstrating higher transcriptional activity levels (Infantino *et al.*, 2013). Together, this suggests that the α exon may have a repressive effect on transcriptional activity.

Both α- variants were found to be expressed in various human tissues, most abundantly in brain and cardiac tissue (see Figure 1.09).

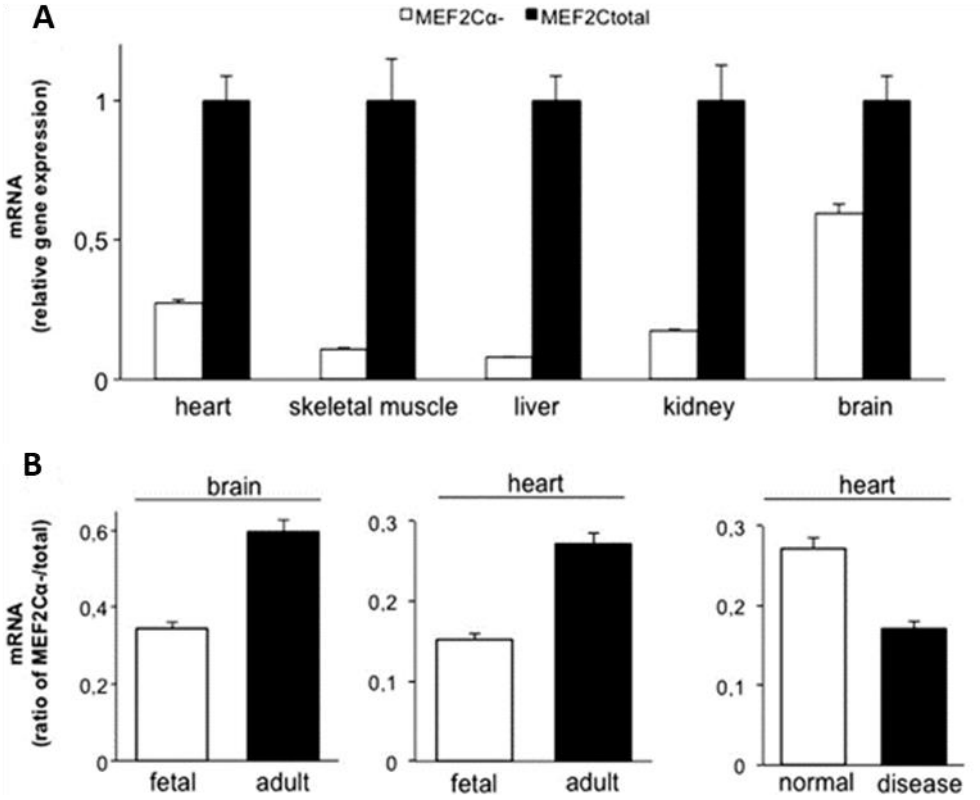


Figure 1.09: Relative expression levels of *Mef2c* α- mRNA isoforms to total *Mef2c* mRNA in (A) adult heart, skeletal muscle, liver, kidney and brain, alongside (B) the normalised ratio of *Mef2c* α- mRNA isoforms to total *Mef2c* mRNA in foetal and adult tissues. Adapted from (Infantino *et al.*, 2013)

### 1.5.4 **α Exon with Fox-1 and PIN1**

Fox-1 is a tissue-specific alternative splicing regulator (Infantino *et al.*, 2013) highly expressed in adult cells of both the heart and brain, with recent studies implicating its role in developing cells (Kalsotra *et al.*, 2008; Hakim *et al.*, 2010; Park *et al.*, 2011). An overexpression of Fox-1 increases the number of transcripts formed containing neither *Mef2c* α exon, suggesting its role as a mediator of α- variant splicing. PIN1, a peptidyl-prolyl isomerase protein, interacts with MEF2C through serines 98 and 110 located within the α exon region through the isomerization of phosphorylated ser/thr-pro peptide bonds, regulating cell differentiation (Infantino *et al.*, 2013). Through the binding of PIN1 to the α exon, MEF2C activity may be repressed (Magli *et al.*, 2010) and this may provide an explanation for the lower transcriptional activity associated with MEF2C variants that include the α exons and provides evidence for its role as, at least in part, an inhibitory region.

### 1.5.5 **β Exon**

The β exon present in *Mef2c* is a skipping exon, which when included in a transcript forms an α-helix secondary structure (Zhu, Ramachandran and Gulick, 2005; Sekiyama, Suzuki and Tsukahara, 2012). This acts as an enhancer of p38 kinase recruitment, a regulator of cellular apoptosis (New and Han, 1998), through manipulation of TAD II, which is involved in tRNA processing (Gerber and Keller, 1999). Proteins formed from β-inclusion transcripts may act in *cis* to facilitate or stabilise the TAD II p38 MAP kinase interaction, enhancing transactivation (Zhu, Ramachandran and Gulick, 2005; Sekiyama, Suzuki and Tsukahara, 2012). As such, this pathway reduces apoptotic cell death during neuronal differentiation in P19 cells (Shu-ichi Okamoto *et al.*, 2000; Sekiyama, Suzuki and Tsukahara, 2012).

MEF2C transcripts excluding the β exon are present in undifferentiated cells (Hakim *et al.*, 2010). During the neural differentiation process, the transcription levels of isoforms excluding the β exon drastically reduced, with greater quantities of β inclusion isoforms then detected (Hakim *et al.*, 2010). Thereafter, a reversal occurs where there is a decrease in β inclusion and a rise in β exclusion isoforms (Hakim *et al.*, 2010). Conversely, cardiac cells do not mirror this regulation of the β exon, with β exclusion transcripts the exclusive isoform type (Hakim *et al.*, 2010), highlighting the differing roles of MEF2C in different tissues. It should be noted that in adult neuronal cells β- transcripts are the predominant transcripts, despite β+ isoforms being more robust in their facilitation of transcriptional enhancement (Zhu, Ramachandran and Gulick, 2005; Hakim *et al.*, 2010).

### 1.5.6 **γ region**

Both γ+ and γ- isoforms have been identified in a wide range of tissue types associated with *Mef2* with the exception of heart tissue, where only γ- isoforms are present, though γ- isoforms are predominant in all cell types (Zhu and Gulick, 2004). MEF2C γ- isoforms have been shown to be more active than those that include the γ region in activating *Mef2* reporter genes in transfected fibroblasts and synergise better with MyoD in promoting myogenic conversion (Zhu and Gulick, 2004). When comparing γ+ isoforms containing either α exon, both are expressed at significantly lower levels compared to γ- isoforms (~20-fold), demonstrating that the influence of the γ region is independent from the α or β exons (Zhu and Gulick, 2004). The influence of the γ region was also shown to be non-cell specific and did not influence *Mef2* transcriptional activity via *cis* effects,

that is to say it does not appear to interfere with DNA binding or MEF2 dimerization (Zhu and Gulick, 2004). The transcriptional repressive effects demonstrated in the presence of the γ region occur as a result of the phosphorylation of Ser residue 396 located in the γ region (Zhu and Gulick, 2004) however substitution of this amino acid dramatically reduces the repressive effect (Zhu and Gulick, 2004).

### 1.5.7 **Transcriptional regulation**

*Mef2c* has long been associated with angiogenesis and cardiac development in *Drosophila*, mice and other animal models. Its recent association with neuronal systems indicated that regulatory mechanisms modify the behaviour of the *Mef2c* gene and its translated protein, mechanisms that differ depending on cell type. The phosphorylation of Ser396 additionally effects of the sumoylation of another amino acid, Lys391 (Kang, Gocke and Yu, 2006). Sumoylation regulates subcellular localisation of proteins, their interactions with other proteins and their stability (Gill, 2004; Johnson, 2004), which can reduce the activity of transcription factors (Poukka *et al.*, 2000; Kim *et al.*, 2002; Ross *et al.*, 2002; Sapetschnig *et al.*, 2002; Kang, Gocke and Yu, 2006). It has been shown that the Sumoylation of Elk-1 and p300 enhances their binding to HDAC2 and 6 respectively, indicating their possible involvement with *Mef2c* transcriptional repression (Girdwood *et al.*, 2003; Yang and Sharrocks, 2004; Kang, Gocke and Yu, 2006). Despite this however, the sumoylation of MEF2C does not affect its DNA binding, HDAC recruitment, nuclear localisation, stability or p38 phosphorylation, indicating that although sumoylation does repress transcription (Grégoire and Yang, 2005), it does not do so through these mechanisms (Kang, Gocke and Yu, 2006).

## 1.6 MEF2C involvement in synapse formation

MEF2C involvement in the brain, including regulation of synapse number and function (Barbosa *et al.*, 2008) differentiation and maturation of neuronal cells (H. Li *et al.*, 2008) among others, may function in accordance with MEF2A and MEF2D given their own involvement in the CNS. Knockdown of MEF2A and MEF2D was found to lead to increased synapse formation and miniature excitatory postsynaptic currents (mEPSCs), indicating that MEF2 functions to reduce the number of synapses receive by a neuron (Flavell *et al.*, 2006) and as such, it should be noted that co-regulation of the MEF2 family of genes in required for full CNS functionality. Moreover, cells in which MEF2C was inhibited produced cells showing neuronal morphology, along with greatly reduced overall numbers of cells, some of which exhibited shortened dendrites and lack of

dendrite spines. This indicates that MEF2C is also required for full neuronal development and maturation from human pluripotent stem cell derived neural precursor cells (NPCs).

### 1.6.1 The effect of MEF2C loss in mice

In MEF2C mouse KO models, effects on neuronal cell types and behaviour differ depending on the nature of the KO. MEF2C null mice are embryonically lethal at E9 due to failure of heart development and angiogenesis. To circumvent this, conditional knockout models are used so as to KO MEF2C in specific target tissues whilst leaving the cardiac and angiogenesis systems unaffected, thereby allowing for viable adult mice to be produced. *Mef2c*$^{loxP/loxP}$ females bred with male *Mef2c*$^{KO/+}$ heterozygous mice containing a cre-transgene attached to a human GFAP promotor is one such model in which MEF2C was knocked out in the brain (Barbosa *et al.*, 2008). These KO mice showed a significant reduction in hippocampal and frontal cortex function as demonstrated in impaired hippocampal-dependant learning, though this was not due to any increase in apoptosis (Barbosa *et al.*, 2008). Loss of MEF2C in dentate gyrus neurons resulted in approximately double the frequency of miniature excitatory postsynaptic currents (mEPSCs) compared to WT neurons, though the amplitude of individual synaptic events was unchanged, indicating that these cells were no less capable of responding to glutamine release or neurotransmitter retention (Barbosa *et al.*, 2008). It is possible therefore that the increased frequency of mEPSCs in MEF2C KO dentate gyrus neurons is due to an increase in synaptic density, through an increase in the probability of neurotransmitter release at the presynaptic site (Hsia, Malenka and Nicoll, 1998; Prange and Murphy, 1999; Barbosa *et al.*, 2008). Furthermore, dentate gyrus neurons exposed to a super-active MEF2C-VP16 protein demonstrated no significant difference in the frequency of mEPSCs, indicating that the role of MEF2C in these neurons is to limit synaptic transmission once synaptic connectivity has been established (Barbosa *et al.*, 2008). Further insight into the role of MEF2C in synaptic transmission was achieved through observing spine densities via Golgi staining, where *Mef2c*$^{BKO/KO}$ neurons showed a significant increase in spine density compared to WT, with an increase of almost 50%. Conversely, MEF2C-VP16 cells showed a significant reduction in spine density. Taken together, in hippocampal neurons MEF2C is an essential regulatory factor for synaptic transmission and spine formation, without which mice exhibit a decreased ability learn in ways that require hippocampal input, such as context-dependent fear conditioning (Barbosa *et al.*, 2008).

Another prominent example of MEF2C KO in the brain is through the loxP-Cre recombinase system attached to a Nestin promoter to target neurons at the much earlier neural progenitor cell (NPC) stage. NESTIN is expressed in many regions of the brain including the cortex. *Nestin-Cre*$^{+}$*/Mef2c*$^{loxP/\Delta 2}$ null conditional KO mice exhibited severe neuronal compaction in the cortical plate at E18.5, disrupting cortical layer formation. The cells most affected by this compaction were post-mitotic neurons rather than precursors (H. Li *et al.*, 2008), indicating MEF2C's role is greater in neuronal cells. These cortical plate abnormalities persisted in both neonatal and adult mice, with MEF2C-null neurons exhibiting immature electrophysiological properties (Shu-ichi Okamoto *et al.*, 2000). Interestingly, patch-clamp analysis of layer 5 cortical MEF2C KO neurons revealed a decrease in the frequency and amplitude of mEPSCs, smaller evoked excitatory postsynaptic currents (EPSCs), and a decrease in the input/output ratio compared with WT (H. Li *et al.*, 2008). This is in stark contrast to the frequency of mEPSCs in dentate gyrus cells lacking MEF2C (MEF2C was knocked out at a later time point in these cells), highlighting that MEF2C function in the brain is dependent on both spatial and temporal factors. (H. Li *et al.*, 2008) also report that fewer synaptic sites were present in MEF2C KO cells, although cellular degradation was ruled out as a cause given cellular expression of the mature neuronal marker microtubule associated protein 2 (MAP2). The behavioural effects of the early-starting global-brain Nestin-Cre MEF2C KO include abnormal anxiety-like behaviours, decreased cognitive function, including fear-dependant and spatial memory, and marked paw wringing/clasping stereotypy, mirroring similar deficits observed in humans suffering from a mutation in even a single MEF2C allele (Hao Li, Radford, Ragusa, Shea, McKercher, Zaremba, Soussou, Nie, Kang, Nakanishi, *et al.*, 2008; Le Meur *et al.*, 2010; Palumbo *et al.*, 2013; Rocha *et al.*, 2016).

## 1.7 Effect of loss of MEF2C expression in Humans

In humans, when only one copy of the *Mef2c* gene is present, severe intellectual disability is the most commonly reported phenotype (Zweier and Rauch, 2012). The 5q14.3q15 deletion syndrome is a rare disorder with approximately 50 reported cases exhibiting a range of phenotypes of varying severity and overlap with Rett syndrome (Zweier and Rauch, 2012; Rocha *et al.*, 2016). These include intellectual disability, seizures and dysmorphic features. *Mef2c* is considered the critical gene involved in the 5q14.3q15 microdeletion syndrome (Zweier *et al.*, 2010; Zweier and Rauch, 2012) and is the most commonly mutated gene among identified patients. This is supported by the observation

that patients who have a *Mef2c* point mutation have similar phenotypes to those whose microdeletions also encompass other genes, including severe mental retardation, an inability to walk freely, impaired or absence of speech, seizures and in many cases a facial gestalt of a broad, high forehead with relatively large backward-rotated ears with prominent ear lobes, mildly upward-slanting palpebral fissures and a cupid bowed or tented upper lip (Cardoso *et al.*, 2009; Engels *et al.*, 2009; Zweier *et al.*, 2010; Zweier and Rauch, 2012). Many patients who underwent magnetic resonance imaging (MRI) analysis showed abnormalities including delayed myelinisation, enlarged ventricles and a hypoplastic or thickened corpus callosum among others, though there was no uniform pattern (Zweier and Rauch, 2012). All human cases reported to date have been *Mef2c* heterozygous *de novo* mutations.

In mice, the homozygous knockout of MEF2C in neural progenitor cells causes an aggregation and compaction of migrating neurons during development in mouse models with a Nestin-Cre, with smaller brains containing less mature neurons even in adulthood, coupled with electrophysiology and behavioural abnormalities comparable to those observed in mouse models of Rett syndrome (Hao Li, Radford, Ragusa, Shea, McKercher, Zaremba, Soussou, Nie, Kang and Nakanishi, 2008; Zweier *et al.*, 2010). Rett syndrome in humans is characterised by apparent normal development for the first 6-18 months of life, followed by developmental stagnation and sharp regression involving a wide range of phenotypes including poor motor skills, language, stereotypic hand movements, emotional instability, episodic apnea and/or hyperpnea, seizures and autistic features (Zweier and Rauch, 2012). Around 90% of classical and 50% of non-classical (abnormal) Rett syndrome patients have a mutation or deletion of the Methyl CpG binding protein 2 (MECP2) gene and in many of those that do not, Cyclin-dependent kinase-like 5 (CDKL5) or Forkhead box G1 (FoxG1) mutations have been detected (Kammoun *et al.*, 2004; Weaving *et al.*, 2004; Fukuda *et al.*, 2005; Archer *et al.*, 2006; Li *et al.*, 2007; Zahorakova *et al.*, 2007; Ariani *et al.*, 2008; Mencarelli *et al.*, 2010; Philippe *et al.*, 2010). Whilst patients suffering from 5q14.3q15 syndrome usually do not share this sharp regression at an early point in their lives after apparent normal development, at least one case has been presented where a patient with a *Mef2c* truncating mutation suffered sharp developmental regression after five months of normal development (Le Meur *et al.*, 2010; Zweier *et al.*, 2010). Furthermore, MECP2 binds to the *Mef2c* promoter region, supressing transcription and subsequently lowering *Mef2c* mRNA levels (Mari *et al.*, 2005; Chahrour *et al.*, 2008; Zweier *et al.*, 2010). This downstream effect on MECP2 and CDKL5 was the same regardless of whether the mutation was missense, truncating or a deletion (Zweier and Rauch, 2012). Haploinsufficiency of the Transcription Factor 4

(TCF4) gene from the bHLH transcription factor family, which are known to regulate *Mef2c* function and/or expression as previously described, is the main cause of Pitt-Hopkins syndrome, which has overlapping phenotypes with Rett and 5q14.3q15 syndrome (Zweier *et al.*, 2008).

Neuropeptide Y (NPY), a neurotransmitter of the sympathetic nervous system, is negatively regulated by MECP2 (Chahrour and Zoghbi, 2007; Fyffe *et al.*, 2008; Chao *et al.*, 2010; Sakai *et al.*, 2013) and was found to be co-expressed with MEF2C in the arcuate nuclei of the hypothalamus. Moreover, *Mef2c* and NPY were found to be epigenetically co-regulated *in vitro* by MECP2 (Chahrour and Zoghbi, 2007; Fyffe *et al.*, 2008; Sakai *et al.*, 2013). MEF2C is believed to regulate expression of genes involved in neuroendocrine homeostasis through increasing NPY expression in mature neurons. Furthermore, it is the deregulation of NPY by MECP2 that creates the molecular phenotype described as one of the mechanisms underlying the metabolic phenotypes of Rett syndrome patients (Chahrour *et al.*, 2008; Fyffe *et al.*, 2008; Sakai *et al.*, 2013). It stands to reason therefore that a loss of MEF2C functionality may bring about an imbalance in NPY modulation in the hypothalamus and as such contribute to neuroendocrine dysfunction.

### 1.7.1 Differential Effects of *Mef2c* Mutations

Patients suffering from either a microdeletion or a truncating mutation in one of their two *Mef2c* alleles were found to have reduced levels of *Mef2c* mRNA. Interestingly, however, those who suffer from a missense mutation in the MADS domain, which may alter DNA-binding affinity, do not have reduced *Mef2c* mRNA levels, likely due to a lack of nonsense-mediated mRNA decay in missense mutations (Zweier *et al.*, 2010). The G27 mutation identified in one patient is present in a structurally important position where the helix of the MEF2C protein is drawn close to the DNA backbone. The role of the alanine is to prevent this proximity through a clash with an adjacent phosphate group. The G27 mutation removes the alanine, replacing it with a glycine (Figure 1.10) (Zweier *et al.*, 2010). The structural changes caused by this mutation ultimately lead to weaker DNA binding (Zweier *et al.*, 2010). The L38Q mutation on the other hand, identified by (Engels *et al.*, 2009), does not directly interact with the DNA, but rather restricts conformational flexibility and relative positioning of long side chains involved in DNA-binding (Figure 1.10) (Santelli and Richmond, 2000; Zweier *et al.*, 2010). This demonstrates that when talking about point mutations in *Mef2c*, one must be aware that although reduced expression of MEF2C is often the end result, the mechanics through which that may

occur can vary significantly, with some mutations in the MADS domain actually not resulting in reduced expression, as previously described.

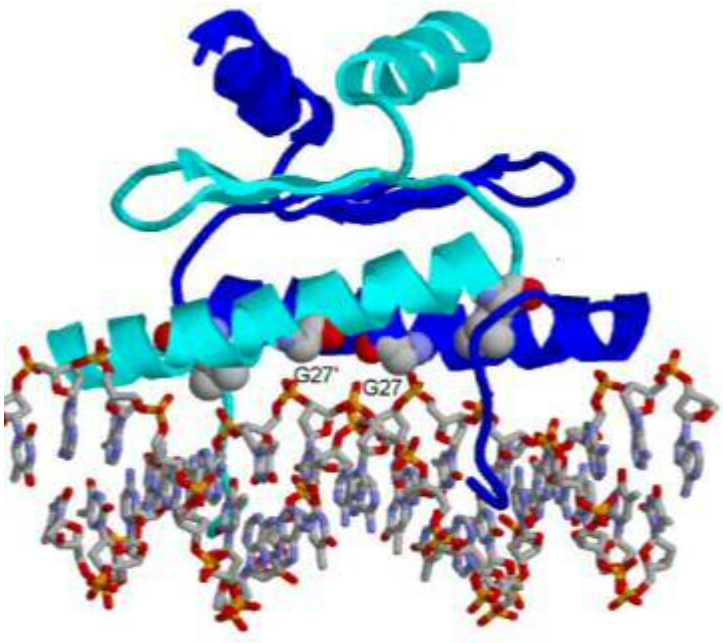


Figure 10: Crystal structure of the MEF2A-DNA binding complex, which is very similar to MEF2C differing only by a single amino acid. The two subunits of the dimeric protein are depicted in cyan and dark blue with DNA in stick-presentation. G27 reference to mutation sites on the protein. Adapted from (Zweier *et al.*, 2010).

### 1.7.2 Diagnosis Issues of *Mef2c* related conditions, and *Mef2c*'s potential impact on neurological conditions

As 5q14.3q15 deletion syndrome is a rare condition only relatively recently described, it is not possible to accurately determine the proportion of humans affected by the disease. This issue is compounded further with the wide range of features associated with the condition and the lack of standardisation and unbiased phenotypic judgement inherent in clinical diagnoses, which can ultimately lead to incorrect diagnoses, for example in regards to the severity of epilepsy (Paciorkowski *et al.*, 2013). Moreover, although it is known that children with *Mef2c* mutations have abnormal movement patterns and neurobehavioral deficits, video examples of these movements and behaviours along with their development as the patient ages have not yet been widely published, adding to the difficulty in distinguishing between abnormal movement patterns caused by *Mef2c* mutations and variety of other conditions (Paciorkowski *et al.*, 2013). It must also be noted that some people simply remain undiagnosed for reasons such as lack of

availability of genetic testing or exhibiting milder symptoms. As such, although the deletion has not been reported in a great number of people, it is thought that *Mef2c* variations or deletions may account for up to 1% of people with intellectual disabilities (Zweier and Rauch, 2012). Furthermore, the MEF2C protein has been linked to other neurodevelopmental features though its ability to regulate various other transcription factors including Dia1, Pcdh10, and Ube3a associated with intellectual disability, epilepsy and autism (Morrow *et al.*, 2008).

## 1.8 Markers of MSN Differentiation

### 1.8.1 **DARRP-32**

DARRP-32 is a signalling molecule activated by a range of neurotransmitters including dopamine, glutamine, gamma-aminobutyric acid and adenosine (Svenningsson *et al.*, 2004; Brami-Cherrier *et al.*, 2005). Within the striatum DARPP-32 is the “gold standard” for MSN identification (Walaas and Greengard, 1984; Tamura *et al.*, 2004). It is also considered a mature MSN marker, as its expression is observed relatively late in embryonic striatal development at E18, with the alternative MSN markers Forkhead box protein 1 (FOXP1) and COUP TF1-interacting protein 2 (CTIP2) expressed earlier (see sections below) (Arlotta *et al.*, 2008; Precious *et al.*, 2016). The identification of a DARPP-32 positive cell within the striatum therefore is a clear marker of a fully differentiated, mature MSN. However, it should be noted that although within the adult striatum all MSNs are expected to be capable of expressing DARPP-32 (Walaas and Greengard, 1984; Tamura *et al.*, 2004), not all MSNs do so at any single point in time, as is evidenced through consistently higher counts of FOXP1 and CTIP2 MSN markers (see sections below).

DARPP-32 is involved in a range of properties of MSNs including nuclear chromatin response, ion channel permeability and synaptic plasticity (Yger and Girault, 2011). Mouse DARPP-32 KO models do not demonstrate severe consequences on spontaneous behaviour, nor have DARRP-32 mutations been clearly associated with human pathology (Heyser *et al.*, 2000; Yger and Girault, 2011). However DARPP-32 may increase evolutionary fitness and allow for a finer balance to be maintained in neurotransmitter signalling and the D1/D2 excitatory/inhibitory signalling pathways (Heyser *et al.*, 2000; Meyer-Lindenberg *et al.*, 2007; Kolata *et al.*, 2010; Yger and Girault, 2011). Human DARPP-32 mutations have, however, been linked to certain personality traits and may predispose to psychopathological states (Yger and Girault, 2011),

strengthening this idea. DARPP-32 is required for mediating the actions or effects of these neurotransmitters, for example in response to drugs of abuse (Svenningsson *et al.*, 2004; Svenningsson, Nairn and Greengard, 2005), playing a particularly important role in biochemical, electrophysiological and behavioural effects of dopamine on dopaminoceptive neurons (Bibb *et al.*, 1999; Greengard, 2001; Svenningsson *et al.*, 2004). The precise role DARRP-32 plays within a neurotransmitter system at any given time depends in part on its state of phosphorylation.

Phosphorylation of DARPP-32 at Thr-34 causes the protein to inhibit protein phosphatase 1 (PP1), a protein required for regulating a range of phosphoproteins including voltage-dependant sodium and calcium channels and neurotransmitter receptors (Hemmings *et al.*, no date; Fienberg *et al.*, 1998; Ouimet, Langley-Gullion and Greengard, 1998; Yan *et al.*, 1999). DARRP-32's inhibition of PP1 causes an increase in phosphorylation of these phosphoproteins, thereby affecting synaptic function and neural plasticity (Svenningsson *et al.*, 2004). Conversely, phosphorylation of DARRP-32 at Thr-75 by cyclin-dependant kinase 5 (CDK5) results in the inhibition of protein kinase A (PKA), increasing phosphorylation of PKA substrates and thereby mediating peak voltage-gated calcium currents (Gray *et al.*, 1998; Yger and Girault, 2011). Thus, DARPP-32 has been shown to play a dual-role as either a kinase- or phosphatase-inhibitor, sensitive to minor post-translational modifications, in dopaminergic neurotransmission (Bibb *et al.*, 1999; Greengard, 2001). It is reasonable to suggest therefore that a cell lacking DARPP-32 may be less able to regulate dopaminergic transmission; an effect compounded when shared by neighbouring cells due to a significant reduction of DARRP-32-expressing cells in the striatum as whole.

Mature MSNs may co-express D1 and/or D2 classes of dopamine receptor, with the activation of either of these receptors influencing DARRP-32 phosphorylation. For example, activation of the D2 receptor decreases cAMP levels, decreasing the activity of PKA and phosphorylation of DARPP-32 and Thr-34 (Yger and Girault, 2011) as shown in Figure 1.11 below. D2 activation also causes an increase in calcium levels and activity of protein phosphatase 2B (PP-2B), thereby increasing de-phosphorylation of DARPP-32 at Thr-34 (Nishi *et al.*, 1999). In a healthy striatum, blockage of the D2 receptor allows for re-phosphorylation of DARPP-32 at Thr-34 (Svenningsson *et al.*, 2000). Thus, it is clear that for the striatum to function properly, MSNs must be mature and fully formed with appropriate D1 and/or D2 receptors, with DARRP-32 protein available for dopaminergic mediation. It is believed that disequilibrium between the direct and indirect pathways in which D1 and D2 receptors play their roles, may account for some of the

striatal alterations in neurological conditions including PD (Di Chiara, 1999; Yger and Girault, 2011).

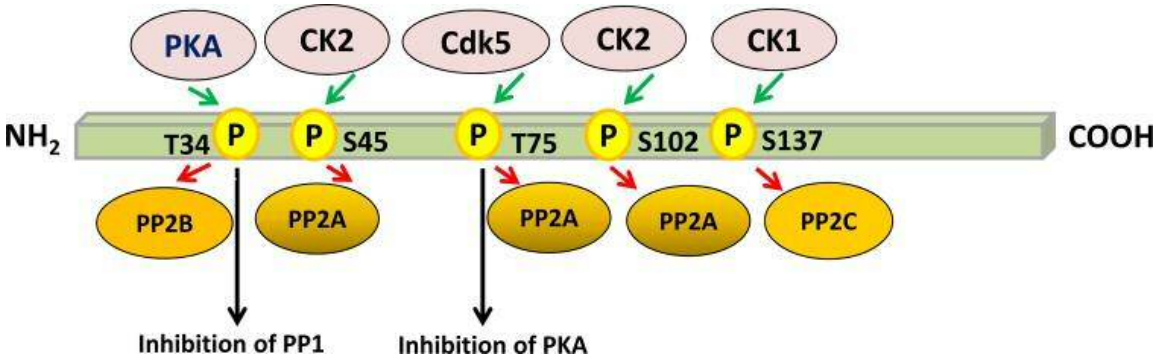


Figure 1.11: Regulation of PP1 and PKA by phosphorylation of DARPP-32. Green arrows indicate phosphorylation by protein kinases, red arrows dephosphorylation by protein phosphatases. Adapted from (Belkhiri, Zhu and El-Rifai, 2016).

DARPP-32 has been associated with neurological conditions including Parkinson's disease and Alzheimer's Disease (AD). In a rodent model of PD chronic administration of L-DOPA induced phosphorylation of DARPP-32 at Thr-34 (Santini *et al.*, 2007), often triggering abnormal involuntary movements (AIMs) mirroring L-DOPA-induced dyskinesia observed in human patients (Cenci, 2007). Interestingly, rodent models in which DARPP-32 was deleted in some but not all striato-nigral neurons showed that D1R-expressing neurons without DARPP-32 did not develop AIMs upon L-DOPA induction, but did so in cells expressing DARPP-32. This highlights the complex relationship DARPP-32 plays with dopamine and motor phenotypes. (Bateup *et al.*, 2008; Darmopil *et al.*, 2009).

In AD, DARPP-32 is cleaved at Thr-153 by calpain, thereby reducing the phosphorylation of important PP1 targets, including the cAMP-response element-binding protein (CREB), a protein associated with cognitive function (Cho *et al.*, 2015; Belkhiri, Zhu and El-Rifai, 2016). In conclusion, AD and PD models suggest DARPP-32 is a required factor for successful motor and cognitive behaviour.

Furthermore, a DARPP-32 reduction in deceased schizophrenic and bipolar patients was detected compared to matched controls (Albert *et al.*, 2002; Torres *et al.*, 2009; Kunii *et al.*, 2011). It should be noted that post-mortem studies of humans are intrinsically limited so it is not possible to determine whether the reduction was a cause or a symptom of the condition, but remains yet another example of DARPP-32s involvement in brain health.

### 1.8.2 **FOXP1**

FOXP1 belongs to the P subfamily of the Forkhead box (FOX) family of transcription factors. FOX transcription factors have several roles during both development and in adulthood in a range of tissues including cardiac muscle cells, the oesophagus and spinal motor neurons. FOX proteins are also responsible for the repression of the transcription of pro-apoptotic genes and by extension, caspase-dependent apoptosis (Bacon and Rappold, 2012; van Keimpema *et al.*, 2014).

During embryonic neural development, FOXP1 has been shown to promote neuronal migration and morphogenesis, and to be important for MSN differentiation (Li *et al.*, 2015; Precious *et al.*, 2016). FOXP1 expression in the developing striatum is detectable from E12.5, where it is highly expressed throughout the developing WGE (Precious *et al.*, 2016). This expression is maintained through to adulthood and it remains expressed in mature MSNs, co-localising with DARPP-32, and is required for its expression *in vitro* (Precious *et al.*, 2016). FOXP1 in the striatum does not co-localise with interneurons however, indicating that it is an MSN-specific marker with the striatum. Furthermore, as previously described FOXP1 labels a significantly greater total number of MSNs relative to DARPP-32. A significant reduction in the total number of surviving cortical and striatal neurons is observed following FOXP1 KO, indicating its necessity not only for the proper development of neurons *in vitro*, but also that FOXP1 harbours a neuroprotective effect and is required for their continued survival *in vivo* (Precious *et al.*, 2016; Louis Sam Titus *et al.*, 2017).

During the development of brain regions other than the striatum, FOXP1 regulates midbrain dopamine neuron differentiation and motor neuron migration (Konstantoulas, Parmar and Li, 2010; Palmesino *et al.*, 2010; Bacon *et al.*, 2015). Cortical-targeted FOXP1 knock-down (KD) via shRNA results in delayed neuronal migration in the developing cerebral cortex (Konstantoulas, Parmar and Li, 2010; Palmesino *et al.*, 2010; Bacon *et al.*, 2015), the effects of which appear to be long-lasting and are not self-correcting. Furthermore, FOXP1 KD was found to significantly affect dendritic length, dendritic maturation and also results in significantly shorter axonal lengths (Li *et al.*, 2015), highlighting the importance of the role FOXP1 plays in the developing striatum. Interestingly however, unlike the effect on MSNs, FOXP1 KD has no effect on the proliferation or differentiation of cortical neurons (Li *et al.*, 2015).

In NPCs FOXP1 was found to induce and bind to 210 genes, with a further 274 repressed and bound (Braccioli *et al.*, 2017). *In vitro*, FOXP1 KD was shown not to affect proliferation, but did affect NSCs thorough reducing neuronal differentiation whilst

maintaining cells with intermediate-progenitor-like characteristics (Braccioli *et al.*, 2017). As well as promoting astrocyte and neuronal differentiation, FOXP1 was also found to promote neurogenesis through repression of the Notch-ligand Jagged1 (JAG1) *in vivo* (Braccioli *et al.*, 2017).

A MEF2C KO model utilising a Nestin-cre mediated loxP recombination system targeted neural progenitor cells (NPCs) in an early stage in the neuronal differentiation programme (Li et al. 2008a). Nestin expression is widespread throughout the brain, but has particularly strong expression in the cortex, within which *n-Cre* $^{+}$/*Mef2c* $^{loxP/\Delta 2}$-null mice were found to have severe neuronal compaction in the cortical plate at E18.5, disrupting cortical layer formation as previously described. This investigation found that important cell adhesion molecules PSA-NCAM and integrin α5 were also expressed in both models, indicating manipulation of these molecules was unlikely to be the cause. Furthermore, it found that signalling pathways are unlikely to be the cause of neuronal migration aberrations, as expression of key radial migration factors such as Diabled1 and p35 remained consistent between KO and control mice. Conditional KO of FOXP1 Nestin-Cre also caused significant structural alterations of the striatum and for mice to exhibit autism-like behaviour, despite the knockout universally affecting all brain regions (Bacon *et al.*, 2015). Moreover, the FOXP1 conditional KO was found to significantly affect dendritic length and dendritic maturation in cortical neurons, also resulting in significantly shorter axonal lengths (Li *et al.*, 2015). A separate investigation of FOXP1 KO *in vitro* showed increased dendritic branching in striatal neurons cultured from E15 brains (Bacon *et al.*, 2015). The suggests that FOXP1 expression is required for normal dendritic formation and dendritic pruning.

KO of FOXP1 has also been shown to reduce excitability in pyramidal neurons of the CA1 hippocampus in early adulthood, without affecting capacitance, input resistance or resting potential (Bacon *et al.*, 2015). These Nestin-Cre KO mice furthermore demonstrated impaired short-term memory, particularly in respect to object recognition, appear hyperactive with increased repetitive behaviours, and increasingly evade social contact. The effect of a striatal-specific FOXP1 KO in the adult mouse has yet to be fully elucidated, however no such observations were made in the mice used within this experiment, although specific behavioural tests assessing these attributes were never fully explored. It would seem, however, that a reduction of FOXP1 in the striatum alone is not sufficient to cause the clear behavioural abnormalities described in full-brain Nestin KO's, suggesting the *in vivo* compensatory measures of the mouse model are sufficient to account for this, or simply that the KO of FOXP1 has just a minor behavioural effect in the neural system, observable only thorough simultaneous KO of several brain regions.

It therefore remains for striatal-specific aimed behavioural tests to be performed in order to assess what may perhaps be a less severe, but present, FOXP1 KO phenotype. This is especially important given FOXP1's (and MEF2C's) well documented loss of function effects in humans, with several behavioural attributes including learning difficulties, repetitive behaviours and decreased social ability present in both animal and human models (Cardoso *et al.*, 2009; Zweier *et al.*, 2010; Zweier and Rauch, 2012; Paciorkowski *et al.*, 2013; Meerschaut *et al.*, 2017).

These studies show that FOXP1 is critical for normal brain development and proper neuronal function in several brain regions, with its mutations now known to be associated with a spectrum of development-associated neurological diseases, the phenotypes of which including speech defects, autism and intellectual disabilities (Horn *et al.*, 2010; Bacon and Rappold, 2012; Le Fevre *et al.*, 2013; Palumbo *et al.*, 2013; Bacon *et al.*, 2015; Lozano *et al.*, 2015; Sollis *et al.*, 2016; Meerschaut *et al.*, 2017). Autism-like behaviour in mice can be induced through cre-mediated FOXP1 deletion through the Nestin-promoter, a significant effect of which is structural alterations of the striatum (Bacon *et al.*, 2015).

Recently, FOXP1 expression was found to be lowered in adult R6/2 Huntington's Disease (HD) mice compared to WT, a trend mirrored in human HD patients (Louis Sam Titus *et al.*, 2017). It is the expression of the mutant htt protein (mut-Htt) that directly results in a decrease of FOXP1 expression (Louis Sam Titus *et al.*, 2017). Although both FOXP1 and mut-Htt are expressed in several brain regions, in HD it is mainly the striatum that is affected by neurodegeneration, along with some cortical neurons, particularly those of layers II, V and VI. Interestingly, reduction of FOXP1 expression does not appear to be universal trait of all neurological diseases (such as PD), nor do all neuronal cell types suffer reduced FOXP1 expression in the presence of the mut-Htt protein, indicating that FOXP1 repression is a cell-specific and disease-specific event (Louis Sam Titus *et al.*, 2017). Furthermore, elevating FOXP1 levels results in an increase in cell survival through mitigation of the mut-Htt neurotoxicity effect, re-enforcing its importance for continued cell survival and its neuroprotective attributes. It is possible that this neuroprotective effect stems from FOXP1's interruption of the cell-cycle, with aberrant cell-cycle activity a classical hallmark and contributing factor of a range of neurological diseases including HD (Becker and Bonni, 2004; Greene *et al.*, 2007; Liu *et al.*, 2015; Louis Sam Titus *et al.*, 2017).

### 1.8.3 **CTIP2**

CTIP2 is a transcription factor involved in a number of neuronal processes including axonal growth, dendrite formation in subcortical neurons (Arlotta *et al.*, 2005) and for the development of MSNs. CTIP2 is first expressed throughout the LGE and MGE and E12.5 in early post-mitotic MSNs and it's expression remains constant through to MSN maturation, with all MSNs believed to express CTIP2 (Arlotta *et al.*, 2008). CTIP2 null mice culled at P0 (null mice die 24 hours after birth) show no differences in terms of MSN birth and migration, but differentiation is impaired as demonstrated through reduction of FOXP1 expression, indicating that CTIP2 is required for normal MSN differentiation (Arlotta *et al.*, 2008). Furthermore, CTIP2 null mice experience a disorganisation of striatal compartments, particularly with striatal patch neurons (Arlotta *et al.*, 2008). Although CTIP2 is expressed in cortical interneurons (Nikouei, Muñoz-Manchado and Hjerling-Leffler, 2016), its expression in the striatum is limited to that of MSNs (Arlotta *et al.*, 2008).

CTIP2, FOXP1 and DARPP-32 are all classified as MSN markers in the striatum, though the exact subset or condition of MSNs within which they express differ. DARPP-32 is thought to be expressed only in mature MSNs as previously described (Walaas and Greengard, 1984; Tamura *et al.*, 2004; Precious *et al.*, 2016) with 100% of DARPP-32 positive cells co-staining with both FOXP1 and CTIP2 (Arlotta *et al.*, 2008; Precious *et al.*, 2016) markers.

FOXP1 and CTIP2 colocalise (Arlotta *et al.*, 2008; Precious *et al.*, 2016) in almost all MSNs in the adult striatum, however ~1% have been found to be CTIP2-positive but FOXP1-negative. This difference could indicate another subset of MSNs is present that expresses CTIP2 without FOXP1 or DARRP-32, although this population is relatively small (Arlotta *et al.*, 2008). Furthermore, only 86% of FOXP1-positive cells are DARPP-32 positive (Precious *et al.*, 2016). These results indicate a number of MSN subsets or MSN states/conditions within which each marker is expressed. Ultimately however, CTIP2 appears to stain the greatest number of MSNs, without staining any other cell type in the striatum, and therefore is likely the best indicator for total MSN count.

### 1.8.4 **NEUN**

The Neuronal nuclei marker (NEUN) is a well-known and widely used marker of post-mitotic neurons that is highly conserved among different species (Mullen, Buck and Smith, 1992; Maxeiner *et al.*, 2014; Wang *et al.*, 2015; Duan *et al.*, 2016). NEUN is a marker for an Rbfox3 epitope, a pre-mRNA alternative splicing regulator (Kim, Adelstein

and Kawamoto, 2009; Dredge and Jensen, 2011). Rbfox3 plays critical roles in neural tissue development and adult brain function. NEUN stains both MSNs and interneurons, although it does not stain glial cells, astrocytes or NPCs. For this reason, NEUN expression is somewhat limited in the developing striatum, particularly at earlier time points, however as post-mitotic neurons develop, NEUN expression increases. In the postnatal/adult striatum NEUN is a consistent and reliable marker of both MSNs and interneurons, whilst not providing positive indications of astrocytes or glial cells.

### 1.8.5 Justification of genetic knockout approach to determine MEF2C striatal function

The purpose of this investigation is to determine the function of MEF2C in the striatum. One way to answer this question is using genetic knockouts in animal models. Knocking out a gene allows for its function to be determined through observation of the differences these mice exhibit compared to unaffected WT littermates. This principle is well established in a range of animal models, including *Drosophila* and mice, with model choice dependent primarily on the reasoning behind the investigation. In this case, MEF2 KO has already been established in *Drosophila* models where somatic, visceral and cardiac muscle phenotypes have been well described, along with loss of function in clock neurons (Blanchard *et al.*, 2010; Soler, Han and Taylor, 2012). The role of MEF2C in neuronal development and maintenance have been less well studied, however as previously described mouse KO models have been produced. In order to study a specific brain region, the animal must of course have the specified region, in this case the striatum, at an appropriate size and level of complexity for differences between WTs and KOs to be observed. Furthermore, mice brains more closely resemble that of humans, allowing for parallels to be drawn between the two systems. This is especially important given the aforementioned severe phenotypic effects of *Mef2c de novo* mutations in humans. Although other animal models, including rat and even chimp, more closely mirror the human brain and so might be better for direct comparisons, considerations such as ethics, breeding time, development time, and cost of animal maintenance result in mouse models as the superior choice. Moreover, no previous investigation has specifically looked for what, if any, role MEF2C has in the developing striatum, so there can be no justification of bringing higher animals such as these into the research at this juncture. These principles are in line with the government's 3Rs programme of Replacement, Reduction and Refinement, with the minimum-tier animal model used that is practically suitable for the investigation.

Following the definition of the animal model to be used, is the method of KO. Mice are well established, understood and historically-used models within which to KO genes; indeed a MEF2C KO was originally achieved in mice many years ago (Lin *et al.*, 1997). Conventional KOs remove the gene in all tissues, which following mating of two mice that are heterozygous for the KO, will produce offspring of which 25% will be homozygous KOs. In the case of *Mef2c* however, this method of gene removal is unsuitable as removal of MEF2C in all tissues in the mouse is embryonically lethal at E9.5, before peak striatal neurogenesis even occurs and is therefore a KO method of very limited use. To circumvent such limitations, conditional genetic KOs can be achieved using systems such as the loxP-Cre system, that allow for the KO to only occur in specified tissue types. This is based on the Cre tyrosine recombinase enzyme isolated from the bacteriophage P1, which catalyses recombination of two small (~34bp) loxP sites that may be deliberately placed either side of a gene or essential exon. Expression of the Cre enzyme alone is not known to cause any noticeable effects in a mouse model, however in the presence of loxP sites recombination excises the DNA sequence located between the two loxP fragments (dependent on the correct orientation of the loxPs), preventing the gene from being transcribed. This principle is well established in mouse KO models as there are no known endogenous loxP sites present in the mouse genome. For the purposes of this investigation, a MEF2C KO model created by (Vong, Ragusa and Schwarz, 2005) was used, where loxP sites flanked exon 2 of the *Mef2c* gene.

The “Cre mouse” is created through attaching the DNA that encodes the Cre enzyme to a specific promoter selected for its temporal and spatial pattern of expression. In the case of this investigation, a “Cre mouse” developed by (Kessaris *et al.*, 2006) was used where the Cre had been attached to the Genetic-Screened Homeobox 2 (Gsx2) promotor. The codon-improved Cre recombinase (iCre) with a nuclear localization signal was fused to the translation initiation codon using a PCR-based approach, followed by an SV40 polyadenylation signal (Kessaris *et al.*, 2006). The Gsx2 promotor was selected for this investigation for a number of reasons: chief of which was that its expression is specific to the striatum, with limited expression in other regions. This allowed for a specific look into the role of MEF2C in the striatum that other promoters such as Nestin and Glial fibrillary acidic protein (GFAP), as used in previous investigations, could not achieve (Barbosa *et al.*, 2008; Hao Li, Radford, Ragusa, Shea, McKercher, Zaremba, Soussou, Nie, Kang and Nakanishi, 2008). This is critical for the purposes of an investigation into the function of MEF2C in the striatum given its already documented involvement in other neighbouring brain regions such as the cortex and hippocampus (Barbosa *et al.*, 2008; Hao Li, Radford, Ragusa, Shea, McKercher, Zaremba, Soussou,

Nie, Kang and Nakanishi, 2008), as KO in these regions could directly influence any phenotypes observed within the striatum or in overall animal behaviour. Furthermore, the temporal expression of GSX2 aligns with that of striatal development, with expression already present at or before E12.5, continuing throughout development and adulthood. This allows for the Cre to be expressed and recombination to subsequently occur in the striatum as soon as it begins to develop and through the key stages of embryonic development (E12.5-E18).

### 1.8.6 **Gsx2-cre expression**

Gsx2-cre expression is first observed at E12.5 in the developing mouse MGE and LGE (Kessaris *et al.*, 2006), with expression persisting throughout the developing telencephalon at E15.5 (Costa *et al.*, 2007). Gsx2-cre expression in the MGE and LGE is shown in Figure 1.12 below:

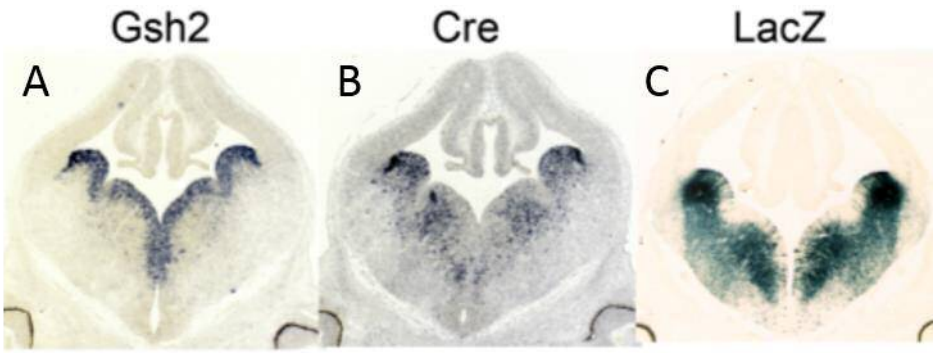


Figure 1.12: Developing telencephalon Gsx2-Cre expression at E12.5. (A) In situ hybridization for endogenous GSX2 (B) Gsx2-Cre in E12.5 Gsh2-Cre mice and (C) b-galactosidase enzymatic labelling in Gsx2-Cre/ Rosa26R-lacZ embryos. Adapted from (Kessaris *et al.*, 2006)

Gsx2-cre expression was further noted at the Pallial–Subpallial Boundary (PSB) between E11.5-E15.5 and throughout the telencephalon at E15.5 (Costa *et al.*, 2007). Expression was also noted in the septum. Although Gsx2-cre lineage expression analysis revealed some expression in the cortex at P0, this is much lower than the WGE (Kessaris *et al.*, 2006). In conclusion, the Gsx2-cre allows for loxP-cre mediated recombinase to occur almost entirely within the developing striatum. Beyond P0, expression of Gsx2-cre is not well documented, although this issue is addressed within this thesis.

## 1.9 Aims of thesis

From the literature outlined in this chapter, it is clear the *Mef2c* transcription factor plays a substantial role in the development of cortical, hippocampal and cultured neural cells. The finding that that *Mef2c* mRNA is significantly up-regulated during the period of peak striatal neurogenesis is novel and led to the experiments in this thesis. The starting point was to establish whether this increase in *Mef2c* mRNA expression is indicative of it having a functional role in striatal development, in particular the MSN content of the striatum. This was done primarily through assessing adult striatal integrity at three months in animals with KO of MEF2C (the principle knockout used in this work was a conditional knockout of MEF2C via the Gsx2 promotor for a loxP-Cre mediated MEF2C KO). Secondly, I sought to understand more about the role of MEF2C in this system by extending these studies to the developing and aged striatum. Specifically, whether MEF2C is involved in early striatal development and whether its absence results in a degenerative phenotype, which might be expected to result in progressive striatal loss after three months. Finally, I used cultured cells in which MEF2C was knocked out to explore some the underlying cellular mechanisms.

## 1.10 Main objectives:

- To establish whether conditional KO of MEF2C via the Gsx2-cre loxP system yields any phenotypic effects in the adult mouse striatum.

- To quantify any effect on the striatum and striatal cell formation at a given time point, and to create a timeline of analyses through which MEF2C function may be tracked in the developing and aged brain.

- To establish cultures of embryonic striatal cells from MEF2C KO mice as a model for addressing the mechanisms whereby MEF2C influences striatal development.

# Chapter 2: Methods

## 2.1 Generation of transgenic mice

All animal experiments were performed in agreement with local ethical guidelines and accepted animal care according to the UK Animals (Scientific Procedures) Act 1986 and its amendments. The mice used in this investigation were of the genetic background C57 BL6 and contain no known allele variants effectual to striatal development.

When increased numbers of each transgenic line were required breeding pairs were set up in the evening and left overnight. For the purposes of experiments requiring embryonic pups the presence of a vaginal plug was recorded as E0.5, with pregnant females sacrificed at the required age and pups extracted from the uterine horn. Tissue harvested from embryos were then immediately plated down for further cell culture use.

Four transgenic lines have been used in this work. The first is the "Null" line with *Mef2c*$^{WT/Tm1}$ mice, with MEF2C knocked-out in a single allele in all tissues, with Tm1 (targeted-mutation 1) the abbreviation originally used to describe the null allele when creating the line (Lin *et al.*, 1998). The second a "conditional" line where MEF2C is knocked-out exclusively in the striatum using a loxP-Cre recombinase system and referred to hereafter as the Striatal MEF2C KO with genotype *Mef2c*$^{loxP/loxP}$ in the presence of the Gsx2-Cre. The third "LoxP-Null" line was generated to produce mice with one null allele and one loxP allele, referred to as *Mef2c*$^{Tm1/loxP}$ in the presence of the Gsx2-Cre. Finally, a 4$^{th}$ transgenic mouse was created through breeding males containing a Gsx2-Cre mediated excised *Mef2c* allele in the testis with *Mef2c*$^{loxP/loxP}$ females to produce *Mef2c*$^{loxP/Tm2}$ offspring, with "Tm2" referring to the new KO variants created through this cross (see below).

### 2.1.1 The "Null" line

This line was a gift from Brian Black, based at the Cardiovascular Research Institute, University of California, San Francisco, USA. It was generated through the deletion of the second protein-coding exon encoding amino acids 18-86, encompassing part of the MADS domain and the entirety of the MEF2 domain, thereby effectively inactivating the gene (Lin *et al.*, 1997). A breeding programme was established from a few *Mef2c*$^{WT/Tm1}$ mice. In this way, although 25% of the litter are of the *Mef2c*$^{Tm1/Tm1}$ genotype and die at

E9, 50% are *Mef2c*$^{WT/Tm1}$. This produced sufficient numbers to ensure the survivability of the line and for selected behavioural/histological analyses.

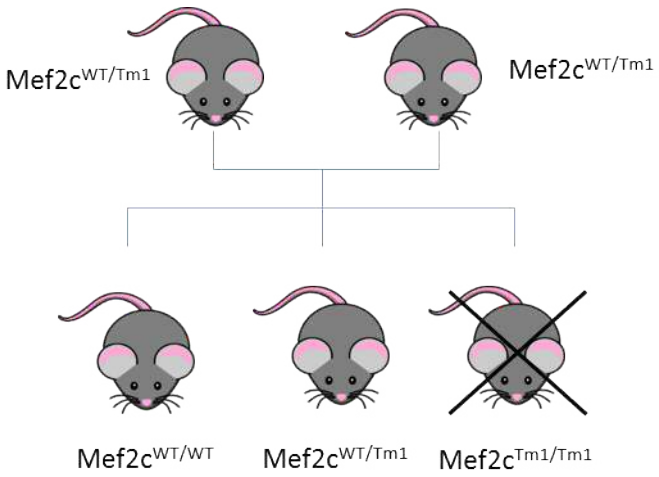


Figure 2.01: The breeding programme for increasing numbers of the Null Line. Mice of the *Mef2c*$^{Tm1/Tm1}$ genotype die at E9.

*Mef2c*$^{Tm1/Tm1}$ mice have loss of MEF2C in all body tissues and die by E9 due to under development of the heart along with a range of vascular defects (Lin, Schwarz et al. 1997, Lin, Lu et al. 1998). This lethality occurs before striatal development; thus, the embryo is of limited use for this work. *Mef2c*$^{WT/Tm1}$ animals however are viable and survive to adulthood.

### 2.1.2 **The "Conditional" KO**

Gsx2-cre mice were originally generated by (Kessaris *et al.*, 2006) and the *Mef2c*$^{loxP/loxP}$ mice were a gift from Eric Olson's lab, based at the South Western medical centre at the University of Texas. The Cre line was generated though the creation of a P1 artificial chromosome containing a codon-improved Cre recombinase with a nuclear signal fused to the initiation codon, with expression recapitulating endogenous expression in the WGE (Kessaris *et al.*, 2006). These two lines were then bred to produce a conditional knockout of striatal MEF2C, with expression of the Cre through the Gsx2 promoter in a mouse containing loxP sites flanking the *Mef2c* gene resulting in the conditional KO of the MEF2C protein (Figures 2.02 and 2.03). In the text this is referred to as "Conditional MEF2C KO". Gsx-2 is expressed in the striatum during striatal neurogenesis from E12.5 (Corbin *et al.*, 2000; Toresson, Potter and Campbell, 2000; Stenman, Toresson and

Campbell, 2003; Kessaris *et al.*, 2006; Cocas *et al.*, 2011) thereby facilitating a KO of MEF2C in the striatum without affecting cardiac tissue, angiogenesis or other tissues. This allowed viable mice to be produced and survive through adulthood with no discernible health differences compared to WT littermates, including no difficulties in breeding, though this was established only through experience of day-to-day handling without any specific behavioural analysis.

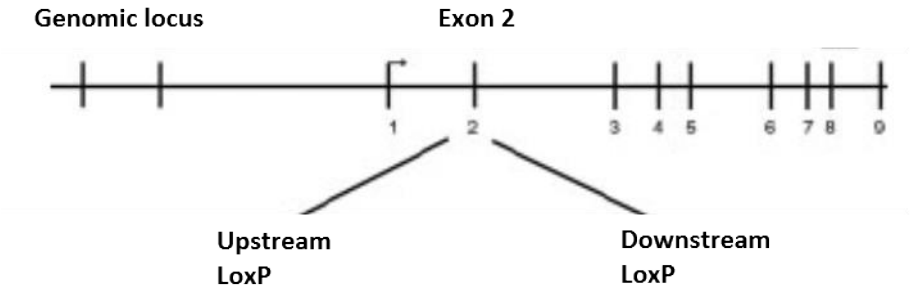


Figure 2.02: Schematic of targeting strategy for MEF2C KO via the loxP-cre system achieved through knocking out exon 2. The first loxP sequence was inserted immediately 3' and the second loxP sequence inserted 150bp 5' of the second coding exon of *Mef2c*, allowing for removal through tissue-specific Gsx2-cre expression. Vertical black bars refer to exons. Adapted from (Vong, Ragusa and Schwarz, 2005).

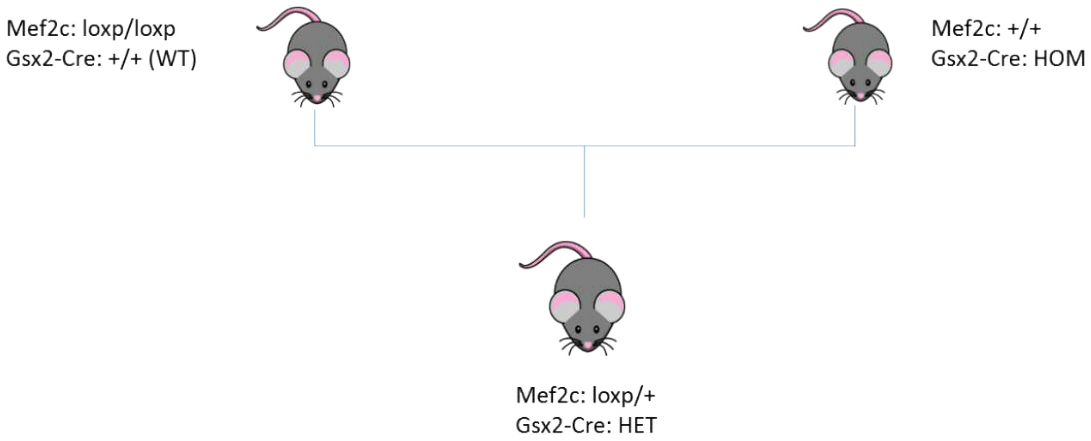


Figure 2.03: Breeding diagram showing the original generation of the *Mef2c*$^{loxP/+}$ KO line through pairing of *Mef2c*$^{loxP/loxP}$ mice with Gsx2-cre mice.

Mice created form this cross were then bred with *Mef2c*$^{loxP/+}$ mice without the Gsx2-Cre, allowing for offspring containing 2 floxed *Mef2c* alleles expressing the Gsx2-cre to be

generated as shown in Figure 2.04 below.

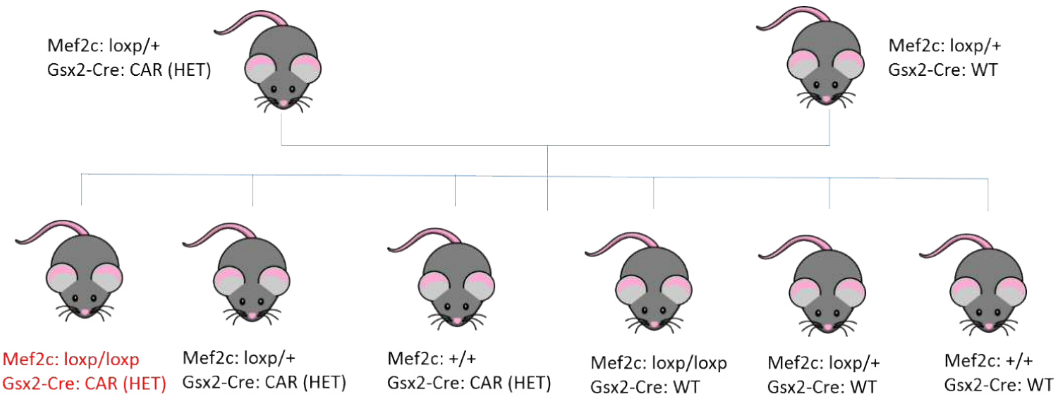


Figure 2.04: Illustration of the breeding programme used to generate *Mef2c*$^{loxP/loxP}$ mice and maintain the conditional KO line. Though zygosity was not determined "CAR" indicates the mouse is a carrier of the Gsx2-cre, the presence of which was determined through genotypic assessment described below. Highlighted in red is the target genotype of the striatal *Mef2c*$^{loxP/loxP}$ KO mouse.

### 2.1.3 **Tm2 KO mouse generation**

Whilst not known at the time of breeding, Gsx2-cre expression was later found to be present within the testis of male mice. When bred, mice expressing the Gsx2-cre had the potential to pass on a *Mef2c* allele that had already undergone loxP-Gsx2-Cre based recombination in the germ line, resulting in the passing of what is an effectively null allele, present in all tissues of the offspring. This allele is referred to as "Tm2" throughout the remainder of this thesis. Mice bred in such a manner produced KO variants as illustrated in Figure 2.05 below:

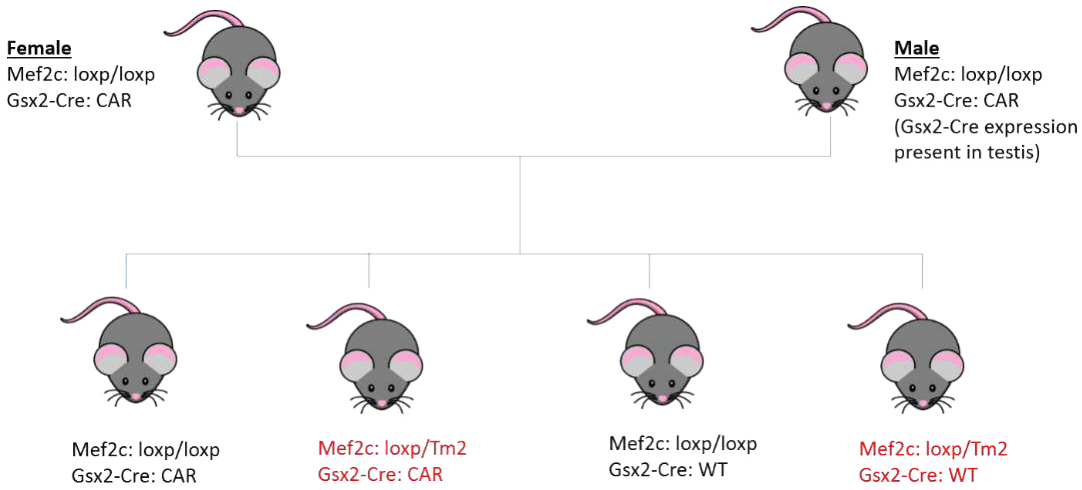


Figure 2.05: Breeding programme and subsequent offspring produced carrying a single copy of the recombined *Mef2c* allele (Tm2). In this strategy, CAR refers to a carrier of the Gsx2-cre, though at least one of the parents must be Heterozygous for offspring to be produced without the Gsx2-cre, which was ensured by using Gsx2-Cre positive breeders originating from breeding pairs where only one parent possessed the Gsx2-Cre.

The *Mef2c* KO variant produced through the passing of a recombined floxed *Mef2c* allele in the parent testis is referred to as TM2. Though ultimately similar in function as TM1 in that the *Mef2c* allele is inactive in all tissues from conception, it remains a distinctive KO variant and must initially be considered individually. As illustrated in Figure 2.05 above, mice of the $Mef2c^{Tm1/Tm1}$, $Mef2c^{Tm2/Tm2}$ and $Mef2c^{Tm1/Tm2}$ genotypes were not found, demonstrating the embryonic lethality brought about through a double-allele KO of *Mef2c*.

### 2.1.4 **The LoxP-Null Line:**

A third mouse line was generated through the breeding of the Null line with the conditional KO line in order to generate mice with one null and one conditional KO gene ($Mef2c^{Tm1/loxP}$) (Figure 2.06). This is valuable because the efficiency of the loxP-Cre recombination is not known. By comparing this with the $Mef2c^{loxP/loxP}$ mouse, one can get an indication of whether the conditional allele in the striatum gives a comparable striatal phenotype to the null allele. If this is not the case, then having one allele fully knocked-out can increase the knock-out effect in the target tissue.

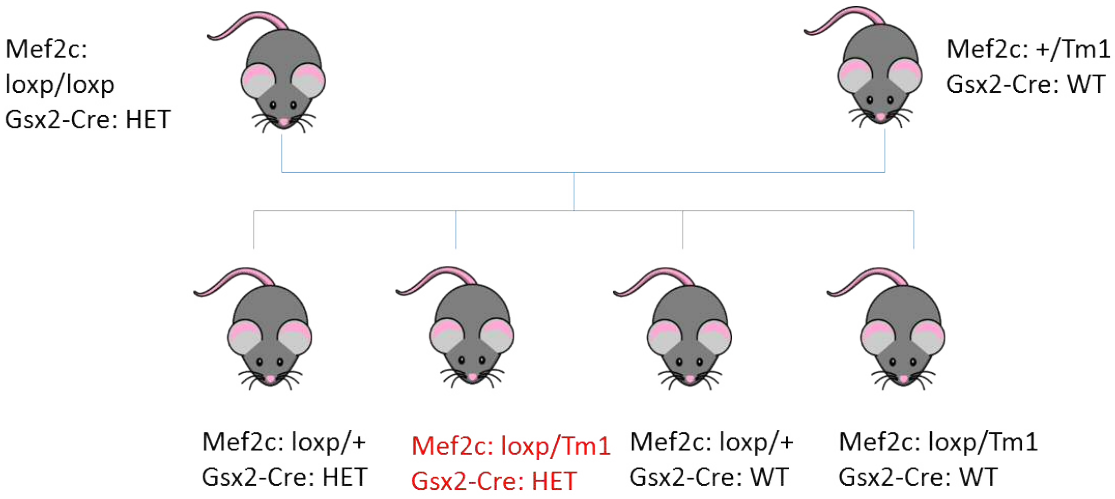


Figure 2.06: Illustration of the first breeding strategy used to generate the "Floxed-Null" line. Highlighted in red is the target genotype of the "KO mouse". As with the previous breeding strategy outline in Figure 2.05, heterozygosity of the Gsx2-Cre parent was ensured through only selecting mice that came from breeding pairs where only one parent was positive for Gsx2-Cre.

In order to increase the number of mice in this third line, a second breeding strategy was adopted where the conditional KO line was bred with the floxed-null line (Figure 2.07).

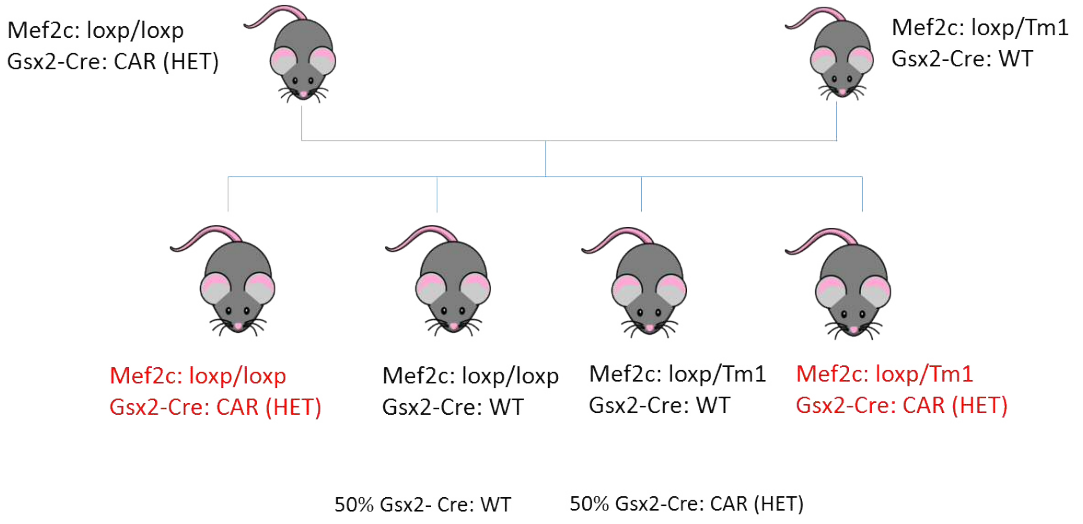


Figure 2.07: Illustration of the second breeding strategy used to generate the "Floxed-Null" line. Red text indicates the two different "KO" variant mice.

### 2.1.5 **ROSA-Lacz reporter line generation**

B6(Cg)-Snca$^{Tm1.1Vlb}$/J ROSA-LacZ reporter mice were donated by Professor Vladimir Buchman with Jackson Laboratory reference #020636 were crossbred with *Mef2c*$^{loxP/loxP}$

mice heterozygous for the Gsx2-Cre. This cross was made to produce a reporter line in which expression of the Gsx2-Cre could be traced through LacZ, which is detectable following X-gal staining. The presence of a single floxed *Mef2c* allele was not an important factor in the development of this reporter line as its intent was to determine which regions of the brain expressed Gsx2-Cre, eliminating any issue that may arise through a minor (if any) cell number loss that may arise following Cre-mediated recombination of the single floxed allele.

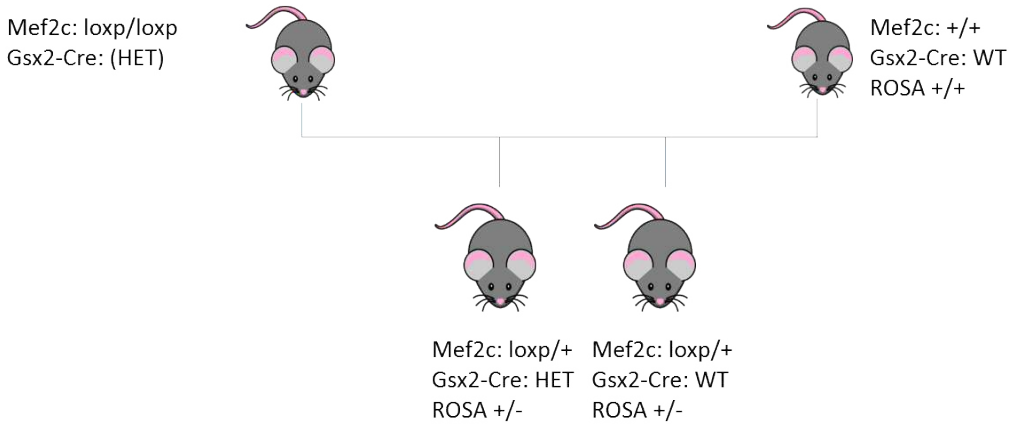


Figure 2.08: Generation of the Lacz-ROSA reporter line. Mice were bred and allowed to age to either P7 or 3-months before being culled as previously described, depending on experimental aim. Brains were then stained with X-gal solution with blue precipitate forming on areas of lacZ expression.

A full list of the *Mef2c* genotypes used in this investigation and their annotations can be seen in Table 2.01 below:

| Term used in text | Genotype |
|---|---|
| WT | *Mef2c*$^{loxP/loxP}$ without Gsx2-Cre |
| Single “null” allele (HET) | *Mef2c*$^{WT/Tm1}$ without Gsx2-Cre |
| “floxed-Null” KO | *Mef2c*$^{loxP/Tm1}$ with Gsx2-Cre |
| “Tm2” KO | *Mef2c*$^{loxP/Tm2}$ with Gsx2-Cre |
| Striatal MEF2C KO | *Mef2c*$^{loxP/loxP}$ with Gsx2-Cre |
| Lacz-ROSA Reporter | *Mef2c*$^{WT/loxP}$ with Gsx2-Cre with ROSA$^{+/-}$ |

Table 2.01: Table summarising the various *Mef2c* genetic loci used in this investigation along with the terms used to describe each variation in the text. Please note that as shown below, *Mef2c*$^{loxP/loxP}$ without Gsx2-Cre are suitable for use as WT controls.

## 2.2 Genotyping

Upon weaning, all animals were tail tipped for genotyping purposes. Ethyl chloride anaesthetic spray (Vidant Pharma Ltd, Surrey, U.K.) was applied to the tip of the tail before removing an approximately 1mm section. The tail was then cauterised with a silver nitrate pen and samples were collected in Eppendorf tubes. Mouse samples were initially shipped on dry ice to Laragen Inc. (Culver City, California, U.S.A), the PCR primers used for each line were identical to those used when each line was initially generated (Lin *et al.*, 1997; Black and Olson, 1998) and were also used after generation of the third line (see Figure 2.07). The genotyping provider was substituted to Transnetyx (Cordova, Tennessee, U.S.A) where a standardised assay was created for each gene of interest (available upon request at Transnetyx), also based on the original primers used in the generation of each line. For identification of alleles that had already undergone loxP-Cre recombinase excision as a result of Gsx2-cre testis expression in the parent mouse, a custom assay was created (also available upon request at Transnetyx).

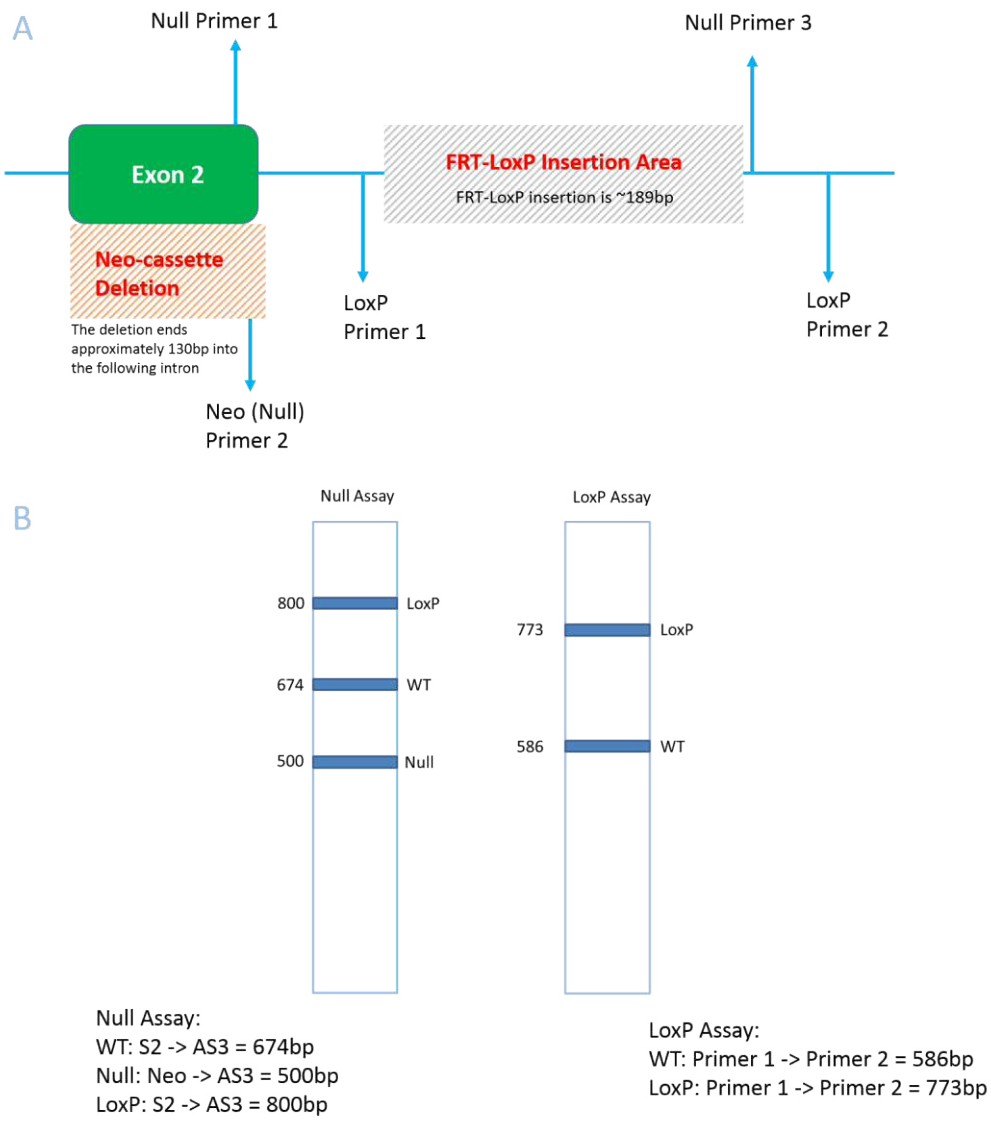


Figure 2.09 Genotyping of the *Mef2c* locus. A) Genotype determination of the Null line used three null primers, with null primers 1 and 2 detecting the presence of a WT allele, and null primers 2 and 3 the null allele. LoxP primers 1 and 2 detect the presence or absence of the second flanking FRT-LoxP insertion. (B) Null and loxP assays are run separately with resulting PCR band lengths shown.

Exon 2 refers to Exon 2 of the *Mef2c* gene that is removed in both the Tm1 and conditional MEF2C striatal KO variants as previously described. The diagram (Figure 2.09) illustrates the position of the Neo-cassette area that results from Tm1 KO, showing that forward Null primer 2 binds to this Neo-cassette with the reverse Null primer 3 placed at the end of the target sequence. Should the allele not contain the neo cassette, Null primer 1 will be able to bind to Exon 2, again using null primer 3 as the end point of the sequence to be amplified by PCR. The downstream FRT-loxP insertion site is flanked by the upstream loxP primer 1, and downstream primer 2, allowing for presence of this area to be determined based on the resulting band-length of 773bp. Furthermore, should an

allele contain the FRT-LoxP insertion site, it is detectable in the “null” assay through a band created between Null primer 1 and Null primer 3, at a longer band-length of 800bp.

| Allele | Supplier | Forward primer | Reverse primer |
|---|---|---|---|
| LoxP | Laragen | TCCCAAGAAAGGACAGGAAATG | CTAGAAATCAAGGTCCAGGGTCA |
| Null | Laragen | GACCGCTATCAGGACATAGCGT | CCTTTATCCATCTGACTTCACGTGT |
| WT | Laragen | CCAGCACTGACATGGATAAGGTGT | CCTTTATCCATCTGACTTCACGTGT |
| LoxP | Transnetyx | Available on request at Transnetyx | Available on request at Transnetyx |
| Null | Transnetyx | Available on request at Transnetyx | Available on request at Transnetyx |
| WT | Transnetyx | Available on request at Transnetyx | Available on request at Transnetyx |
| Excised LoxP | Transnetyx | Available on request at Transnetyx | Available on request at Transnetyx |

Table 2.02: List of primers used for genotype identification in throughout this investigation. At the request of Transnetyx, primer sequences used by this company are not published.

### 2.2.1 **Perfusion**

Mice were terminally anaesthetised by intraperitoneal (i.p.) administration of 0.3ml of 0.2 mg/ml sodium pentobarbital (Euthatal) and thereafter perfused initially with a prewash solution (Phosphate-buffered saline (PBS), pH 7.3) for 1 minute followed by 4% PFA solution at pH7.3 for 6 minutes. The brains were then removed and post-fixed in 4% PFA for 4 hours before being transferred to 25% sucrose (Sigma) in PBS solution O/N at room temperature.

## 2.3 Histology

Brains were weighed and a single sided razor blade (40mm) used to remove the cerebellum. The brains were then weighed again and frozen with distilled water onto a freezing platform of a sliding sledge freezing microtome (Leitz, Wetzlar). Once frozen,

brains were cut coronally into a 1 in 12 series of 40µm sections and collected into 48 well plates (Thermo, Fisher Scientific) containing an anti-freeze solution of di-sodium hydrogen orthophosphate and stored at -20°C. For staining purposes, a 1:12 series of sections was then selected from a single well and placed into an immuno-pot for free-floating section staining.

At each stage of the immunohistochemistry procedure 1ml of fluid was used for each pot both to completely immerse the tissue to ensure complete uptake of the antibodies and to ensure adequate washing volume, whilst minimising waste. Sections were washed in tris-buffered saline (TBS) (0.05M Tris-HCL, 0.15M NaCl, pH7.4) to remove residual antifreeze with endogenous peroxidase activity quenched for 5 minutes using 10% $H_2O_2$ (VWR, West Sussex, UK) and 10% methanol (Sigma-Aldrich, Dorset, UK) in distilled water, followed by 3x TBS washes. Sections were blocked in 3% normal serum in Triton-X tris-buffered saline (TXTBS) for 1 hour to block non-specific binding sites. Sections were incubated in a solution of TXTBS, 1% serum and primary antibody, overnight at room temperature. The primary antibody information and their working concentrations can be found in Table 2.03 below.

| Primary Antibody | Species raised | Supplier | Normal Serum | Dilution | Secondary Antibody (DAB) | Secondary Antibody (Fluorescent) | Dilution |
|---|---|---|---|---|---|---|---|
| DARRP-32 | Mouse | Santa-Cruz | Horse | 1:200 | Horse Anti-Mouse | Goat Anti-Mouse | 1:200 |
| FOXP1 | Rabbit | Abcam | Goat | 1:200 | Goat Anti-Rabbit | Goat Anti-Rabbit | 1:200 |
| CTIP2 | Rat | Abcam | Goat | 1:500 | Goat Anti-Rabbit | Goat Anti-Rat | 1:200 |
| NUEN | Mouse | Abcam | Horse | 1:2000 | Horse Anti-Mouse | Goat Anti-Mouse | 1:200 |
| MEF2C | Rabbit | Protein-Tech | Goat | 1:500 | Goat Anti-Rabbit | Goat Anti-Rabbit | 1:200 |
| KI67 | Mouse | Abcam | Goat | 1:200 | n/a | Goat Anti-Mouse | 1:200 |
| CASPASE-3 | Rabbit | Abcam | Goat | 1:400 | n/a | Goat Anti-Rabbit | 1:200 |
| BrdU | Rat | Abcam | Goat | 1:500 | Goat Anti-Rat | n/a | 1:200 |

Table 2.03: Primary and Secondary antibodies used for Immunohistochemistry or immunocytochemistry in mouse brains. All secondary DAB antibodies used in this experiment were manufactured by Vector and all fluorescent secondary antibodies were manufactured by Invitrogen.

Following overnight incubation in a primary antibody solution, sections underwent 3x TBS wash before incubation in an appropriate biotinylated secondary antibody solution at a concentration of 1:200 for 2 hours at room temperature. Sections were then washed

in TBS and ABC kit (Vector Laboratories Ltd, Peterborough, Cambridgeshire) added, using a 1:200 dilution in TBS of both solutions A and B for 2 hours. The secondary antibodies used are listed in Table 2.03 above.

Sections were then washed in TRIS non-saline (TNS) comprised of 6g Trizma base (Sigma) in 1L of water, before addition of the chromogen 3-3'-diaminobenzadine (DAB) supplied from DAKO. DAB was allowed to defrost at room temperature in the absence of light with the 2ml vial (0.66mg/ml) then added to 40ml of fresh TNS in the presence of 12µl of $H_2O_2$. This solution was then further diluted to a 1:5 concentration in fresh TNS and 1ml added to the tissue. The reaction was allowed to develop until the stain could be clearly seen under a light microscope, with time kept consistent for each primary antibody. Sections were washed in TBS to stop the reaction before being mounted on to double-subbed 1% gelatinised slides (Thermo Scientific, Menzel Gläser). Slides were allowed either to air dry O/N or through incubation at 37°C for 2 hours before dehydration in an industrial methylated spirit (IMS) alcohol ladder of increasing concentrations (70%, 95% and 100%). Samples were then cleared in 100% xylene and cover slipped using distyrene plasticizer and xylene (DPX) (Thermo Scientific, Raymond Lamb, Leicestershire, UK) mountant and allowed to dry O/N in a fume hood.

### 2.3.1 **X-gal staining protocol**

Adult and P7 brain slices prepared as previously described (prior to immunohistochemistry) were washed (3x10 minute with 1ml PBS) in an 30ml immuno-pot. Following the final wash, 100µl of 20mg/ml X-gal in DMF stock solution was added to 900µl of "X-gal buffer solution" from a stock solution comprised of:

4ml PBS
0.5ml 50nM $K_4ClFe(CN)_6$
0.5ml 50nM $K_3ClFe(CN)_6$

Tissue was then incubated for 24 hours at 30°C before it was removed, washed 3x 5 mins in PBS then dried and mounted as previously described.

### 2.3.2 **Cresyl violet**

Cresyl violet (CV) staining was used to gain an overall visualisation of cellular morphology by staining for Nissl substance in the cytoplasm of neurons and glia. It was

also used as a means to define striatal, cortical and corpus-collosum structures. A 1 in 12 series of sections was selected from the 48 well plate and mounted onto glass slides double subbed with 1% gelatine and allowed to air dry. Once dry, slides were placed for 5 minutes in each of the following solutions: 70% IMS, 95% IMS, 100% IMS, 50/50 chloroform alcohol, 95% IMS, 70% IMS, distilled water, Cresyl violet solution and distilled water. Sections were then dehydrated in 70% and 95% IMS for 5 minutes each, then agitated gently in acid alcohol solution for up to 5 minutes until an appropriate level of staining was obtained. Additional dehydration in 100% IMS was performed, before clearing in xylene and cover slipping using DPX mountant.

### 2.3.3 **Stereological Analysis**

Throughout this investigation, all assays and gathering of data was conducted in a blind fashion, with no matching of genotype to sample made until all raw data had been entered for that particular assay.

Stereological quantification was conducted using Visiopharm Integrator System (VIS, version 4.4.6.9) software on an Olympus Canada Inc. Q-Imaging Microscope. For each slide striatal sections were initially photographed using a 1.25X objective lens under a Leica DFC420 Camera using the Leica Application Core V3.6 software. Defined striatal sections were then randomly sampled from a gird via the software under a consistent step length, with cells counted manually with oil and optical condenser used under the 40X objective lens to improve resolution. A 500$\mu m^2$ counting frame size was used with cells either within the frame or touching the green lines included in the count and cells that touched either of the red lines excluded as shown in Figure 2.10 below:

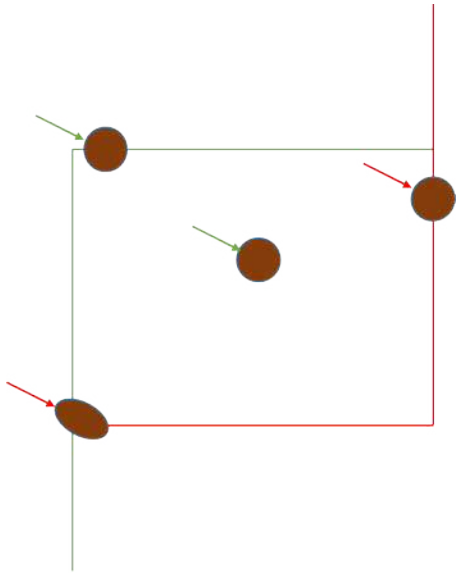

Figure 2.10: Illustration of which cells (brown ellipses) within a counting frame are accepted and which are rejected. Red arrows indicate those rejected; green arrows indicate those accepted.

Six striatal sections per mouse brain were counted in order to minimise the effect any potential inconsistencies that may arise in histological staining due to variable tissue exposure to any reagent at any given part of the protocol that could cause any single section to be less-well stained. These six striatal regions were selected by their morphology so that they were taken after the appearance of the lateral ventricle, and before the appearance of the pyramidal.

The number of animals used in each stereological analysis differed depending on the experiment, the precise number will be provided in each experimental chapter. The total number of cells (C) in each striatal section was calculated using the following formula:

$$C = \Sigma c \times (\Sigma A \times (\Sigma n \times a)) \times f$$

Where:

C = estimated total number of cells

Σc = total number of cells counted

ΣA = sum of all striatal areas

Σn = total number of frames allocated to the included striatal area

a = area of sampling user grid (500μm$^2$)

f = frequency of sectioning

x= multiplication

An Abercrombie correction (AC) factor was then applied to the total number of calculated cells using the following formula (Abercrombie 1946):

aC = C x (ST /(ST+D)
Where:
aC = Abercrombie corrected cell count
C = estimated total number of cells
ST = section thickness
D = cell diameter.

This value is referred to as total cell count per unit of striatum.

Representative images of the stained sections were acquired using a Leica Microsystems Ltd microscope (Heerbrugg, Switzerland, Model CH-9435) and Leica Application Suite (LAS, version 3.8) software.

### 2.3.4 **Striatal volume and cell density calculation**

Striatal volume was calculated through the following equation:

$V = (\Sigma A \times ST \times 12)/1000000000$.

In order to determine cells/mm$^3$, the Abercrombie correction value was divided by the volume (V) as shown:

Cells/mm$^3$ = Ac/V

In order to keep count and volume calculations consistent across mouse samples, clearly defined striatal structural start and end points were defined. Coronally sliced mouse striatum between approximately the following locations were used:

Bregma 1.54mm : Interaural 5.34mm
to
Bregma -0.1mm : Interaural 3.7mm

This area encompasses the vast majority of the striatum and for the purposes of this paper is used to relate the total striatum.

### 2.3.5 Defined striatal limits of P7 mice

Only certain regions of the striatum were included for counting in order to maximise consistency and reliability of results. This was kept to the same principles in terms of structural start and end points, though due to the changing size of the striatum and the brain as a whole, it is difficult to quantify Bregma/Interaural values. As a point of reference however the Allen brain atlas provides a series of images of the P7 coronally sliced brain, found at the following link: http://developingmouse.brain-map.org. Using this resource, images 139-202 encompass the region observed in this chapter, deemed to be the vast majority of the striatum whilst allowing for consistent and accurate data collection.

### 2.3.6 Statistical analysis

SPSS was the principal statistical software package used in analysis of all histological data. For all experiments, where applicable, analysis of variance (ANOVA) were used in alongside Bonferroni post-hoc analysis when applicable. Furthermore, where stated, two-Way ANOVAs and MANOVAs were used also with Bonferroni post-hoc analysis. These statistical approaches were selected for maximum statistical power and suitability in the specific cases of the data gathered in this investigation and in alignment with similar investigations. T-Tests were also utilised only when ANOVAs or other statistical analysis methods were not possible.

## 2.4 BrdU analysis

### 2.4.1 Uptake and Staining

50mg/kg of 5-bromo-2′-deoxyuridine (BrdU) (Sigma Aldrich) was injected into the striatum of postnatal litters containing MEF2C conditional KO and WT littermates bred with the breeding strategy described in Figure 2.04 above, with a 30G needle 3 days prior to the date of culling. Following this, pups were culled visa cervical dislocation and post fixed for 24 hours in 4% PFA and coronally sliced as previously described in section 1.3. Sections were treated with 2M HCL for 30 minutes at 37 degrees before being histologically stained with an anti-BrdU antibody (see Table 2.03) and each cell manually counted. As cells originating from the SVZ migrate to brain regions other than the striatum, only cells that had proliferated and/or migrated into the striatum itself were counted.

## 2.5 Behavioural analysis

### 2.5.1 Activity Box

Clear plastic activity boxes were fitted with a water bottle and an adequate amount of powdered food for a 32-hour period. Mice were placed singularly into each box and placed immediately in the holding rack. Each mouse number was assigned to a corresponding box and analysis begun immediately. Four infra-red beams permeated each box with the number of non-perseverative breaks recorded for intervals of an hour over a 32-hour period. For the first 3 hours mice were allowed to acclimatise to their surroundings before they entered the dark phase which was timed according to their normal light and dark phase cycle. Mice were then removed and placed back into their cages after this time, with data collected between 15:00-15:00$^{+1}$ used for analysis.

## 2.6 Golgi-Cox

The Golgi-Cox method is a variation of the original Golgi recipe in which silver nitrate is replaced with mercury chloride to foster the impregnation of neurons (Van Der Loos, 1956; Glaser and Van der Loos, 1981; Levine *et al.*, 2013). This method impregnates neurons in thin brain tissue sections (80μm) while minimizing any crystallization artefact (Levine *et al.*, 2013). Once a neuron has been impregnated with the crystal present in the silver chromate, every dendrite is fully labelled. It should be noted it is not yet fully understood by what principles which neurons are ultimately affected by the Golgi-Cox and which are not.

### 2.6.1 Preparation:

Solutions for the Golgi-Cox analysis are made as follows:

Solution A: 5% Potassium Dichromate solution

- 5g potassium dichromate solution stirred into 100ml $dH_2O$ heated to 45°C

Solution B: 5% Mercuric Chloride solution

- 5g Mercuric Chloride solution stirred into 100ml $dH_2O$ heated to 75°C

Solution C: 5% Potassium Chromate solution

- 5g potassium chromate solution stirred into cold water.

Once all solutions have been made, 100ml of solution A is added to 100ml of solution B and 80ml of solution C is added to 200ml $dH_2O$. The A/B solution is slowly poured into diluted solution C whilst being constantly stirred until dissolved. Solution is then kept in the dark for 3 days and filtered before use with filter paper. At no point are metallic instruments used during this process.

### 2.6.2 **Mouse brain preparation**

Animals are perfused in 4% PFA as outlined above but after 4 hours and placed in the Golgi-Cox solution. Solution was replaced every 3 days for a total of 14 days. Brains were then removed with blotting paper used to absorb excess fluid, then placed in 25% sucrose solution overnight. Brains were then cut at 80µm and stored in anti-freeze at 4°C. The tissue was then mounted onto slides and allowed to dry for 24 hours, before receiving 2x $dH_2O$ and incubated in 20% ammonium solution for 10mins. The tissue then received a further 2x $dH_2O$ wash before being dehydrated and cover-slipped with DPX as previously described.

### 2.6.3 **Dendrite and spine analysis**

Samples were visualised under Visiopharm Integrator System (VIS, version 4.4.6.9) software on an Olympus Canada Inc. Q-Imaging Microscope and region of interests (ROI's) identified based on presence of striatum. Software-generated randomly allocated frames were set along each ROI viewed at x400 magnification, with the first spiny neurons containing "suitable dendrites" isolated and analysed. "Suitable Dendrites" in this case refers to clear separation of axonal cell body from others, dendrites to be for the most part un-broken so as to ensure Golgi-Cox staining of the dendrite was not interrupted, and that not too many axons and their dendrites overlapped so as to make distinguishing between them impossible. No special allocation was given for any other variable and all samples were counted blind from genotype. Following axon selection, the following parameters were recorded:

- Cell body diameter (average taken from width and height measurements)
- Number of Dendrites

- Dendritic length
- Number of Spines on each dendrite
- Spine density (Number of spines / dendrite length)
- Spines per Neuron

Spinal measurements and analysis of type/maturity was begun but not completed on sufficient numbers of samples due to time constraints.

## 2.7 E18 Mouse WGE cell culture

### 2.7.1 Collecting embryos and plating cells

Mouse embryos were collected at E18 and placed in Dulbecco's Modified Eagle Medium F-12 Nutrient Mixture (Ham) (DMEM/F12) (Gibco, Life Technologies), with the brains removed and whole ganglionic eminence (WGE) dissected out as shown in Figure 2.11. Dissections were performed under a dissecting microscope in a laminar flow hood.

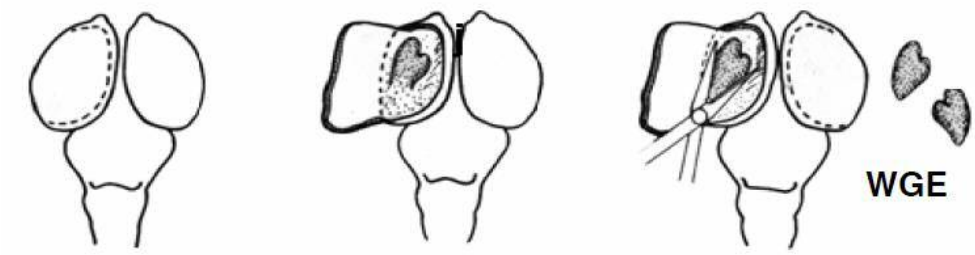


Figure 2.11 Dissection of striatal eminences. Once the brain has been removed, a longitudinal cut is made close to the midline of the cortex, which was then opened to reveal the striatal primordium. The WGE was then cut out with care taken not to include cortical tissues and placed in Hanks Balanced Salt Solution (HBSS) (Gibco). Figure adapted from Dunnett and Bjorklund 1992.

Once dissected the tissue was washed in DMEM/F12 before being transferred to a solution of 50µl TrypLE Express (Gibco, Life Technologies) and 2µl dornase alpha, before incubation for 10 minutes at 37°C. 1ml of DMEM/F12 was then added to the tissue and the solution centrifuged at 1000rpm for 3 mins. Supernatant was then removed and

tissue resuspended in 200µl of DMEM/F12 through 10 successive pipette titrations. Cells were then counted using a haemocytometer and trypan blue (sigma), with 10µl of cell suspension diluted with 40µl of 0.4% trypan blue (repeated twice), before adding to 10µl of trypan blue. Cells were counted on a haemocytometer covered with a glass cover-slip, with cells within 5 of the squares counted and their sum taken into the following equation:

Cells counted/squares counted x dilution factor x 10 = cells/µl

Cells were then plated at a density of 100,000 cells per well in 30µl of solution (DMEM/F12 solution used to raise the final volume to 30µl) onto pre-prepared 24-well plates. Plates were prepared by inserting a single 13mm diameter glass cover-slip which had been coated with Poly-lysine (PLL) and incubated for a minimum of 1 hour at 37°C, thereafter washed 3 times with PBS and left to dry overnight under ultraviolet (UV) light. After 3 hours, wells containing cells had 500µl of Neural differentiation medium (50ml DMEMF/12, 1ml 2% B27 (Thermo Fisher), 500µl fetal calf serum (FBS) and 500µl pen-strep) added and incubated overnight at 37°C. Cells then selected for fixing were then removed through lifting of their coverslip and placed in a separate 24-well plate for fixing (see below). The remaining cells were fed every three days for up to 2 weeks before fixing (depending on the experiment). Cells were fixed first by washing once with 1 X PBS, then with freshly made 4% Paraformaldehyde (PFA) for 20mins at 4°C. This was followed by 3 x 5-minute washes in 1 X PBS with plates sealed with parafilm to prevent drying and stored at 4°C until required for staining analysis.

### 2.7.2 **Immunocytochemistry**

Cells were permeabilised with 100% ethanol for 2 minutes, followed by 3 x 5-minute washes in PBS. In order to reduce background staining through preventing non-specific binding of the primary antibody, cells were “blocked” for 1 hour in 3% of the correct normal serum (NS) required, 3% bovine serum albumin (BSA) in PBS. The block was then removed and all required primary antibodies added simultaneously, provided they were raised in different species, in block solution and incubated overnight at room temperature. A full list of antibodies used for all immunocytochemistry experiments can be found Table 2.03 above. Removal of the primary antibody (retained and re-used up to 2 times) was followed by 3x 5-minute washes in PBS. All secondary antibodies used are optimal at a 1:200 and made up as such in block solution before being added to the cells for two hours. From this time point onwards, cells were wrapped in tin-foil to ensure the secondary antibodies remained in the dark and not be “bleached” by light. Following

this, the secondary antibody was removed and kept as previously described and cells washed for 3x 5 minutes in 1 X PBS, before adding the nuclear stain Hoechst (10µg/ml) (1:10:000) (Sigma) for 4.5 minutes in PBS. Cells then received 3x 5-minute washes in PBS before the slides were removed from the 24-well plates and placed on slides (Thermo-Scientific) and sealed with clear nail polish (L'Oréal shock-proof) and thereafter stored in the dark at room temperature until used for cell count analysis.

### 2.7.3 **Fluorescence microscopy**

Cells were visualised using UV fluorescence under a Lecia DRMBE microscope and photos captured on a Lecia DFC420 Camera in Lecia Application suite software. Hoechst positive nuclei were first detected under 346nm- "blue" wavelength and counted to obtain a total cell count. Cells were then checked for primary antibody staining under fluorescence using different UV wavelengths (560nm-red; 494nm- green).

# Chapter 3: Establishing a MEF2C Conditional KO Model

## 3.1 Introduction

In a microarray screen conducted in my host lab at Cardiff University designed to detect genes differentially expressed during peak embryonic murine striatal development (Precious et al. 2016), *Mef2c* was one gene found to be prominently up-regulated. *Mef2c* encodes a transcription factor involved in the differentiation of a variety of cell types, including muscle and nerve. Although most initial *Mef2c* research was centred on its role in muscle, it has also been implicated in nervous system development and function. For example, the conditional KO of MEF2C in Nestin-expressing neural stem/progenitor cells in mouse models impaired neuronal differentiation and maturation, resulting in aberrant compaction of cortical neurons and smaller somal size in adult mice. (Li et al. 2008a). Furthermore, a conditional KO of MEF2C via the GFAP-Cre promotor has been shown to affect hippocampal based learning and memory in adult mice, inhibiting context-fear dependant learning with mice exhibiting fewer instances of stereotypical “freezing” behaviour in response to pre-conditioned environmental cues, and greater dendritic spine densities (Barbosa et al. 2008). However, post-natal (P10-14) hippocampal KO of MEF2C has been shown not to affect learning and memory (Adachi et al. 2016), in contrast to the pre-natal KO achieved through the GFAP-Cre (Barbosa et al. 2008). This suggests that it is during the embryonic development of these neurons that MEF2C plays a key role, however the increased spine number, synaptogenesis and hyperactive behaviour observed in the post-natal KO mice also suggest MEF2C plays an important role in later development (Adachi et al. 2016). The requirement of MEF2C for normal development of hippocampal and cortical cells, combined with its upregulation during embryonic striatal development, suggests that *Mef2c* could be an important gene in the development of the striatum and proper formation of MSNs. It is reasonable to anticipate that phenotypes resulting from the loss of MEF2C during striatal development will be detectable in the adult mouse, as they were in cortical and hippocampal knockouts (Barbosa et al. 2008; Li et al. 2008b; Adachi et al. 2016).

In vitro, using the P19 cell line, use of a dominant negative Mef2 construct indicated that MEF2C proteins directly influence neuronal development including dendrite morphogenesis, the differentiation of post synaptic structures and the excitatory synapse number (Flavell et al. 2006; Shalizi et al. 2006; Potthoff and Olson 2007). Moreover,

the knockdown of MEF2C prior to the formation of NPCs in vitro causes a ~2-fold greater amount of cell death, with smaller than normal neurospheres forming, demonstrating a neuroprotective role via the prevention of apoptosis (Mao and Wiedmann 1999; Mao et al. 1999; Okamoto et al. 2000).

The majority of MEF2C-related CNS investigations to date have been focused on the cortex and hippocampus, as MEF2C was not shown to be linked to striatal development prior to identification of its upregulation between E12.5 and E18 in the developing mouse striatum; a time during which the majority of MSNs are thought to be born (Evans 2013; Precious et al. 2016). In the next two Chapters, I explored whether knock down of MEF2C in the developing mouse stratum affected its development, in particular the differentiation of striatal MSNs. In this first Chapter I establish the *in vivo* tools to achieve this and in Chapter 4 I go on to report the effects of striatal specific knock down of MEF2C.

### 3.1.1 Gsx2-Cre expression occurs throughout the entirety of the P7 and Adult striatum

The main experimental model used in my research is a conditional striatal KO of MEF2C, made using the loxP-cre system, with Gsx2 as the Cre-promoter (Kessaris et al. 2006). In order to determine whether Cre expression is driven in the striatum and not (extensively) in other brain regions, mice carrying the Gsx2-Cre were crossbred with mice homozygous for the ROSA-LacZ reporter gene (see Chapter 2). Gsx2-cre expression has previously been shown to be present within the developing striatum from E12.5 (Kessaris et al. 2006), with substantial expression observed by E15.5 (Costa et al. 2007), although the expression patterns in post-natal mice have not been reported.

LacZ is a bacterial gene that may be used as a reporter construct in transfected eukaryotic cells as the expressed protein produced is β-galactosidase, which is resistant to proteolysis in cellular lysates and its activity is therefore easily assayed. In order to first determine whether the Gsx2-cre is active in a significant proportion of striatal cells at P7, ROSA-lacZ reporter mouse brains were collected and prepared as described in Chapter 2 with X-gal staining to visualise cells expressing Gsx2-cre. As shown in Figure 3.01 below, Gsx2-cre expression is seen throughout the entirety of the striatum, with comparatively lighter staining in the cortex and septum, as seen in the original publication of this Cre-promotor construct (Kessaris et al. 2006). This confirms the striatal expression of the Gsx2-Cre that was anticipated, with the widespread staining throughout the striatum indicating that recombination has taken place in a high proportion of striatal cells during their development.


Figure 3.01: LacZ staining in Gsx2-Cre LacZ-Rosa mice at P7, showing expression of the LacZ reporter (blue) throughout most cells of the striatum (red arrow), with some staining in the septum (black arrow) and minor expression in the cortex (green arrow).

Brains were also collected from ROSA-lacZ reporter mice at 3 months and stained with X-gal solution. As shown in Figure (3.02), lacZ expression was identified primarily in the striatum and the septum, with little staining seen in other brain regions.

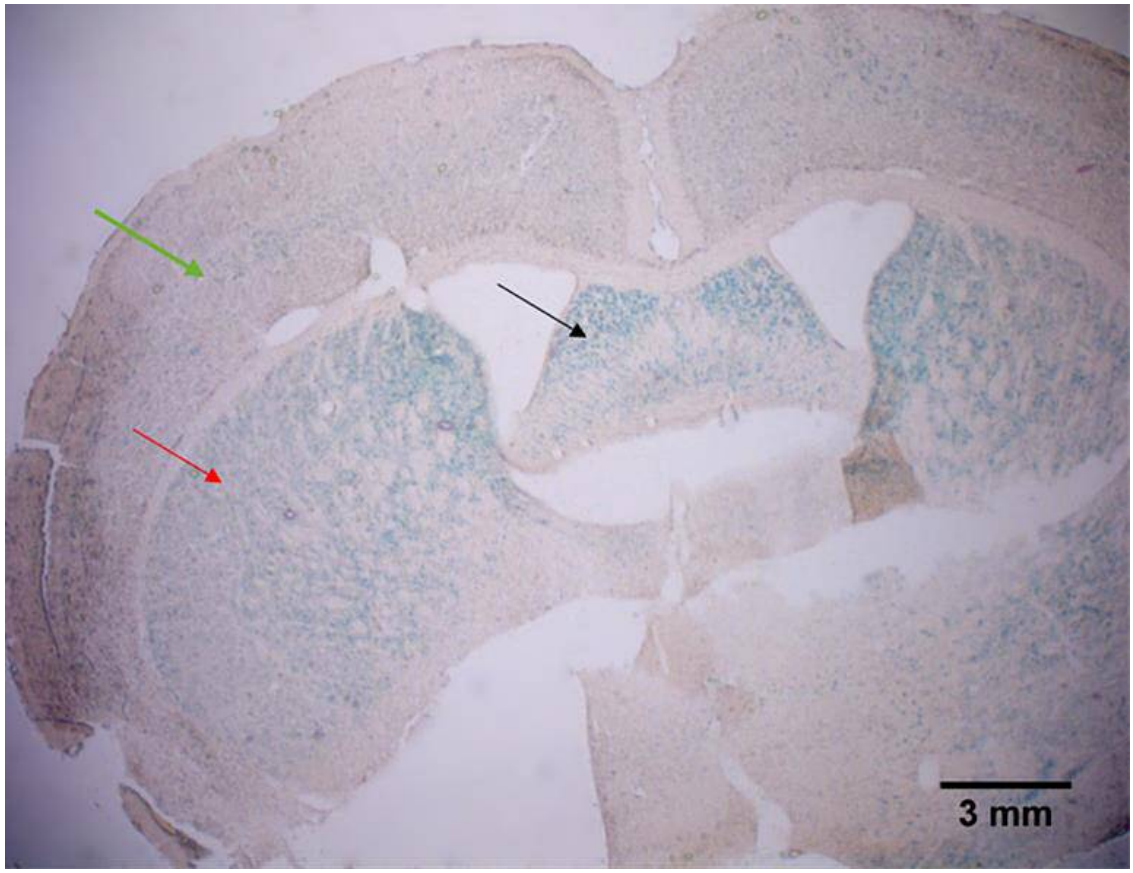


Figure 3.02: X-gal staining of the 3-month adult striatum and septum in mouse brain expressing both the Gsx2-cre and ROSA reporter constructs. There is strong positive staining in the striatum (red arrow) and in the septum (black arrow). There is also some slight staining in the cortex (green arrow).

This indicates that the Gsx2 Cre is predominantly expressed in striatum and septum, and thus, the *Mef2c*$^{LoxP/loxP}$ Gsx2-Cre$^{+}$ mice are highly likely to have substantial knock out of MEF2C in the P7 and adult striatum.

Whilst expression of Gsx2-Cre within the developing (Kessaris et al. 2006; Costa et al. 2007) and postnatal striatum has been confirmed (Figures 3.01 and 3.02), Gsx2-Cre has not yet been shown to be expressed during the development of MSNs specifically. In order to determine whether Gsx2-Cre is expressed at some point during the differentiation or maturation of MSNs, and thereby capable of facilitating a KO of MSN MEF2C, Gsx2-Cre LacZ-Rosa mice were double-stained with CTIP2 and MEF2C antibodies. Fluorescence microscopy and manual cell counting analysis revealed that 91.67% (n= 220 of 240 cells) of CTIP2 positive cells co-expressed β-galactosidase (see Figure 3.03 below). Moreover, 11.35% of β-galactosidase positive cells were found not to co-label with CTIP2 (n= 60 of 555 cells), indicating that one or more other striatal cell types are also affected by the Gsx2-Cre and thus loss of MEF2C will occur in those cells.

However, time restrictions prevented further co-labelling and so the classification of these cells has not been confirmed.

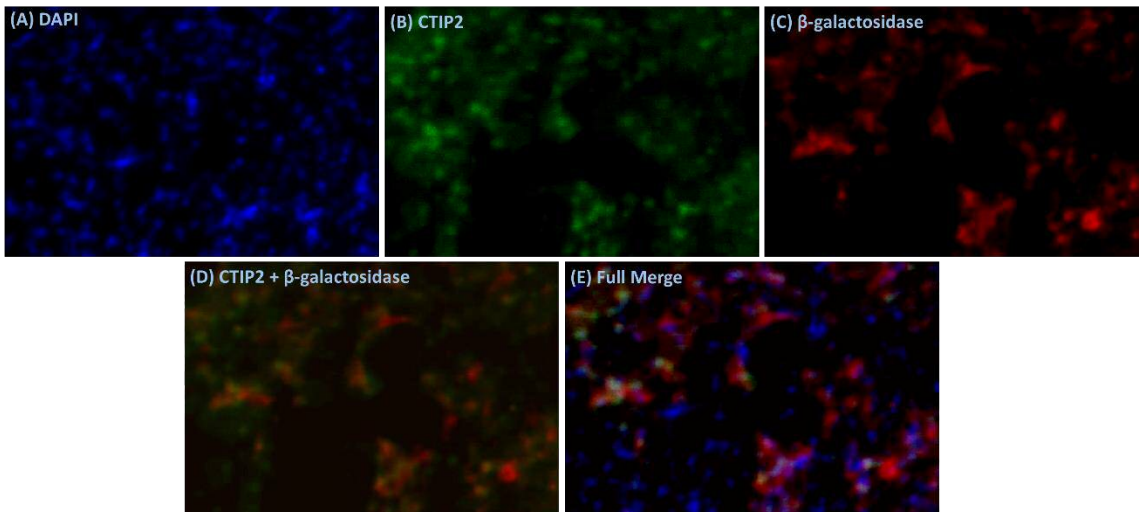


Figure 3.03: Fluorescence microscopy image of CTIP2 and anti-β-galactosidase double stain with DAPI co-label on adult Gsx2-Cre LacZ-Rosa mice, showing a high proportion of CTIP2$^+$ cells co-expressing β-galactosidase. (A) x200 magnification image DAPI co-labelled cells (blue), (B) CTIP2 positive cells (green), (C) β-galactosidase positive cells (red), (D) merged image showing co-expression of CTIP2$^+$/ β-galactosidase$^+$ cells and (E) merged with DAPI.

Taken together, these results demonstrate that Gsx2-Cre expression is prevalent throughout the striatum not only during embryonic development (Kessaris et al. 2006; Costa et al. 2007) but also in the early postnatal and adult mouse, affecting the vast majority of CTIP2$^+$ MSNs and possibly one or more additional striatal cell types.

Whilst this investigation was being conducted, it was discovered that progeny of male mice carrying a LoxP allele were found not to pass this allele to its offspring in the expected mendelian ratio. Furthermore, the original deriver of the Gsx2-Cre line (Kessaris et al. 2006) informed us that Gsx2-Cre may also be expressed within the testis, causing a recombined LoxP (and thus "knocked out" *Mef2c*) allele, referred to as "Tm2", to be inherited by the offspring (see Chapter 2 for breeding diagram). This was confirmed through the design of an additional genetic test (see Figure 3.04 below), where primers were aligned with endogenous *Mef2c* sequence upstream and downstream of the LoxP fragments flanking Exon2.

**A**

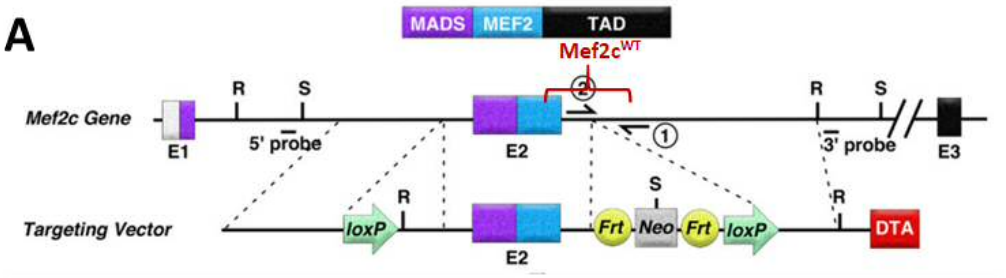


Mef2c endogenous at FRT-neo-FRT-loxP insertion site (denoted with *)

ACCTCATTTGAACCTTATTATGTATGTCACCTCTTTCTAACTCATTCTCTCTCTCTGTCTCTCTGTCTCTCTGTCTCTCTCTCTCTGT
CTCTCTCTCTCTGTCTCTCTCTCTCTCTCTCTCTGTCTCTCTCTCTCTGGAAAAGACAGCTAGTTATAAAAATACTGCTTTTCCTCAAA
ATGAT*ATCATTATAGCATTGAAAACTGTTAATACACGTGAAGTCAGATGGATAAAGGGCCATAGAATCTCAGTGAACCTTCTAA
TGTATTTTCAACATGTGTCCTATTTAAATGGTGCTTT

**B**

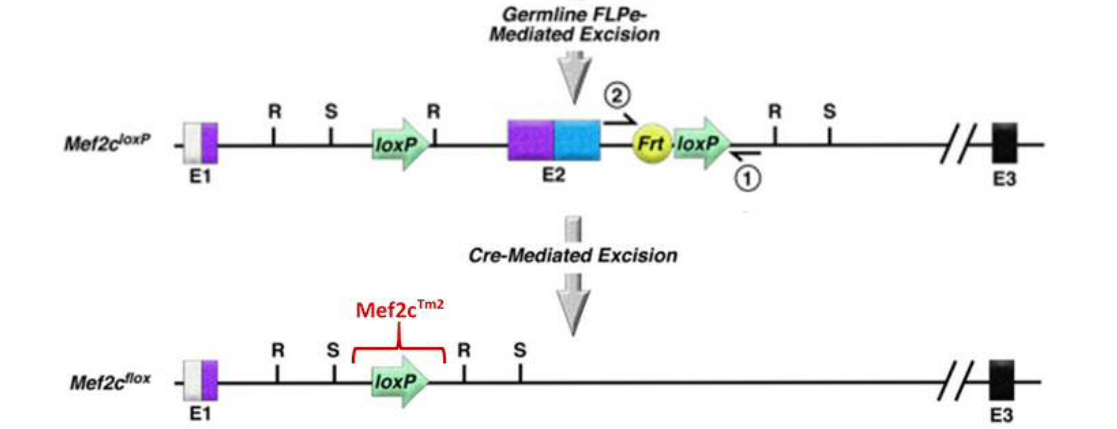


GTTCCCCAGTAGTTCCCAGTAGTCCCCAGTAGTTCCCCAGTGCCCAGCCAAGTTTCTAGAGAGAGAGAGTAAACTGGCTGAGAGT
TGTACCCACAAGCTGCAAGGGTTGTCAAATAAGTGGCACAAGAGTAACCAGTTTTGTGTGTGTGTTGTTTTAACACAGATCTAAA
ATATTAGGTTTATAATTGCGATGCTAC**AACTAGTGGATCGGCCG**CTCTAGAACTAGTGGATCCGGAACCCTTAATATAACTTCGTAT
**AATGTATGCTATACGAAGTTATTAGG**TCCCTCGACCTGCAGCCCAAGCTAGCTTATCGA**TACCGTCGA**CATTGAAAACTGTTAATA
CACGTGAAGTCAGATGGATAAAGGGCCATAGAATCTCAGTGAACCTTCTAATGTATTTTCAACATGTGTCCTATTTAAATGGTGCT
TTCTTATGAGCAATGGCTCC

**Recombined sequence** **LoxP** **Endogenous Sequence**

Fwd. Primer Seq: GCCATGCTAGAACTAGTGGATCGGCCG

Rev. Primer Seq: CTTCACGTGTATTAACAGTTTTCAATGTCGACGGTA

Reporter 1 Seq: AATGTATGCTATACGAAGTTATTAGG

Figure 3.04: Illustration of the FRT-loxP complex located either side of Exon 2, with the design of the Taq-Man probe genetic tests developed to differentiate between WT and Tm2 mice. (A) Diagram of *Mef2c* sequence with the MADS and MEF2 domains highlighted, along with Exon2, showing the forward WT probe present within Exon 2 and the reverse probe in the downstream intron. (B) Diagram showing the FLP-mediated excision of the Neo Cassette and subsequent loxP-Cre mediated excision following expression of the Gsx2-Cre, along with the approximate location of the *Mef2c*$^{Tm2}$ assay. The endogenous *Mef2c* sequence (blue font) is shown alongside the loxP sequence (red font) and the recombined sequence (black font) and how they relate to the forward (green highlight), reverse (yellow highlight) and reporter (blue highlight) primer sequences. Diagrams adapted from (Arnold et al. 2007).

The discovery of this allele in the tail-tissue of adult mice, where Gsx2-Cre expression does not occur, confirmed that Gsx2-Cre is passed on to offspring due to expression within the adult testis. This allele was thereafter named "Tm2", in accordance with nomenclature convention and its similarity to the previously established "Tm1" knockout through removal of *Mef2c* Exon 2 (Lin et al. 1997).

### 3.1.2 Establishment of *Mef2c*$^{loxP/loxP}$ Cre$^{-}$ mice as a WT control

In accordance with similar breeding practices in MEF2C KOs (Black and Olson 1998; Vong et al. 2005), mice which were homozygous for the loxP allele but negative for the Cre, were used as a pseudo-WT control in place of *Mef2c*$^{WT/WT}$ mice. This genotype is not expected to have any significant effect on the animal, as without the presence of the Cre there is no excision of the *Mef2c* gene between the loxP sites, however it remains possible that the presence of inactive loxP sites are enough to change splicing activity, gene/promoter availability or other unforeseen effects. With the breeding strategy described In Chapter 2, it was not practically feasible to have *Mef2c*$^{WT/WT}$ littermates to use as controls against striatal *Mef2c*$^{loxP/loxP}$ Gsx2-Cre$^{+}$ KO mice, therefore a range of striatal comparisons were made between *Mef2c*$^{WT/WT}$ and *Mef2c*$^{loxP/loxP}$ mice.

The most straightforward way to analyse effects on the mouse striatum is to assess its cellular composition through analysis of neuronal and MSN markers. MSNs make up 85-90% of striatal neurons as described in Chapter 1, identifiable through the early MSN markers FOXP1 and CTIP2 and the mature MSN marker DARRP-32, with NEUN identifying both MSNs and interneurons in the striatum. Furthermore, alongside comparing the total cell counts for these markers, the striatal volume may also be

compared so that any effects of genotype alterations on the structural formation of the striatum may be identified. These alterations in tandem, alongside possible effects on migration of terminally-differentiated cells from the SVZ into the striatum during development (DeDiego et al. 1994; Schiffmann 1997; Tamamaki et al. 1997; Lambert de Rouvroit and Goffinet 1998; Hamasaki et al. 2003), may also bring about changes in striatal cell density, which therefore must also be considered for each neuronal and MSN marker. Therefore, in order establish this genotype as being functionally identical to *Mef2c*$^{WT/WT}$ mice, total cell count for each marker, cell densities and striatal volumes were compared as shown in Figure 3.05 below.

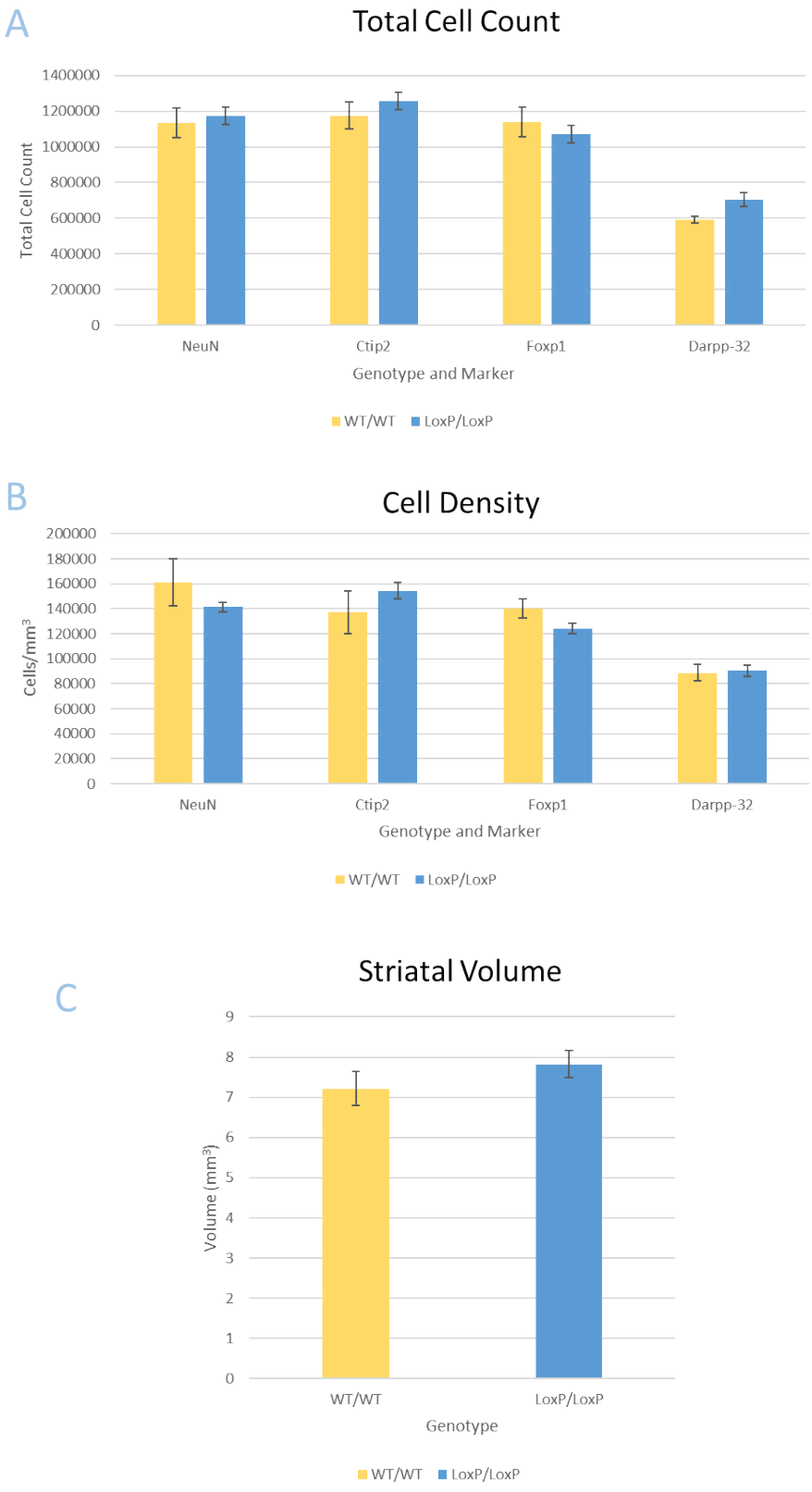


Figure 3.05: *Mef2c*$^{WT/WT}$ and *Mef2c*$^{loxP/loxP}$ mice show no significant difference in (A) total positive cell counts or (B) expression density of NEUN, FOXP1, CTIP2 and DARRP-32 markers, nor in (C) striatal volume. *Mef2c*$^{WT/WT}$ n=5 and *Mef2c*$^{loxP/loxP}$ n=10.

A MANOVA revealed no significant difference between the genotypes for total cell count or cell density for any marker or in striatal volumes (Cell counts ($F_{1,13}$ =0.002 p=0.965), cell density ($F_{1,13}$ =0.206 p=0.658) or volume ($F_{1,13}$ =3.554 p=0.082)).

These findings demonstrate that *Mef2c*$^{loxP/loxP}$ mice are a suitable WT control, in alignment with the standard practice of considering loxP/loxP mice (without the presence of the Cre) as WT.

### 3.1.3 Heterozygous MEF2C KO mice show no significant differences to WT mice.

Severe craniofacial, motor and cognitive phenotypes are observed in humans when only one copy of the *Mef2c* gene is functional and are attributed to loss, or improper formation of, MEF2C protein in the brain (Zweier et al. 2010; Zweier and Rauch 2012; Shim et al. 2015; Rocha et al. 2016) as described in Chapter 1, so physiological and phenotypical differences were also sought in the *Mef2c*$^{WT/Tm1}$ compared to WT. As described in Chapter 2, previous investigations have used a heterozygous MEF2C KO (HET) mouse as a WT control, on the basis that no discernible differences were discovered between the genotypes in neuronal models, both in terms of behaviour and physiological examination (Black and Olson 1998; Lin et al. 1998; Li et al. 2008b). Whilst the Nestin-Cre knockout model (Li et al. 2008a) included a knockout of MEF2C in the striatum alongside other brain regions, no MEF2C KO model has targeted the striatum exclusively, observing in detail the protein expression and striatal development measurements over time as has been done in this investigation. It was therefore necessary to determine whether there are striatal differences between HET and WT models, and if the HET model should therefore be included as a KO model for further study.

Alongside the *Mef2c*$^{WT/Tm1}$ mouse, additional MEF2C heterozygous KO genotypes were generated over the course of this project; *Mef2c*$^{WT/Tm2}$ and *Mef2c*$^{WT/LoxP}$ Gsx2-Cre$^{+}$. These HET variants are very similar in their genetic composition to each other and to *Mef2c*$^{WT/Tm1}$, thus are expected to achieve complete loss of MEF2C protein from a single allele due to the excision of exon 2; totally and conditionally respectively. The inclusion of these HET variants allows for a greater number of HET mice to compared to WT, thus allowing for greater reliability and accuracy of results at each time point, whilst also allowing for direct comparisons to be made to the original *Mef2c*$^{WT/Tm1}$ investigations (Black and Olson 1998; Lin et al. 1998; Li et al. 2008b).

Heterozygous MEF2C KO mice and WT mice collected at P7, 3, 12 and 18 months of age and stained for each of the 4 neuronal and MSN markers used in this investigation. MANOVA analysis of both genotypes including all markers over all time points revealed no significant differences revealed no significant difference in total NEUN positive cell count between genotypes at any age, indicating no significant difference in total striatal cell count at P7 ($F_{1,43}$ =0.425, p=0.518), 3-months ($F_{1,43}$ =0.414, p=0.523), 12-months ($F_{1,43}$ =3.543, p=0.067) or 18-months ($F_{1,43}$ =2.870, p=0.097) as shown in Figure 3.06 below. Furthermore, no difference was found at any time point in CTIP2 (P7 ($F_{1,44}$ =0.013, p=0.909) 3-month ($F_{1,44}$ =0.436, p=0.513), 12-month ($F_{1,44}$ =<0.001, p=0.999), 18-month ($F_{1,44}$ =0.164, p=0.688)), FOXP1 (P7 ($F_{1,47}$ =0.179, p=0.674) 3-month ($F_{1,47}$ =0.356, p=0.544), 12-month ($F_{1,47}$ =0.072, p=0.789), 18-month ($F_{1,47}$ =1.717, p=0.196)) or DARRP-32 (P7 ($F_{1,47}$ =0.535, p=0.468) 3-month ($F_{1,47}$ =0.031, p=0.862), 12-month ($F_{1,47}$ =0.872, p=0.355), 18-month ($F_{1,47}$ =0.001, p=0.971)) expression between genotypes, indicating that MSNs remain unaffected by a single allele loss of *Mef2c* in terms of their key protein expression markers. Moreover, no significant difference was found in striatal volume between genotypes ((P7 ($F_{1,49}$ =0.211, p=0.648) 3-month ($F_{1,49}$ =2.133, p=0.299), 12-month ($F_{1,49}$ =0.020, p=0.887), 18-month ($F_{1,49}$ =0.487, p=0.489)), suggesting the normal structural development of the striatum also remains unaffected by a single allele loss of *Mef2c*.

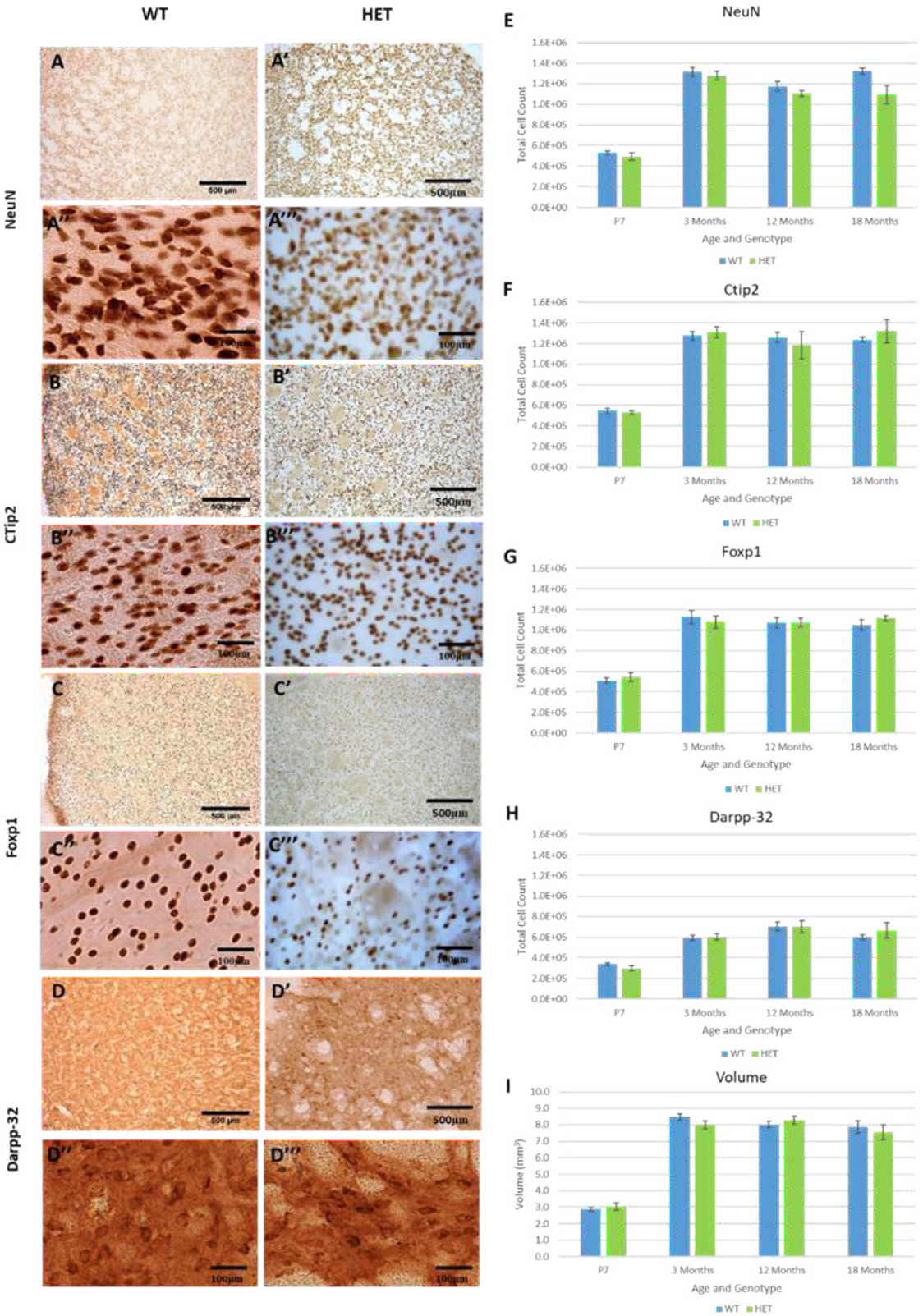
WT
HET
NeuN
CTip2
Foxp1
Darpp-32
A
A'
A''
A'''
B
B'
B''
B'''
C
C'
C''
C'''
D
D'
D''
D'''
500µm
100µm
E
NeuN
F
Ctip2
G
Foxp1
H
Darpp-32
I
Volume
Total Cell Count
Volume (mm³)
P7
3 Months
12 Months
18 Months
Age and Genotype
WT
HET

Figure 3.06: There are no significant differences between the WT and HET mouse striatum at P7, 3, 12 and 18 months of age as shown in images taken at 125X (A, A', B, B', C, C', D, D') and 400X A", A"', B", B"', C", C"', D", D"')) stained with an anti-NEUN antibody (A -A"'), CTIP2 (B – B"'), FOXP1 (C-C"'), DARRP-32 (D-D"'). Total striatal cell counts for WT and KO mice at all ages for NEUN (E), CTIP2(F), FOXP1(G) and DARRP-32(H), along with striatal volumes (I). Group numbers were: P7, WT n=8, HET n=6; 3 months, WT n=6, HET n=10; 12 months, WT n=15, HET n=7; and 18 months, WT n=4, HET n=4.

These findings demonstrate that a single allele loss of *Mef2c* is insufficient to significantly alter the expression profiles of key striatal neuronal and MSN markers or striatal volume, and are comparable to previous heterozygous *Mef2c* investigations (Black and Olson 1998; Vong et al. 2005).

*Mef2c*$^{WT/Tm1}$ and *Mef2c*$^{WT/WT}$ mice were also compared for cortical and corpus callosum thickness, and the presence of MEF2C positive cells in the motor and cingulate cortex. Furthermore, as motor deficiencies are a common phenotype in humans suffering from a mutation or entirely lacking a single *Mef2c* allele (Zweier et al. 2010; Zweier and Rauch 2012; Shim et al. 2015; Rocha et al. 2016), mouse movement over a period of 24-hours was tested using automated Activity Boxes.

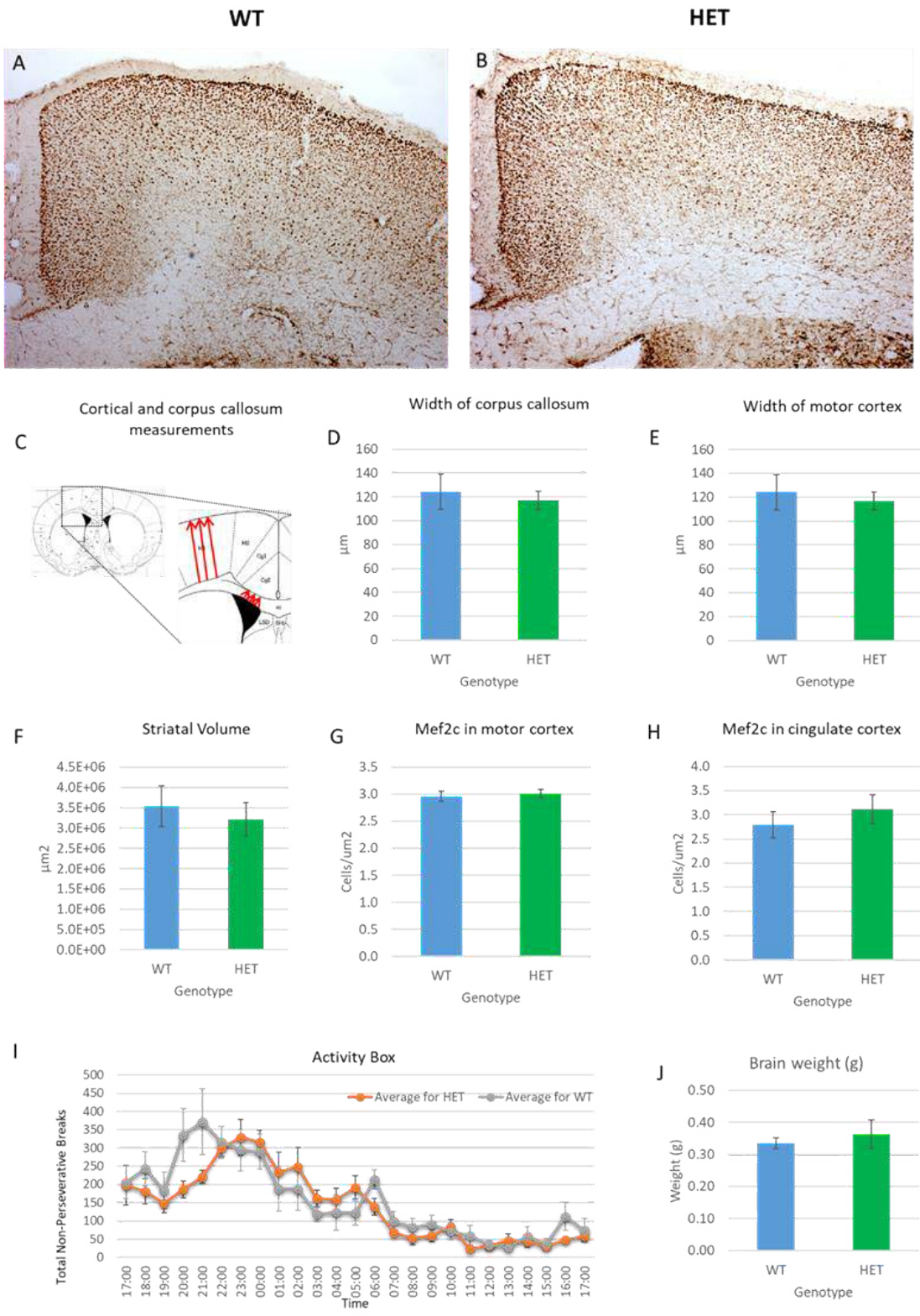
WT
HET
A
B
Cortical and corpus callosum measurements
C
Width of corpus callosum
D
µm
Genotype
WT
HET
Width of motor cortex
E
Striatal Volume
F
µm2
Mef2c in motor cortex
G
Cells/um2
Mef2c in cingulate cortex
H
Activity Box
I
Total Non-Perseverative Breaks
Average for HET
Average for WT
Time
Brain weight (g)
J
Weight (g)

Figure 3.07: There are no significant differences between any measurements made comparing WT and *Mef2c*$^{WT/Tm1}$ mice at 12 months of age. 40x magnification photos (A) WT and (B) HET cingulate and motor cortex. (C) red arrows illustrate measurements (in triplicate) taken for motor cortex and corpus callosum. No differences between WT (n=3) and *Mef2c*$^{WT/Tm1}$ (n=4) were found for (D) width of the corpus callosum and (E) width of the motor cortex. (F) Striatal volume for *Mef2c*$^{WT/WT}$ and *Mef2c*$^{WT/Tm1}$ mice (*Mef2c*$^{WT/WT}$ n=4, *Mef2c*$^{WT/Tm1}$n=2). No difference was seen in the number of MEF2C-expressing cells between *Mef2c*$^{WT/WT}$ and *Mef2c*$^{WT/Tm1}$ mice in (G) the Motor Cortex and (H) Cingulate Cortex (WT n=8, WT/Tm1 n=5). (I) Activity Box results indicating the number of non-perseverative beam-breaks over a 24-hour period. (J) There is no significant difference in brain weight (WT n=9, WT/Tm1 n=13).

No significant difference was observed between *Mef2c*$^{WT/Tm1}$ mice and their WT littermates through comparison of Motor cortex width ($T_{1,5}$ =0.032, p=0.866), Cingulate cortex width ($T_{1,5}$ =0.08, p=0.788), the number of MEF2C expressing cells in the Motor cortex ($T_{1,11}$ =0.144, p=0.712) or cingulate cortex ($T_{1,11}$ =0.594, p=0.4587). Moreover, there were no significant differences in striatal volume or brain weight ($T_{1,14}$ =1.568, p=0.139). As no differences in any of these measures were found between a single allele KO and WT mice, these data demonstrate that the motor cortex, cingulate cortex and striatum appear to be resilient to a HET KO of MEF2C, in line with what has been shown in mouse cortical and hippocampal KO models (Lyons et al. 1995; Barbosa et al. 2008) and not mirroring the effect observed in single-allele *Mef2c* loss in humans.

### 3.1.4 Conditional KO of MEF2C results in reduced protein expression in the adult striatum and fewer MEF2C-expressing MSNs

In order to show that MEF2C protein expression is reduced in the KO striatum through the conditional knockout mechanism previously described, immunohistochemistry was performed using a carefully selected anti-MEF2C antibody, different to those used in previous MEF2C KO publications (Martin et al. 1993; Lin et al. 1997; Vong et al. 2005). Previous investigations, including the original generation of the *Mef2c*$^{loxP/loxP}$ construct which utilised both the EIIa promotor (expressing Cre in all cells through the germ line) and MLC2V (expressing Cre from E8.5 in the heart) promoters (Vong et al. 2005), used MEF2C antibodies to demonstrate MEF2C protein loss in a range of tissues. However, the peptide sequence used as the antigen, and thus the epitope to which these commercial antibodies (antibody code SC-313, Santa Cruz Biotechnology, renamed as MEF2A antibody as of September 2018) appear to bind is the MEF2 domain, which is highly conserved (Shore and Sharrocks, 1995) and present in other MEF2 variants (see Figure 1.01, Chapter 1) as previously described in Chapter 1. Thus, it is unlikely the

antibodies used in these previous investigations are specific to MEF2C. These antibodies may have been selected to circumvent the issue of isoform selection (two of the eight alternatively spliced isoforms produced by *Mef2c* transcription are not expressed in neuronal tissue), however there remains the possibility of cross-protein reactivity.

In order for an antibody to be MEF2C specific, it must be comprised from an amino acid sequence located towards the C-terminus of the protein after the MADS and MEF2 domains, where the protein sequences are most varied between the four MEF2 homologs. Therefore, a MEF2C antibody raised against a peptide downstream of the MADS/MEF2 domains was selected for this experiment (see Figure 3.08), with careful consideration taken to ensure its target sequence was present in neuronally-present isoforms (Hakim et al. 2010) (see Chapter 1). It must be noted however than even this peptide contains sequence overlaps with MEF2A and MEF2D, which are also expressed in the adult striatum, thus it is possible that this antibody will detect MEF2A and MEF2D, but not MEF2B.


Figure 3.08: MEF2C antibodies designed against the human protein are also suitable for mouse tissue given the high degree of similarity between human and mouse MEF2C proteins, however the selected peptide has small sequence-target overlaps with MEF2A and MEF2D. (A) Human and Mouse MEF2C protein sequences are very similar, with differences highlighted in red, MADS and MEF2 domains in green and the selected antibody target sequence in blue. (B) Amino acid sequence comparison of MEF2A, B, C and D showing a 3 and 5 peptide amino acid sequence overlap with the target peptide sequence in MEF2A and MEF2D respectively, indicating the remaining but reduced possibility of cross-reactivity.

Using this antibody, the WT striatum was found to contain approximately 913,176 MEF2C positive cells (Abercrombie correction, see Chapter 2), compared to only 250,065 cells in the conditional KO. Due to limited antibody supply and the presence of faint cells after exposure to DAB indicating cross-reactivity with other MEF2 proteins, increasing the likelihood of incorrectly identifying MEF2C positive cells, analysis was conducted on a small number of tissues (n=2 each) in order to initially show reduced MEF2C expression in the conditional KO striatum as shown in Figure 3.09 below.

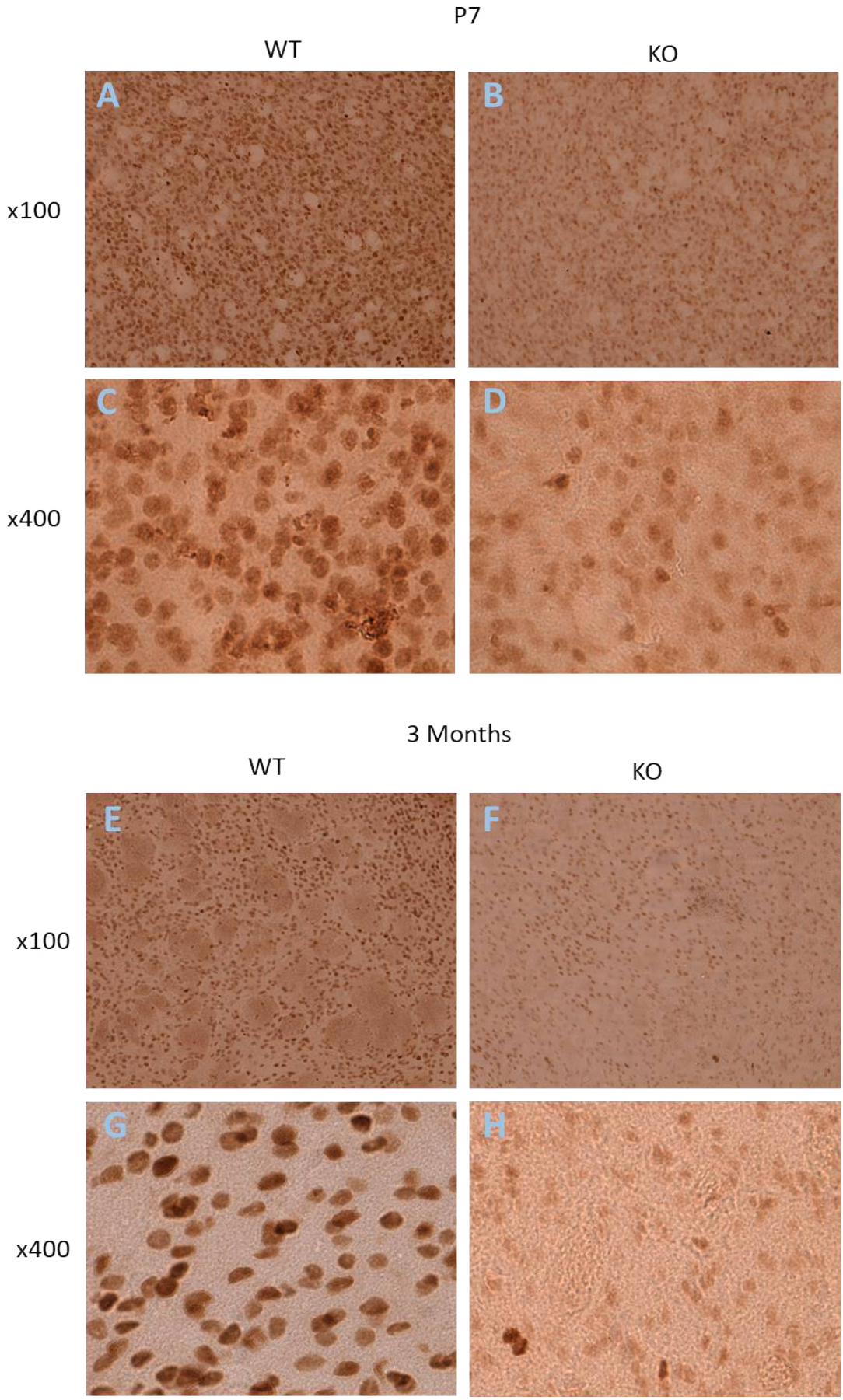
P7
WT
KO
A
B
x100
C
D
x400
3 Months
WT
KO
E
F
x100
G
H
x400

Figure 3.09: MEF2C conditional KO mouse contain fewer MEF2C positive cells in the striatum than WT mice in both adult (A-D) and P7 postnatal mice (E-H) as shown at 100X (A, B, E, F) and 400X (C, D, G, H,).

Furthermore, as shown in Figure 3.10, cortical MEF2C expression remains strong in the 3-month adult mouse in the conditional KO model, further demonstrating the specificity of the Gsx2-Cre mediated KO.

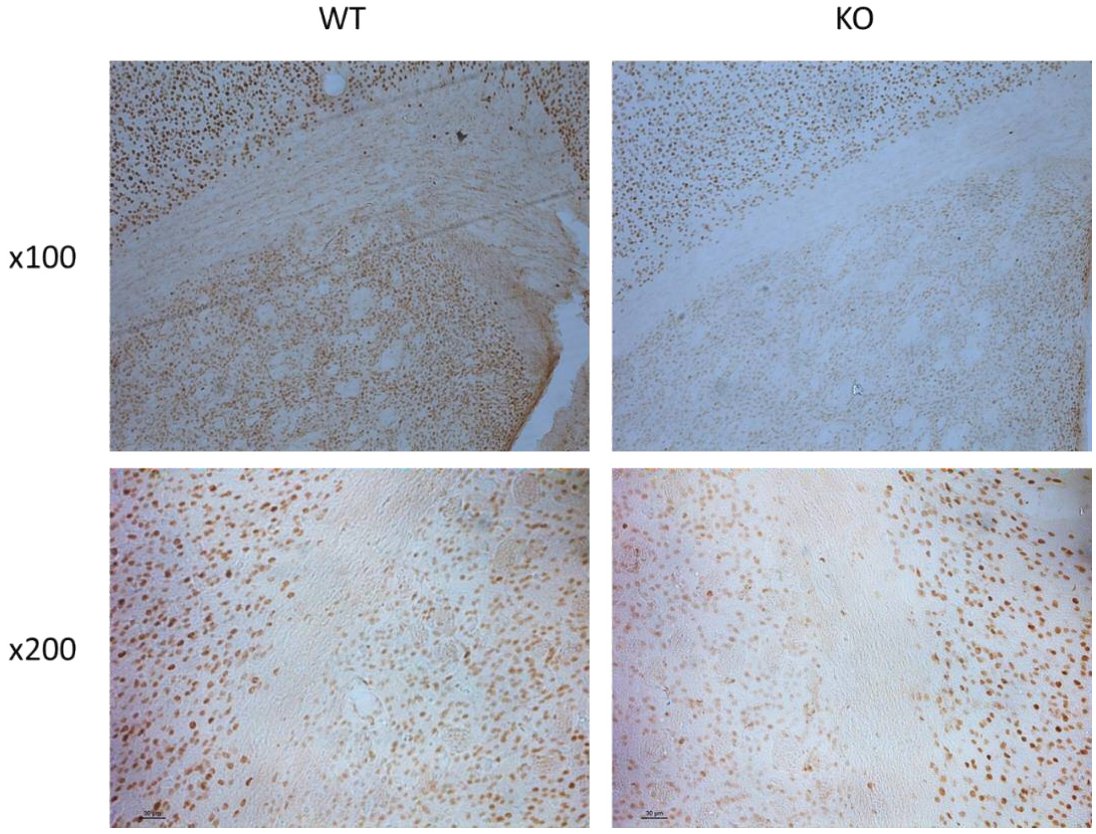


Figure 3.10: Cortical expression of MEF2C appears unaffected in 3-month adult conditional KO mice, though there are clearly more MEF2C positive cells within the striatum of WT mice compared to KO.

These data support both the regional-specific nature of the Gsx2-Cre mediated conditional KO MEF2C genetic construct as detailed in Chapter 2, and the LacZ reporter data evidenced in Figure 3.02 above in demonstrating significant loss of MEF2C protein in the striatum, without affecting the cortex.

Whilst expression of MEF2C within striatal cells has been confirmed, it remains necessary to confirm whether MEF2C is expressed specifically within MSNs, and if the conditional MEF2C KO striatum contains fewer $MEF2C^{+}$ MSNs as a result of Gsx2-Cre expression. To this end WT and MEF2C conditional KO mice were double-stained with CTIP2 and MEF2C antibodies. Fluorescence microscopy and manual cell counting analysis revealed that 88.7% of MSNs (n=469 of 529 cells) were confirmed to co-express CTIP2 and MEF2C (see Figure 3.11 below) in the WT striatum, compared to only 1.6% (n=6 of 377 cells) in the conditional KO striatum.

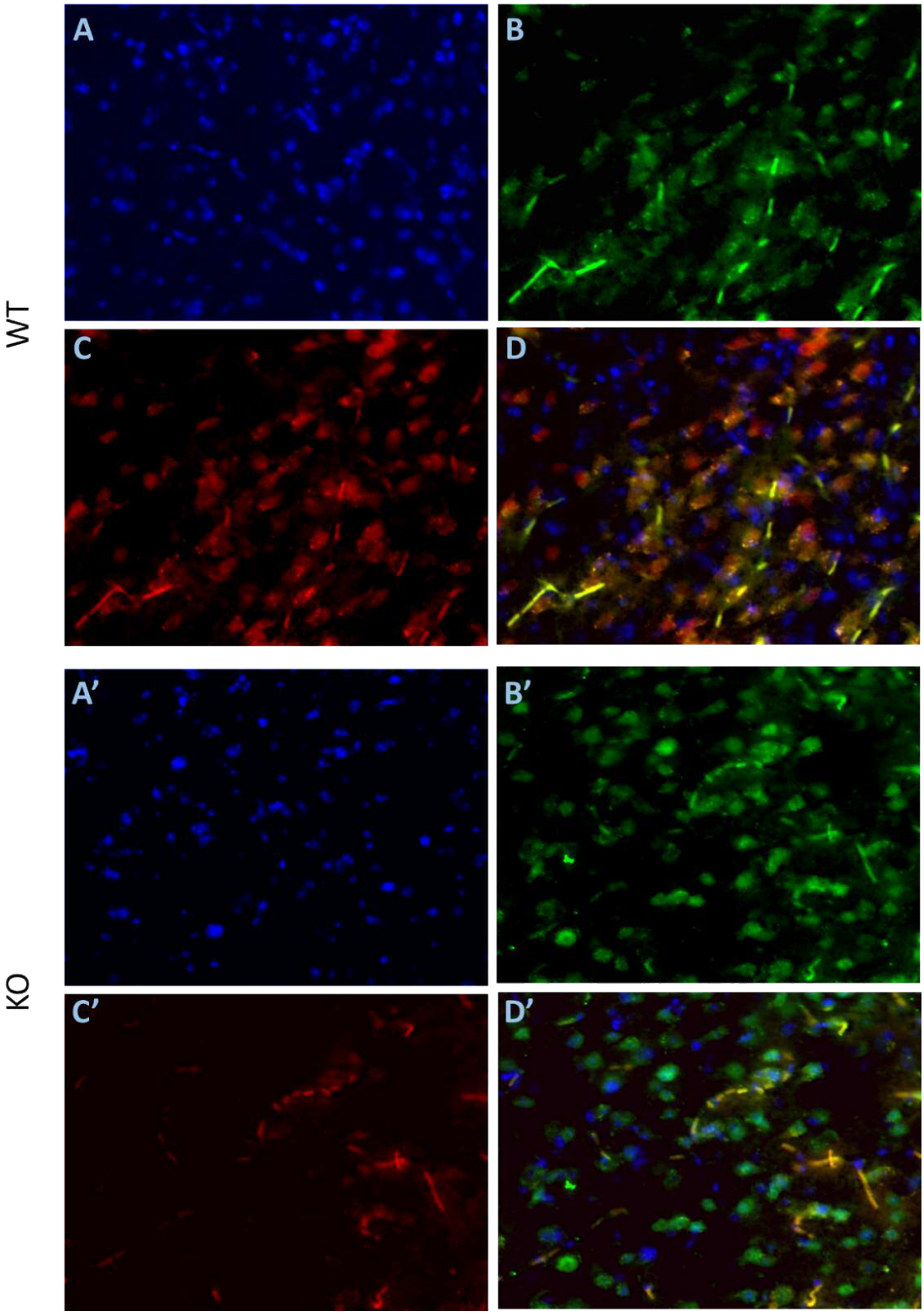


Figure 3.11: Fluorescence microscopy images of MEF2C and CTIP2 histological double staining showing fewer CTIP2$^+$ / MEF2C$^+$ striatal cells in the 3-month adult conditional MEF2C KO striatum compared to WT. x200 magnification images of striatum labelled for (A, A') DAPI, (B, B') CTIP2, (C, C') MEF2C and (D, D') merged image for WT (A,B,C, D) and KO' (A',B',C',D') respectively.

Taken together, these results demonstrate that expression of the Gsx2-Cre produces a knockdown of MEF2C in the vast majority of conditional MEF2C KO striatal MSNs, supporting the lineage tracing analysis illustrated in Figures 3.01 and 3.02 and thus providing a KO model for subsequent analysis. Due to possibility that this antibody also detects (to an as yet unquantified degree) MEF2D and MEF2A (see Figure 3.08), it is not possible to use these results to determine the extent of KO, other than to recognise that it is likely to be under-estimated.

## 3.2 Discussion

This Chapter describes attempts to find an in vivo mouse model in which to explore the effects on downregulating MEF2C on the development of the striatum. The specific interest in this thesis was the development of MSNs. Homozygous MEF2C null mice are embryonically lethal (probably due to developmental failure of major musculature, including the heart). Options therefore included using a heterozygous MEF2C null or establishing a conditional KO of MEF2C in the brain.

Early studies into cardiac tissue reported no differences between *Mef2c*$^{WT/Tm1}$ mice and their WT littermates (Black and Olson 1998; Lin et al. 1998; Vong et al. 2005), with no differences also found in the cortex or hippocampal cells (Li et al. 2008b). However, no studies to date have specifically considered the striatal effects of a single *Mef2c* allele KO. Furthermore, being able to use the *Mef2c*$^{WT/Tm1}$ mouse as a model of MEF2C KO would have been substantially easier and cheaper, given that it already existed, so a comparison of striatal structure in the *Mef2c*$^{WT/Tm1}$ and WT littermates was undertaken. No statistically significant differences were found between WT and *Mef2c*$^{WT/Tm1}$ mice in any cortical or striatal measurements as shown in Figures 3.04 and 3.05. Furthermore, activity box analysis showed no significant difference in the number of non-perseverative beam-breaks between genotypes indicating that activity levels are similar over a 24-hour period. *Mef2c*$^{WT/Tm1}$ mice were found to have no difference in overall weight, ability to breed, life expectancy (data not shown) or brain-weight compared to WT mice. Although this does not exclude a subtle structural or behavioural phenotype in these animals, activity testing is a well-accepted and reasonably sensitive screening test and together these findings strongly suggest that the loss of a *Mef2c* single allele is not sufficient to interfere with striatal development. Furthermore, although *Mef2c*$^{WT/Tm1}$ were not used as controls in this thesis, they have been used as pseudo WT controls in other studies (Black and Olson 1998; Lin et al. 1998; Li et al. 2008b) and could be considered for use as controls in future experiments.

Having failed to establish a detectable histological striatal phenotype for the *Mef2c*$^{WT/Tm1}$ mouse, the next strategy was to develop a KO that was specific for brain. A mouse possessing a *Mef2c* gene flanked by loxP constructs was sourced from Olson (See Chapter 2) and a mouse containing a Cre on the Gsx2 promoter originally generated by (Kessaris et al. 2006) was used to attempt to create a conditional KO of MEF2C in the developing striatum.

The Lineage tracing results illustrated in Figures 3.1 and 3.2 demonstrate high levels of staining in the striatum and substantially lower levels in the septum and cortex. This suggests that findings using the Gsx2 conditional KO can be largely attributed to loss of MEF2C expression from striatal cells. Furthermore, as shown in Figure 3.03, over 90% of CTIP2 positive cells in the adult striatum co-labelled with LacZ, suggesting that the resultant loss of MEF2C in striatal MSNs should be extensive. Time constraints precluded characterisation of the remaining approximately 10% of cells. An antibody to MEF2C was also used to compare conditional MEF2C KO and WT brain sections from at both P7 and 3 months. This demonstrated lower numbers of cells staining for this antibody in both the developing and adult brain, which further confirms the conclusion that the conditional KO has indeed reduced striatal MEF2C expression. Nevertheless, these results do increase confidence in the validity of the conditional KO model.

There are relatively high numbers of septal cells stained positive for LacZ, but according to the Allen brain atlas MEF2C is not expressed in the septum (http://mouse.brain-map.org/experiment/show/79567505, 2013), so presence of the Gsx2-Cre in these cells would not be expected to have any effect. The presence of Gsx2-Cre-lineage cells in the cortex is not unexpected and has been previously reported (Kessaris et al. 2006; Costa et al. 2007). A proportion of ganglionic eminence cells migrate through the striatum into the cortex. Most of these cells originate from the MGE and are destined to become cortical interneurons (Wonders and Anderson 2006; Xu et al. 2008; Miyoshi et al. 2010; Rudy et al. 2011; Hu et al. 2017). Furthermore, single cell sequencing of cortical interneurons and their precursors and showed expression of MEF2C in the early precursors of Parvalbumin interneurons, suggesting a requirement for MEF2C in the normal development of these cells (Mayer *et al.*, 2018). Despite this, it seems unlikely that loss of MEF2C in small numbers of cortical interneurons will impact substantially, given no differences in MEF2C staining in the adult HET KO vs WT cortex were seen as shown in Figure 3.07 above.

As shown in Figure 3.05, no significant differences were found between *Mef2c*$^{loxP/loxP}$ and *Mef2c*$^{WT/WT}$ mice, demonstrating that the loxP insertion sites have no noticeable effect on transcription of the MEF2C protein. Therefore, *Mef2c*$^{loxP/loxP}$ mice are suitable for use as a WT control, as is standard practice in conditional KO models, allowing for any differences observed between WT and KO models to be attributed solely to the expression of the Gsx-Cre.

### 3.2.1 **Summary**

*Mef2c*$^{loxP/loxP}$ mice were established as a WT control. Heterozygous mice were not significantly different to WT, therefore necessitating the use of a conditional KO model. LacZ and protein expression analysis revealed that Gsx2-Cre is expressed throughout the striatum at both P7 and 3 months, appearing to dramatically reduce the numbers of MEF2C positive MSNs, thus is suitable to serve as the KO model.

# Chapter 4: The Effect of Conditional Loss of MEF2C on the Adult and Postnatal Mouse Striatum.

## 4.1 Introduction

The results of Chapter 3 demonstrated that MEF2C is conditionally knocked out in the striatum of *Mef2c*$^{LoxP/loxP}$ Gsx2-Cre$^{+}$ mice. In this chapter the effects of conditional homozygous loss of MEF2C protein from striatal cells was determined. At 3-months of age mice are considered fully developed and mature adults and are capable of reproducing and display normal behaviours and cognitive abilities expected of adult mice. This was used as the starting point for these studies as a convenient adult age in terms of generating experimental animals.

## 4.2 Analysis of WT and MEF2C conditional KO Mice at 3 months

### 4.2.1 There is a significant reduction in striatal volume and striatal cell counts of neuronal and MSN markers in conditional MEF2C KO at 3 months.

There was a small, but significant decrease of 8.1% in the conditional MEF2C KO striatal volume compared to WT at 3 months ($t=2.896$, $df=9$, $P=0.018$), although macroscopically the structure of the KO striatum appeared normal. NEUN, found in both MSNs and interneurons in the striatum, was significantly reduced in the striatum of KO mice compared to their WT littermates by 21% ($F_{1,9}=18.75$, $p=0.002$) (Figure 4.01).

In order to determine whether embryonic striatal KO of MEF2C affected the development of MSNs in adulthood, 3-month adult brains were stained immunohistochemically using known markers for striatal MSNs: CTIP2, FOXP1 and DARPP-32. Estimates for cell counts per striatum were analysed through a MANOVA incorporating all four markers, which demonstrated statistical significance between the WT and conditional KO genotypes ($F_{1,9}=15.096$ $p=0.003$). Subsequent Post-Hoc (Bonferroni) analysis showed that DARPP-32, the gold-standard of MSN identification and associated with mature MSNs (Yger and Girault, 2011; Belkhiri, Zhu and El-Rifai, 2016; Precious *et al.*, 2016) was significantly reduced by 48% in KO mice compared to their WT littermates ($F_{1,9}=39$ $p=<0.001$) (Figure 4.01). FOXP1 was also found to be significantly reduced in KO mice

compared to WT littermates (by 39%; $F_{1,9}$ =27.832 p=0.001). In WT brains FOXP1 co-localised with all DARPP-32 positive cells in the striatum whilst also marking a further subset of MSNs, as described by Precious et al (Precious *et al.*, 2016). CTIP2 also exclusively stains MSNs within the striatum and has been found to colocalise with ~99% of FOXP1 positive cells (Arlotta *et al.*, 2008). CTIP2 was also found to be significantly reduced ($F_{1,9}$ =5.155 p=0.049), although only by 12%.

As well as assessing cell counts per striatum, counts were also expressed as counts per $mm^3$. The relatively greater loss of FOXP1 and DARPP-32 was reflected in this analysis where MANOVA revealed a significant difference between genotypes ($F_{1,9}$ =11.282 p=0.006) with Bonferroni post-Hoc analysis showing a significant decrease in KO mice of 27% for Fox ($F_{1,9}$ =12.761 p=0.006) and 41.8% for DARPP-32 ($F_{1,9}$ =32.866 p=<0.001) compared to WT, but no significant difference in NEUN ($F_{1,9}$ =4.781 p=0.057) or CTIP2 ($F_{1,9}$ =0.130 p=0.727) cell densities.

In other words, the overall smaller striatum is reflected in the lower striatal counts of NEUN and CTIP2, but these markers appear to be normal in terms of striatal density. In contrast, the much greater reduction in DARPP-32 and FOXP1 positive cells suggests that a substantial proportion of $CTIP2^+$ “MSNs” in the KO mouse brain do not co-express FOXP1 and DARPP-32. This was therefore studied in more detail in the next section using double staining with CTIP2 and FOXP1.

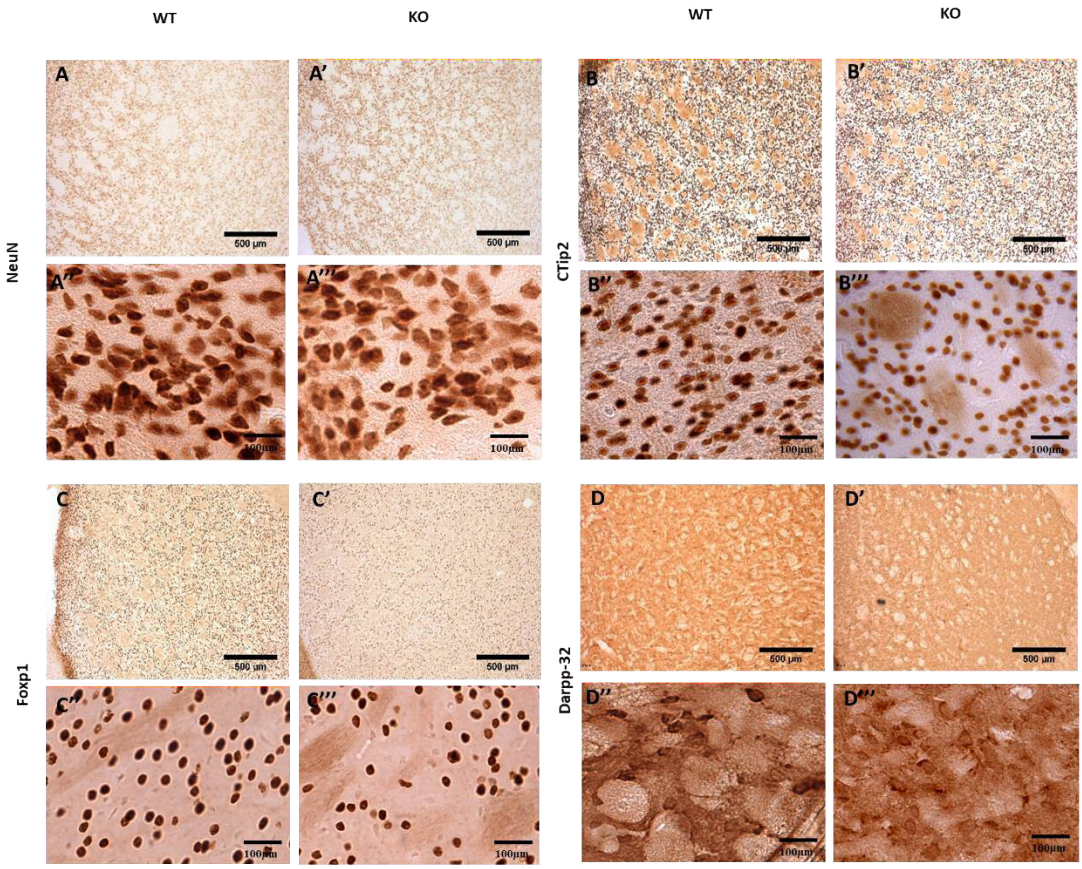
WT
KO
WT
KO
NeuN
CTip2
Foxp1
Darpp-32
A
A'
A''
A'''
B
B'
B''
B'''
C
C'
C''
C'''
D
D'
D''
D'''
500 µm
100µm

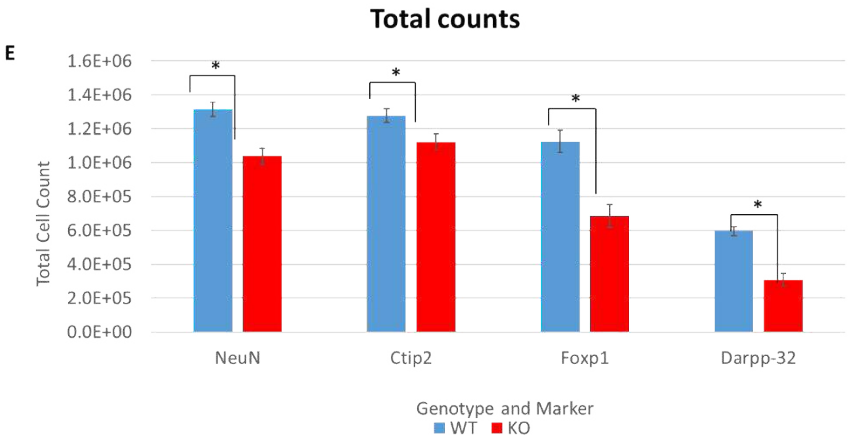
E
Total counts
Total Cell Count
1.6E+06
1.4E+06
1.2E+06
1.0E+06
8.0E+05
6.0E+05
4.0E+05
2.0E+05
0.0E+00
*
NeuN
Ctip2
Foxp1
Darpp-32
Genotype and Marker
WT
KO

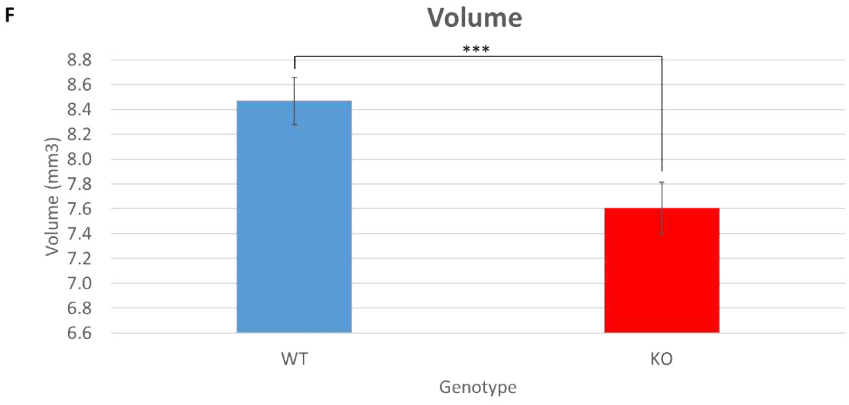
F
Volume
***
Volume (mm3)
8.8
8.6
8.4
8.2
8.0
7.8
7.6
7.4
7.2
7.0
6.8
6.6
WT
KO
Genotype

Figure 4.01: Photos of the 3-month striatum following DAB staining taken at 125x magnification (top) and 500x (bottom) for NeuN in WT (A, A'') and KO (A', A'''); CTIP2 in WT (B – B'') and KO (B', B'''); FOXP1 in WT (C-C'') and KO (C', C'''); and DARPP-32 in WT (D,D'') and KO (D', D'''). (E) Counts per striatum comparison of neuronal and MSN markers showing a significant reduction in striatal MEF2C KO mice compared to WT at 3 months of age along with (F) a significant reduction in volume (WT n=6, KO n=5).

### 4.2.2 Conditional loss of MEF2C in the striatum results in CTIP2 positive / FOXP1 negative cells

CTIP2 and FOXP1 colocalise in normal adult mouse striatal MSNs (Arlotta *et al.*, 2008; Precious *et al.*, 2016) with very few neurons expressing either protein alone (<1%). Although the number of both CTIP2 and FOXP1 expressing cells was reduced in the KO mouse, the number of FOXP1 expressing cells was reduced proportionately more. From this it would be predicted that the KO striatum would contain a greater proportion CTIP2 positive/FOXP1 negative neurons. In order to confirm this finding and quantify the number of cells affected, WT and KO brain sections were double-stained for CTIP2 and FOXP1. Figure 4.02 shows confocal images of CTIP2/FOXP1 staining illustrating that most cells are clearly double labelled in the WT striatum, but a large number of cells stained positive for CTIP2 but not FOXP1 in the KO striatum. Counting of these images was performed by first counting every $CTIP2^+$ cell without any detectable FOXP1 expression ($CTIP2^+/FOXP1^-$), then counting every cell expressing CTIP2 with any detectable FOXP1 expression (low or high) as "double-stained". Counts were then presented as the percentage of $CTIP2^+/FOXP1^-$ cells relative to double-stained cells.

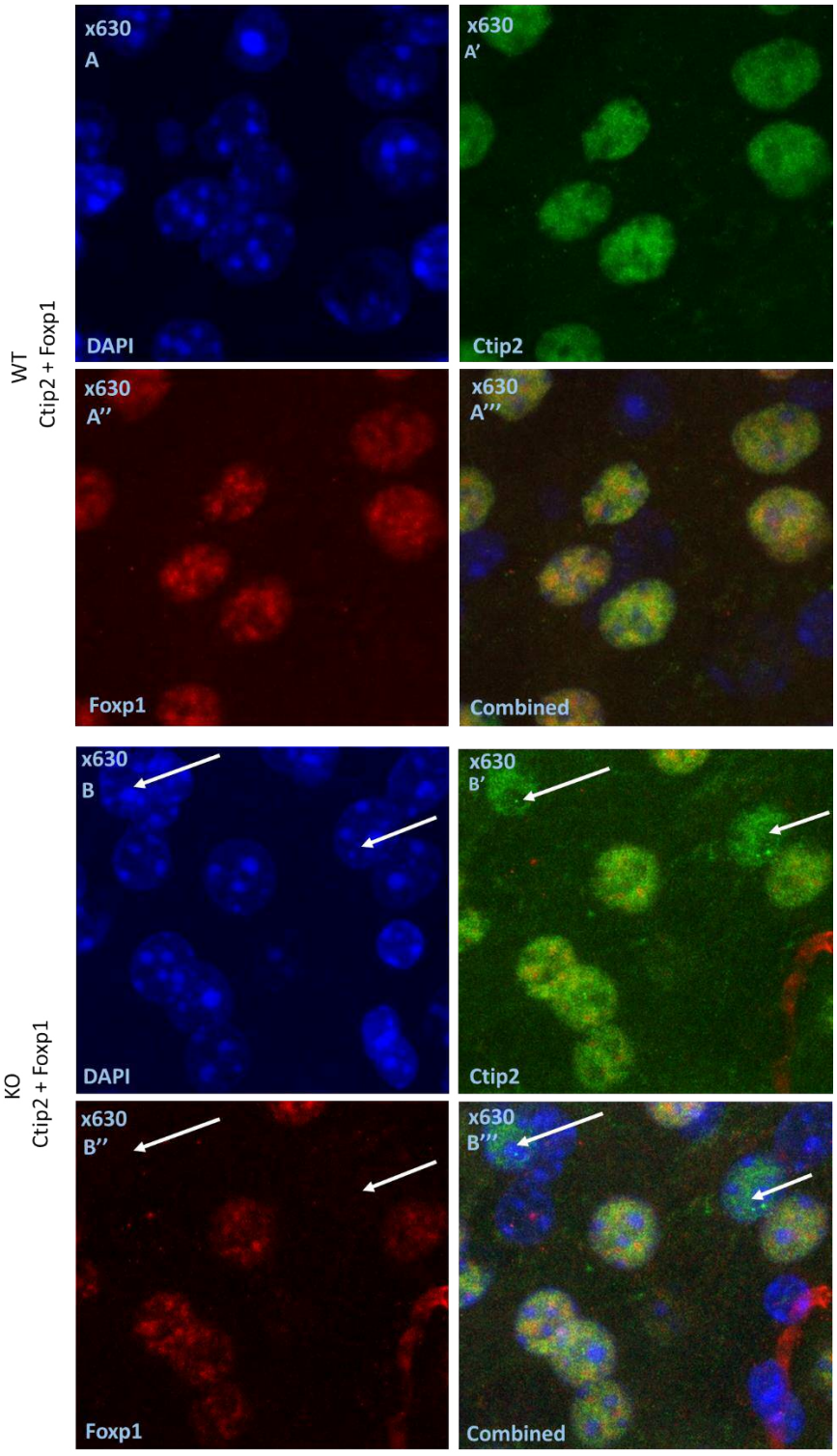
WT
Ctip2 + Foxp1
x630
A
DAPI
x630
A'
Ctip2
x630
A''
Foxp1
x630
A'''
Combined
KO
Ctip2 + Foxp1
x630
B
DAPI
x630
B'
Ctip2
x630
B''
Foxp1
x630
B'''
Combined

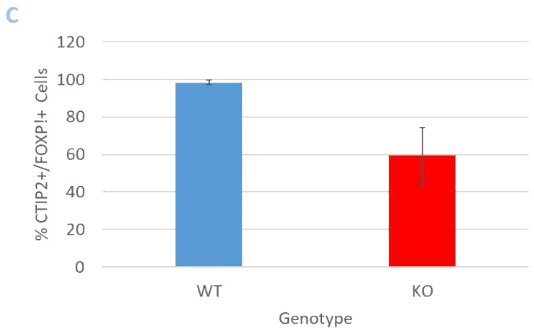
C
120
100
80
60
40
20
0
% CTIP2+/FOXP1+ Cells
WT
KO
Genotype

Figure 4.02: Representative confocal microscope images of 3-month striatal tissue double-stained for CTIP2 (green) and FOXP1 (red) at x630 magnification. WT striatal tissue stained for (A) DAPI, (A') CTIP2, (A'') FOXP1 and (A''') merged; and MEF2C conditional KO for (B) DAPI, (B') CTIP2, (B'') FOXP1'', and (B''') merged. These high-power images, with z-stacking scanning, show that in the WT there are almost no instances of $CTIP2^{+}/FOXP1^{-}$ cells, whereas in KO there are many CTIP2+ cells with weak FOXP1 staining and some with none. (C) Percentage of $CTIP2^{+}/FOXP1^{-}$ cells relative to total double-stained cells counted.

Confocal images were taken and individually counted so that only cells with a complete detectable loss of FOXP1 expression were regarded as FOXP1 negative. Quantification confirmed the finding in Figure 4.01 that FOXP1 was disproportionately reduced compared to CTIP2 in the KO striatum, with 30.5% (n=436 of 1476 cells) of $CTIP2^{+}$ cells found to contain no detectable trace of FOXP1 expression. It should be noted however that FOXP1 expression was greatly reduced in a large proportion of conditional KO striatal cells, with high power confocal microscopy and z-stack imaging required to detect low levels of protein. In the WT striatum however almost no (<1%, n=9 from 959 cells) CTIP2 positive cells were also FOXP1 negative (Figure 4.02 C), in alignment with previous reports (Arlotta *et al.*, 2008; Precious *et al.*, 2016).

CTIP2 and FOXP1 show near identical temporal expression patterns, with both present at E12.5 (Arlotta *et al.*, 2005; Precious *et al.*, 2016) and a high rate of co-labelling (~99%), with both regarded as reliable markers for total MSN counts. These results demonstrate that embryonic loss of striatal MEF2C disturbs the development of normal MSN populations in the striatum, suggesting MEF2C is necessary for proper MSN differentiation.

## 4.3 Analysis of the striatum in MEF2C KO at P7

As part of the process of understanding the mechanisms underlying the changes seen in the MEF2C conditional KO at 3 months of age, it was necessary to start by asking when these changes first occurred. For example, it is possible that a subpopulation of striatal MSNs initially developed normally and then failed to mature or underwent a degenerative process before adulthood. Alternatively, there may have been a failure of MSN production or specification at an early developmental stage. A first step towards addressing the underlying cause, and thereby determine the role of MEF2C, was to perform a developmental study to assess when the changes, with respect to the wild type, are first seen. It is reasonable to suggest that as striatal MEF2C protein expression

increases, so does the likelihood that it is performing a necessary role within the striatal system. The *Mef2c* gene is highly expressed during embryonic development and the early postnatal period as shown by qPCR in Figure 3.16 (Evans et al unpublished data) (Leifer, Golden and Kowall, 1994; G E Lyons *et al.*, 1995; Adachi *et al.*, 2016), suggesting that protein expression will be increased at this period. P7 was selected as it followed peak levels at P0 (see Figure 4.03) and tissues were processed using the same tissue preparation and histological methodologies as for adult tissues to allow comparisons to be made.

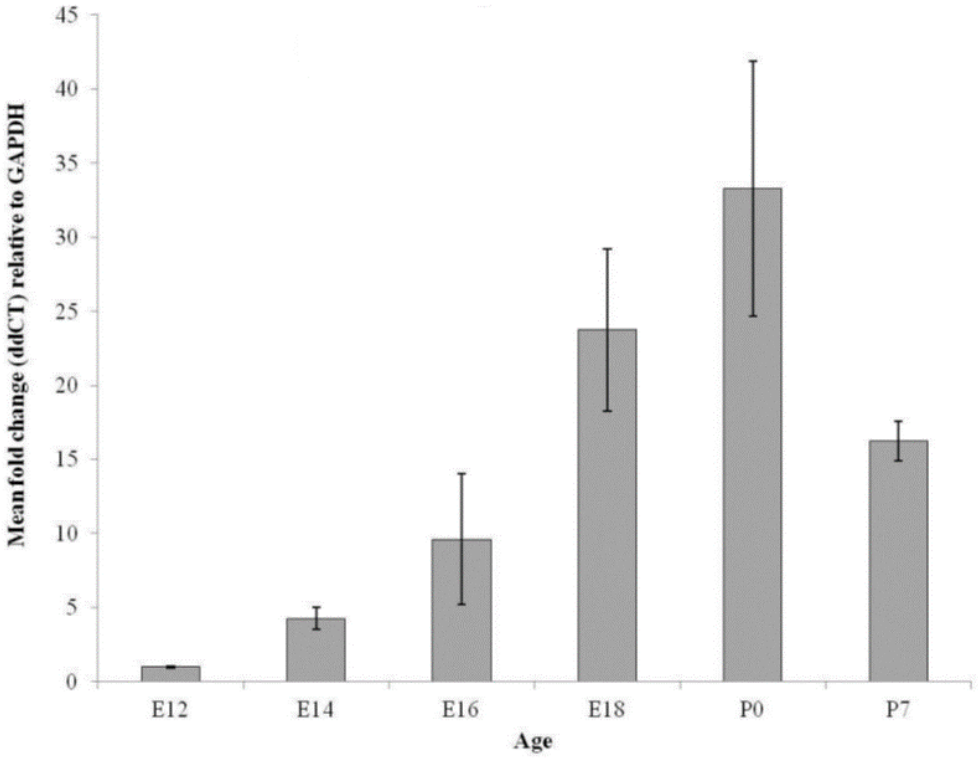


Figure 4.03: Expression of *Mef2c* relative to GAPDH “house-keeping” gene through embryonic and early post-natal WT striatal development (Evans et al unpublished data).

### 4.3.1 Numbers of DARPP-32 positive cells alone were significantly lower in the conditional MEF2C KO mouse striatum at P7.

A direct comparison was made between the histological results of P7 and 3-month MEF2C striatal KO and WT mice for each marker using two-way ANOVAs comparing both genotypes and age with Bonferroni post-hoc analysis performed thereafter. This analysis revealed a significant interaction between age and genotype for each marker (NEUN ($F_{1,22}$ = 17.204, p=<0.001), CTIP2 ($F_{1,17}$ = 4.586, p=0.047), FOXP1 ($F_{1,23}$ = 32.209, p=<0.001) and DARPP-32 ($F_{1,23}$ = 27.545 p=<0.001)). NEUN, CTIP2 and

FOXP1 were not significantly reduced in P7 KO tissues compared to WT littermates (p=0.699, p=0.574 and p=454 respectively) (Figure 4.04 and 4.05). In contrast, the number of DARPP-32 expressing cells was found to be significantly reduced (by 17.5%) in the conditional KO striatum at P7 compared to WT (p=0.015). These findings differ to the those at 3 months in that there are no differences between MEF2C KO for total striatal NEUN, CTIP2 or FOXP1 counts, and only a small reduction in DARPP-32.

Bonferroni post-hoc analysis also revealed an increase in total striatal cell counts of WT 3-month mice compared to P7 for NEUN, CTIP2, FOXP1 and DARPP-32, with an increase of 248%, 234%, 220% and 175% respectively as shown in Figure 4.05 (NEUN (p=<0.001), CTIP2 (p=<0.001), FOXP1 (p=<0.001) and DARPP-32 (p=<0.001)). However, although MEF2C striatal KO mice show a significant increase in total striatal cell counts for NEUN (189%, p=<0.001) and CTIP2 (192%, p=<0.001), similar to that observed in WT mice, total striatal counts of FOXP1 and DARPP-32 KO mice showed no significant increase between the P7 and 3-months (p=0.224 and p=0.490 respectively).

An ANOVA of striatal volume for both time points showed a significant interaction effect of genotype and age ($F_{1,23}$ = 8.974, p=0.006), along with genotype ($F_{1,23}$ = 8.038, p=0.009) and age ($F_{1,23}$ = 1215.070, p=<0.001) separately. At P7, Bonferroni post-hoc analysis revealed no significant differences between WT and conditional KO striatal volumes (p=0.426), further demonstrating the phenotypic effect seen at 3 months is not present by P7. The significant increase in striatal volume at 3 months relative to P7 was 199% and 161% for WT and conditional KO mice respectively.

These results reveal two key findings:

- The continued increase in size and neuronal cell number of the striatum between P7 and 3 months (albeit less in the KO than WT) indicates that striatal development continues well into the postnatal period in both WT and KO.
- Although the number of NEUN, CTIP2, FOXP1 and DARPP-32 positive cells were significantly lower in the 3-month adult conditional KO striatum, the P7 KO striatum was not different to the WT striatum in terms of volume or neuronal markers, apart from slightly lower DARPP-3 counts. This suggests that striatal KO of MEF2C is having its principle effect on postnatal striatal development, although an earlier effect cannot be absolutely ruled out based on the experiments here.

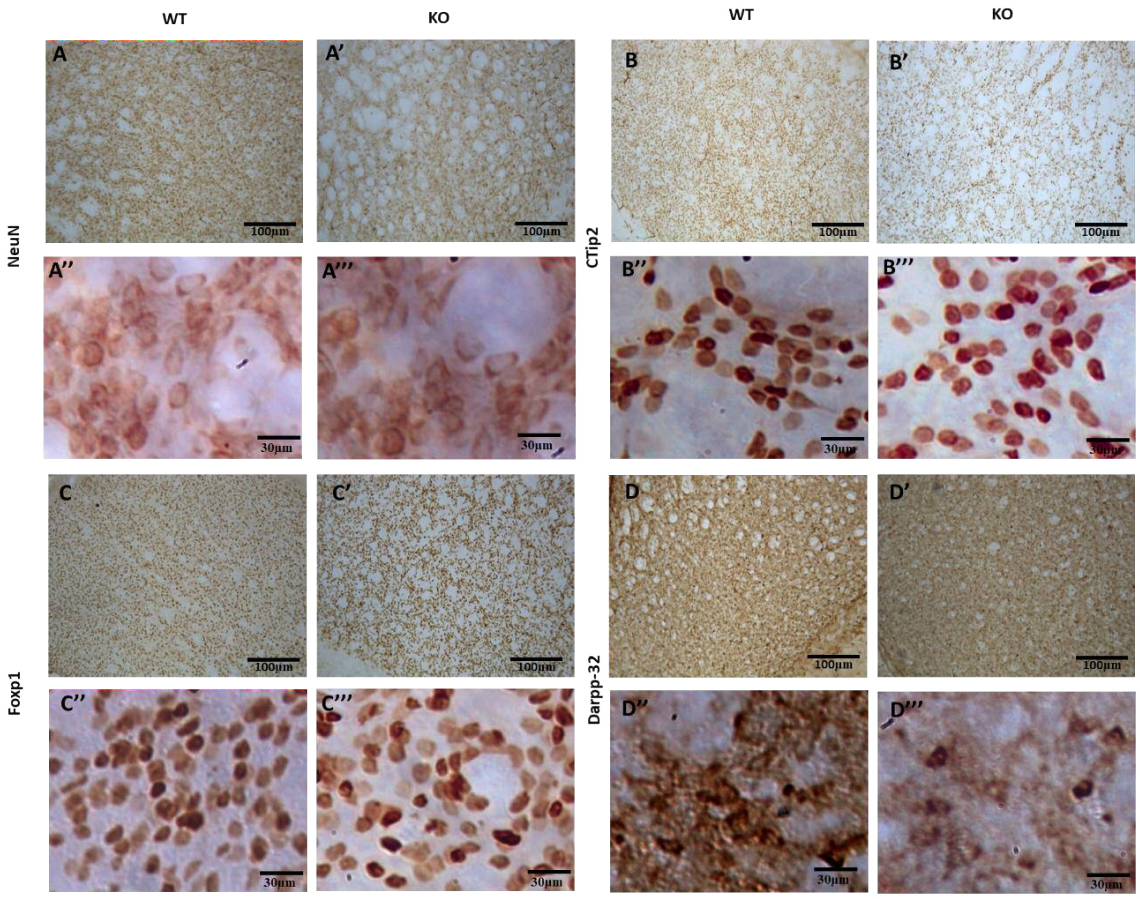


Figure 4.04: (A) WT and (A') KO Photos of P7 striatal tissue taken at 125x and 400x magnification respectively for NEUN in WT (A, A'') and KO (A', A'''); CTIP2 in WT (B, B'') and KO (B', B'''); FOXP1 in WT (C, C'') and KO (C'', C'''); and DARPP-32 for WT (D,D'') and KO (D'', D''').

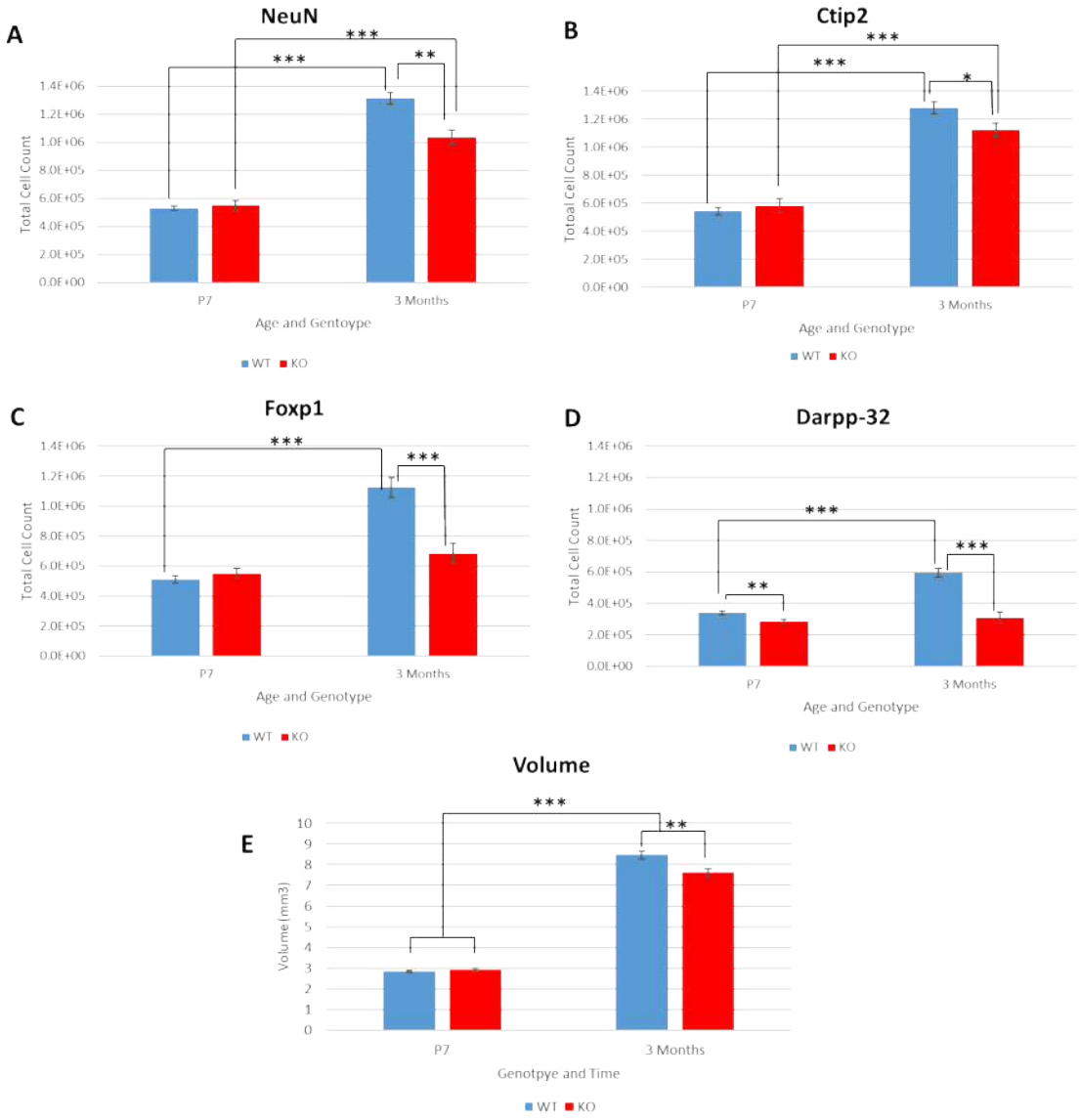


Figure 4.05: Comparison of striatal neuron markers and volume between P7 and 3 months. Total positive striatal cell counts for WT and KO at P7 and 3-months for (A) NEUN, (B) CTIP2, (C) FOXP1 and (D) DARPP-32 antibodies and (E) striatal volume. There are no differences in the general neuronal marker, NeuN, and the MSN marker, CTIP2, at P7. Counts of both markers increase between P7 and 3 months for both genotypes, albeit with a smaller rise in the KO. There is no difference in FOXP1 between genotypes at P7, but a small difference in DARPP-32. Between P7 and 3 months both FOXP1 and DARPP-32 rise significantly in WT striatum, but fail to rise in the KO striatum. P7 WT n=6, KO=5; 3-month WT n=6, KO n=5.

## 4.4 There is substantial striatal cell proliferation between P14-P16, though this is significantly reduced in MEF2C conditional KO mice

The increase in striatal volume and neuronal numbers suggests that neurogenesis continues after P7, with the accompanying increase in CTIP2, FOXP1 and DARPP-32 positive cells suggesting that the neurons generated over this period include MSNs. The postnatal neurogenic period has not been extensively studied. Early investigations into postnatal murine striatal development identified few newly-proliferated cells in the striatum after P4 (Fentress, Stanfield and Cowan, 1981) using $^{3}$H-thymidine labelling, but there are no reports focussed on striatal development at later postnatal periods.

Here, 5-bromo-2′-deoxyuridine (BrdU) injections were used to assess the proliferation activity within the mouse striatum at later postnatal stages to confirm whether cell proliferation occurs in the striatum after P7 and whether this was different between conditional KO and WT animals. Mice were injected with BrdU each day for 3 days before they were culled at P16 or at P23 and stained with an anti-BrdU antibody (Abcam) by Heba Ali as described in Chapter 2, with cell counting and analysis performed myself.

A Two-way ANOVA of total striatal BrdU counts for both genotypes at both ages revealed a significant effect of both genotype ($F_{1,14}$ = 4.857, p=0.045) and age ($F_{1,14}$ = 37.862, p=<0.001), with subsequent Bonferroni post-hoc analysis confirming significantly more $BrdU^{+}$ cells in the WT striatum compared to KO (86.8% more) at P16 (p=0.011), but not at P23 (p=0.839) (Figure 4.06). This indicates that striatal loss of MEF2C results in fewer proliferating cells between P14-P16, aligning with the lower cell counts found in conditional KO striatum at 3 months compared to WT as previously shown in Figure 4.01.

These results also showed there are significantly more $BrdU^{+}$ cells at P16 compared to P23 for both WT and KO mice, with the number of $BrdU^{+}$ cells sharply decreasing between P20-P23 by 91% and 89.4% respectively. These results demonstrate firstly that a substantial number of cells proliferate between P13-P16 in the striatum, confirming neuronal striatal proliferation continues beyond P7. Furthermore, the number of $BrdU^{+}$ cells sharply decreases between P20-P23 to only 8% of that seen between P13-P16 in WT mice (10.6% in KO), indicating the number of recently differentiated cells has decreased by this time.

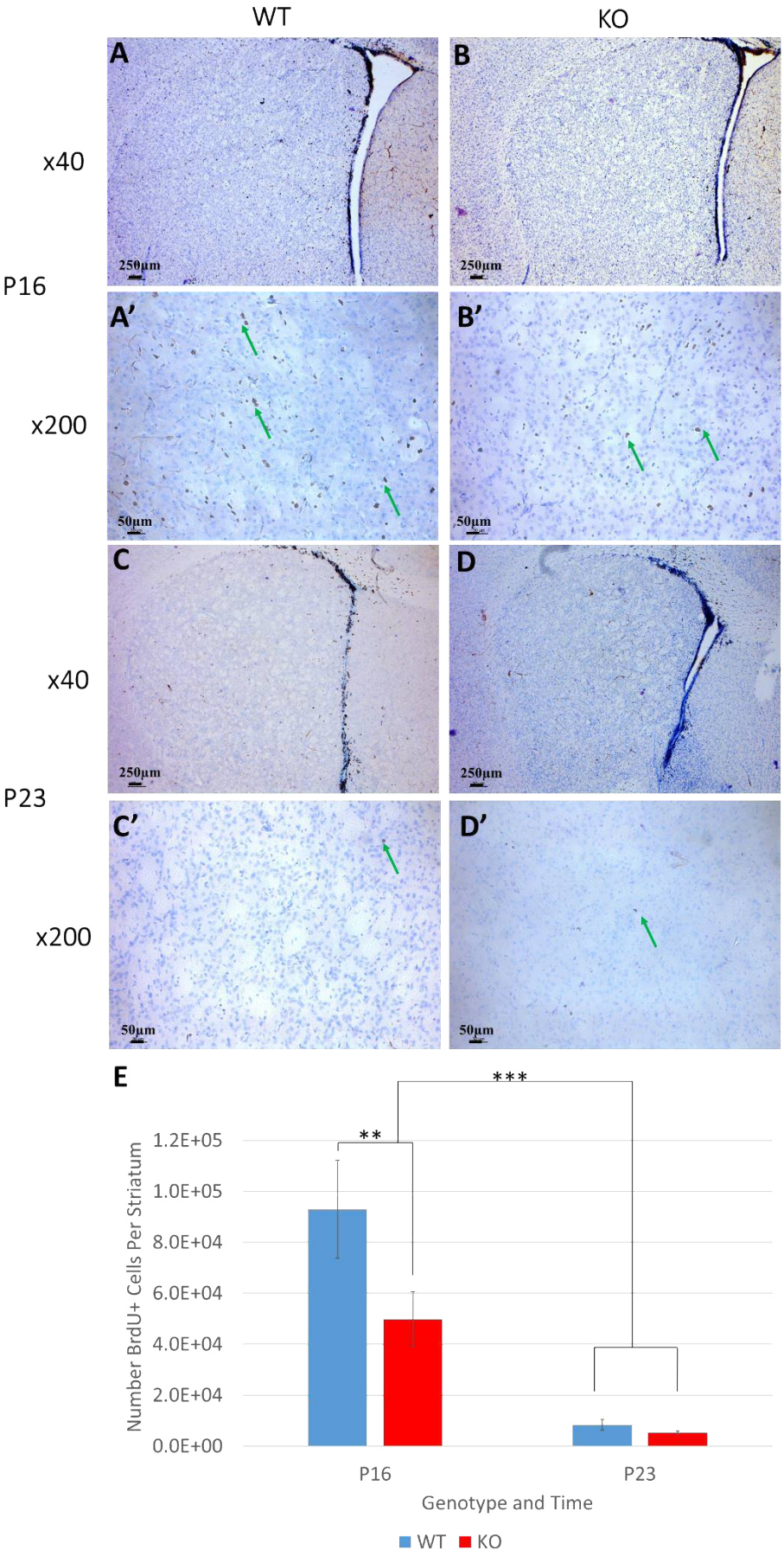
WT
KO
A
B
x40
P16
250µm
A'
B'
x200
50µm
C
D
x40
P23
250µm
C'
D'
x200
50µm
E
***
**
1.2E+05
1.0E+05
8.0E+04
6.0E+04
4.0E+04
2.0E+04
0.0E+00
Number BrdU+ Cells Per Striatum
P16
P23
Genotype and Time
WT
KO

Figure 4.06: DAB staining with anti-BrdU antibody to assay proliferation (with Cresyl violet background stain) showing a large number of $BrdU^+$ cells at P16, with significantly more in WT compared to KO striatum and fewer $BrdU^+$ cells overall at P23. (A) WT and (B) KO Photos of BrdU staining (brown, green arrows) in striatal tissue at x40 and x200 magnification respectively for P16 WT (A, A'), P16 KO (B, B'), P23 WT (C, C') and P23 KO (D, D'). (E) Counts showed fewer $BrdU^+$ cells relative to WT at P16, with no significant difference between genotypes at P23. P16 WT n=4, KO=5; P23 WT n=5, KO n=4.

## 4.5 Conditional KO mice show loss of FOXP1 and DARPP-32 expressing cells in 12- and 18-month Mice

Whilst a role for MEF2C in the postnatal development of the striatum has been identified, there remains the possibility that MEF2C may also play a role in the maintenance of adult striatal cells in the environment of the ageing brain by rendering cells more vulnerable to neurodegeneration, as has been observed in other MEF2C KO models (Okamoto, Li, Ju, Scholzke, *et al.*, 2002; Pon and Marra, 2016), as well as in neurological conditions, including Parkinson's disease and Huntington's disease. Furthermore, an alternative hypothesis to explain the loss of FOXP1 and DARPP-32 expressing cells in the 3-month mice is through loss of already terminally differentiated MSNs, rather than due to an interruption of the cell differentiation program as suggested above. If the latter hypothesis is true, then it may be expected that the loss of striatal neurons will continue as the striatum ages. In order to address this question, striatal MEF2C KO and WT controls were maintained until 12 and 18 months of age for histological analysis.

As shown in Figure 4.08 below, a two-way ANOVA showed no significant effect of genotype in NEUN and CTIP2 positive cell counts between the WT and conditional KO striatum between 12 and 18 months ($F_{1,24}$ =4.025, p=0.056 and $F_{1,23}$ =1.811, p=0.191 respectively). However, there was a significant effect of genotype for FOXP1 and DARRP-32 ($F_{1,24}$ =10.690, p=0.003 and $F_{1,23}$ =30.716, p=<0.001 respectively), with a reduction of 18% and 47% respectively at 12 months and 21% and 16% respectively at 18 months (Figure 4.07 and 4.08). This demonstrates that the reductions in FOXP1 and DARPP-32 positive cell counts seen in conditional KO mice at 3 months persist in older mice, though the reduction was not as marked.

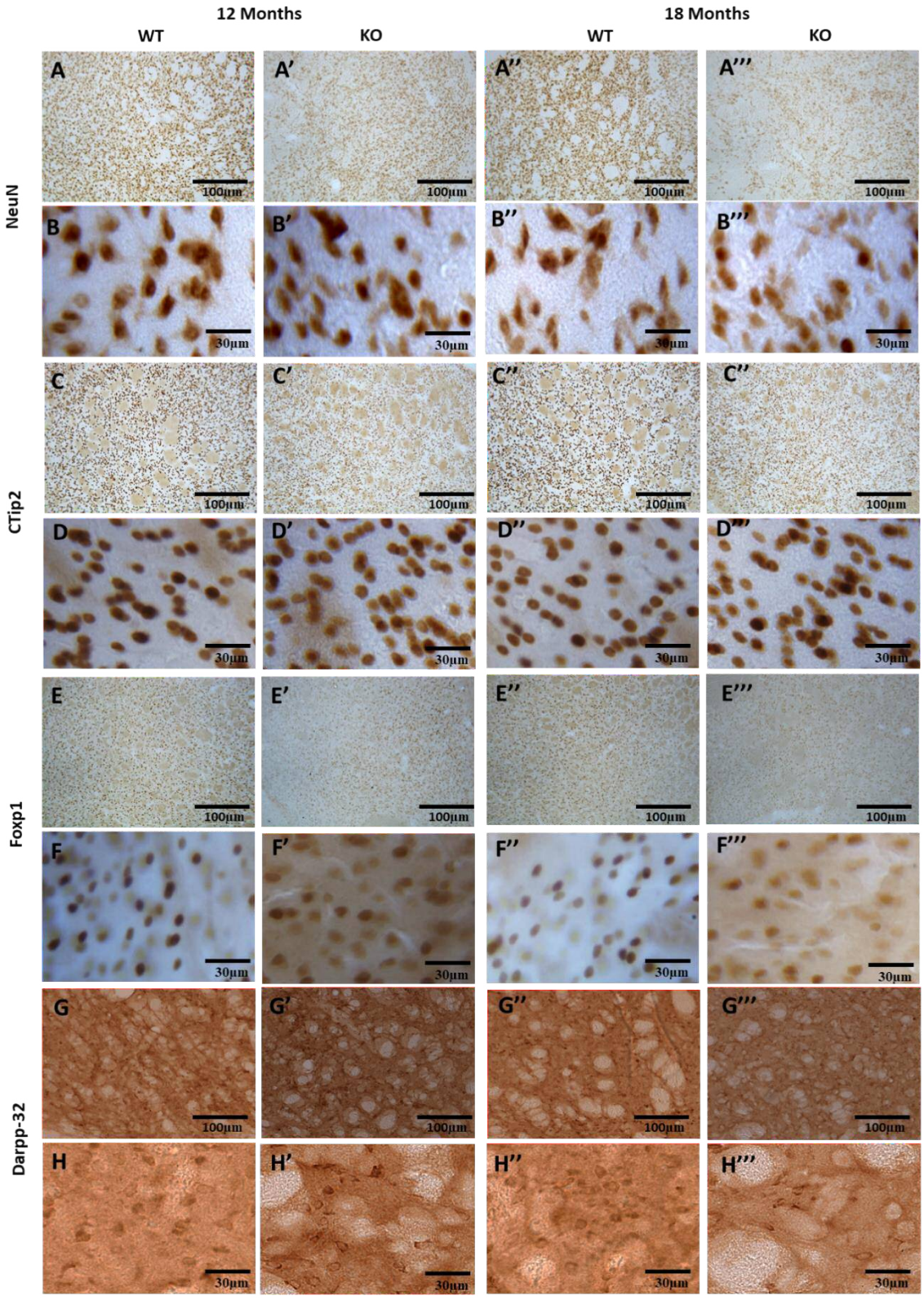


Figure 4.07: Representative photos from 12-month old animals for WT and KO mice respectively, stained using antibodies to NEUN (A,B,A',B'); CTIP2 (C,D,C',D'); FOXP1 (E,F,E',F') and DARPP-32 (G,H,G',H'). Typical examples from 18-month old animals for WT and KO mice respectively, stained using antibodies to NEUN (A'',B'',A''',B'''); CTIP2 (C'',D'',C''',D'''); FOXP1 (E'',F'',E''',F''') and DARPP-32 (G'',H'',G''',H''').

This suggests that while there remains a significant difference in the protein expression profile of striatal MSNs in terms of FOXP1 and DARPP-32 expression, the total neuronal count no longer differs between WT and MEF2C conditional KO mice.

As shown in Figure 4.08, all markers remained stable in WT striatum between 3 and 18 months. As reported in Figure 4.01 there was reduction of all four markers, compared to WT, in KO striatum at 3 months but by 12 months this difference was no longer significant for NEUN and CTIP2. Counts of FOXP1 and DARPP-32 remained significantly lower, but in this study there was some evidence of recovery of DARPP-32 levels between 3 and 18 months (significant increase of 64.4% between 3 and 18 months ($F_{2,30} = 4.022$, p=0.026). Numbers of NEUN, CTIP2 and FOXP1 positive cells did not change significantly over the same period ($F_{2,31} = 0.25$, p=0.781; $F_{2,30} = 0.885$, p=0.423 and $F_{2,31} = 2.384$, p=0.109 respectively).

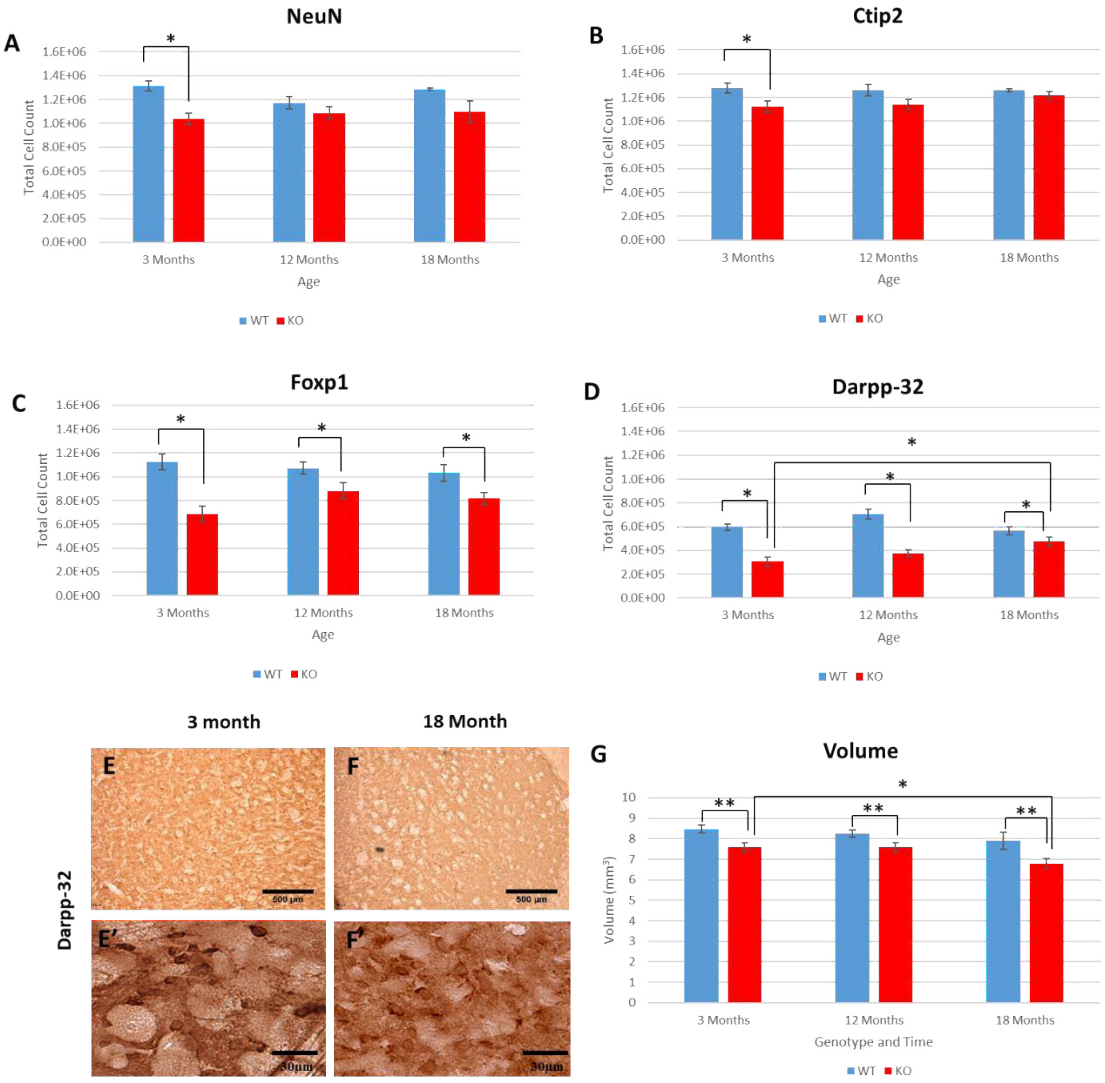


Figure 4.08: Total striatal cell counts for WT and KO mice from 3 to 18 months for (A) NEUN, (B) CTIP2, (C) FOXP1 and (D) DARPP-32, showing stability of all markers in the WT striatum, and reduction of all four markers in KO striatum, compared to WT, at 3 months. There is a loss of this differential by 12 months for NEUN and CTIP2, but continued a reduction of FOXP1 and DARPP-32 cells in the conditional KO striatum compared to WT. There is some evidence of recovery of DARPP-32 levels between 3 and 18 months. Representative photos at 3 (E, E') and 18 (F, F') months of DAB staining with an anti-DARPP-32 antibody showing (some recovery of striatal DARPP-32. (G) 18-month KO striatal volume is significantly reduced relative to 3-months. (3-month WT n=6, KO n=5; 12-month WT n=11, KO n=8; 18-month WT n=4, KO n=5).

ANOVA of striatal volumes over all adult ages showed a significant effect between genotypes ($F_{1,33}$ =11.104 p=0.002), with subsequent Bonferroni post-hoc analysis showing a slight but significant decrease of 8.1% in the MEF2C KO striatal volume compared to WT at 3 months as previously described, 10.2% at 12 months (p=0.008) and 14.3% at 18 months (p=0.01).

Given the sharp increase in striatal volume observed between P7 and 3-month adult mice, the question remained as to whether striatal volume continues to change once adulthood has been reached and the mouse ages, or whether the volume at 3-months is maintained throughout. No significant differences were found between WT mice over time (Figure 4.08) demonstrating that the WT mouse striatal volume remains consistent into old age, comparable to previous investigations that found no differences between young-adult and old-age rats (Kelly *et al.*, 2009) or in mice even after 2 years (Bayram-Weston *et al.*, 2012). It is interesting to note however that these results differ to what is seen in humans, where the striatum was found to be the second most affected in terms of volume decline in old age after the prefrontal cortex (Peters, 2006).

However, as shown in Figure 4.08 there is a significant reduction in volume of 10.8% in the 18-month conditional KO striatum compared to the 3-month ($F_{2,29}$ =3.234 p=0.048), but no significant difference relative to 12-months. This suggests that further investigation into older age groups may be warranted in order to see whether these changes a meaningful, and to determine with certainty whether or not total cell counts are reduced in the conditional KO 12-18-month striatum relative to WT. Due to the reduced volume of the adult KO striatum at 18 months relative to 3 months, NEUN, FOXP1 and DARPP-32 positive cell densities were found to significantly increase in the conditional KO mouse between 3 and 18 months by 26.5%, 24.1% and 32.3% for NEUN, FOXP1 and DARPP-32 respectively ($F_{3,44}$ =18.092, p=0.005, $F_{3,45}$ =68.138, p=0.02 and $F_{3,43}$ =60.884, p=0.05), although not for CTIP2 ($F_{3,38}$ =18.068, p=0.984) as confirmed by ANOVA and Bonferroni Post-Hoc analysis. Taken together with total cell counts this suggests that the striatum reduces in structure, but not due to a reduction of MSNs.

## 4.6 Comparison of MEF2C Conditional KO with a Conditional/null KO.

The extent of loss of MEF2C in the *Mef2c*$^{loxP/loxP}$ Gsx2-Cre$^{+}$ mouse is dependent on the extent of Cre-mediated excision, i.e. a high loxP/Cre recombination efficiency will result in gene deletion in a high proportion of cells. The LacZ-Gsx2-Cre result reported in Chapter 3 suggests that Cre expression is widespread in the striatum, but it is nevertheless possible that recombination is less efficient than hoped. In order to provide further evidence that the results discussed in this chapter in the conditional KO mouse were brought about through a substantial loss of striatal MEF2C, a comparison was made with models containing one conditional KO allele and one null allele (i.e. complete

loss of that allele in all tissues). Two such mice were available to this project: *Mef2c*$^{loxP/Tm1}$ Gsx2-Cre$^{+}$ and *Mef2c*$^{loxP/Tm2}$ Gsx2-Cre$^{+}$ KO. For the purposes of this analysis, both the *Mef2c*$^{WT/Tm1}$ and *Mef2c*$^{WT/Tm2}$ KO variants have been categorised together as "Floxed-Null" genotypes, as molecularly they both achieve excision of *Mef2c* exon 2 and therefore should functionally achieve identical knockdown of MEF2C protein formation. It is necessary therefore to compare these KO variations with conditional KO mice in order to determine whether there are any differences that may occur through inefficient recombination.

"Floxed-Null" and MEF2C conditional KO mice were collected at P7, 3, 12 and 18 months of age and stained for each of the 4 neuronal and MSN markers used in this investigation. A series of two-way ANOVAs were conducted on both genotypes with all ages, for a single marker. No significant effects of genotype nor any significant interaction between age and genotype were found in NEUN positive cell counts (($F_{1,45}$ =0.030, p=0.863) and ($F_{1,45}$ =1.649, p=0.192) respectively). The same was found for CTIP2 (($F_{1,35}$ =0.343, p=0.562), ($F_{1,35}$ =1.064, p=0.377)); FOXP1 (($F_{1,45}$ =1.425, p=0.239), ($F_{1,45}$ =0.404, p=0.751)) and DARRP-32 (($F_{1,44}$ =0.637, p=0.429) ($F_{1,44}$ =0.789, p=0.506)). This indicates that MSNs remain equally affected by MEF2C KO in terms of their key protein expression markers (Figure 4.09). Moreover, no significant difference between genotype nor any significant interaction between age and genotype was found in striatal volume (($F_{1,46}$ =0.601, p=0.442) and ($F_{1,46}$ =0.507, p=0.679) respectively), suggesting the striatum develops structurally similarly in both genotypes (Figure 4.09).

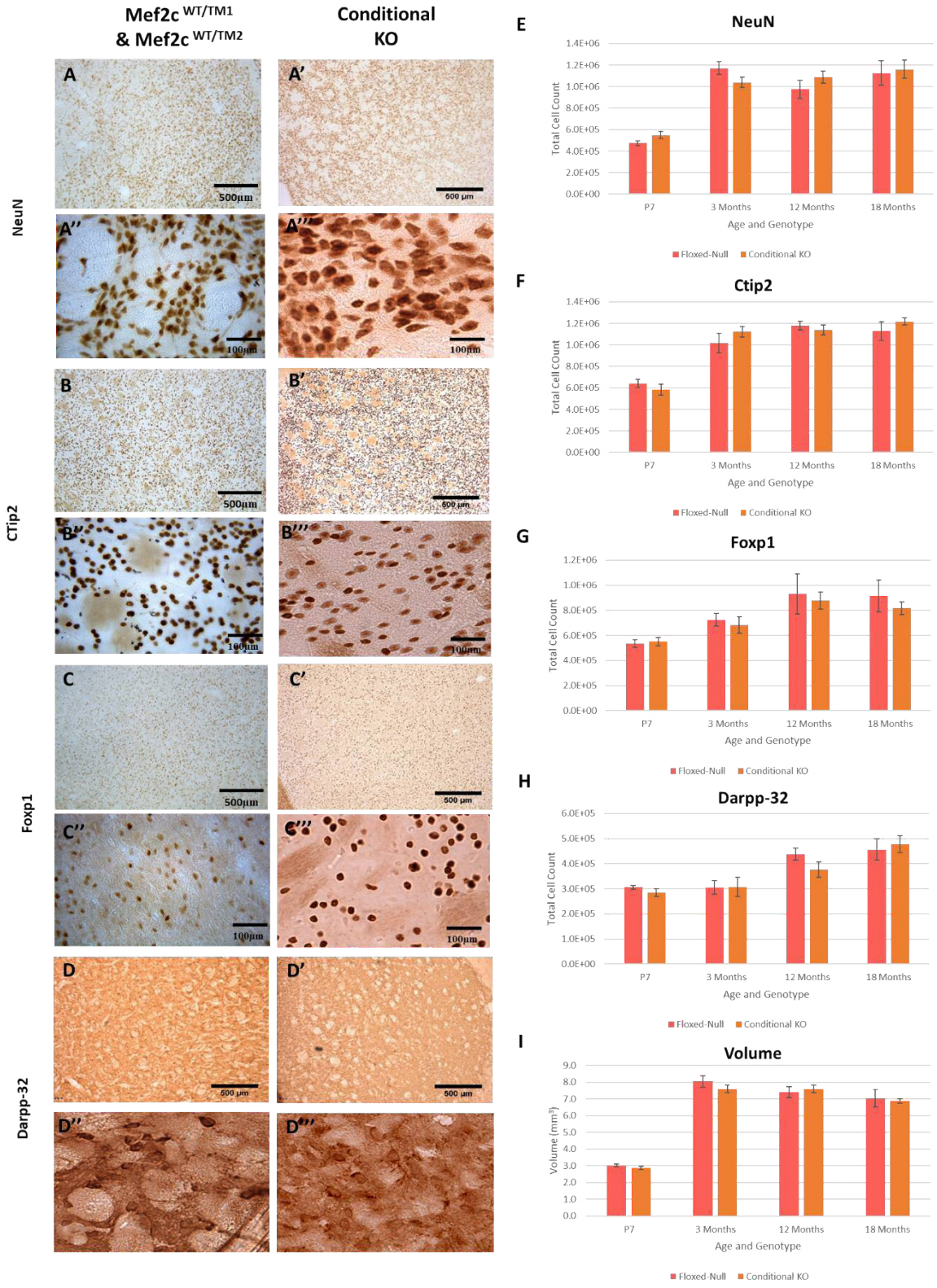
Mef2c WT/TM1 & Mef2c WT/TM2
Conditional KO
NeuN
CTip2
Foxp1
Darpp-32
A
A'
A''
A'''
B
B'
B''
B'''
C
C'
C''
C'''
D
D'
D''
D'''
500µm
100µm
E
NeuN
F
Ctip2
G
Foxp1
H
Darpp-32
I
Volume
Total Cell Count
Volume (mm³)
P7
3 Months
12 Months
18 Months
Age and Genotype
Floxed-Null
Conditional KO

Figure 4.09: Comparison of neuronal and MSN markers of the conditional/null (*Mef2c*$^{loxP/Tm1}$ / *Mef2c*$^{loxP/Tm2}$ Gsx2-Cre$^{+}$ ) and conditional (*Mef2c*$^{loxP/loxP}$ Gsx2-Cre$^{+}$) mice, showing no significant differences in the total striatal number of any of the MSN/neuronal markers used in this investigation between genotypes, nor any difference in striatal volume. Representative images taken at 125X or 400X magnification respectively for anti-NEUN antibody for floxed/null (A,A'') and conditional KO (A',A'''); CTIP2 for floxed/null (B,B'') and conditional KO (B', B'''), FOXP1 for floxed/null (C,C'') and conditional KO (C', C''') and DARPP-32 for floxed/null (D,D'') and conditional KO (D', D'''). Total striatal cell counts for WT and KO mice at all ages for NEUN (E), CTIP2(F), FOXP1(G) and DARRP-32(H), along with striatal volumes (I). P7 (Floxed-null n=10, Conditional KO n=8), 3-months (Floxed-null n=7, Conditional KO n=5) 12-months (Floxed-null n=4, Conditional KO n=8), 18-months (Floxed-null n=5, Conditional KO n=4).

In summary, there were no significant differences between the *Mef2c*$^{loxP/loxP}$ Gsx2-Cre$^{+}$ (double conditional KO) mice and the other KO variants (one conditionally KO allele and one null; either Tm1 or Tm2) in striatal or cortical tissues. This indicates that the recombination efficiency of the Gsx2 promoted loxP/Cre is high enough to be functionally similar to a single complete allele loss of *Mef2c* and so further studies were undertaken with the *Mef2c*$^{loxP/loxP}$ Gsx2-Cre$^{+}$ (double conditional KO). Whilst it remains possible that there may be other differences between these genotypes given the loss of a single *Mef2c* allele in all brain tissues, no discernible differences were found in cortical or striatal tissues between WT and *Mef2c*$^{WT/Tm1}$ mice (see Chapter 3). Moreover, this selection provided an additional advantage for selecting the *Mef2c*$^{loxP/loxP}$ Cre$^{-}$ genotype as the WT control, as it allows for a clear genetic distinction between the WT and KO cohorts and the observed differences between these genotypes to be attributed directly to the presence of the Gsx2-Cre, without the possibility of loss of MEF2C in other brain regions influencing results.

## 4.7 Dendrite and Spine analysis

### 4.7.1 Neurons of the MEF2C conditional KO striatum have significantly greater spine/neuron ratio and spine density than WT neurons at 12 months

Conditional GFAP-Cre mediated loss of MEF2C has previously been reported to increase spine density and alter dendrite formation in Hippocampal cells (Barbosa *et al.*, 2008), whilst also affecting excitatory synapse function (Adachi *et al.*, 2016), though striatal MSNs were not assessed in this study. In the developing mouse cortex and

striatum there is an early phase of dendritic spine addition and synaptogenesis followed by spine pruning and synaptic refinement, during which unnecessary spiny synapses are eliminated (Brand and Rakic, 1979; De Felipe, 1997; Holtmaat *et al.*, 2005; Zuo *et al.*, 2005). Thus, spine shrinkage and elimination appear to be essential for fine tuning of neural circuits both when they are established during development and during learning in adults.

To determine whether there are effects on dendrites or spines of striatal neurons lacking MEF2C, Golgi-Cox analysis was performed in 12-month old mice to assess whether conditional *Mef2c* KO mouse striatal neurons show any signs of abnormal development or degeneration as is seen in hippocampal cells (Barbosa *et al.*, 2008). Analysis was undertaken from a total of 290 dendrites, from 12 and 23 neurons from 4 WT and 6 KO mice respectively. The parameters assessed were: the numbers of dendrites per neurons, dendritic length, numbers of spines per dendrite and spines per neuron, spine density and the proportions of primary, secondary and tertiary dendrites.

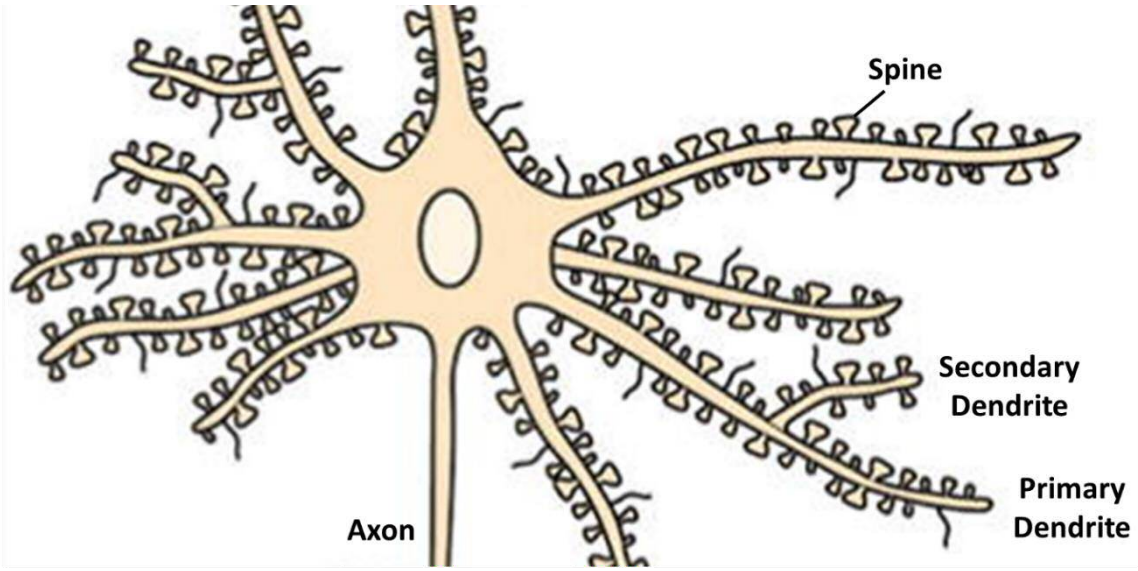


Figure 4.10: Diagram illustrating a neuron with Primary and Secondary dendrite types labelled (tertiary dendrites originate from secondary) and spines lining each dendrite. Adapted from (Smrt and Zhao, 2010).

Analysis of spinal counts was conducted using a mixed-effect model. Typically, investigations involving spinal counts (including the dendritic/spinal effect of MEF2C KO in hippocampal cells (Barbosa *et al.*, 2008)) use standard ANOVA analysis (or students t-test) utilising either dendrites or neurons as the biological replicate, with only 1 of 19 total investigations found to use the more appropriate two-level nested ANOVA (Paternoster *et al.*, 2018). Standard ANOVA analyses in this way grossly overestimate

statistical effect, and is strictly incorrect as a biological replicate if no test has been made to note the effect of “dendrite” or “neuron” in such analyses. The solution of simply averaging data at the animal level (aggregating data) effectively throws away information and thus statistical power of detection is lost, though in this instance the error is on the conservative side and will likely therefore only produce Type 2 errors. Furthermore, relying on aggregated data poses the risk of ecological fallacy, where a false inference about spines may be drawn based on the higher levels – in this case, animal. The most appropriate statistical test therefore is the mixed-effect analysis, where data is analysed in levels: Level 0 = dendrite, level 1 = neuron, level 2 = mouse, with “genotype” set as the fixed variable and mouse, neuron and dendrite within each genotype the random variables, as is the recommended practice (Paternoster *et al.*, 2018).

The number of spines per dendrite increased by 58.1% between MEF2C conditional KO and WT mice ($F_{1,8.6}$ = 5.422, p=0.046), with no difference between genotypes found in dendrite length ($F_{1,8.9}$ = 0.162, p=0.697), as shown in Figure 4.11 below. Therefore, there was a significant increase in spine density of 78% between MEF2C conditional KO mice and WT ($F_{1,8.3}$ =7.552, p=0.024). Whilst this finding can be compared with the increase in spine density of 71.4% previously reported in hippocampal neurons with loss of MEF2C function (Barbosa *et al.*, 2008), it is difficult to confidently do so due to the choice of statistical analysis used in that investigation, however I have taken the assumption that their findings are true.

Furthermore, there was no significant difference in dendrite number ($F_{1,6.8}$ =0.936, p=0.366) or ratios of primary, secondary or tertiary dendrite types between genotypes ($F_{1,8.8}$ = 0.373, p= 0.557; $F_{1,7.5}$ = 0.053, p=0.824 and $F_{1,33}$ = 0.037, p=0.849 respectively) between MEF2C conditional KO and WT mice, thus there was a significant increase of 60% in the total number of spines per neuron ($F_{1,8.3}$ = 5.012, p=0.049).

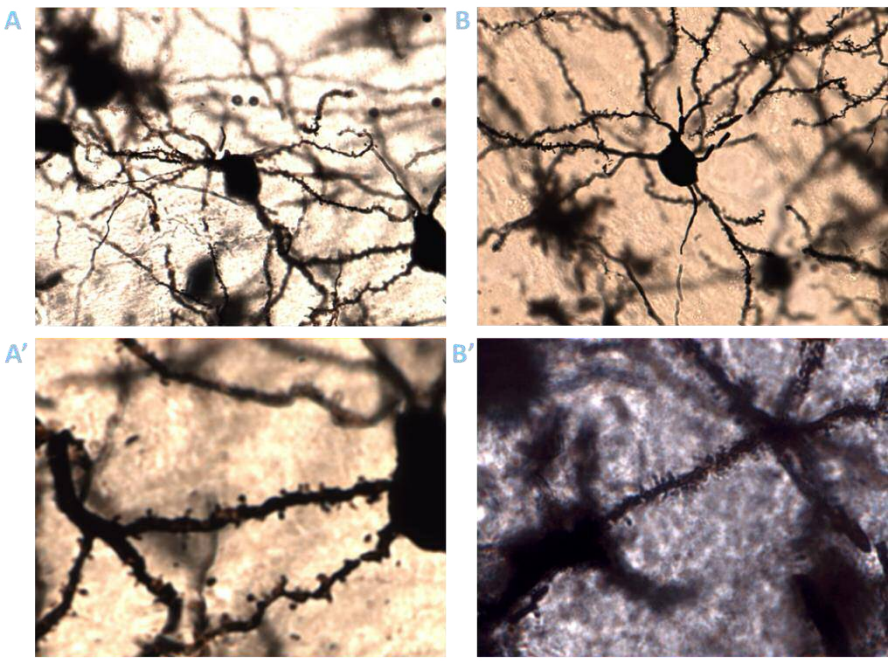
A
B
A'
B'

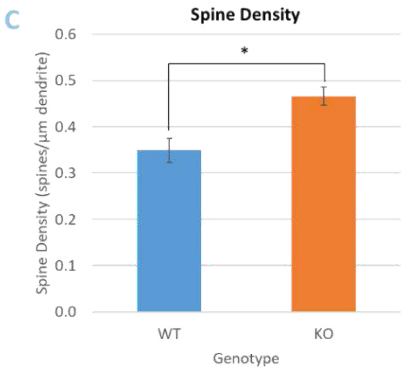
C
Spine Density
Spine Density (spines/µm dendrite)
0.6
0.5
0.4
0.3
0.2
0.1
0.0
*
WT
KO
Genotype

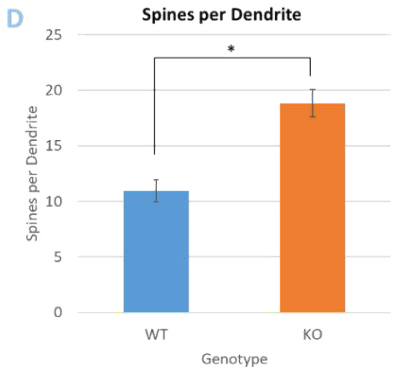
D
Spines per Dendrite
Spines per Dendrite
25
20
15
10
5
0
*
WT
KO
Genotype

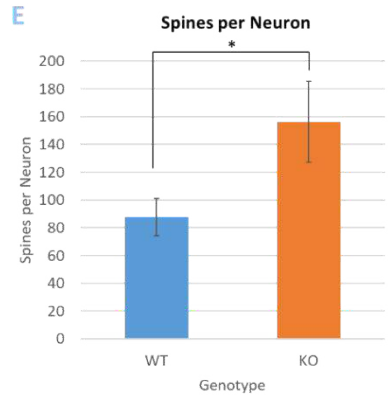
E
Spines per Neuron
Spines per Neuron
200
180
160
140
120
100
80
60
40
20
0
*
WT
KO
Genotype

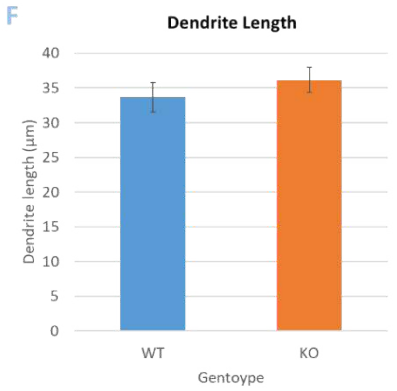
F
Dendrite Length
Dendrite length (µm)
40
35
30
25
20
15
10
5
0
WT
KO
Gentoype

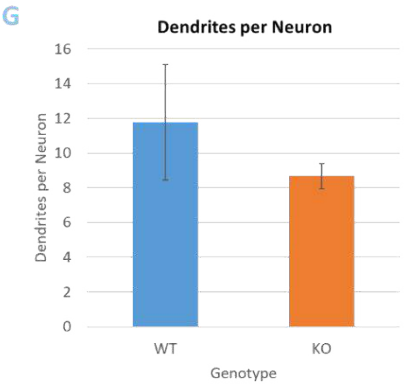
G
Dendrites per Neuron
Dendrites per Neuron
16
14
12
10
8
6
4
2
0
WT
KO
Genotype

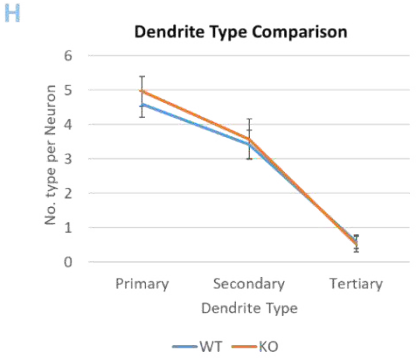
H
Dendrite Type Comparison
No. type per Neuron
6
5
4
3
2
1
0
Primary
Secondary
Tertiary
Dendrite Type
WT
KO

Figure 4.11: Comparisons of dendrite and dendritic spine parameters in WT and striatal MEF2C KO mice following Golgi-Cox staining. Representative photos of Golgi-Cox staining in (A, A') WT and (B, B') KO at 200x and 400x magnification respectively. A significant increase was found in MEF2C striatal KO compared to WT samples for (C) spine density, (D) number of spines per dendrite and (E) the number of spines per neuron. No difference between WT and KO was observed in (F) dendritic length, (G) the number of dendrites per neuron or (H) the ratio between primary, secondary and tertiary dendrites (WT n=4, KO=6).

This demonstrates that loss of MEF2C results in abnormal spinal count of MSNs, without affecting dendritic formation.

## 4.8 Discussion

Examination of adult post-mortem mouse brains revealed that the striatal KO of MEF2C interfered with development of the striatum and specifically, the MSN content. First, there was evidence that by three months the striatum was smaller in the MEF2C KO, whereas the volume of the adjacent motor cortex was unchanged. This suggested a selective effect on the striatum, although further measurements of other brain regions would be needed to confirm this. A significant reduction was seen in the total numbers (per striatum) of total neurons (according to NEUN staining) and the three MSN markers CTIP2, FOXP1 and DARPP-32. Interestingly, the numbers of CTIP2 cells per $mm^2$ (referred to as density) was not different in KO and WT, suggesting that the drop in CTIP2 positive cells may be related to the overall loss of striatal tissue. However, it was notable that the proportionate loss of FOXP1 and DARPP-32 was greater than that of CTIP2 (39%, 41.8% and 12% respectively). Previous studies have demonstrated almost complete co-expression of CTIP2 and FOXP1 in the normal mouse striatum and approximately 65% of co-expression of DARPP-32 with CTIP2, despite the fact that DARPP-32 is considered the "gold standard" MSN marker (Precious *et al.*, 2016), so it would be anticipated that there should be substantial numbers of CTIP2 cells that do not express FOXP1 in the MEF2C KO striatum. This was confirmed by CTIP2/FOXP1 co-labelling studies in which a substantial proportion of cells in the MEF2C KO striatum were positive for CTIP2 but not FOXP1. It is important to note that careful inspection of the confocal images revealed that many apparent $CTIP2^{+}/FOXP1^{-}$ cells did in fact contain very low levels of FOXP1. This change in the characteristics of the MSNs suggest that MEF2C may be important for regulating the numbers of MSNs and for their proper differentiation.

As shown in Chapter 3 (Figure 3.10), no significant difference was found between the conditional MEF2C striatal KO and the Floxed-Null (*Mef2c*$^{loxP/TM1}$ / *Mef2c*$^{loxP/Tm2}$) KO variants. Floxed-Null variants ensure that a single allele is knocked out in all cells throughout all stages of development, with only on allele capable of expressing MEF2C in all other cells. The lack of any significant difference between the conditional MEF2C striatal KO and the Floxed-Null variants suggests that the Gsx2-Cre inhibits a substantial proportion of MEF2C striatal expression, as it must be capable of reducing MEF2C expression to the extent same extent as if one allele was fully knocked-out. It should be noted that a single allele mutation is not enough to generate the phenotypes described in the conditional KO mice, providing further evidence that a very large proportion of MEF2C expression is achieved through the MEF2C conditional KO mouse.

The significant increase in DARRP-32 total cell counts in the MEF2C striatal KO at 18 months relative to earlier time points may suggest that the KO phenotype is recovering over time and whilst there is no significant increase of any other marker, a similar (though non-significant) trend can be seen in the FOXP1 and NEUN positive cell counts. It should be noted however that a return to WT levels of total cell expression of these for markers does not necessarily demonstrate recovery, as other components of the striatum, such as its structure, appear to be changing as reflected by the reduction in overall striatal volume. Overall, these results show that the expression of neuronal and MSN markers in the MEF2C conditional KO mouse does not appear to deteriorate as mice progress through adulthood, suggesting loss of striatal MEF2C does not lead to MSN degeneration. Thus, MEF2C is required during the development of the striatum and MSNs, rather than for MSN maintenance. This is important to consider in the context of known MEF2C-related conditions such as the 5q14 syndrome, particularly as MEF2C's recent discovery as a critical component of the neuronal system suggest it could be functionally involved in a range of further conditions.

However, the consistency of striatal volume in WT over 3, 12 and 18 months does not appear to be replicated in the conditional KO model, where there is a relative decrease of striatal volume at 18 months in conditional MEF2C KO mice compared to 3- and 12-month mice (see Figure 3.21). Whilst further investigation is warranted to determine the meaningfulness of this finding, this suggests the MEF2C is integral not only in the structural formation of the developing striatum, but also in its maintenance into old age. Moreover, DARPP-32 positive cell counts were found to have increased between 3-18 months. This may indicate that should any recovery be taking place over time, it is strictly on a cellular expression basis and not through correction of striatal structure. Adult neurogenesis and cell turnover have previously been noted in the adult hippocampus and olfactory bulb (Belluzzi *et al.*, 2003; Stenman, Toresson and Campbell, 2003; Kempermann, Song and Gage, 2015), thus there remains the possibility of some adult neurogenesis occurring in the striatum (or cells migrating to the striatum) (Das and Altman, 1970; Luzzati *et al.*, 2014), however there are to date no examples of striatal volume increasing after 3 months of age.

Conditional striatal MEF2C KO at P7 resulted in a small but significant decrease of DARPP-32 cell counts, while there was little effect on NEUN, CTIP2 and FOXP1, in contrast to the phenotype observed at 3 months. However, there is a reduction of DARPP-32 expression in the conditional KO striatum compared to WT at P7, suggesting that loss of MEF2C affects proper differentiation and/or maturation of MSNs at this time point. This is supported by the findings that MEF2C is a required factor for neuronal

maturation (Barbosa *et al.*, 2008) (and thus expression of the mature MSN marker DARPP-32), alongside cell fate determination and as an anti-apoptotic factor (S Okamoto *et al.*, 2000), with both effects observed postnatally. Moreover, at P7 there is extensive striatal LacZ staining in Gsx2-Cre animals, suggesting that it is unlikely that the relative lack of differences between genotypes at P7 are due to a poor/incomplete KO of MEF2C. This further suggests that MEF2C has a greater role in the development of the striatum after P7.

Comparatively little has been written about the development of the mouse striatum postnatally, since the publication of key early papers (Smart and Sturrock, 1979; Fentress, Stanfield and Cowan, 1981) which suggested no significant change in rat striatal development after P7. Most striatal investigations have typically focused on embryonic and adult models (Gary E Lyons, Micales, Schwarz, J. F. Martin, *et al.*, 1995; S Okamoto *et al.*, 2000; Barbosa *et al.*, 2008; Paciorkowski *et al.*, 2013). The results of this chapter show that in WT mice there is a substantial and significant increase between P7 and all adult ages in terms of both striatal volume and the total number of cells expressing each of the four markers. This is supported by previous observations of mass increase of brain regions including the striatum between postnatal and adult murine models (Baydyuk *et al.*, 2011), as an increased striatal mass is only possible through volumetric expansion as a result of an increase in the total number of cells, despite early claims that rat striatal volumes remained unchanged between thee time points (Fentress, Stanfield and Cowan, 1981). This strongly suggests that a second period of neurogenesis occurs between P7 and 3-months of age, or that the first period of neurogenesis is still ongoing. The observed increases should be unsurprising given the comparatively small size and mass of P7 brains compared to adult, although there has been little focus on this in the literature. There are however suggestions that this secondary period may indeed occur in other species including the guinea pig and in striatal in-vitro cultures (Luzzati *et al.*, 2014; Maya-Espinosa *et al.*, 2015). These results also demonstrate that it is likely during this latter postnatal period of striatal development that MEF2C plays its most prominent role, as evidenced by the phenotypic differences observed in the adult conditional KO mouse.

BrdU studies confirmed that proliferation is still ongoing at P13-P16 and that this is reduced following loss of MEF2C, suggesting MEF2C is required for normal proliferative activity in the later post-natal striatum. These results align with the increase in total striatum cell counts between P7 and 3 months and suggest that the lower total cell counts seen in the 3-month conditional KO striatum could be due to reduced proliferative activity following loss of MEF2C. Furthermore, this provides further evidence that MEF2C has

important functions in the later postnatal striatum. However, double staining with neuronal/MSN markers was not undertaken so it is not possible to confirm whether the proliferation was predominantly in neurons/MSNs.

As shown in Figure 3.23, dendrite formation is unaffected following loss of MEF2C, suggesting that the processes governing their development and maintenance are un-reliant on MEF2C expression. However, the significant increase in spine density, the number of spines per dendrite and the number of spines per neuron observed in conditional KO striatal cells compared to WT shows that MEF2C expression is critical for proper spinal development and/or maintenance. This is consistent with embryonic and postnatal deletion of MEF2C in the forebrain, where an increased excitatory synapse function and dendritic spines in vivo in granule cells of the hippocampal dentate gyrus was found (Barbosa *et al.*, 2008; Adachi *et al.*, 2016) whilst also being required for synapse elimination following induction of extracellular signals (Elmer *et al.*, 2013) and synaptic pruning (Pfeiffer *et al.*, 2010). Abnormal spinal formation will likely have an effect on striatal-cell electrophysiology in the adult mouse, possibly with increased excitatory synapse function as seen in hippocampal cells (Barbosa *et al.*, 2008; Adachi *et al.*, 2016) which is an important consideration when attempting to understand the pathology of human *Mef2c*-related conditions such as the 5q14 syndrome (Zweier *et al.*, 2010; Zweier and Rauch, 2012; Shim *et al.*, 2015; Rocha *et al.*, 2016), despite such phenotypes not being detected in mice. Further experiments are required to determine whether MEF2C is required for proper initial spinal development, and/or the maintenance of striatal cell spines.

An increased differential between CTIP2/FOXP1 and DARPP-32 positive cells may be due to a variety of reasons, such as: the presence of a greater percentage of immature MSNs (particularly in embryonic and early post-natal striatum); a proportion of cells having undergone aberrant development; or some cells containing undetectably low protein expression levels at the point of tissue fixation.

As previously described, CTIP2 does not co-label with any interneuron markers, but co-localises with FOXP1 in ~99% of MSNs (Arlotta *et al.*, 2008), suggesting there is a small subset of MSNs within the adult striatum that express CTIP2, but not DARPP-32 or FOXP1. Immunohistochemistry analysis with CTIP2 also showed a significant decrease of 21% in the total number of CTIP2 expressing cells in the KO striatum compared to WT, though this is substantially less than the other striatal markers FOXP1 (39%) and DARPP-32 (48%), more closely resembling the loss observed with NEUN (12%). This

may indicate that the MSN subset that exclusively expresses CTIP2 without DARPP-32 or FOXP1 is proportionally increased in the conditional MEF2C KO.

MEF2C has previously been described as a crucial factor for cell fate determination in non-neural cell types including myeloid cells (Schüler *et al.*, 2008), where its holds key roles in immune development. Sox genes have demonstrated a critical role in neuronal cell fate determination (Lefebvre *et al.*, 2007) with an already established role for Sox18 in the MEF2C regulation of cardiac tissue (Hosking *et al.*, 2001). Furthermore P38 MAPKs, a known regulator of MEF2C, have demonstrated involvement in neuronal cell fate determination, possibly altering its behaviour dependant on stress response to generate cell required cell types (Takeda and Ichijo, 2002). Moreover, MEF2C has been shown to be important for the proper differentiation of hippocampal and cortical plate neurons in-vivo and also of neuronal cells in-vitro (Barbosa *et al.*, 2008; Hao Li, Radford, Ragusa, Shea, McKercher, Zaremba, Soussou, Nie, Kang, Nakanishi, *et al.*, 2008). It is therefore reasonable to suggest that without MEF2C, MSNs are driven down a differentiation path different to that which they otherwise would, possibly towards an MSN subtype that expresses CTIP2 without FOXP1 and DARPP-32.

DARPP-32 has also classically been described as a mature marker for MSNs (Ouimet, Langley-Gullion and Greengard, 1998; Kelly *et al.*, 2009; Evans *et al.*, 2012; Precious *et al.*, 2016) which could indicate that a KO of MEF2C in the developing striatum prevents many MSNs from reaching maturity, interrupting their differentiation program at some stage. This hypothesis is supported by the reduced expression of FOXP1 observed in the 3-month conditional KO striatum, as FOXP1 expression occurs earlier in MSN differentiation than DARPP-32 (Arlotta *et al.*, 2008; Precious *et al.*, 2016), indicating therefore a limitation or early-termination of MSN differentiation or maturation following FOXP1 expression. However CTIP2, like FOXP1, is also expressed in early post-mitotic cells (Arlotta *et al.*, 2008) with its expression remaining present throughout MSN differentiation through to their mature state. As CTIP2 expression is affected to a lesser degree than FOXP1 in the conditional KO, it is possible that any differentiation-cycle interruption occurs after the induction of CTIP2 expression, but at the point of FOXP1 expression, though further experiments are required to determine if this is correct.

Whilst it is possible that $CTIP2^{+}$ $FOXP1^{-}$ neuronal migration occurs from other brain regions such as the cortex and may begin to replace lost neurons of the conditional MEF2C KO striatum, given the substantial number of migratory neurons that would be required, along with the need for replacing cells to be capable of functional activity to the extent that no obvious phenotype is present, this is an unlikely prospect. However,

neuronal migration from other brain regions into the striatum has not been extensively studied in postnatal mice after P7, thus it is not possible to say for certain whether or to what extent neuronal migration may be encouraged following loss of striatal MEF2C.

### 4.8.1 **Summary:**

This investigation has shown that conditional KO of MEF2C results in striatal changes – specifically a smaller striatum with disturbed MSN marker expression. This appears to occur predominantly in the period between P7 and 3 months, with initial BrdU studies demonstrating a reduction in striatal proliferation in the KO by P14-16. There do not appear to be substantial changes in later adulthood, thus these effects of MEF2C KO appear to be having an effect largely on postnatal striatal development, with at least one mechanism suggested through reduction in cell proliferation during this period.

# Chapter 5: Effect of Conditional MEF2C KO in E18 Primary Cell Cultures

## 5.1 Introduction

In Chapter 4 it was demonstrated that conditional knock down of MEF2C during development led to a reduction in the number of normal striatal MSNs (as defined by CTIP2 expression) in adulthood and also a change in their character (a lower proportion of CTIP2 neurons that co-expressed substantial levels of DARPP-32 and FOXP1), although, with the exception of DARPP-32, these changes were not detectable at P7. This chapter attempts to explore some of the cellular events that precede the changes seen by adulthood by investigating the effects of MEF2C KO in the embryonic striatum at E18 in an *in vitro* analysis. MEF2C expression is detected from E12 and increases through to E18 in the developing mouse brain and peaks in the early postnatal period (See Chapter 4 – Figure 4.03), so taking cells at E18 includes cells generated before peak expression and so may be expected to provide the opportunity of detecting the effects of conditional MEF2C knock down that result in the changes seen at 3 months. *In vitro* culture systems can allow manipulations of cells that are difficult or impossible to undertake *in vivo*. Furthermore, *in vivo* systems have compensatory mechanisms that may prevent phenotypes from developing, thus masking the effect of a gene knockdown. Such compensatory mechanisms may be weaker or not present *in vitro*, particularly as MEF2C is a transcription factor, which are typically sensitive to environmental cues and the presence of other activity-mediating proteins and factors.

The reduced total MSN count demonstrated in Chapter 4, following striatal KO of MEF2C, may be due to reduced proliferation, increased cell death or both. An *in vi*tro analysis allows for these aspects to be assessed in genetically defined cells that can be plated over several individual wells, so that cells from a single pup can be analysed in multiple ways over a range of time points in culture. *In vitro* analysis also circumvents the issue of cells migrating from other regions of the brain, thus allowing for clearer interpretations of proliferation or apoptotic activity in striatal cells. Expression of the CTIP2 and FOXP1 MSN markers is present at this time point (Evans et al. 2012; Precious et al. 2016) and, as striatal neurogenesis continues beyond P0 (Smart and Sturrock 1979; Fentress et al. 1981), neural and glial progenitors will also be present. Upon plating of striatal tissue in neural culture media, neural progenitors will begin to proliferate and differentiate primarily into MSNs and interneurons, with glia progenitors

differentiating into astrocytes and other glial lineage cells. It should be noted that DARPP-32 is not as reliable as a marker *in vitro* as it is *in vivo* (Precious et al. 2016), and so was not used in these experiments.

## 5.2 Preliminary Experiment 1

This preliminary study was undertaken to allow several methodological factors to be determined. These include the time frame of culture, and the culture medium.

Primary mono-layer cell culture experiments often range between 24 hours and 3 weeks. A greater time in culture allows more time for cells to mature, but this needs to be balanced with longer periods being associated with more cell death. 2 and 3 week time points were selected to allow enough time for cells to develop and to provide an indication as to the stability of E18 WGE cells under *in vitro* conditions.

In previous *Mef2c in vitro* investigations loss of MEF2C affected cell survival with decrease in total neuron count (Mao et al. 1999; Okamoto et al. 2000; Okamoto et al. 2002a), therefore the outputs in this preliminary study were total cell count and neuronal count of KO compared to WT, assayed using DAPI and NEUN antibodies respectively.

Given that the *Mef2c*$^{loxP/loxP}$ and *Mef2c*$^{loxP/Tm2}$ KO variants were not found to differ significantly in any striatal measurement in Chapter 3, cultures taken from these animals were combined in this experiment to increase the power.

MEF2C KO is expected to occur upon expression of LacZ-Cre, which occurs from E12.5 in the developing striatum (Lyons et al. 1995; Kessaris et al. 2006). The MEF2C conditional KO is therefore expected to occur in the striatum from E12.5 in *Mef2c*$^{loxP/loxP}$ mice, following expression of the Gsx2-Cre throughout the striatum (Kessaris et al. 2006; Costa et al. 2007). Additionally, histological evidence of loss of MEF2C expression in E18 expression is provided in section 5.8.1 below.

### 5.2.1 Methods

Homozygous knockouts possessing one conditionally knocked out allele and one null allele were generated. The null allele was achieved following germline KO of *Mef2c* in the testis as a result of testicular Gsx2-cre expression, as described in Chapter 2 (*Mef2c*$^{loxP/Tm2}$ with Gsx2-Cre; referred to as KO1). It is possible that a proportion of neurons may be left unaffected by the conditional KO method at the E18 developmental stage, for example, due to Gsx2-cre mediated excision not yet occurring in a cell as it may still be too-immature. With the inclusion of the Tm2 variant, loss of MEF2C is achieved in all tissues for one allele, with the second allele conditionally knocked out only in the presence of the striatal Gsx2-cre expression. This KO variant provided

potential for partial compensation for any cells that are not affected through Gsx2-cre expression at this point in development, ensuring that every cell has at least one non-functional copy of *Mef2c*.

Unless otherwise stated, ANOVAs were utilised for all statistical analysis and included all genotypes at all time points.

WGE was dissected from E18 mouse pups, with each individual pup representing a single experimental unit. As described in Chapter 2, 100,000 dissociated WGE cells were suspended in 30µl of neural differentiation medium and pipetted in a single droplet onto a PDL-coated coverslip placed inside a 24-well plate. In this way the starting cell count, the area covered by the cells, and therefore the cell plating density was kept consistent for each sample. Following plate-down, cells were incubated at 37°C for the relevant time frame then fixed with 4% PFA.

Following staining, five photographs of each coverslip at 400X magnification for each wavelength were taken as shown in Figure 5.01 below, covering a significant portion of the droplet area. Images were then collected and manually counted using ImageJ (Schneider et al. 2012). Control samples processed without secondary fluorescent antibodies were used to ensure no endogenous fluorescent signal detection. Furthermore, control samples containing only one secondary antibody colour were used to check for channel “bleed through”, with red channels found to exclusively detect the red fluorescence, and green channels to exclusively detect green fluorescence.

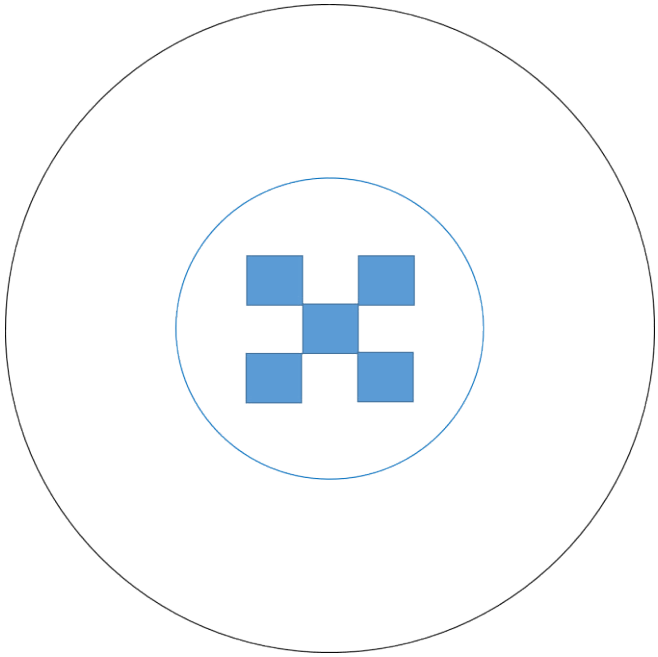

Figure 5.01: Diagram illustrating the counting frame pattern used for *in vitro* analyses, with the black circular outline representing the coverslip, the blue circle the area of the 30µl droplet, and each blue square representing one 400X magnification image (not to scale).

### 5.2.2 **Results**

DAPI co-staining identifies all cell nuclei. As can be seen in Figure 5.02 A-D, DAPI staining of striatal neuronal cultures reveals nuclei of two distinct types; one that is larger in size and fainter under fluorescence and another more compact and brightly stained. Examples of each can be seen in the coloured arrows in Figure 5.02-C. There was a trend towards lower total cell counts in KO, compared to WT, cultures but this was not significant ($F_{1,11}$ =0.061 p=0.809) (Figure 5.02-E). This trend appeared to be more marked when considering the cells with larger nuclei (Figure 5.02-F), but this also did not reach significance ($F_{1,11}$ =3.382 p=0.093).

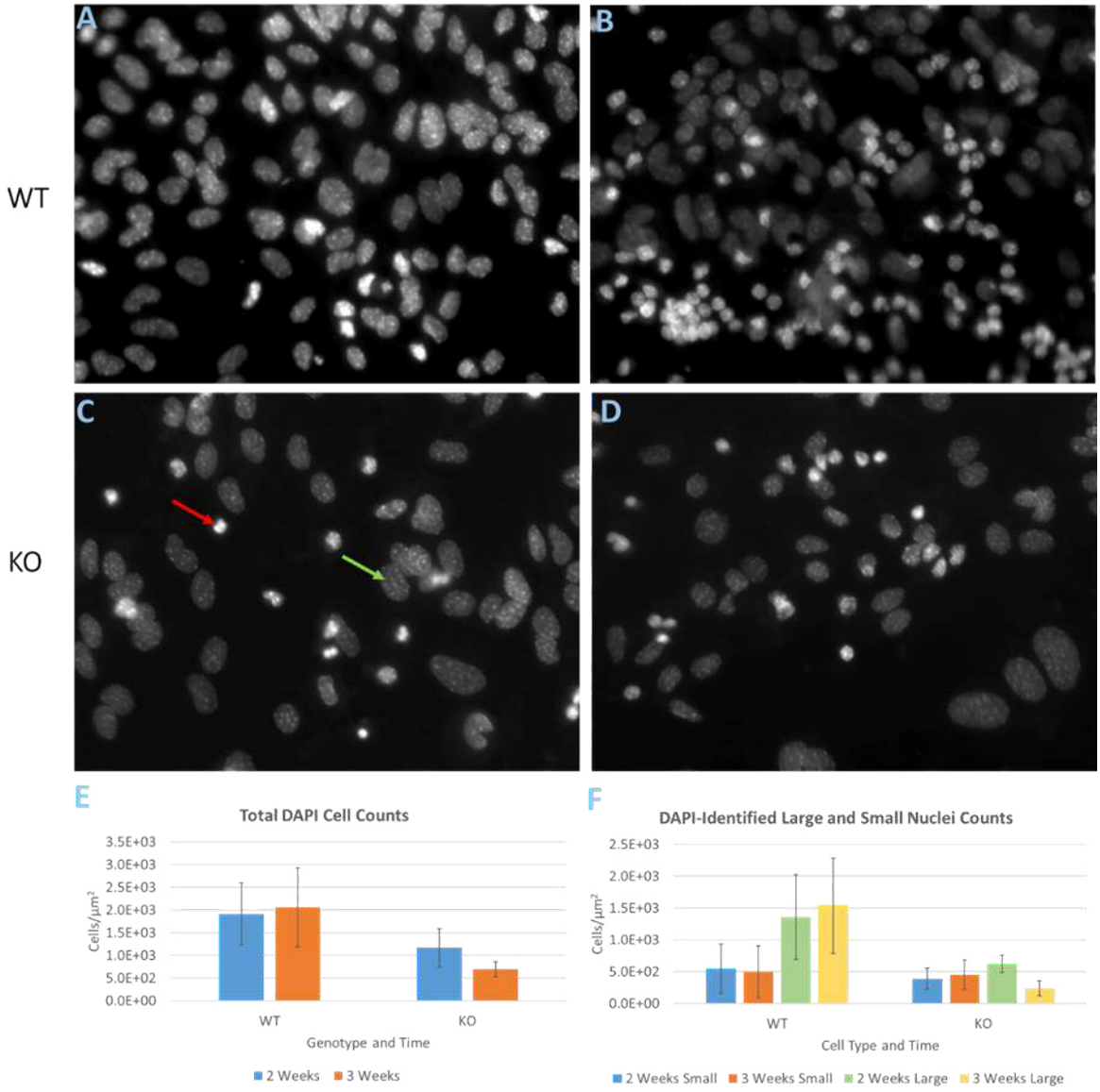


Figure 5.02: There was a trend for lower total cell numbers in KO, compared to WT, cultures, although this did not reach significance. It also appeared that the numbers of cells with large nuclei increased over time in WT cultures but failed to increase in KO cultures. Images of WT cells at (A) 2 weeks, and (B) 3 weeks showing a greater proportion of cells with large nuclei by this time point. In contrast, the proportions of cells with large and smaller nuclei appeared to change little in KO cultures between 2 (C) and 3 weeks (D). (E) Total DAPI cell counts and (F) large and small DAPI-identified cell counts. The red arrow shows example of "small nuclei" and green arrow shows example of "large nuclei" identified by DAPI. Images are x400 magnification; WT n=4, KO n=4.

Differences in nuclei size may indicate different neural cell-type populations (van Deijk et al. 2017), although more specific (e.g. neuronal/non-neuronal expression) markers

are required to determine this. NEUN, which labels neuronal nuclei (Bentivoglio et al. 1980), is a reliable indicator for most types of post mitotic neurons. NEUN counterstained with DAPI confirmed the presence of neuronal cells within each culture and was found to only stain cells with small nuclei. As shown in Figure 5.03, there are no significant differences in the number of NEUN-expressing cells between WT and KO cultures ($F_{1,10}$ =0.956 p=0.351), nor any significant differences between 2-3 weeks ($F_{1,10}$ =0.241 p=0.634).

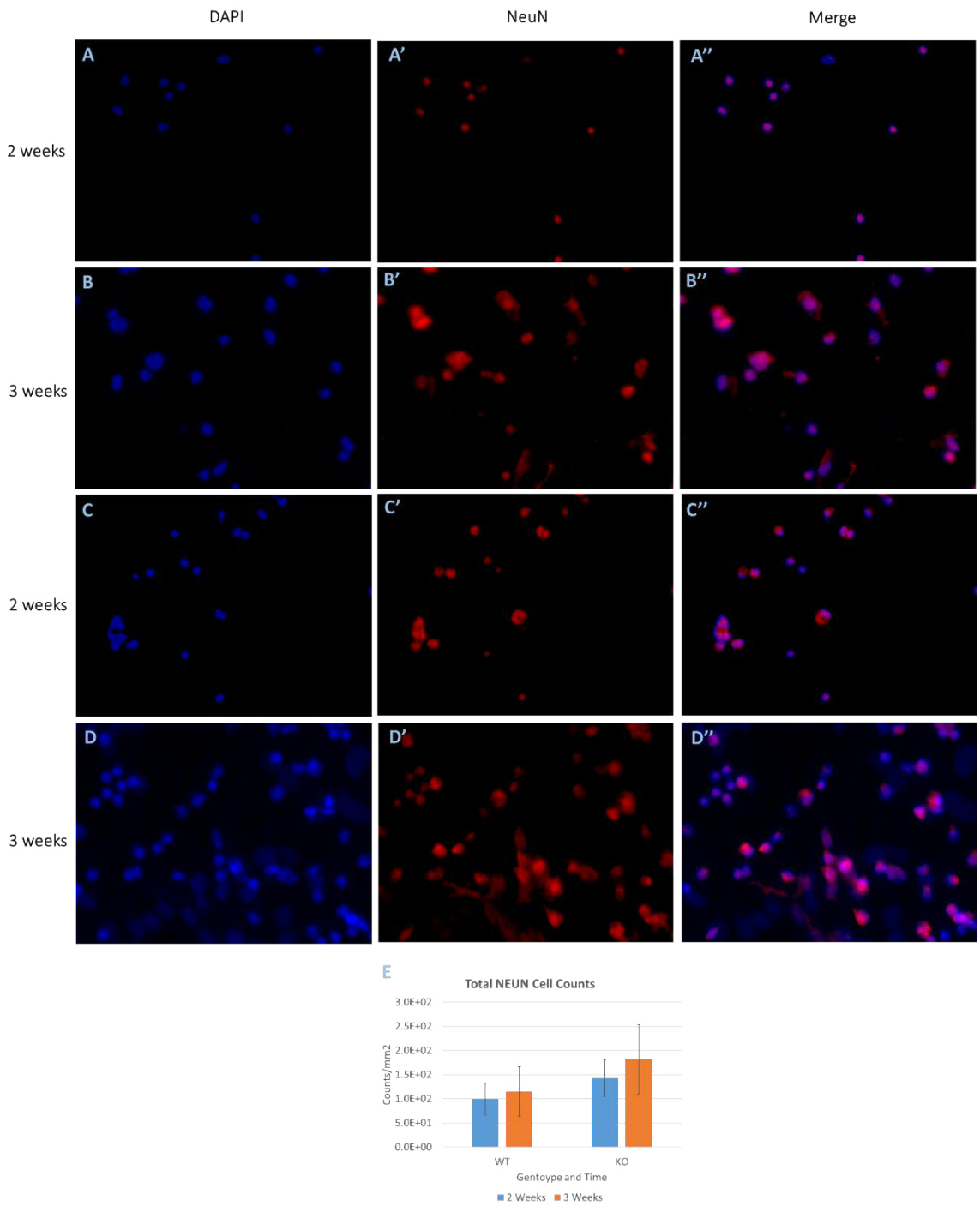


Figure 5.03: There was no significant differences in the number per $\mu m^2$ of NEUN-expressing cells between groups or across time. WT cells at 2 weeks or 3 weeks respectively showing positive staining for DAPI (A, B), CTIP2 (A'B') and merged (A'', B'') and KO cultures at 2 weeks and 3 weeks respectively stained for DAPI (C, D), CTIP2 (C', D') and merged (C'', D''). All images are x400 Magnification; WT n=4, KO n=4.

Some of the DAPI-positive cells with small nuclei were not positive for NEUN, indicating that some of these cells may be non-neuronal or could represent pyknotic nuclei. The large standard errors in these data almost certainly relate to the small n's and also to the

relatively small numbers of counting frames (and thus small proportion of all cells) counted per coverslip. For these reasons, a further experiment with methodological adaptations was undertaken.

## 5.3 Preliminary Experiment 2

Adjustments were made to the counting methodology (Figure 5.04) in order to increase the number of total cells counted, the magnification of each counting frame was reduced from 400X to 200X and an additional 4 frames per coverslip were counted for the 2-week samples.

A 24-hour time point included in order to provide a baseline of cellular condition following plating (to better assess the quality of the cultures, viability etc at an early stage) and the 2-week time point was kept as a latter-reference point.

The main aims of this experiment were (i) to assess whether the non-significant trends towards lower cell counts in KO cultures compared to wildtype are meaningful, (ii) if seen, whether differences in cell number are due to differences in proliferation, or in apoptotic activity, as has been shown in cortical cells (Okamoto et al. 2000; Cho et al. 2011). To this end, a Cysteine-aspartic acid protease 3 (CASPASE-3) antibody suited to detecting cells marked for apoptosis (Porter and Jänicke, 1999) was included alongside Antigen KI-67 (KI67), a factor expressed in the G1, G2, S and M phases of cells undergoing mitosis and is a standard marker to assess proliferation (Gerdes 1990; Kee et al. 2002).

A heterozygous KO group was also included in Preliminary Experiment 2. The heterozygous KO variant (HET) was also generated through this cross (see table 5.1 below for description of each genotype and abbreviation). This provides a reference point from which to assess what effect the loss of only a single copy of *Mef2c* has on the differentiation of E18 striatal cells *in vitro*, relative to WT and double-allele KO variants. This genotype was used in Preliminary Experiment 2 only (see below).

| Abbreviation | Genotype |
|---|---|
| WT | *Mef2c*$^{loxP/loxP}$ without Gsx2-Cre |
| HET | *Mef2c*$^{loxP/Tm2}$ without Gsx2-Cre |
| KO | *Mef2c*$^{loxP/Tm2}$ with Gsx2-Cre or<br>*Mef2c*$^{loxP/loxP}$ with Gsx2-Cre |

Table 5.1: Description of genotypes used in this chapter along with their abbreviation.

Although no significant differences were found between the WT and HET (single *Mef2c* allele KO) in Chapter 3 nor in previous reports of conditional MEF2C loss in the cortex and hippocampus (Black and Olson 1998; Barbosa et al. 2008; Li et al. 2008a) in vivo phenotypic observations in adult mice may not reflect all events in embryonic

development, where cell development and differentiation are occurring in the context of an intact developmental brain environment. Furthermore, given the severity of the heterozygous KO of MEF2C in the human brain, the HET genotype cannot be overlooked in an investigation in the pre-natal brain.

### 5.3.1 **Methods**

Unless otherwise stated, the methods used in this experiment match those previously stated within this Chapter and Chapter 2.

Following dissection of the WGE from E18 pups and cultures for 24 hours and 2 weeks, cells were fixed and stained with one of the following primary antibody double stain pairs: NEUN plus CASPASE-3; CTIP2 plus KI67 (see antibody list in Chapter 2), each co-stained with DAPI. Following staining, photographs were taken and cells subsequently counted in 5 frames for each coverslip at 200X magnification for 24-hour samples (fewer photographs due to a lesser spread of cells following plating in a 30µl droplet), with 9 frames used for 2 weeks as shown in Figure 5.04.

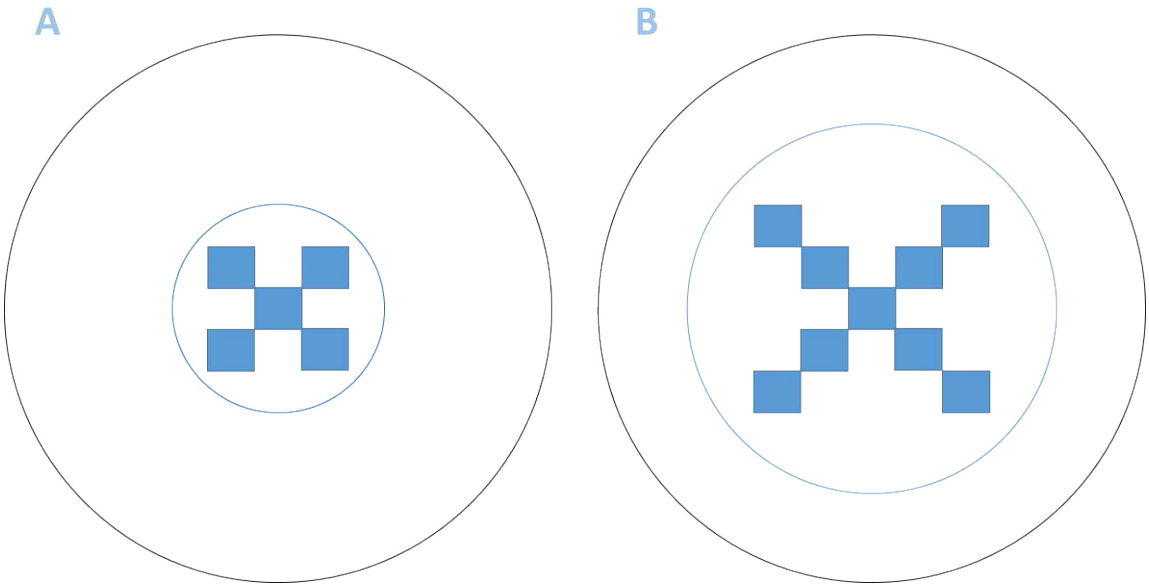


Figure 5.04: The counting frame pattern used for E18 cultured cells in Preliminary Experiment 2 in (A) 24-hour samples and (B) 2-week samples. The black circular outline represents the coverslip, the blue circle the area of the 30µl droplet and each blue frame represents one sample image at 200X magnification.

Cells were then checked for primary antibody staining under fluorescence using different appropriate UV wavelengths (560nm-red; 494nm- green) and counted in the same format as described in Preliminary Experiment 1.

### 5.3.2 **Results**

There was a trend towards fewer cells in 2 week KO cultures relative to WT, as in Preliminary Experiment 1, but again there were no significant differences between genotypes ($F_{2,17}$ =1.084 p=0.359) or time in culture ($F_{1,18}$ =2.18 p=0.157) (Figure 5.05).

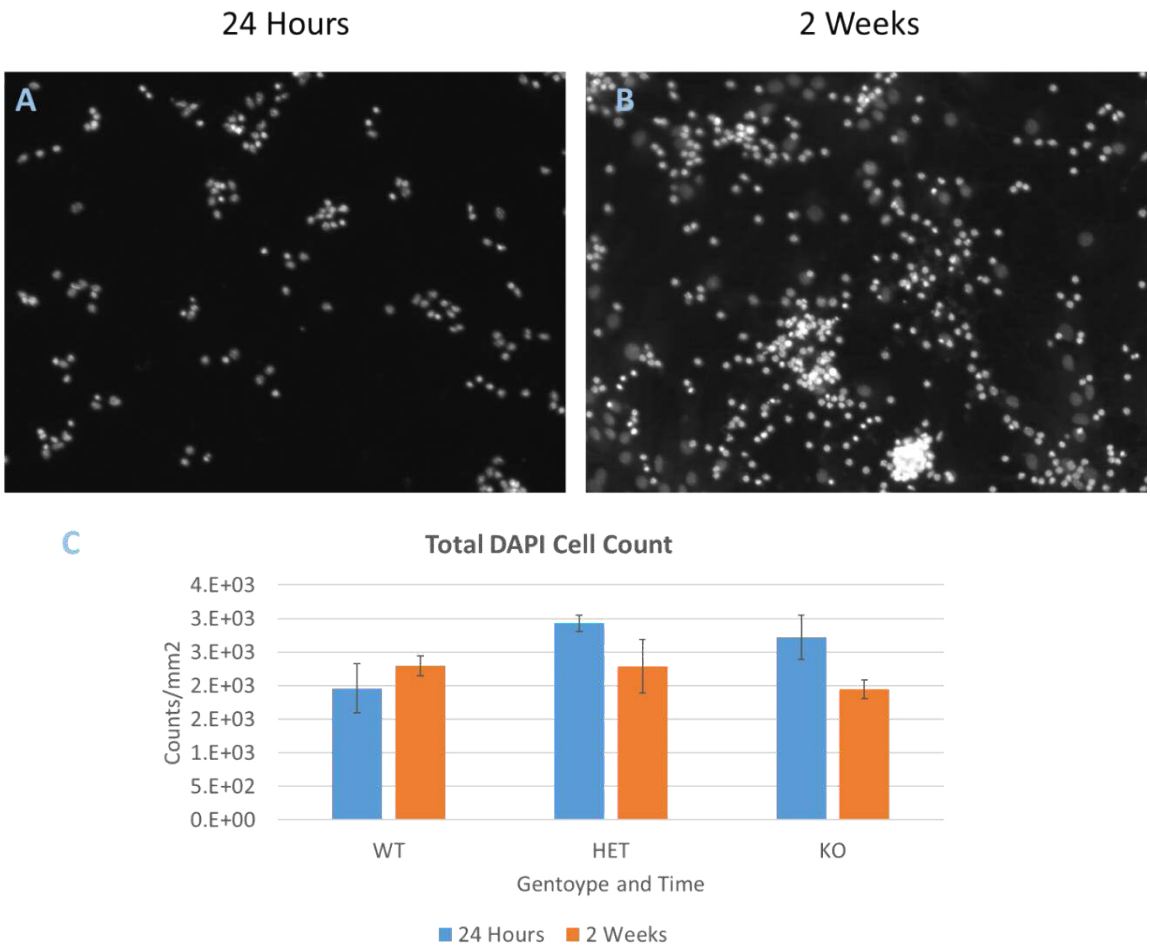


Figure 5.05: WT DAPI: (A) at 24 hours and (B) 2 weeks. (C) There were no significant differences in total cell counts between genotypes or time points. Images at x200 Magnification WT n=3, HET n=3, KO n=6.

By 2 weeks of culture (but not at 24 hours), DAPI staining revealed cultured cells to have either small dense nuclei or large nuclei with more dispersed punctate staining (Figure 5.06). As previously observed in Preliminary Experiment 1 (Figure 5.03), a trend towards a reduction in the number of large nuclei in conditional KO cultures compared to WT may be observed in 2 week cultures, though ANOVA showed no significant main effect between genotypes ($F_{2,18}$ =0.377 p=0.691).

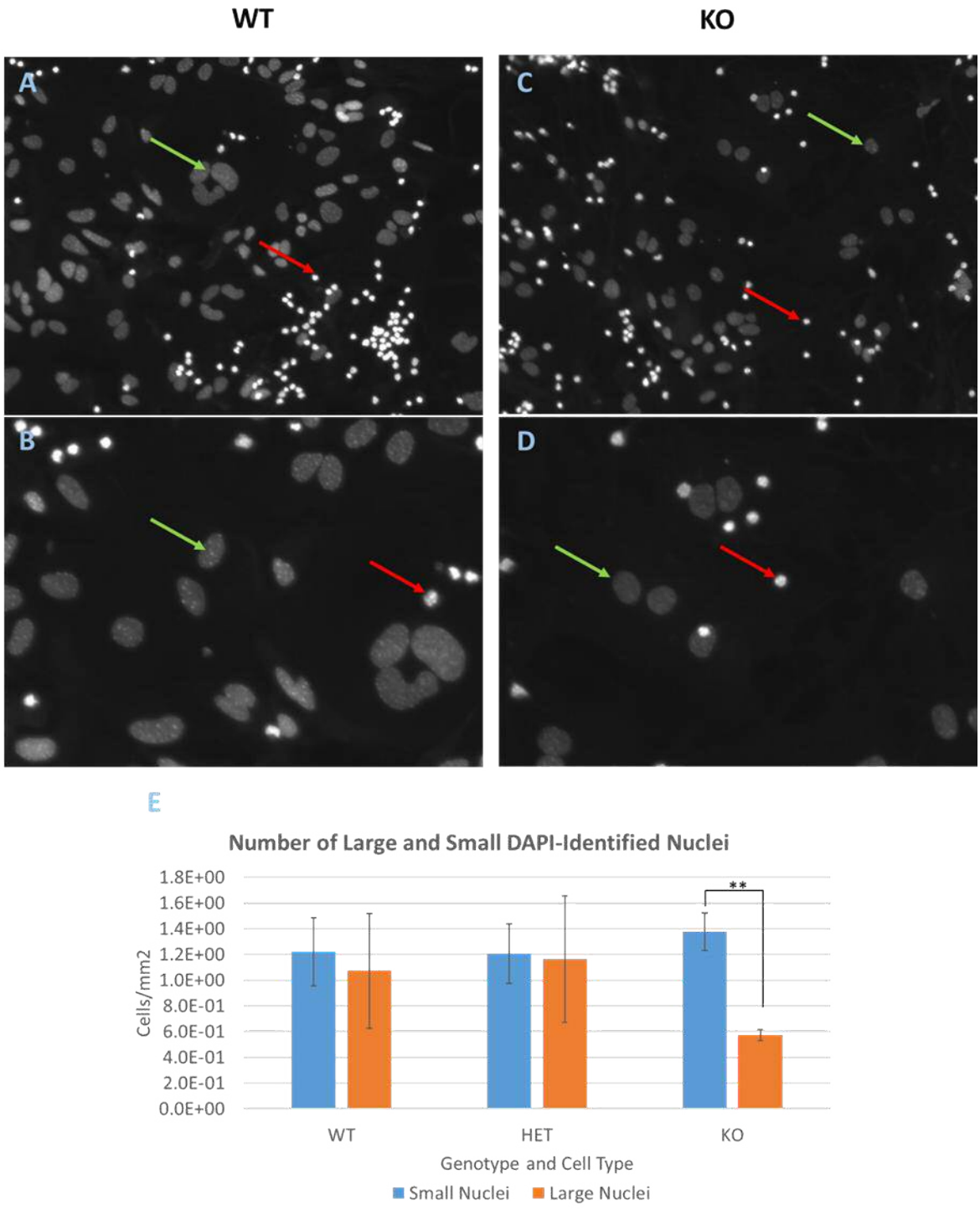


Figure 5.06: Photograph of DAPI stained WT cells at 2 weeks of culture at (A) x200 and (B) x400 magnification, alongside KO cells of the same magnifications (C and D respectively), suggesting fewer cells with large nuclei compared to small nuclei in KO cultures relative to WT. Green arrows indicate large nuclei cells, red indicates small nuclei cells. There is a significant difference between "large" and "small" nucleated counts (E) in KO cultures only, with WT cultures containing significantly more large nucleated cells (WT n=3, HET n=3, KO n=6).

Classification of cells by size of nucleus on DAPI staining is not a robust means of identifying specific cell types and may relate more to cell health (i.e. undergoing cell-death) or stage of development/differentiation. Therefore, additional marker staining was required. A Two-way ANOVA of NEUN total cell counts revealed a significant difference in the total NEUN positive cells between 24 hours and 2 weeks ($F_{1,17}$ =12.186 p=0.003), however no significant difference was found between genotypes ($F_{2,17}$ =1.127 p=0.347). Furthermore, as can be seen in Figure 5.07-(H), when considering NEUN as a proportion of DAPI, a two-way ANOVA showed there is a significant reduction in the proportion of NEUN to total cell count between 24 hours and 2 weeks ($F_{1,17}$ =21.346 p=<0.001), however again there was no difference between genotypes ($F_{2,17}$ =0.066 p=0.936).

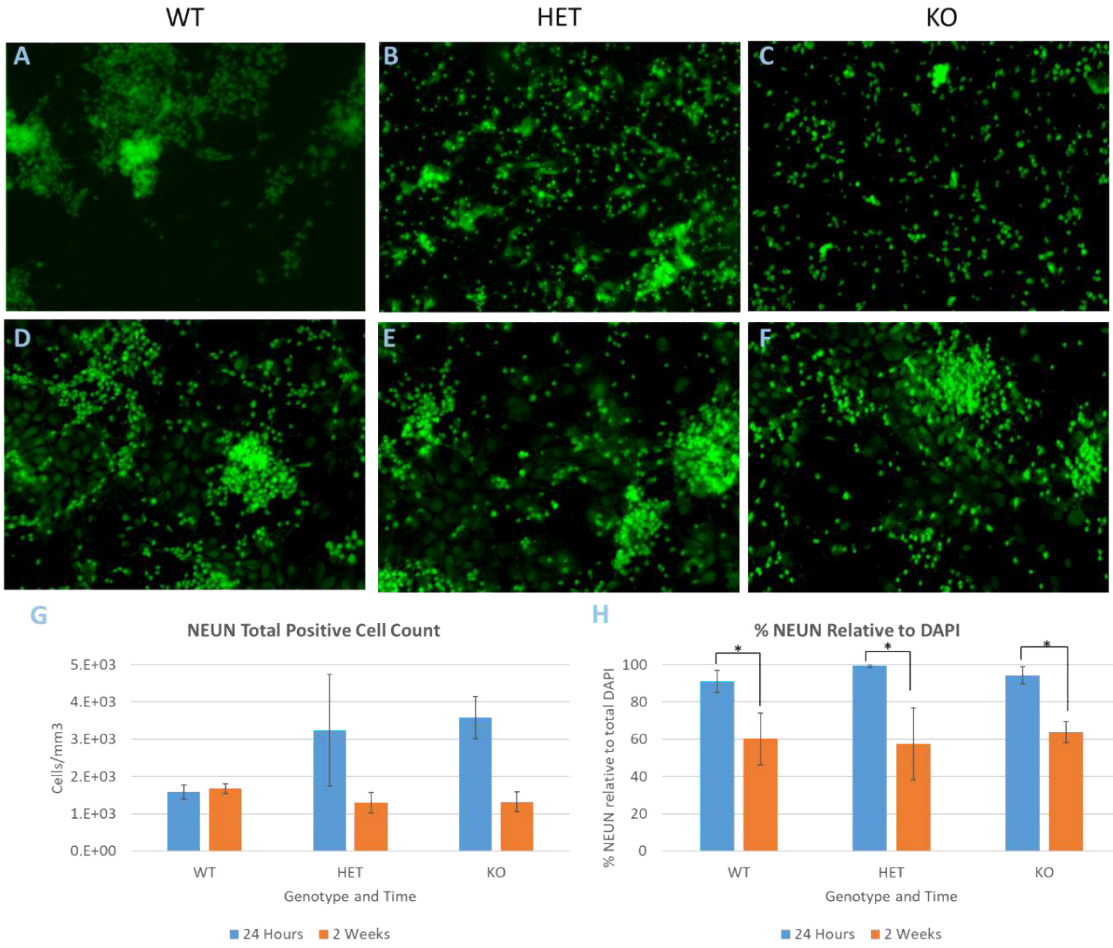


Figure 5.07: NEUN cell counts after 24 hours and 2 weeks of culture at x200 magnification for WT, HET and KO cells at 24 hours (A, B and C respectively) and at 2 weeks (D, E and F respectively), with counts at 24 hours and 2 weeks shown in (G). HET and KO NEUN counts appear to decrease in number more dramatically than WT between 24 hours and 2 weeks. When NEUN is expressed as a proportion of total DAPI (H) a significant reduction in the proportion of NEUN is found in all genotypes by 2 weeks. (WT n=3, HET n=3, KO n=6).

The reduction of NEUN positive cells relative to DAPI in 2-week cultures may be due to the development of large DAPI-identified nuclei, which did not express NEUN. Given the variance in counts and relatively small n's, it is difficult to know how robust any differences between genotypes are and whether they are meaningful. However, as there was a suggestion that the proportion of NEUN cells declined in KO cultures by 2 weeks, it was decided to explore whether any differences in proliferation (using KI67) or cell death (using CASPASE-3) could be detected.

Staining with the proliferation marker KI67 revealed a significant difference between 24 hours and 2 weeks in culture ($F_{1,16}$ =23.964 p=<0.001) (Figure 5.08-G) following a two-way ANOVA of cell counts of both time points and all three genotypes, though no significant difference was detected between genotypes at either time point ($F_{2,16}$ =9.83 p=0.396).

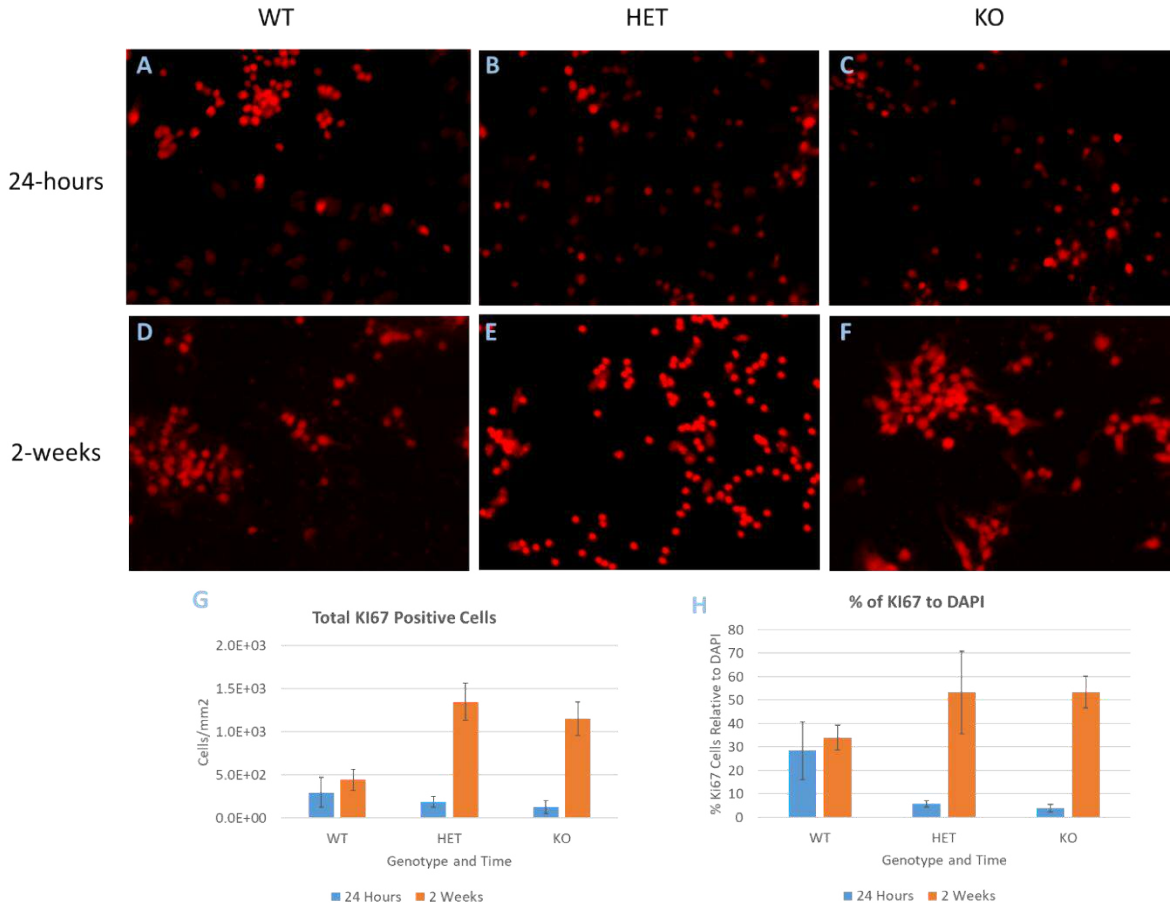


Figure 5.08: KI67 cell counts after 24 hours and 2 weeks of culture at x400 magnification for WT, HET and KO cells at 24 hours (A, B and C respectively) and at 2 weeks (D, E and F respectively), with counts at 2 weeks shown in (G). KI67 counts significantly increase between 24 hours and 2 weeks, but there is no difference between genotypes. This is also seen when KI67 is expressed as a proportion of total DAPI (H). (WT n=3, HET n=3, KO n=6).

The same is observed with KI67 expression relative to DAPI, with a two-way ANOVA of total cell counts including both time times and all three genotypes showing a significant increase at 2 weeks compared to 24 hours ($F_{1,16}$ =18.578 p=0.001), but no significant difference between genotypes ($F_{2,16}$ =0.052 p=0.950).

A two-way ANOVA comparing total CASPASE-3 cell counts of all genotypes in both 24 hour and 2 week cultures showed no significant differences between genotypes ($F_{2,16}$ =1.460 p=0.262) or time points ($F_{1,16}$ =3.129 p=0.096) (Figure 5.09).

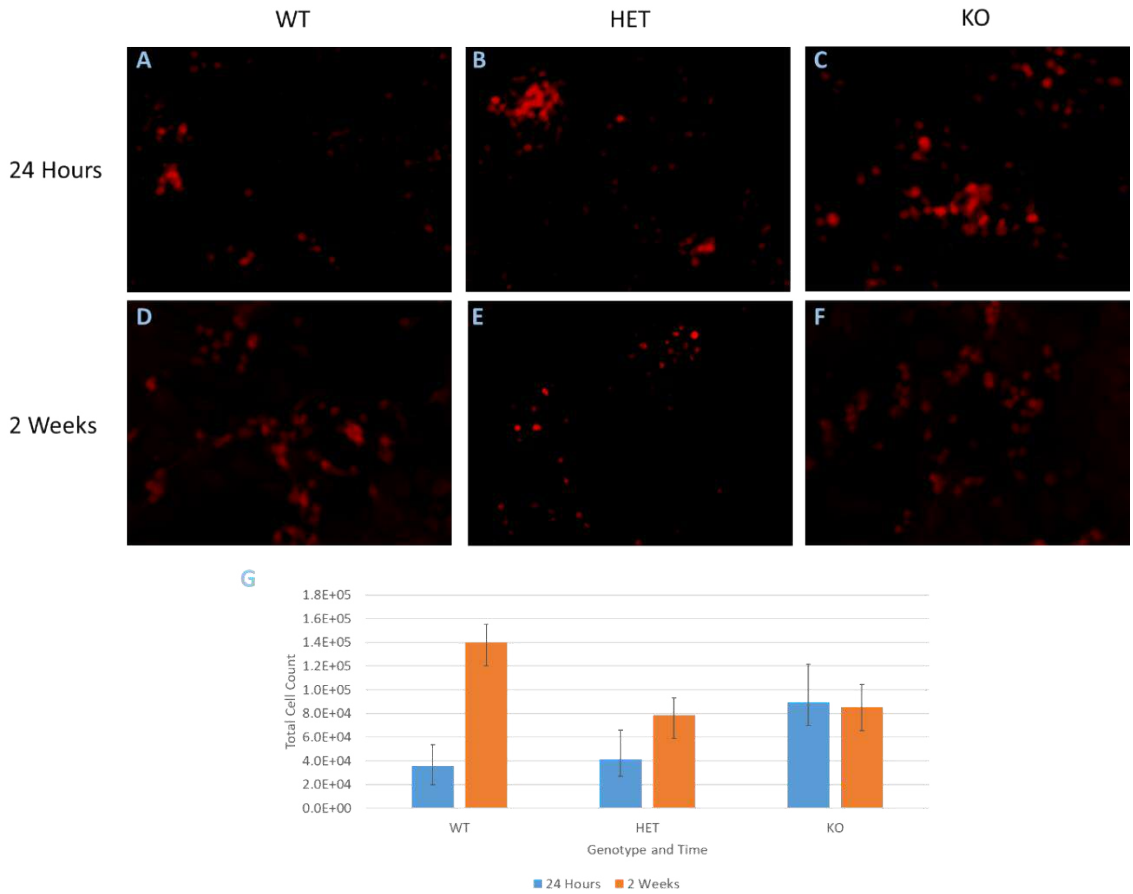


Figure 5.09: CASPASE-3 activity over time between WT, HET and KO cells. A) x200 Magnification image of WT, (B) HET and (C) KO cells at 24 hours and at 2 weeks (D, E and F respectively), showing no significant differences in the number of CASPASE-3 positive cells between genotypes and over time. WT n=3, HET n=3, KO n=6.

Whilst there appear to be no significant differences between genotypes, the inconclusive nature of these results make it difficult to explain the effect of MEF2C in influencing NEUN cell and total cell numbers. Therefore, another experiment was needed to more clearly understand the effect of MEF2C on proliferation and apoptotic activity.

## 5.4 E18 Experiment 3

The preliminary experiments showed a trend to reduced numbers of cells per mm2 in the KO compared to WT between 2 and 3 weeks, and also suggested that this may have been predominantly due to loss of large nucleated cells with very little change in the small nucleated cells, which were predominantly NeuN positive. As astroglia are reported to form the majority of large nucleated cells (van Deijk et al. 2017), this could lead to the conclusion that the major effect of MEF2C loss was on astroglia.

A final experiment was undertaken with some changes to the methodology. The main aims of this experiment were (i) to assess whether the non-significant trends towards lower cell counts in KO cultures compared to WT are meaningful; (ii) if seen, whether differences in cell number are due to predominantly to differences in MSNs using CTIP2 (CTIP2 is expressed in MSN progenitors from as early as E12.5 (Arlotta et al. 2008) thereby allowing for MSN identification from the progenitor stage onwards), or astrocytes using GFAP. MEF2C loss has been found to influence the differentiation of neuronal cells (Barbosa et al. 2008; Li et al. 2008b), but the effect of its loss on glial lineages is unknown, although overexpression of MEF2C has been shown to increase astrocyte proportions in DA Neuron rich regions in Parkinsonian Rats *in vivo* (Cho et al. 2011). (iii) determine whether loss of MEF2C affects proliferation, or apoptosis, as has been shown in cortical cells (Okamoto et al. 2000; Cho et al. 2011). To this end, a CASPASE-3 antibody suited to detecting cells marked for apoptosis (Porter and Jänicke, 1999) was included alongside KI67, a factor expressed in the G1, G2, S and M phases of cells undergoing mitosis and a standard marker to assess proliferation (Gerdes 1990; Kee et al. 2002).

The 2-week time point was retained. A 4-hour time point was included instead of the 24 hours point in order to better assess the quality of the cultures (viability etc) and to provide a baseline of cellular condition following plating, and a 7-day time point was included as an intermediary point of assessment. Unfortunately, survival of cells at 2 weeks was very poor and so this data is not presented.

Whilst Preliminary Experiment 2 included the heterozygous *Mef2c* genotype, the greatest phenotypic differences were between the WT and KO genotypes. Foregoing this genotype allowed for a more efficient breeding strategy to be utilised (see Figure 2.04, Chapter 2,) increasing the total number of biological replicates for each genotype. Therefore, the final experiment consisted of cells from only WT and conditional KO mice.

The question remains as to the quantity of MSNs within each culture and how they may be affected by loss of MEF2C over time.

The antibody pairings selected for double stain analysis were CTIP2 with CASPASE-3, CTIP2 with KI67, and CTIP2 with GFAP, each pair co-labelled with DAPI. This allowed a number of co-labelling comparisons to be made, including determining the proportion of $CTIP2^{+}$ MSNs that are also undergoing CASPASE-3 meditated apoptosis. Additionally, although a cell undergoing mitosis does not usually express protein markers of mature differentiated MSNs such as DARPP-32, CTIP2 has been shown to co-label KI67 positive neurons at the border between the VZ and the SVZ in gestational week 9-10 humans, suggesting that residual KI67 protein remains immediately following terminal differentiation and CTIP2 expression (Cipriani et al. 2016). This allows for proliferation rates of recently differentiated MSNs to be compared alongside differences in total MSN numbers between genotypes.

Additionally, a small number of WT and conditional KO cultures were double-stained for MEF2C and CTIP2 to confirm MEF2C knockdown at E18.

### 5.4.1 **Methods**

In this experiment, total cell counts represent the total number counted within a set counting frame and are reported as cells/$mm^2$. The counting frame used in this experiment is a variation of that used in Preliminary Experiment 2, with nine 20x magnification images (571µm x 428µm each) taken, though in this instance in a 3x3 grid with images automatically stitched together to allow for more efficient manual counting thereafter (Figure 5.10). This was performed in the same way for both 4-hour and 7-day cultures.

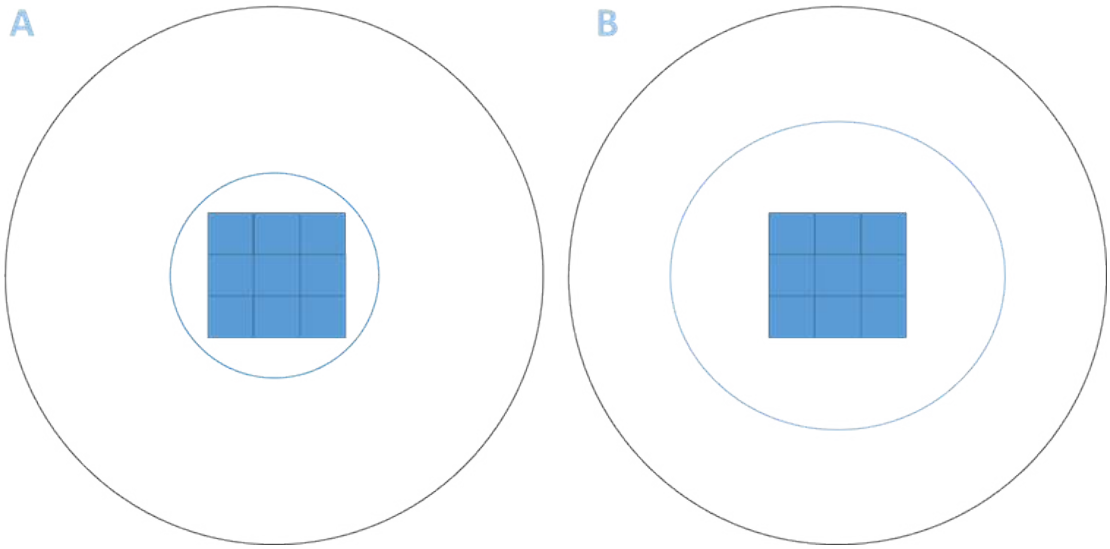


Figure 5.10: The photograph and counting frame pattern used for E18 cultured cells in experiment 3 for (A) 4-hour samples and (B) 7-day samples. The black circular outline represents the coverslip, the blue circle the area of the 30µl droplet and each blue frame represents one sample image at 200X magnification (not to scale).

In this experiment, cell counts were also expressed as a proportion of total DAPI-identified allowing for a proportional representation of expression patterns within populations. Two technical replicates were used for each biological replicate for every stain.

Unless otherwise stated, ANOVA statistical analysis was conducted in each instance, with Bonferroni post-hoc analysis performed thereafter.

## 5.5 Results

### 5.5.1 MEF2C expression is reduced in the Conditional KO striatum

MEF2C and CTIP2 co-labelling of WT and conditional KO cultures followed by fluorescence microscopy and manual cell counting analysis revealed that 91.49% of CTIP2 positive cells (n=3226 of 3526 cells) co-expressed MEF2C in WT cultures, compared to only 4.44% (n=230 of 5175 cells) in conditional KO cultures (Figure 5.11).

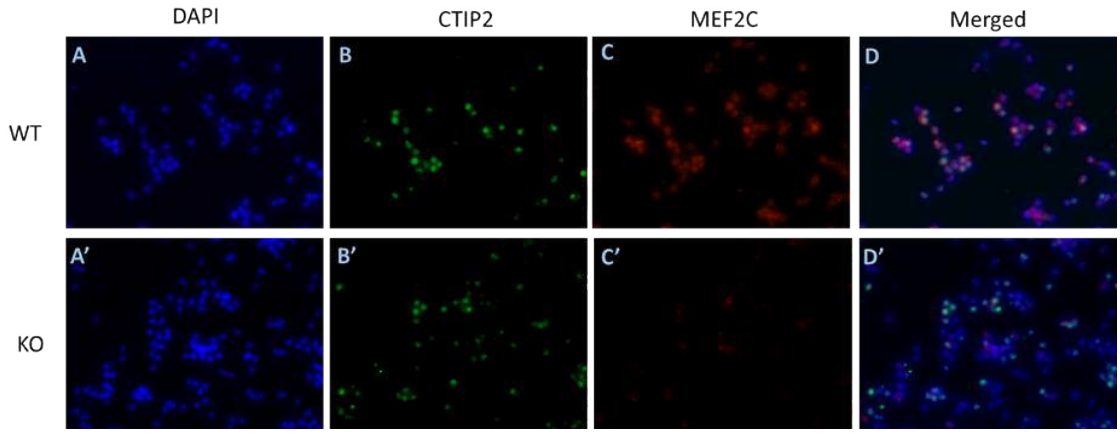


Figure 5.11: Fluorescence microscopy of MEF2C and CTIP2 double-stained cells show markedly fewer MEF2C - expressing cells in the conditional KO striatum compared to WT. Images at x400 Magnification at 4 hours for WT (A, B, C, D) and KO (A', B', C', D'). WT n=2 KO n=2.

These results support the premise that a loss of MEF2C in a substantial proportion of E18 striatal cells in conditional KO tissues compared to WT occurs due to the previously established widespread Gsx2-cre expression in the early embryonic striatum (Kessaris et al. 2006; Costa et al. 2007). Interestingly, these results also show that CTIP2-expressing neurons are able to differentiate in the absence of MEF2C. Due to limited tissue availability, stains were only conducted with n of 2 for each genotype, with the intention of showing loss of MEF2C in KO cultures. For this reason, statistical analysis was not undertaken.

### 5.5.2 DAPI

Cells fixed at 4 hours and 7 days were co-stained with DAPI alongside every antibody staining pair. No significant differences were found in the total cell count between WT and conditional KO cultures at either time point ($F_{1,58}$ =0.062 p=0.804). These results

align with those gathered in the Preliminary Experiments 1 and 2, which also found no significant difference in total cell counts between genotypes.

It is important to note that although the number of DAPI cells is lower at 7 days compared to 4 hours (Figure 5.12 G-H), this reflects the number of cells counted per $mm^2$ and does not therefore account for the increased spread of cells across the coverslip and thus the cell count of the entire coverslip.

Preliminary Experiments 1 and 2 highlighted a trend towards an increase in the proportion of large nucleated cells and small nucleated cells between WT and KO cultures following extended periods of culture. So, although interpretation of changes based on nuclei size alone is limited, this analysis was repeated for comparison with these preliminary results. 4-hour cultures contained very few large DAPI-identified nuclei for either genotype, in alignment with the 24-hour cultures described in Preliminary Experiment 2.

A two-way ANOVA incorporating large and small nuclei counts for both genotypes and time points showed a significant difference between 4-hour and 7-day cultures ($F_{1,24}$ =49.121 p=<0.001) and between nuclei size ($F_{1,24}$ =55.399 p=<0.001), with Bonferroni post-hoc analysis showing that at 7 days there were significantly more large DAPI-identified nuclei compared to small (p=0.001) in both WT and KO cultures (increase of 105%). No significant differences found between genotypes ($F_{1,24}$ =0.215 p=0.647) (Figure 5.12).

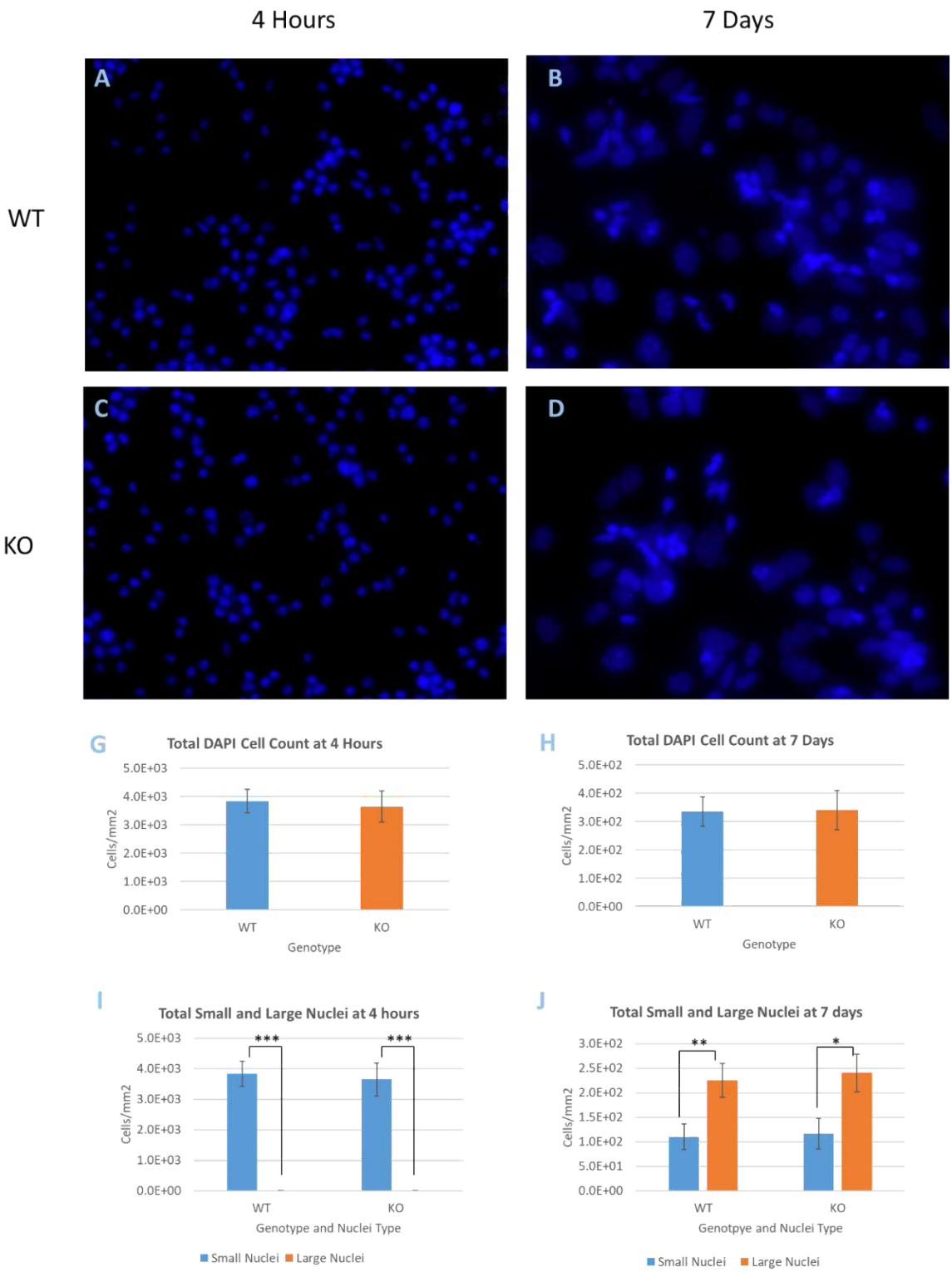


Figure 5.12: DAPI cell counts per mm$^2$ remain consistent between genotypes, however the proportion of small to large DAPI identified nuclei changes over time. DAPI cell counts after 4 hours and 7 days of culture for WT (A, B) and KO (C-D) cultures. There is no difference in total DAPI cell counts between genotypes at 4 hours (G) or 7 days (H). Few DAPI-identified nuclei were seen at 4 hours (I), increasing substantially by 7 days (J), but with no differences between genotypes. Magnification x400, WT n=4, KO n=4.

### 5.5.3 **CTIP2**

No significant difference was found in the total number of CTIP2 positive cells per $mm^2$ between genotypes at either time point ($F_{1,12}$ =1.482 p=0.247) (Figure 5.13). However, when CTIP2 counts are represented relative to the total (DAPI) cell count, two-way ANOVA revealed significant differences between genotypes ($F_{1,12}$ =5.883 p=0.032), with KO cultures found to contain a significantly lower proportion of CTIP2 positive cells after 7 days in culture in KO (10.46 +/- 1.5 %) compared to WT (42.4% +/- 0.67) following Bonferroni post-hoc analysis (p=0.047). This difference was not apparent at 4 hours (p=0.248). This suggests that loss of MEF2C may negatively impact the formation of $CTIP2^+$ MSNs. There was also a decrease in the proportion of CTIP2 positive cells relative to total DAPI positive cells after 7 days compared to 4 hours ($F_{1,12}$ =59.582 p=<0.001) for both WT ($F_{1,12}$ =9.897 p=0.003) and KO ($F_{1,12}$ =25.630 p=<0.001) cultures, although this is likely simply due to the presence of large DAPI-identified nuclei at 7-days.

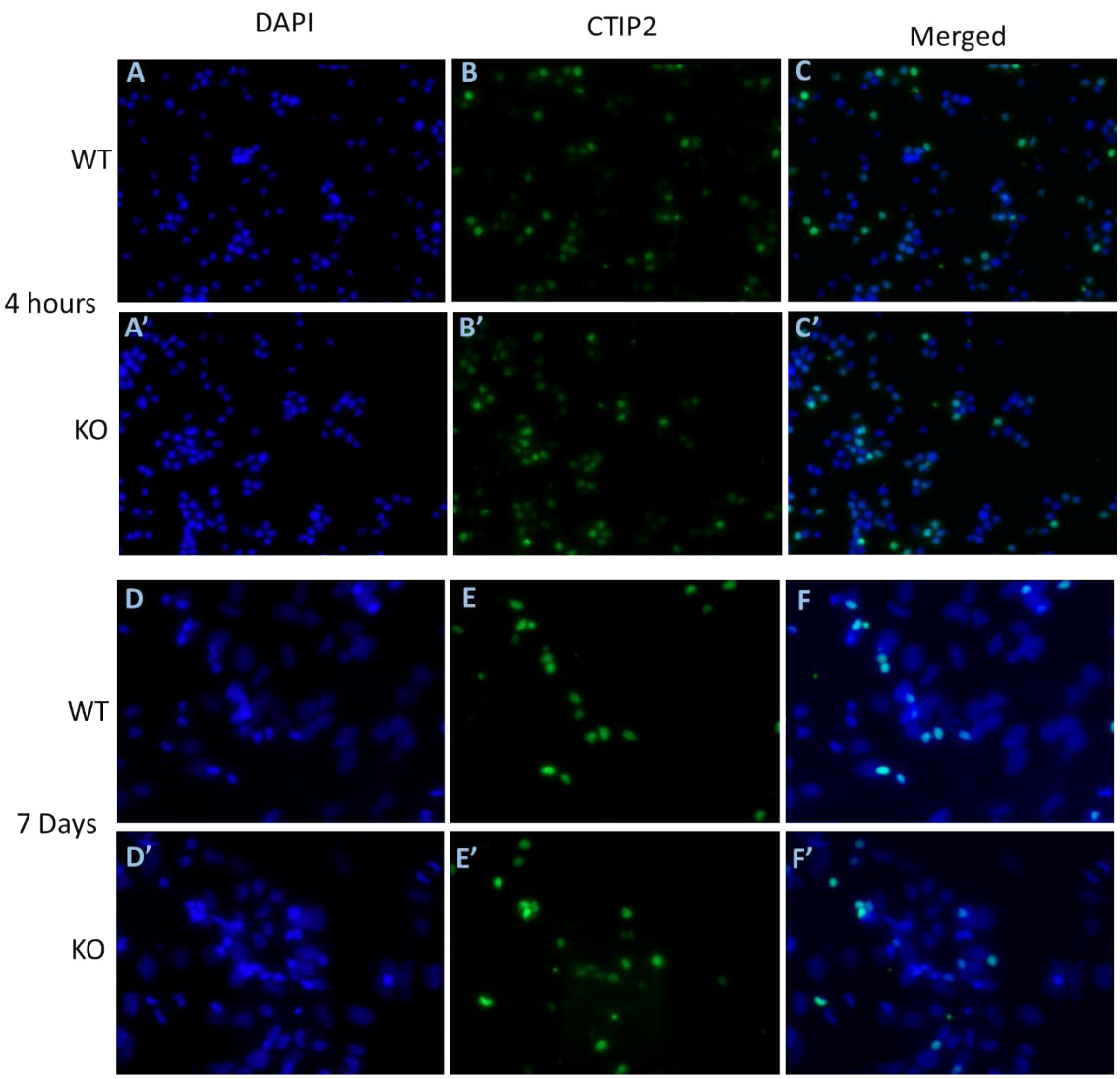
DAPI
CTIP2
Merged
A
B
C
WT
4 hours
A'
B'
C'
KO
D
E
F
WT
7 Days
D'
E'
F'
KO

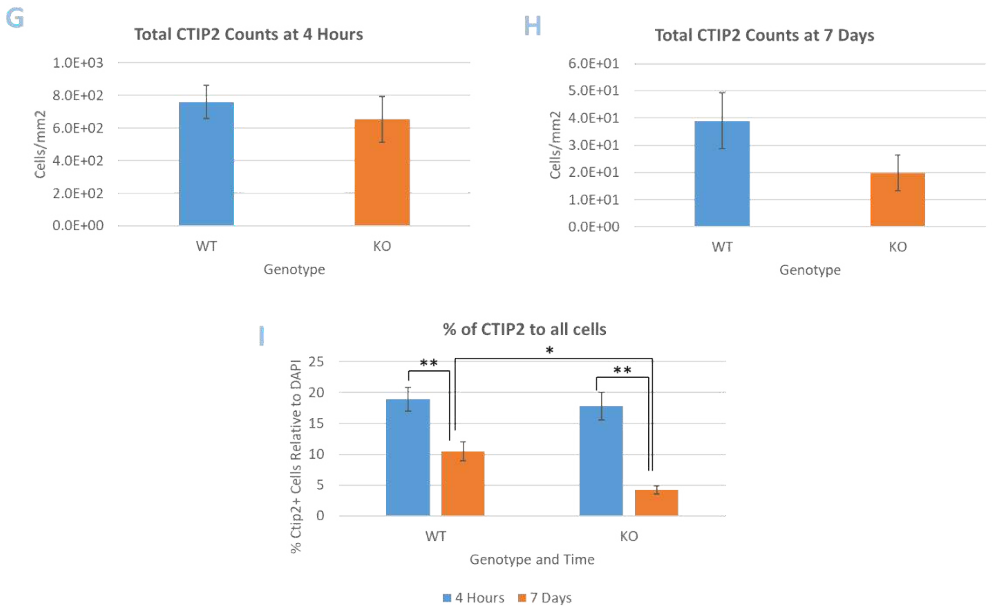
G
Total CTIP2 Counts at 4 Hours
Cells/mm2
1.0E+03
8.0E+02
6.0E+02
4.0E+02
2.0E+02
0.0E+00
WT
KO
Genotype
H
Total CTIP2 Counts at 7 Days
Cells/mm2
6.0E+01
5.0E+01
4.0E+01
3.0E+01
2.0E+01
1.0E+01
0.0E+00
WT
KO
Genotype
I
% of CTIP2 to all cells
% Ctip2+ Cells Relative to DAPI
25
20
15
10
5
0
**
*
**
WT
KO
Genotype and Time
4 Hours
7 Days

Figure 5.13: Photographs of DAPI, CTIP2 and merged cells at 4 hours for WT (A, B, C) and KO (A',B',C'), and at 7 days for WT (D, E, F) and KO (D', E', F') respectively. There are no significant differences in total CTIP2$^+$ counts between genotypes at any either time point (G, H). There was a significant decrease in the proportion of CTIP2$^+$ cells relative to total DAPI positive cells by 7 days compared to 4 hours in both genotypes, and significantly fewer CTIP2+ cells as a proportion of DAPI in KO cultures by 7 days (I). x400 magnification; WT n=4, KO n=4.

### 5.5.4 **GFAP**

GFAP staining was performed alongside DAPI as a marker for astrocytes. GFAP staining is non-nuclear unlike the other markers used in this investigation, so positive cell counts were attributed to DAPI identified cells that were entirely enveloped by GFAP staining (Figure 5.14). No GFAP positive cells were identified in 4-hour cultures, somewhat aligning with the previous finding of almost no large DAPI-identified nuclei in 4-hour cultures (Figure 5.12). In 7-day cultures, as shown in Figure 5.14 below, a t-test revealed no significant difference in the total GFAP positive cell counts between WT and KO cultures (t=0.4826, df=5, p=0.646). The proportion of GFAP positive cells relative to total DAPI identified cell counts in conditional KO cultures was 76.9% +/- 5.4, compared to WT at 53.1% +/-12.7, though this difference was not found to reach statistical significance (t=1.544, df=5, p=0.183).

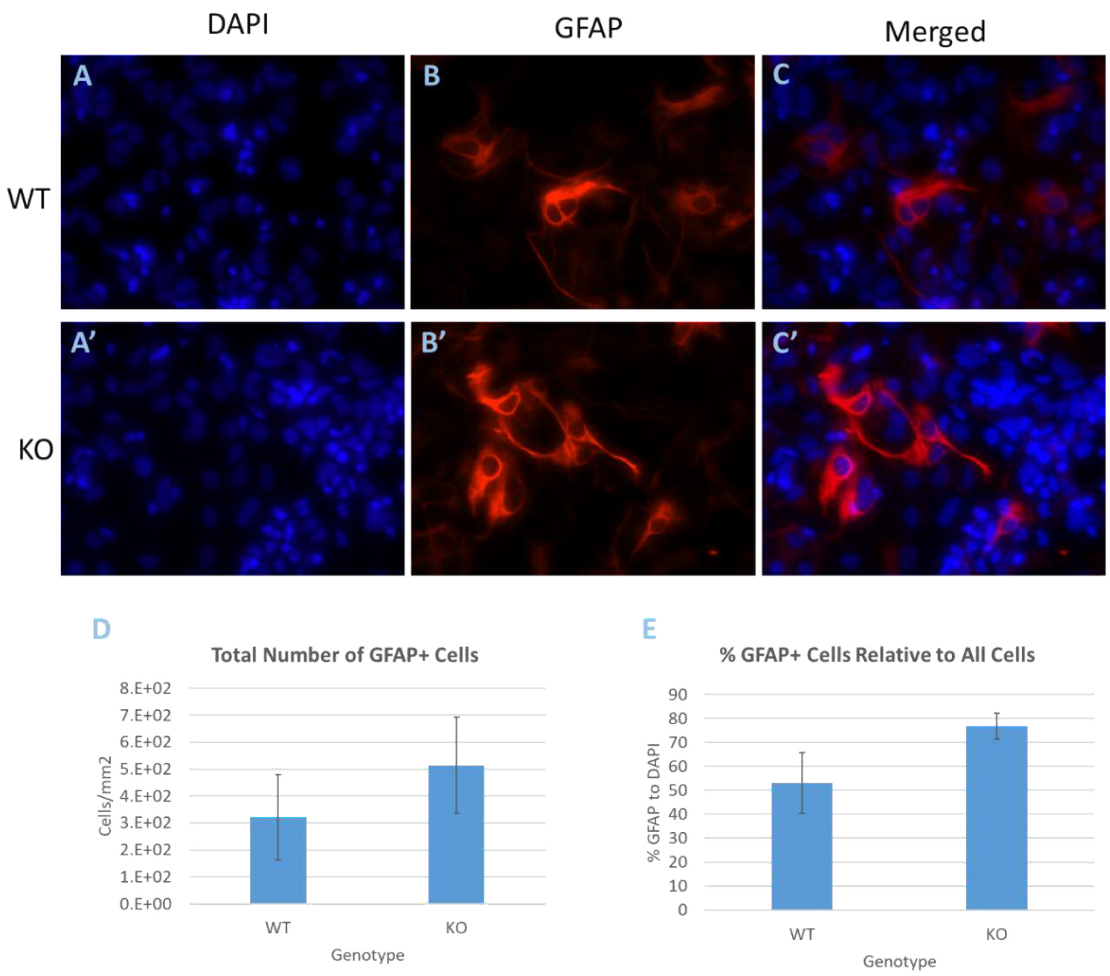


Figure 5.14: DAPI, GFAP and merged at 7 days for WT (A, B, C) and KO (A',B',C') respectively. There were no significant differences between WT and KO in the total number of GFAP positive cells or GFAP as a proportion of DAPI in 7day cultures (D, E). x400 Magnification WT n=4, KO n=4.

### 5.5.5 **CASPASE-3**

Two-way ANOVA of total CASPASE-3$^+$ cells showed a significant interaction of genotype and time point ($F_{1,11}$ =6.194, p=0.030), with Bonferroni post hoc analysis showing that at 4 hours, the number of CASPASE-3$^+$ cells was significantly higher in KO cultures compared to WT (p=0.05), but not at 7 days (p=0.216) (Figure 5.15). It is important to note, however, that the number of CASPASE-3$^+$ cells is very low at 4 hours (WT 4 +/- 2, KO 17 +/- 6), so although this finding is significant and the KO an order of magnitude higher than the WT, the proportion of cells affected remain small for both genotypes.

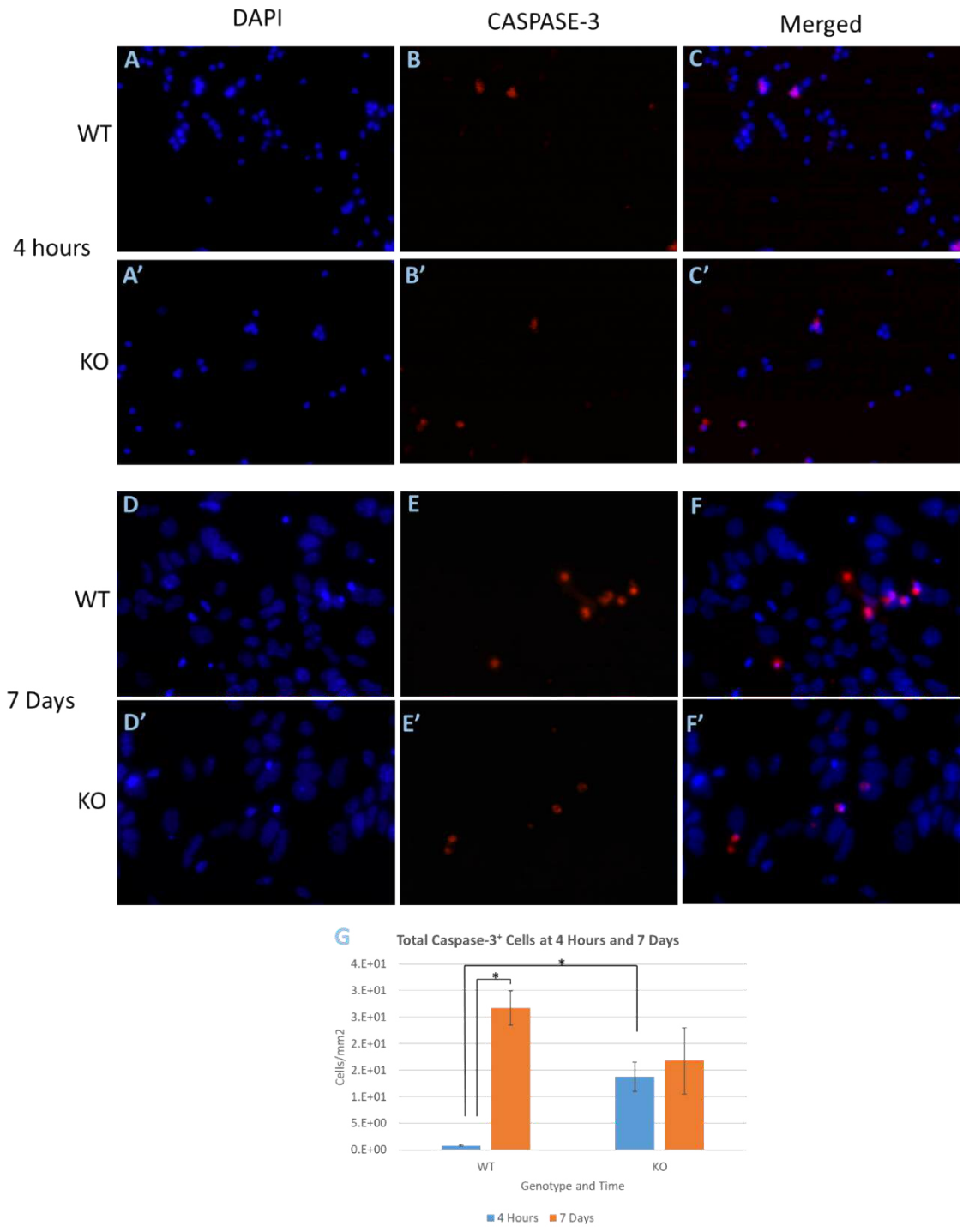


Figure 5.15: DAPI, CASPASE-3 and merged expression at 4 hours for WT (A, B, C) and KO (A', B', C'), and at 7 days for WT (D, E, F) and KO (D', E', F'). There are significantly more CASPASE-$3^+$ cells in conditional KO cultures at 4 hours compared to WT, though no difference after 7 days (G). Furthermore, WT cultures shown an increase in CASPASE-$3^+$ cells between 4 hours and 7 days, however KO cultures do not. Magnification x400; WT n=4, KO n=4.

This suggests that the total number of cells undergoing CASPASE-3 mediated apoptosis may be higher in the E18 conditional KO striatum compared to WT as evidenced by its increased express in 4-hour cultures. However, following a week of culture, this effect is lost. There is a significant increase in the number of CASPASE-3 positive cells at 7 days compared to 4-hour WT cultures (p=0.002), though conditional KO culture CASPASE-3 counts remain similar in each time point (p=0.520).

In order to determine whether MSN's in WT and conditional KO cultures were differently affected by Capase-3 mediated apoptosis, CASPASE-$3^+$/CTIP$2^+$ cells were identified at each time point. A two-way ANOVA showed a significant interaction effect of age and genotype ($F_{1,11}$ =8.143, p=0.016), with Bonferroni post-hoc analysis show significantly more (3.5x) CASPASE-$3^+$/CTIP$2^+$ cells in 4-hour KO cultures compared to WT at (p=0.049), though not in 7-day cultures (p=0.093).

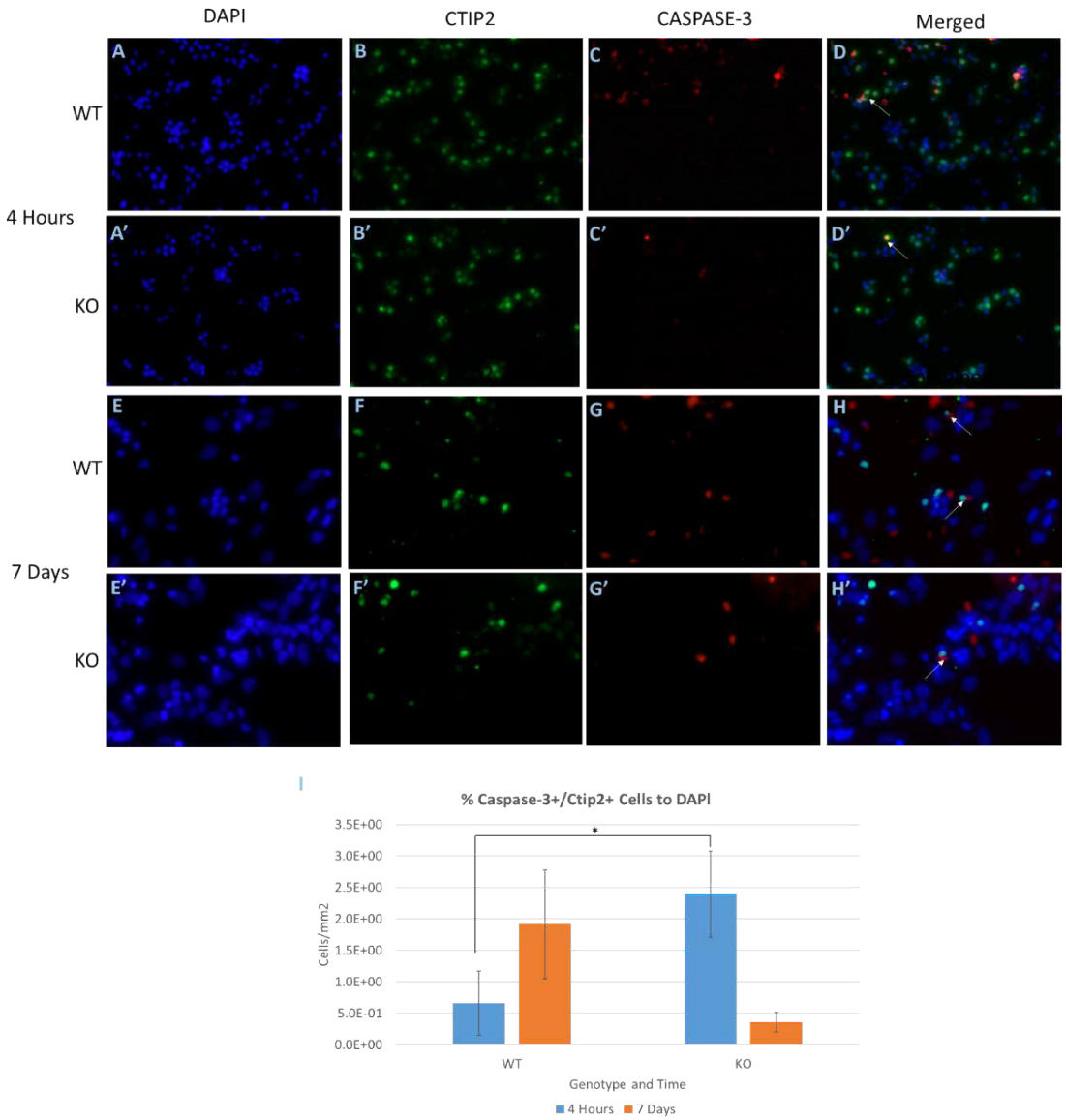


Figure 5.16: Fluorescent images of DAPI, CTIP2, CASPASE-3, and merged images respectively at 4 hours for WT (A, B, C, D) and KO (A', B', C', D'), and at 7 days for WT (E, F, G, H) and KO (E', F', G', H'). (I) There is a greater number of CTIP2$^{+}$/CASPASE-3$^{+}$ cells in KO cultures at 4 days compared to WT. x200 magnification; WT n=4, KO n=4.

This suggests that a higher proportion of MSNs are affected by CASPASE-3 mediated apoptosis in KO cultures compared to conditional WT at 4 days, though it should be noted that the proportions are very low for both genotypes.

### 5.5.6 **KI67**

A two-way ANOVA revealed a significant difference in KI67 cell counts between genotypes ($F_{1,12}$ =7.243 p=0.020) and time points ($F_{1,12}$ =12.944 p=0.001), with Bonferroni post-hoc analysis showing significantly less staining in KO cultures compared to WT at 4 hours (p=0.007), but not at 7 days (p=0.594). When KI67 counts were expressed relative to DAPI, a two-way ANOVA also revealed a significant difference between genotype ($F_{1,12}$ =11.824 p=0.005) with Bonferroni post-hoc analysis showing a significant decrease of 21% in KO cultures compared to WT in 7 day cultures (p=0.020) but not at 4-hours (p=0.350) (Figure 5.17-G). Furthermore, there was a significant increase in KI67 counts relative to DAPI between 4-hour and 7 days ($F_{1,12}$ =47.914 p=<0.001), with an increase of 246% and 174% in WT and KO cultures respectively. WT cultures also contained significantly more KI67 positive cells relative to DAPI compared to KO ($F_{1,12}$ =250.4 p=<0.001), with an increase of 35% and 52% at the 4-hour (p=0.05) and 7-day (p=<0.001) time points respectively.

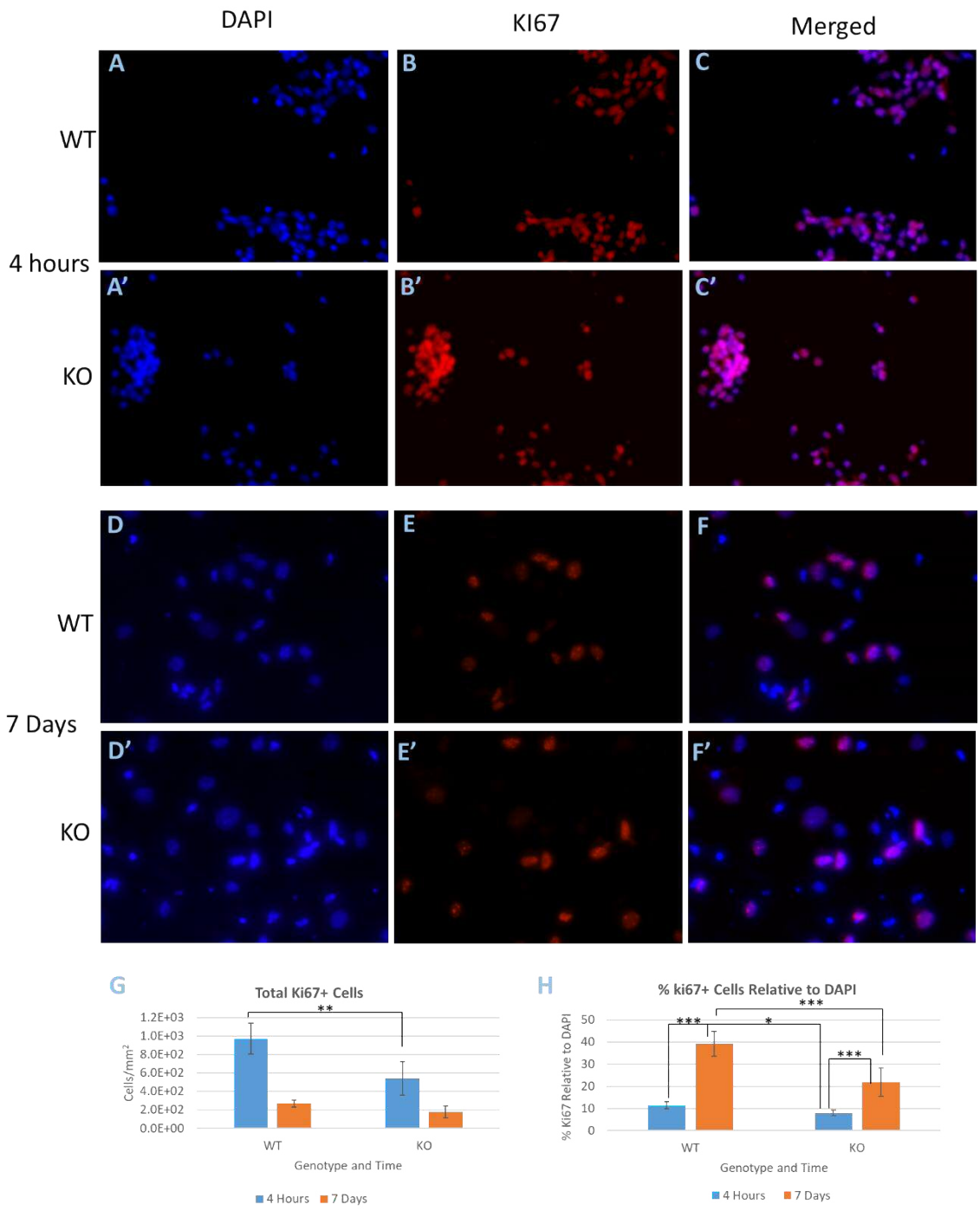


Figure 5.17: Photos for DAPI, KI67 and merged expression at 4 hours for WT (A, B, C) and KO (A', B', C'), and at 7 days for WT (D, E, F) and KO (D', E', F'). WT cultures contain more KI67 positive cells than KO at 4 hours (G) and both genotypes show increased KI67 expression relative to total cell counts between 4 hours and 7 days (WT=15%, KO=6%), although KO cultures have a lower proportion compared to WT at both time points (H). x200 magnification; WT n=4, KO n=4.

KI67 co-staining with CTIP2 was analysed in order in an attempt to identify newly differentiated MSNs. Very few CTIP2$^{+}$ cells were found to co-label with KI67, which is perhaps not surprising as most CTIP2 positive cells would be expected to be post mitotic.

The fact that some co-label may indicate that there is a window in which cells very recently having left the cell cycle contain detectable amounts of both proteins. A two-way ANOVA showed a significant increase in the number of KI67$^{+}$/CTIP2$^{+}$ cells in 7 day cultures ($F_{1,11}$ =11.768 p=0.006) and a significant difference between genotypes ($F_{1,11}$ =4.864 p=0.050), with Bonferroni post-hoc analysis showing significantly fewer (71%) KI67$^{+}$/CTIP2$^{+}$ cells in conditional KO cultures compared to WT after 7 days in culture (p=0.016), but not at 4 days (p=0.860) (Figure 5.18).

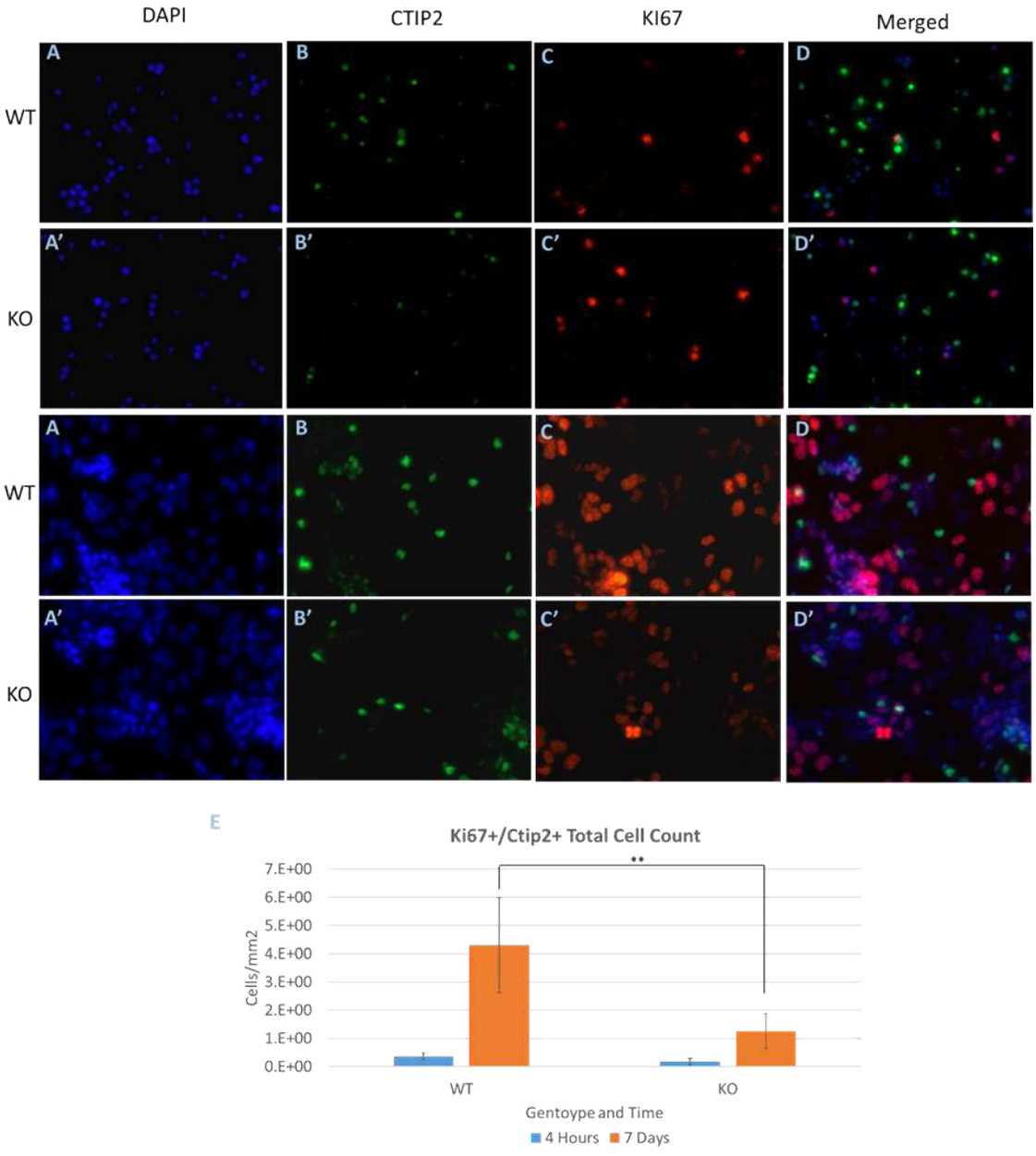


Figure 5.18: Photos at 7 days for WT (A, B, C, D) and KO (A', B', C', D'), showing a significantly greater number of KI67$^{+}$/CTIP2$^{+}$ cells in 7 day WT cultures compared to conditional KO (E). Magnification x200 WT n=4, KO n=4.

## 5.6 Discussion

In this Chapter primary foetal striatal cells with a genetically defined conditional MEF2C KO were used. Previous *in vitro* investigations into MEF2C were conducted on the established P19 and H9 cell lines (Okamoto et al. 2000; Cho et al. 2011). These cell lines have undergone multiple passages *in vitro* and cells are therefore adapted towards survival in an *in vitro* system, and hence may behave differently to primary striatal cells. Extensive passages of cells often result in cellular, genetic or epigenetic modifications that could influence the extent to which a protein's function is necessary for differentiation of particular cell types. The primary striatal foetal cells used in this chapter provide a clear advantage over established cell-line based experiments. Dominant negative knock-down constructs or lenti-shRNA's may fail to effectively knockdown MEF2C in all cells, with cultured primary cell lines also known to accumulate a series of random genetic mutations and adaptions to culture conditions after several passages. The cells within the primary conditional KO cultures used in this investigation however are all the same genetically defined mutant cells (*Mef2c*$^{loxP/loxP}$) and are not adapted to *in vitro* culture conditions, ensuring less cell-to-cell variation within cultures and more accurate representation of MEF2C function.

MEF2C staining demonstrated a marked reduction of MEF2C in KO cultures relative to WT, further confirming that the conditional KO results in widespread KO of MEF2C expression. Interestingly, cells with confirmed KO of MEF2C are still able to develop into neurons expressing CTIP2, a recognised MSN marker. This is consistent with the findings in Chapter 4, where CTIP2 cell numbers were only slightly reduced in the conditional KO striatum. However, in Chapter 4 it was also demonstrated that many of these CTIP2 cells in the KO striatum did not co-label with FOXP1, suggesting that they may reflect aberrant differentiation of "normal" MSNs. Whilst FOXP1 expression within E18 striatal KO cultures would be an interesting marker to compare to WT, particularly given its reduced expression in the adult KO striatum, FOXP1 staining was not undertaken in this investigation due to limited tissue availability. Furthermore, despite FOXP1 expression reduction in adult tissue, the numbers of FOXP1 expressing cells at P7 was not different to wild type, so it may be expected that that FOXP1 expression would not be impaired in E18 KO cultures.

Both preliminary experiments showed non-significant trends towards lower total numbers of DAPI positive cells by 2-3 weeks in the KO. However, this was not born out in

Experiment 3 where no significant differences were found in total cell numbers between genotypes.

Similarly, an analysis of small nuclei vs large nuclei cells showed a non-significant trend to lower numbers of large nuclei cells in the KO by 2 and 3 weeks, which was again not born out in the third Experiment. The larger nuclei cells are most likely to be astrocytes, and GFAP staining in Experiment 3 also showed no significant different in counts between genotypes, indicating that MEF2C did not have a marked effect on astrocyte differentiation in this experimental system. As before, there are differences in the longest time points assessed in the Preliminary Experiments (2-3 weeks) and in the 3rd Experiment (7 days), so it remains possible that a significant effect on larger nuclei cells may have been seen with longer periods of time in culture.

NEUN staining in Preliminary Experiment 2 identified neuronal proportions within each culture and demonstrated a decline in the proportion of neurons over time, though there was no convincing difference between genotypes. Unfortunately, there weren't enough cells in Experiment 3 to repeat the NEUN staining which would have been ideal. However, these results do confirm there is a significant portion of post-mitotic neuronal cells within each culture, and that the proportion of these neurons decreases after 2 weeks, though this does not show what proportion of these neuronal cells are MSNs.

Therefore, in Experiment 3, CTIP2 staining was used as a marker of MSNs. CTIP2 is also known to only stain neurons. The CTIP2 staining conducted in Experiment 3 showed an increase in CTIP2 between 4 hours and 7 days in both WT and KO cultures, suggesting that substantial numbers of MSNs are born/differentiate from precursors after E18, at least in vitro. Interestingly, CTIP2 was reduced in the KO at 7 days, although only when assessed as a percentage of total cells (DAPI). This aligns with Chapter 4 where levels of CTIP2 were lower in the conditional KO striatum (although this reduction was less than that of FOXP1 and DARPP-32).

The reduction in cells labelling for MSN markers, both in this in vitro experiment and in Chapter 4, raises the possibility that KO of MEF2C results in an increase in the number of cells undergoing cell death, reduces the proliferation of these cells, or both. CASPASE-3 staining at 24 hours and 2 weeks in Preliminary Experiment 2 did not show any genotype differences, however Experiment 3 revealed higher levels of CASPASE-3 in the KO at 4 hours (immediately after plating) but not at 7 days. Furthermore, an analysis of CASPASE-3 staining of CTIP2 cells produced a similar result with higher numbers of CTIP2 cells at 4 hours co-labelling with CASPASE-3, suggesting that apoptosis of MSNs/MSN progenitors was greater in the KO cultures immediately after

plating. This effect appears to have disappeared by 7 days. An effect of MEF2C on apoptosis in neuronal cells has been previously been described (Mao et al. 1999; Okamoto et al. 2000; Cho et al. 2011). Specifically, *In vitro* analysis of MEF2C knockdown was previously undertaken using a mutated dominant negative MEF2 construct (pGK-DNmt) (Okamoto et al. 2000). Cultures derived from an established P19 cell line were differentiated for 3 days with the addition of retinoic-acid. This revealed an increase in apoptosis of immature neuronal cells identified through Hoechst staining, whilst also preventing differentiation of mature neuronal cells, as indicated through MAP2 antibody staining. Furthermore, the knockdown of MEF2C in neural stem cells of the established H9 cell line through the introduction of lenti-shRNA prior to the formation of NPCs *in vitro*, has been shown to increase cell death by ~2-fold at 14 days post infection, following TUNEL assay (Cho et al. 2011). After 33 days, however, the degree of cell death returned to levels consistent with control samples. It should be noted that this investigation used neurosphere culture rather than traditional monolayer cultures, although it is reasonable to expect that the same patterns of cell behaviour apply for each method, albeit over differing time points. Loss of MEF2C also resulted in smaller than normal neurospheres, adding further weight to the notion that MEF2C plays a role in cell survival (Mao et al. 1999; Okamoto et al. 2000; Cho et al. 2011).

In Experiment 3, both genotypes show a significant increase in the proportion of cells that express KI67 after 7 days of culture, demonstrating that proliferative activity increases over time. However, the numbers of KI67 positive cells was lower in KO compared to WT at 4 hours and trended towards lower levels at 7 days. When compared to total DAPI, the KI67 was again reduced in KO cultures, but this time significantly so at 7 days with a trend to being lower at 4 hours. When the total number of $KI67^{+}/CTIP2^{+}$ cells are compared, there was again a significant drop in the KO at 7 days and a trend to being lower at 4 hours relative to WT. These results are consistent with the lower $CTIP2^{+}$ cell proportion identified in 7-day KO cultures compared to WT, and with the reduced numbers of MSNs seen in the striatum of the MEF2C KO mouse in Chapter 4. They are also consistent with the notion that loss of MEF2C could lead to a reduction in the differentiation of normal MSNs. An effect on neuronal proliferation following knock down of MEF2C has been reported previously. Knockdown of Mef2C via the lenti-shMEF2C-1 virus has been shown to cause a decline or delay of neurogenesis in 33 day post-infection cultures as evidenced through both a significant reduction in mRNA levels of MAP2 and quantitative reduction of cells of neuronal morphology compared to controls (Cho et al. 2011). It should be noted however that this investigation did not utilise proliferation markers such as KI67, the inclusion of which would add significant weight

to these findings. However, it is also important to point out that in Preliminary Experiment 2, although a trend to lower levels of KI67 were seen at 4 hours in both the KO and the HET, by 2 weeks this trend was reversed with a trend to higher levels of KI67 in the KO and HET at 2 weeks. Thus, it will be important to repeat these experiments to have a greater level of confidence in these findings, and if/how they may change over different times in culture.

Taken together, these results are consistent with the notion that MEF2C is required for normal proliferation and survival of striatal cells, in particular MSNs from the late embryonic period onwards and are largely consistent with the findings in Chapter 4. It can't be excluded from these results that MEF2C is important for the generation/survival of non-MSNs and glia, although no evidence has been found for this to date. The results are consistent with a role for MEF2C in both proliferation and reduction of cell death, and this is in line with previous reports in the literature, although more work is required to confirm this. The culture model used in this Chapter may provide a useful system for future investigations of the mechanisms by which MEF2C is affecting striatal MSN differentiation.

### 5.6.1 **Summary**

Loss of MEF2C has a range of significant effects on cells isolated from the developing E18 striatum and analysed *in vitro*, altering the cellular composition of striatal culture populations both immediately after plate down and following several days of cultures. MEF2C expression is required for normal proliferative activity, apoptotic activity and the *in vitro* differentiation of MSNs.

# Chapter 6: Discussion

The key finding in this thesis is that conditional striatal KO of MEF2C disturbs normal striatal development in the mouse; in particular the number and character of striatal MSNs. The major period over which MEF2C appears to be exerting its influence in this context is the postnatal period. This conclusion is drawn largely from the result of histological comparison of the conditional KO and WT brain. The volume of the striatum is decreased in the MEF2C striatal KO compared to the WT at 3 months, whereas there was no significant difference between these genotypes in the striatal volume at P7. This suggests that MEF2C is of greater functional importance in the postnatal period after P7. Striatal volumes were stable in WT adult animals through to 18 months, aligning with other studies (Kelly *et al.*, 2009; Bayram-Weston *et al.*, 2012). However, a small but significant reduction in volume was seen in the MEF2C striatal KO by 18 months, suggesting that loss of MEF2C renders the structure of the striatum vulnerable to degeneration in old-age mice. Furthermore, it should be noted that despite the decrease of striatal volume there is no continued decrease in FOXP1 or DARPP-32 expressing MSNs after 3 months, indicating that MEF2C does not have a degenerative effect on striatal neurons into old age.

A reduction in striatal volume in humans is strongly linked to behavioural and cognitive impairments and to various diseases, including Huntington's, Parkinson's and schizophrenia (Bogerts, Meertz and Schönfeldt-Bausch, 1985; Rosas *et al.*, 2001; Aylward *et al.*, 2012; Pitcher *et al.*, 2012). MEF2C loss in humans is also linked to brain volume loss, with reduced forebrain volume seen in the 5q14.3q15 microdeletion syndrome, a condition driven through *de novo* mutations of MEF2C (Zweier *et al.*, 2008, 2010; Rocha *et al.*, 2016), although striatal volume loss has not been recorded. Loss of MEF2C has also been shown to foster development of a thicker corpus callosum and enlarged ventricles, which may bring about striatal volume reduction (Cardoso *et al.*, 2009; Zweier *et al.*, 2010; Zweier and Rauch, 2012; Rocha *et al.*, 2016). Furthermore, cocaine has been shown to supress MEF2 activity in the striatum, both acutely during the drug use and long-term following repeated exposure (Dietrich, 2013). Humans dependant on cocaine have been shown to have smaller striatal volumes relative to controls.

Striatal volume increased between P7 and 3 months in both genotypes, however this increase was less in the conditional KO striatum. A striatal volume increase between P7 and 3 months may be unsurprising, given the brains of P7 mice are smaller relative to

adults, although it does seem to somewhat contradict early work into striatal development, which found no increase in volume over this period (Fentress, Stanfield and Cowan, 1981). The increase in striatal volume may result from a number of processes, including continued neurogenesis, gliogenesis and an increase in the number and/or thickness of white matter tracts travelling through the striatum. The observation of increased NEUN and CTIP2 positive cells per striatum over this period indicates that ongoing neurogenesis is a major contributor of volume increase, and the demonstration of proliferation within the P13-P16 striatum described in this investigation provides further evidence that there is indeed an extended period of postnatal development in the mouse. However, it should also be acknowledged that no double-staining of BrdU and neuronal markers was undertaken, so it is not possible at this stage to confirm whether this represents neurogenesis, gliogenesis or both. Furthermore, a wider range of time points could be undertaken to more accurately identify postnatal striatal proliferation patterns.

At P7, the reduction in cell marker expression seen at 3 months in the MEF2C striatal KO is not present. FOXP1 and DARPP-32 MSN counts were not found to increase between P7 and 3 months in conditional KO mice in contrast to the increase that occurs in the WT. This indicates that MEF2C is required for post-natal differentiation of MSNs.

The reduction of DARPP-32 expression observed in KO mice compared to WT at 3 months may indicate reduced formation of mature MSNs at this age, thereby potentially hindering normal striatal function. DARPP-32 has a well-documented role in MSN function and striatal pathology and has been associated with neurological conditions including Parkinson's Disease and Alzheimer's. Rodent models of Parkinson's Disease show that phosphorylation of DARPP-32 at Thr-34 triggers abnormal involuntary movements (AIMs), mirroring l-DOPA-induced dyskinesia observed in human patients (Cenci, 2007; Santini *et al.*, 2007). DARPP-32 KO mice, however, do not exhibit particularly severe phenotypes in regards to spontaneous behaviour (Heyser *et al.*, 2000; Meyer-Lindenberg *et al.*, 2007; Kolata *et al.*, 2010; Yger and Girault, 2011). Whilst no formal behaviour analysis was conducted in my investigation, day-to-day handling of the mice showed no obvious movement differences between genotypes. However, DARPP-32 expression may increase evolutionary fitness and allow for a finer balance to be maintained in neurotransmitter signalling and the D1/D2 excitatory/inhibitory signalling pathways (Heyser *et al.*, 2000), suggesting DARPP-32 may be a required factor for higher motor and cognitive behavioural functions.

As described in Chapter 1, FOXP1 has a number of significant roles in neurological diseases and is associated with a range of phenotypes including speech defects, autism

and intellectual disabilities (Horn *et al.*, 2010; Le Fevre *et al.*, 2013; Palumbo *et al.*, 2013; Lozano *et al.*, 2015; Sollis *et al.*, 2016; Meerschaut *et al.*, 2017). Autism-like behaviour in mice can be induced through Nestin-Cre mediated FOXP1 deletion, significantly altering striatal structure (Bacon *et al.*, 2015). The loss of FOXP1 expression shown in my investigation may be a contributing factor to the reduction of MSN differentiation in the postnatal-adult mice period. This is supported through the finding that increased FOXP1 expression helps to maintain post-mitotic cell count in the presence of mutant-Huntingtin (mut-Htt), likely as a result of allowing smooth running of the cell cycle, the interruption of which is a common aspect in neurological disease (Becker and Bonni, 2004; Greene *et al.*, 2007; Liu *et al.*, 2015).

Furthermore, FOXP1 KO was found to significantly affect dendrite length, maturation and also significantly shorten axonal lengths in cortical neurons (Li *et al.*, 2015). The suggests that FOXP1 expression is required for normal dendritic formation and pruning. Despite the reduction of FOXP1 observed in this investigation, no changes to dendritic length or maturation was observed. However, significant increases in spine number and spine density were observed in striatal cells of the conditional KO striatum. It is important to note, however, that at 12 months of age, there has been significant time for striatal dendrites to adjust and correct. The combination of these two findings therefore may suggest that the dendritic effect of FOXP1 in the MEF2C conditional KO model is compensated for by the time 12-month adulthood is reached, therefore analysis at an earlier time point may be justified, or simply that the reduction of FOXP1 due to MEF2C KO is insufficient to produce these dendritic alterations.

A striking finding in this investigation is the differential expression levels of CTIP2 and FOXP1 in the adult conditional KO model. FOXP1 and CTIP2 have been shown to co-localise in almost all striatal MSNs in WT mice from their initial detection in the developing embryonic striatum at E12.5 through to adulthood, with only 1% of cells shown to be $CTIP2^{+}/FOXP1^{-}$ (Arlotta *et al.*, 2008; Precious *et al.*, 2016). Considering both FOXP1 and CTIP2 mark significantly higher numbers of MSNs than DARPP-32, it is clear that there are different subsets of MSNs that differentially express these factors, either temporally or permanently. This is supported by the well documented differences in MSN function not only through patch and matrix classifications, but also the differing direct and indirect pathways that exist throughout the basal ganglia system. In this respect, it is reasonable to suggest therefore that as there are differing functions of MSNs, there may be a $CTIP2^{+}/FOXP1^{-}$ subset of MSNs, although more analysis into the $CTIP2^{+}/FOXP1^{-}$ MSNs is required to confirm whether this is indeed a unique subset. One possible explanation therefore for the conserved CTIP2+ cell count between WT and KO mice, despite the

observed reduction in FOXP1+ cells in the KO model, is that the hypothesised CTIP2$^{+}$/FOXP1$^{-}$ MSN subset increases under this model.

It is also possible, however, that these CTIP2$^{+}$/FOXP1$^{-}$ cells represent an aberrant population of MSNs that have not properly differentiated. The relatively low proportion of CTIP2$^{+}$/FOXP1$^{-}$ MSNs in WT mice may be due to MEF2C facilitating the normal differentiation of the vast majority of MSNs, however loss of MEF2C results in an increase in the number of improperly differentiated MSNs. It is not known whether CTIP2$^{+}$/FOXP1$^{-}$ MSNs are functionally dissimilar to other MSNs, and indeed it may be unlikely that the striatum would maintain a proportion of improperly differentiated MSN, however this small proportion may simply not have been sufficiently impactful on an evolutionarily basis.

Alternatively, the reduction in FOXP1+ cells observed in this investigation may be due to reduced migration of neurons originating within the striatum and bound for the cortex. Whilst FOXP1 expression is present in the cortex, it is not present in all cortical cell types or in all layers, therefore if cortical-bound cells were unable to migrate through the striatum they would not necessarily be expected to express FOXP1. This may provide an explanation for the comparatively high number of CTIP2 positive cells observed within the striatum compared to the other MSN markers. Moreover, restriction of the migration of cortical-bound cells has been shown upon expression of Family Zinc Finger 2 (Fezf2), a protein that has been shown to co-localise with CTIP2 (Chen *et al.*, 2008). However, it is uncertain whether this is the case, particularly since there remains a reduction in striatal volume in the striatal MEF2C KO mouse and drop in total cell number. Furthermore, a substantial number of migrating projection neurons would be required and would need to provide some degree of functionality similar to MSNs, thereby masking severe phenotypes.

Although MSNs have an essential role in signal transfer between multiple brain regions, severe behavioural phenotypic deficits may not be noticed until there is a significant reduction in total MSN count, such as that seen following mut-Htt aggregation in HD. In this investigation, there was a significant decrease in total MSN count in 3-month conditional MEF2C KO mice, however the CTIP2 positive cell reduction was relativity small in relation to the total number of cells. If phenotypic differences were to be found in MEF2C striatal KO mice, it is likely this would occur at some point between mid-postnatal development and early adulthood (between P7 and 3 months), as it is between these periods that the biggest differences are likely to be observed.

A decrease of cell density in neuronal populations is a common pathological effect of a range of neurodegenerative conditions. Significant decreases of neuronal density in the hippocampus have been observed in Alzheimer's patients, particularly in later stages of the disease (Ross *et al.*, 2004). A similar observation has been made in the striatum of Parkinson's and Huntington's Disease patients, with lower neuronal density observed in the substantia nigra, particularly in the latter stages of the diseases (Ross *et al.*, 2004). Non-neurodegenerative diseases also show variations in cell density, however, with reduced neuronal density observed in the putamen, nucleus accumbus and amygdala of schizophrenia patients. MEF2C has increasingly been shown in recent years to be a contributing factor to an ever-growing range of neurological conditions, therefore the significance of striatal volume reduction in my MEF2C KO model should not be understated. These results open up avenues of investigations where targeted therapies of MEF2C may bring about therapeutic treatments for a range of conditions in which decreases in striatal volume and cell densities are of pathological consequence.

This investigation also undertook a series of small studies to determine whether KO of MEF2C has any significant effect in the embryonic developing striatum, as assayed in E18 WGE cultures. The main findings were that loss of MEF2C results in reduced proliferation, increased apoptosis, and fewer CTIP2 positive MSNs. These results indicate that striatal MEF2C function is not limited to post-natal mice and suggest it is functionally important in differentiating neurons isolated from embryonic stages. These experiments could be extended to a larger scale with several litters analysed over several time points, to analyse this observation further.

These results would appear to align with those obtained in the P19 cell investigation of MEF2C KO, confirming that the immediate effect on embryonic cells *in vitro* following reduction of MEF2C function is inhibited differentiation and increased apoptosis (S Okamoto *et al.*, 2000). It is important to consider, however, that my investigation was conducted on primary cells, which are more indicative of true MEF2C embryonic function. In contrast, established cell lines are often passaged numerous times and are selected in part for their stability in the *in vitro* culture conditions and the ease with which differentiation may be induced.

### 6.1.1 Future directions

Following BrdU analysis on the P13-P16 striatum which showed that MEF2C is required for normal proliferation of striatal cells during this period, the next step would be to determine whether the anti-apoptotic effect of MEF2C previously shown *in vitro* in this chapter and literature (Zixu Mao *et al.*, 1999; S Okamoto *et al.*, 2000) is also present *in vivo*. This will allow for a more complete understanding of why there is significant MSN loss, particularly of FOXP1 and DARPP-32 expressing MSNs, in the 3-month striatum.

In order to explore the remarkably unaffected CTIP2 expression profile relative to FOXP1 following striatal MEF2C KO, histological analysis of the adult mouse striatum with Fezf2 antibodies could be undertaken to search for cortical bound neurons originating from the SVZ that may have had their migration interrupted following loss of striatal MEF2C. Furthermore, it would be informative to further investigate the nature of $CTIP2^{+}/FOXP1^{-}$ MSNs in terms not only of their expression profile, but also electrophysiological activity.

Moreover, with the cellular phenotypes described in this investigation, particularly in 3-month mice, it remains to be known what functional effects, if any, arise from striatal loss of MEF2C. A series of striatum-oriented behavioural experiments could be conducted on conditional KO mice compared to WT littermates to determine what motor or cognitive effects arise as a result of this and whether any parallels may be drawn with human conditions of MEF2C loss (Zweier *et al.*, 2010; Zweier and Rauch, 2012; Rocha *et al.*, 2016). Although it is perhaps unlikely that phenotypes as severe as they are in humans may be found in this striatal MEF2C KO mouse model, phenotypic detection may allow for better understanding of the disease pathology, with links possibly drawn to what effect the human striatum is involved in cognitive and motor phenotypes exhibited in this condition.

It remains to be determined exactly what mechanisms underpin my results on the functional effects of the MEF2C striatal KO. MEF2C is a transcription factor associated not only with neuronal processes, but also processes in other tissues including angiogenesis and cardiac development (see Chapter 1). In order for MEF2C to facilitate different roles in different cell types, specific post-translational modifications and protein interactions are likely within each tissue to ensure MEF2C acts to regulate gene expression in the appropriate way for the cell type. Novel MEF2C protein-protein interactors present within the embryonic brain were identified over the course of my investigation, however the data are not shown due to their incomplete status. Further work could be undertaken to identify MEF2C protein-protein interactors that are present in the striatum during its development that may influence MEF2C activity, to include the

effects of loss of MEF2C on these proteins. Moreover, investigating what the effect of various different mutations of MEF2C proteins have in terms of their ability to bind to key proteins may be key to understanding how specific mutations in the human MEF2C gene can result in serve phenotypes, such as those seen in the 5q14.3q15 condition (Cardoso *et al.*, 2009; Zweier *et al.*, 2010; Zweier and Rauch, 2012; Rocha *et al.*, 2016).

# Bibliography

Adachi, M. *et al.* (2016) 'Postnatal Loss of Mef2c Results in Dissociation of Effects on Synapse Number and Learning and Memory', *Biological Psychiatry*. Elsevier USA, 80(2), pp. 140–148. doi: 10.1016/j.biopsych.2015.09.018.

*Affymetrix* (2020). Available at: https://www.affymetrix.com/site/mainPage.affx (Accessed: 4 February 2020).

Albert, K. A. *et al.* (2002) 'Evidence for decreased DARPP-32 in the prefrontal cortex of patients with schizophrenia.', *Archives of general psychiatry*, 59(8), pp. 705–12. Available at: http://www.ncbi.nlm.nih.gov/pubmed/12150646 (Accessed: 29 January 2018).

Albin, R. L., Young, A. B. and Penney, J. B. (1989) 'The functional anatomy of basal ganglia disorders', *Trends in Neurosciences*. Elsevier Current Trends, 12(10), pp. 366–375. doi: 10.1016/0166-2236(89)90074-X.

Anderson, S. A. *et al.* (1997) 'Interneuron migration from basal forebrain to neocortex: Dependence on Dlx genes', *Science*, 278(5337), pp. 474–476. doi: 10.1126/science.278.5337.474.

Anderson, Stewart A *et al.* (1997) 'Mutations of the Homeobox Genes Dlx-1 and Dlx-2 Disrupt the Striatal Subventricular Zone and Differentiation of Late Born Striatal Neurons', *Neuron*. Cell Press, 19(1), pp. 27–37. doi: 10.1016/S0896-6273(00)80345-1.

Arber, C. *et al.* (2015) 'Activin A directs striatal projection neuron differentiation of human pluripotent stem cells.', *Development (Cambridge, England)*. Oxford University Press for The Company of Biologists Limited, 142(7), pp. 1375–86. doi: 10.1242/dev.117093.

Archer, H. L. *et al.* (2006) 'CDKL5 mutations cause infantile spasms, early onset seizures, and severe mental retardation in female patients', *Journal of medical genetics*, 43(9), pp. 729–734.

Ariani, F. *et al.* (2008) '< i> FOXG1</i> Is Responsible for the Congenital Variant of Rett Syndrome', *The American Journal of Human Genetics*, 83(1), pp. 89–93.

Arlotta, P. *et al.* (2005) 'Neuronal Subtype-Specific Genes that Control Corticospinal Motor Neuron Development In Vivo', *Neuron*. Cell Press, 45(2), pp. 207–221. doi: 10.1016/J.NEURON.2004.12.036.

Arlotta, P. *et al.* (2008) 'Ctip2 Controls the Differentiation of Medium Spiny Neurons and the Establishment of the Cellular Architecture of the Striatum', *Journal of Neuroscience*, 28(3), pp. 622–632. doi: 10.1523/JNEUROSCI.2986-07.2008.

Arnold, M. A. *et al.* (2007) 'MEF2C Transcription Factor Controls Chondrocyte Hypertrophy and Bone Development', *Developmental Cell*, 12(3), pp. 377–389. doi: 10.1016/j.devcel.2007.02.004.

Aubry, L. *et al.* (2008) 'Striatal progenitors derived from human ES cells mature into DARPP32 neurons in vitro and in quinolinic acid-lesioned rats.', *Proceedings of the National Academy of Sciences of the United States of America*. National Academy of Sciences, 105(43), pp. 16707–12. doi: 10.1073/pnas.0808488105.

Aylward, E. H. *et al.* (2012) 'Striatal Volume Contributes to the Prediction of Onset of Huntington Disease in Incident Cases', *Biological Psychiatry*. Elsevier, 71(9), pp. 822–828. doi: 10.1016/J.BIOPSYCH.2011.07.030.

Bacon, C. *et al.* (2015) 'Brain-specific Foxp1 deletion impairs neuronal development and causes autistic-like behaviour', *Molecular Psychiatry*. Nature Publishing Group, 20(5), pp. 632–639. doi: 10.1038/mp.2014.116.

Bacon, C. and Rappold, G. A. (2012) 'The distinct and overlapping phenotypic spectra of FOXP1 and FOXP2 in cognitive disorders', *Human Genetics*. Springer-Verlag, 131(11), pp. 1687–1698. doi: 10.1007/s00439-012-1193-z.

Barbosa, A. C. *et al.* (2008) 'MEF2C, a transcription factor that facilitates learning and memory by negative regulation of synapse numbers and function', *Proceedings of the National Academy of Sciences*, 105(27), pp. 9391–9396.

Bateup, H. S. *et al.* (2008) 'Cell type–specific regulation of DARPP-32 phosphorylation by psychostimulant and antipsychotic drugs', *Nature Neuroscience*, 11(8), pp. 932–939. doi: 10.1038/nn.2153.

Baydyuk, M. *et al.* (2011) 'TrkB receptor controls striatal formation by regulating the number of newborn striatal neurons', *Proceedings of the National Academy of Sciences of the United States of America*, 108(4), pp. 1669–1674. doi: 10.1073/pnas.1004744108.

Bayram-Weston, Z. *et al.* (2012) 'Light and electron microscopic characterization of the evolution of cellular pathology in YAC128 Huntington's disease transgenic mice', *Brain Research Bulletin*, 88(2–3), pp. 137–147. doi: 10.1016/j.brainresbull.2011.05.005.

Becker, E. B. . and Bonni, A. (2004) 'Cell cycle regulation of neuronal apoptosis in

development and disease', *Progress in Neurobiology*. Pergamon, 72(1), pp. 1–25. doi: 10.1016/J.PNEUROBIO.2003.12.005.

Bedogni, F. *et al.* (2010) 'Tbr1 regulates regional and laminar identity of postmitotic neurons in developing neocortex', *Proceedings of the National Academy of Sciences*, 107(29), pp. 13129–13134.

Belkhiri, A., Zhu, S. and El-Rifai, W. (2016) 'DARPP-32: from neurotransmission to cancer.', *Oncotarget*. Impact Journals, LLC, 7(14), pp. 17631–40. doi: 10.18632/oncotarget.7268.

Belluzzi, O. *et al.* (2003) 'Electrophysiological differentiation of new neurons in the olfactory bulb.', *The Journal of neuroscience : the official journal of the Society for Neuroscience*. Society for Neuroscience, 23(32), pp. 10411–8. doi: 10.1523/jneurosci.1114-05.2005.

Bentivoglio, M. *et al.* (1980) 'Two new fluorescent retrograde neuronal tracers which are transported over long distances', *Neuroscience Letters*. Elsevier, 18(1), pp. 25–30. doi: 10.1016/0304-3940(80)90208-6.

Bernard, V., Normand, E. and Bloch, B. (1992) 'Phenotypical characterization of the rat striatal neurons expressing muscarinic receptor genes', *Journal of Neuroscience*. Society for Neuroscience, 12(9), pp. 3591–3600. doi: 10.1523/JNEUROSCI.12-09-03591.1992.

Bertran-Gonzalez, J. *et al.* (2010) 'What is the Degree of Segregation between Striatonigral and Striatopallidal Projections?', *Frontiers in neuroanatomy*. Frontiers Media SA, 4. doi: 10.3389/fnana.2010.00136.

Bibb, J. A. *et al.* (1999) 'Phosphorylation of DARPP-32 by Cdk5 modulates dopamine signalling in neurons', *Nature*, 402(6762), pp. 669–671. doi: 10.1038/45251.

Black, B. L., Lu, J. and Olson, E. N. (1997) 'The MEF2A 3'untranslated region functions as a cis-acting translational repressor', *Molecular and cellular biology*, 17(5), pp. 2756–2763.

Black, B. L. and Olson, E. N. (1998) 'Transcriptional control of muscle development by myocyte enhancer factor-2 (MEF2) proteins', *Annual review of cell and developmental biology*, 14(1), pp. 167–196.

Blanchard, F. J. *et al.* (2010) 'The transcription factor Mef2 is required for normal circadian behavior in Drosophila', *Journal of Neuroscience*, 30(17), pp. 5855–5865. doi: 10.1523/JNEUROSCI.2688-09.2010.

Bogerts, B., Meertz, E. and Schönfeldt-Bausch, R. (1985) 'Basal Ganglia and Limbic System Pathology in Schizophrenia', *Archives of General Psychiatry*. American Medical Association, 42(8), p. 784. doi: 10.1001/archpsyc.1985.01790310046006.

Bolam, J. P. *et al.* (1986) 'Substance P-Containing terminals in synaptic contact with cholinergic neurons in the neostriatum and basal forebrain: a double immunocytochemical study in the rat', *Brain Research*, 397(2), pp. 279–289. doi: 10.1016/0006-8993(86)90629-3.

Bolam, J. P. *et al.* (2000) 'Synaptic organisation of the basal ganglia', *Journal of Anatomy*. Wiley-Blackwell, 196(4), pp. 527–542. doi: 10.1046/j.1469-7580.2000.19640527.x.

Bour, B. A. *et al.* (1995) 'Drosophila MEF2, a transcription factor that is essential for myogenesis', *Genes & development*, 9(6), pp. 730–741.

Braccioli, L. *et al.* (2017) 'FOXP1 Promotes Embryonic Neural Stem Cell Differentiation by Repressing Jagged1 Expression.', *Stem cell reports*. Elsevier, 9(5), pp. 1530–1545. doi: 10.1016/j.stemcr.2017.10.012.

Brami-Cherrier, K. *et al.* (2005) 'Parsing Molecular and Behavioral Effects of Cocaine in Mitogen- and Stress-Activated Protein Kinase-1-Deficient Mice', *Journal of Neuroscience*, 25(49), pp. 11444–11454. doi: 10.1523/JNEUROSCI.1711-05.2005.

Brand, S. and Rakic, P. (1979) 'Genesis of the primate neostriatum: [3H]thymidine autoradiographic analysis of the time of neuron origin in the rhesus monkey', *Neuroscience*. Pergamon, 4(6), pp. 767–778. doi: 10.1016/0306-4522(79)90005-8.

Braunlich, K. and Seger, C. (2013) 'The basal ganglia', *Wiley Interdisciplinary Reviews: Cognitive Science*. Wiley-Blackwell, 4(2), pp. 135–148. doi: 10.1002/wcs.1217.

Bromberg-Martin, E. S., Matsumoto, M. and Hikosaka, O. (2010) 'Dopamine in Motivational Control: Rewarding, Aversive, and Alerting', *Neuron*. Cell Press, 68(5), pp. 815–834. doi: 10.1016/J.NEURON.2010.11.022.

Campbell, K., Olsson, M. and Björklund, A. (1995) 'Regional incorporation and site-specific differentiation of striatal precursors transplanted to the embryonic forebrain ventricle', *Neuron*. Cell Press, 15(6), pp. 1259–1273. doi: 10.1016/0896-6273(95)90006-3.

Cardoso, C. *et al.* (2009) 'Periventricular heterotopia, mental retardation, and epilepsy associated with 5q14. 3-q15 deletion', *Neurology*, 72(9), pp. 784–792.

de Carlos, J. A., López-Mascaraque, L. and Valverde, F. (1996) 'Dynamics of cell

migration from the lateral ganglionic eminence in the rat.', *The Journal of neuroscience : the official journal of the Society for Neuroscience*. Society for Neuroscience, 16(19), pp. 6146–56. doi: 10.1523/JNEUROSCI.16-19-06146.1996.

Cenci, M. A. (2007) 'Dopamine dysregulation of movement control in l-DOPA-induced dyskinesia', *Trends in Neurosciences*, 30(5), pp. 236–243. doi: 10.1016/j.tins.2007.03.005.

Chahrour, M. *et al.* (2008) 'MeCP2, a key contributor to neurological disease, activates and represses transcription', *Science*, 320(5880), pp. 1224–1229.

Chahrour, M. and Zoghbi, H. Y. (2007) 'The story of Rett syndrome: from clinic to neurobiology', *Neuron*, 56(3), pp. 422–437.

Chang, S. *et al.* (2006) 'Histone deacetylase 7 maintains vascular integrity by repressing matrix metalloproteinase 10', *Cell*, 126(2), pp. 321–334.

Chao, H.-T. *et al.* (2010) 'Dysfunction in GABA signalling mediates autism-like stereotypies and Rett syndrome phenotypes', *Nature*, 468(7321), pp. 263–269.

Chen, B. *et al.* (2008) 'The Fezf2-Ctip2 genetic pathway regulates the fate choice of subcortical projection neurons in the developing cerebral cortex.', *Proceedings of the National Academy of Sciences of the United States of America*. National Academy of Sciences, 105(32), pp. 11382–7. doi: 10.1073/pnas.0804918105.

Di Chiara, G. (1999) 'Drug addiction as dopamine-dependent associative learning disorder.', *European journal of pharmacology*, 375(1–3), pp. 13–30. Available at: http://www.ncbi.nlm.nih.gov/pubmed/10443561 (Accessed: 29 January 2018).

Cho, E.-G. *et al.* (2011) 'MEF2C enhances dopaminergic neuron differentiation of human embryonic stem cells in a parkinsonian rat model', *PLoS One*, 6(8), p. e24027.

Cho, K. *et al.* (2015) 'Calpain-mediated cleavage of DARPP-32 in Alzheimer's disease', *Aging Cell*, 14(5), pp. 878–886. doi: 10.1111/acel.12374.

Cipriani, S. *et al.* (2016) 'Dynamic Expression Patterns of Progenitor and Pyramidal Neuron Layer Markers in the Developing Human Hippocampus', *Cerebral Cortex*. Narnia, 26(3), pp. 1255–1271. doi: 10.1093/cercor/bhv079.

Clark, R. I. *et al.* (2013) 'MEF2 is an in vivo immune-metabolic switch', *Cell*, 155(2), pp. 435–447.

Cocas, L. A. *et al.* (2011) 'Pax6 Is Required at the Telencephalic Pallial–Subpallial Boundary for the Generation of Neuronal Diversity in the Postnatal Limbic

System', *The Journal of neuroscience*, 31(14), pp. 5313–5324. doi: 10.1523/jneurosci.3867-10.2011.

Corbin, J. G. *et al.* (2000) 'The Gsh2 homeodomain gene controls multiple aspects of telencephalic development', *Development*, 127(23).

Costa, M. R. *et al.* (2007) 'The Marginal Zone/Layer I as a Novel Niche for Neurogenesis and Gliogenesis in Developing Cerebral Cortex', *The Journal of neuroscience*, 27(42), pp. 11376–11388. doi: 10.1523/jneurosci.2418-07.2007.

Coulombe, P. and Meloche, S. (2007) 'Atypical mitogen-activated protein kinases: structure, regulation and functions', *Biochimica et Biophysica Acta (BBA)-Molecular Cell Research*, 1773(8), pp. 1376–1387.

Darmopil, S. *et al.* (2009) 'Genetic Inactivation of Dopamine D1 but Not D2 Receptors Inhibits L-DOPA–Induced Dyskinesia and Histone Activation', *Biological Psychiatry*, 66(6), pp. 603–613. doi: 10.1016/j.biopsych.2009.04.025.

Das, G. D. and Altman, J. (1970) 'Postnatal neurogenesis in the caudate nucleus and nucleus accumbens septi in the rat', *Brain Research*. Elsevier, 21(1), pp. 122–127. doi: 10.1016/0006-8993(70)90026-0.

Deacon, T. W., Pakzaban, P. and Isacson, O. (1994) 'The lateral ganglionic eminence is the origin of cells committed to striatal phenotypes: neural transplantation and developmental evidence', *Brain Research*. Elsevier, 668(1–2), pp. 211–219. doi: 10.1016/0006-8993(94)90526-6.

DeDiego, I., Smith Fernández, A. and Fairén, A. (1994) 'Cortical Cells That Migrate Beyond Area Boundaries: Characterization of an Early Neuronal Population in the Lower Intermediate Zone of Prenatal Rats', *European Journal of Neuroscience*, 6(6), pp. 983–997. doi: 10.1111/j.1460-9568.1994.tb00593.x.

van Deijk, A.-L. F. *et al.* (2017) 'High Content Analysis of Hippocampal Neuron-Astrocyte Co-cultures Shows a Positive Effect of Fortasyn Connect on Neuronal Survival and Postsynaptic Maturation.', *Frontiers in neuroscience*. Frontiers Media SA, 11, p. 440. doi: 10.3389/fnins.2017.00440.

Delli Carri, A. *et al.* (2013) 'Developmentally coordinated extrinsic signals drive human pluripotent stem cell differentiation toward authentic DARPP-32+ medium-sized spiny neurons.', *Development (Cambridge, England)*. Oxford University Press for The Company of Biologists Limited, 140(2), pp. 301–12. doi: 10.1242/dev.084608.

Dequiedt, F. *et al.* (2003) 'HDAC7, a thymus-specific class II histone deacetylase,

regulates Nur77 transcription and TCR-mediated apoptosis', *Immunity*, 18(5), pp. 687–698.

Dietrich, J.-B. (2013) 'The MEF2 family and the brain: from molecules to memory', *Cell and Tissue Research*. Springer-Verlag, 352(2), pp. 179–190. doi: 10.1007/s00441-013-1565-2.

Difiglia, M. (1987) 'Synaptic organization of cholinergic neurons in the monkey neostriatum', *Journal of Comparative Neurology*, 255(2), pp. 245–258. doi: 10.1002/cne.902550208.

Dodou, E. and Treisman, R. (1997) 'The Saccharomyces cerevisiae MADS-box transcription factor Rlm1 is a target for the Mpk1 mitogen-activated protein kinase pathway', *Molecular and cellular biology*, 17(4), pp. 1848–1859.

Dredge, B. K. and Jensen, K. B. (2011) 'NeuN/Rbfox3 Nuclear and Cytoplasmic Isoforms Differentially Regulate Alternative Splicing and Nonsense-Mediated Decay of Rbfox2', *PLoS ONE*. Edited by J. Valcarcel. Public Library of Science, 6(6), p. e21585. doi: 10.1371/journal.pone.0021585.

Duan, W. *et al.* (2016) 'Novel Insights into NeuN: from Neuronal Marker to Splicing Regulator', *Molecular Neurobiology*. Springer US, 53(3), pp. 1637–1647. doi: 10.1007/s12035-015-9122-5.

Eckenhoff, M. F. and Rakic, P. (1984) 'Radial organization of the hippocampal dentate gyrus: A Golgi, ultrastructural, and immunocytochemical analysis in the developing rhesus monkey', *Journal of Comparative Neurology*, 223(1), pp. 1–21. doi: 10.1002/cne.902230102.

Edley, S. M. and Herkenham, M. (1984) 'Comparative development of striatal opiate receptors and dopamine revealed by autoradiography and histofluorescence', *Brain Research*. Elsevier, 305(1), pp. 27–42. doi: 10.1016/0006-8993(84)91116-8.

Edmondson, D. G. *et al.* (1994) 'Mef2 gene expression marks the cardiac and skeletal muscle lineages during mouse embryogenesis', *Development*, 120(5), pp. 1251–1263.

Elmer, B. M. *et al.* (2013) 'MHCI requires MEF2 transcription factors to negatively regulate synapse density during development and in disease', *Journal of Neuroscience*, 33(34), pp. 13791–13804. doi: 10.1523/JNEUROSCI.2366-13.2013.

Engels, H. *et al.* (2009) 'A novel microdeletion syndrome involving 5q14. 3-q15: clinical and molecular cytogenetic characterization of three patients', *European Journal of Human Genetics*, 17(12), pp. 1592–1599.

Evans, A. E. *et al.* (2012) 'Molecular Regulation of Striatal Development: A Review', *Anatomy Research International*. Hindawi, 2012, pp. 1–14. doi: 10.1155/2012/106529.

Evans, A. E. (2013) *Characterisation of Foxp1 in striatal development and the adult brain*. Cardiff University.

Feliciano, D. M. and Bordey, A. (2013) 'Newborn cortical neurons: only for neonates?', *Trends in neurosciences*. NIH Public Access, 36(1), pp. 51–61. doi: 10.1016/j.tins.2012.09.004.

De Felipe, J. (1997) 'Inhibitory synaptogenesis in mouse somatosensory cortex', *Cerebral Cortex*, 7(7), pp. 619–634. doi: 10.1093/cercor/7.7.619.

Fentress, J. C., Stanfield, B. B. and Cowan, W. M. (1981) 'Observation on the development of the striatum in mice and rats.', *Anatomy and embryology*, 163(3), pp. 275–98. Available at: http://www.ncbi.nlm.nih.gov/pubmed/7340556 (Accessed: 1 February 2018).

Le Fevre, A. K. *et al.* (2013) '*FOXP1* mutations cause intellectual disability and a recognizable phenotype', *American Journal of Medical Genetics Part A*. Wiley-Blackwell, 161(12), pp. 3166–3175. doi: 10.1002/ajmg.a.36174.

Fienberg, A. A. *et al.* (1998) 'DARPP-32: regulator of the efficacy of dopaminergic neurotransmission.', *Science (New York, N.Y.)*, 281(5378), pp. 838–42. Available at: http://www.ncbi.nlm.nih.gov/pubmed/9694658 (Accessed: 29 January 2018).

Flavell, S. W. *et al.* (2006) 'Activity-dependent regulation of MEF2 transcription factors suppresses excitatory synapse number', *Science*, 311(5763), pp. 1008–1012.

Foster, G. A. *et al.* (1987) 'Development of a dopamine- and cyclic adenosine 3':5'-monophosphate-regulated phosphoprotein (DARPP-32) in the prenatal rat central nervous system, and its relationship to the arrival of presumptive dopaminergic innervation.', *The Journal of neuroscience : the official journal of the Society for Neuroscience*. Society for Neuroscience, 7(7), pp. 1994–2018. doi: 10.1523/JNEUROSCI.07-07-01994.1987.

Fukuda, T. *et al.* (2005) 'Methyl-CpG binding protein 2 gene (< i> MECP2</i>) variations in Japanese patients with Rett syndrome: pathological mutations and polymorphisms', *Brain and Development*, 27(3), pp. 211–217.

Fyffe, S. L. *et al.* (2008) 'Deletion of Mecp2 in Sim1-expressing neurons reveals a critical role for MeCP2 in feeding behavior, aggression, and the response to stress', *Neuron*, 59(6), pp. 947–958.

Gerber, A. P. and Keller, W. (1999) ‘An adenosine deaminase that generates inosine at the wobble position of tRNAs’, *Science*, 286(5442), pp. 1146–1149.

Gerdes, J. (1990) ‘Ki-67 and other proliferation markers useful for immunohistological diagnostic and prognostic evaluations in human malignancies.’, *Seminars in cancer biology*, 1(3), pp. 199–206. Available at: http://www.ncbi.nlm.nih.gov/pubmed/2103495 (Accessed: 30 December 2019).

Gerfen, C. R. (1984) ‘The neostriatal mosaic: compartmentalization of corticostriatal input and striatonigral output systems’, *Nature*. Nature Publishing Group, 311(5985), pp. 461–464. doi: 10.1038/311461a0.

Gerfen, C. R. *et al.* (1990) ‘D1 and D2 dopamine receptor-regulated gene expression of striatonigral and striatopallidal neurons.’, *Science (New York, N.Y.)*. American Association for the Advancement of Science, 250(4986), pp. 1429–32. doi: 10.1126/SCIENCE.2147780.

Gerfen, C. R. (1992) ‘The Neostriatal Mosaic: Multiple Levels of Compartmental Organization in the Basal Ganglia’, *Annual Review of Neuroscience*. Annual Reviews 4139 El Camino Way, P.O. Box 10139, Palo Alto, CA 94303-0139, USA , 15(1), pp. 285–320. doi: 10.1146/annurev.ne.15.030192.001441.

Gerfen, C. R., Baimbridge, K. G. and Miller, J. J. (1985) ‘The neostriatal mosaic: compartmental distribution of calcium-binding protein and parvalbumin in the basal ganglia of the rat and monkey.’, *Proceedings of the National Academy of Sciences of the United States of America*. National Academy of Sciences, 82(24), pp. 8780–4. doi: 10.1073/PNAS.82.24.8780.

Gill, G. (2004) ‘SUMO and ubiquitin in the nucleus: different functions, similar mechanisms?’, *Genes & development*, 18(17), pp. 2046–2059.

Girdwood, D. *et al.* (2003) ‘P300 transcriptional repression is mediated by SUMO modification’, *Molecular cell*, 11(4), pp. 1043–1054.

Glaser, E. M. and Van der Loos, H. (1981) ‘Analysis of thick brain sections by obverse-reverse computer microscopy: application of a new, high clarity Golgi-Nissl stain.’, *Journal of neuroscience methods*, 4(2), pp. 117–25. Available at: http://www.ncbi.nlm.nih.gov/pubmed/6168870 (Accessed: 31 January 2018).

Gossett, L. A. *et al.* (1989) ‘A new myocyte-specific enhancer-binding factor that recognizes a conserved element associated with multiple muscle-specific genes’, *Molecular and cellular biology*, 9(11), pp. 5022–5033.

Gray, P. C. *et al.* (1998) 'Primary structure and function of an A kinase anchoring protein associated with calcium channels.', *Neuron*, 20(5), pp. 1017–26. Available at: http://www.ncbi.nlm.nih.gov/pubmed/9620705 (Accessed: 29 January 2018).

Graybiel, A. M. (2005) 'The basal ganglia: learning new tricks and loving it', *Current Opinion in Neurobiology*. Elsevier Current Trends, 15(6), pp. 638–644. doi: 10.1016/J.CONB.2005.10.006.

Greene, L. A. *et al.* (2007) 'Cell cycle molecules define a pathway required for neuron death in development and disease', *Biochimica et Biophysica Acta (BBA) - Molecular Basis of Disease*. Elsevier, 1772(4), pp. 392–401. doi: 10.1016/J.BBADIS.2006.12.003.

Greengard, P. (2001) 'The neurobiology of slow synaptic transmission.', *Science (New York, N.Y.)*. American Association for the Advancement of Science, 294(5544), pp. 1024–30. doi: 10.1126/science.294.5544.1024.

Grégoire, S. and Yang, X.-J. (2005) 'Association with class IIa histone deacetylases upregulates the sumoylation of MEF2 transcription factors', *Molecular and cellular biology*, 25(6), pp. 2273–2287.

Haber, S. N. *et al.* (2006) 'Reward-related cortical inputs define a large striatal region in primates that interface with associative cortical connections, providing a substrate for incentive-based learning', *Journal of Neuroscience*, 26(32), pp. 8368–8376. doi: 10.1523/JNEUROSCI.0271-06.2006.

Haber, S. N. (2016) 'Corticostriatal circuitry', *Dialogues in Clinical Neuroscience*. Les Laboratoires Seriver, 18(1), pp. 7–21.

Haber, S. N. and McFarland, N. R. (1999) 'The concept of the ventral striatum in nonhuman primates', in *Annals of the New York Academy of Sciences*. New York Academy of Sciences, pp. 33–48. doi: 10.1111/j.1749-6632.1999.tb09259.x.

Haberland, M. *et al.* (2007) 'Regulation of HDAC9 gene expression by MEF2 establishes a negative-feedback loop in the transcriptional circuitry of muscle differentiation', *Molecular and cellular biology*, 27(2), pp. 518–525.

Hakim, N. H. A. *et al.* (2010) 'Alternative splicing of Mef2c promoted by Fox 1 during neural differentiation in P19 cells', *Genes to Cells*, 15(3), pp. 255–267.

Halliday, A. L. and Cepko, C. L. (1992) 'Generation and migration of cells in the developing striatum', *Neuron*. Cell Press, 9(1), pp. 15–26. doi: 10.1016/0896-6273(92)90216-Z.

Hamasaki, T. *et al.* (2003a) 'Neuronal cell migration for the developmental formation of

the mammalian striatum', *Brain Research Reviews*. Elsevier, 41(1), pp. 1–12. doi: 10.1016/S0165-0173(02)00216-3.

Hamasaki, T. *et al.* (2003b) 'Neuronal cell migration for the developmental formation of the mammalian striatum', *Brain Research Reviews*. Elsevier, 41(1), pp. 1–12. doi: 10.1016/S0165-0173(02)00216-3.

Hamburger, V., W, B.-B. and J. and Yip (1981) 'NEURONAL DEATH IN THE SPINAL GANGLIA OF THE CHICK EMBRYO AND ITS REDUCTION BY NERVE GROWTH FACTOR'', 1(1), pp. 60–71. Available at: https://pdfs.semanticscholar.org/769a/1d97c7b0a0b93542e9d8929ea684f6733bba.pdf (Accessed: 3 February 2018).

Han, J. *et al.* (1997) 'Activation of the transcription factor MEF2C by the MAP kinase p38 in inflammation'.

Heiman, M. *et al.* (2008) 'A Translational Profiling Approach for the Molecular Characterization of CNS Cell Types', *Cell*. Cell Press, 135(4), pp. 738–748. doi: 10.1016/J.CELL.2008.10.028.

Hélie, S., Ell, S. W. and Ashby, F. G. (2015) 'Learning robust cortico-cortical associations with the basal ganglia: An integrative review', *Cortex*. Elsevier, 64, pp. 123–135. doi: 10.1016/J.CORTEX.2014.10.011.

Hemmings, H. C. *et al.* (no date) 'DARPP-32, a dopamine-regulated neuronal phosphoprotein, is a potent inhibitor of protein phosphatase-1.', *Nature*, 310(5977), pp. 503–5. Available at: http://www.ncbi.nlm.nih.gov/pubmed/6087160 (Accessed: 29 January 2018).

Heyser, C. J. *et al.* (2000) 'DARPP-32 knockout mice exhibit impaired reversal learning in a discriminated operant task', *Brain Research*. Elsevier, 867(1–2), pp. 122–130. doi: 10.1016/S0006-8993(00)02272-1.

Hoffarth, R. M. *et al.* (1995) 'The mouse mutation reeler causes increased adhesion within a subpopulation of early postmitotic cortical neurons.', *The Journal of neuroscience : the official journal of the Society for Neuroscience*. Society for Neuroscience, 15(7 Pt 1), pp. 4838–50. doi: 10.1523/JNEUROSCI.15-07-04838.1995.

Holtmaat, A. J. G. D. *et al.* (2005) 'Transient and persistent dendritic spines in the neocortex in vivo', *Neuron*, 45(2), pp. 279–291. doi: 10.1016/j.neuron.2005.01.003.

Horn, D. *et al.* (2010) 'Identification of FOXP1 deletions in three unrelated patients with mental retardation and significant speech and language deficits', *Human Mutation*.

Wiley-Blackwell, 31(11), pp. E1851–E1860. doi: 10.1002/humu.21362.

Hosking, B. M. *et al.* (2001) 'SOX18 Directly Interacts with MEF2C in Endothelial Cells', *Biochemical and Biophysical Research Communications*. Academic Press Inc., 287(2), pp. 493–500. doi: 10.1006/bbrc.2001.5589.

Hsia, A. Y., Malenka, R. C. and Nicoll, R. A. (1998) 'Development of Excitatory Circuitry in the Hippocampus', *Journal of Neurophysiology*, 79(4), pp. 2013–2024. doi: 10.1152/jn.1998.79.4.2013.

http://mouse.brain-map.org/experiment/show/79567505 (2013) 'Experiment Detail :: Allen Brain Atlas: Mouse Brain'. Available at: http://mouse.brain-map.org/experiment/show/79567505 (Accessed: 3 February 2020).

Hu, J. S. *et al.* (2017) 'Cortical interneuron development: A tale of time and space', *Development (Cambridge)*. Company of Biologists Ltd, pp. 3867–3878. doi: 10.1242/dev.132852.

Hughes, A. (1961) 'Cell Degeneration in the Larval Ventral Horn of Xenopus laevis (Daudin)', *Development*, 9(2).

Ince, E., Ciliax, B. J. and Levey, A. I. (1997) 'Differential expression of D1 and D2 dopamine and m4 muscarinic acetylcholine receptor proteins in identified striatonigral neurons', *Synapse*. Wiley-Blackwell, 27(4), pp. 357–366. doi: 10.1002/(SICI)1098-2396(199712)27:4<357::AID-SYN9>3.0.CO;2-B.

Infantino, V. *et al.* (2013) 'MEF2C exon α: Role in gene activation and differentiation', *Gene*, 531(2), pp. 355–362.

Jain, M. *et al.* (2001) 'Cellular and molecular aspects of striatal development', *Brain Research Bulletin*. Elsevier, 55(4), pp. 533–540. doi: 10.1016/S0361-9230(01)00555-X.

Johnson, E. S. (2004) 'Protein modification by SUMO', *Annual review of biochemistry*, 73(1), pp. 355–382.

Johnston, J. G. *et al.* (1990) 'Mechanisms of striatal pattern formation: conservation of mammalian compartmentalization', *Developmental Brain Research*, 57(1), pp. 93–102. doi: 10.1016/0165-3806(90)90189-6.

Joshua, M., Adler, A. and Bergman, H. (2009) 'The dynamics of dopamine in control of motor behavior', *Current Opinion in Neurobiology*, pp. 615–620. doi: 10.1016/j.conb.2009.10.001.

Kakita, A. and Goldman, J. E. (1999) 'Patterns and Dynamics of SVZ Cell Migration in

the Postnatal Forebrain: Monitoring Living Progenitors in Slice Preparations', *Neuron*. Cell Press, 23(3), pp. 461–472. doi: 10.1016/S0896-6273(00)80800-4.

Kalsotra, A. *et al.* (2008) 'A postnatal switch of CELF and MBNL proteins reprograms alternative splicing in the developing heart', *Proceedings of the National Academy of Sciences*, 105(51), pp. 20333–20338.

Kamath, S. P. and Chen, A. I. (2019) 'Myocyte Enhancer Factor 2c Regulates Dendritic Complexity and Connectivity of Cerebellar Purkinje Cells', *Molecular Neurobiology*. Humana Press Inc., 56(6), pp. 4102–4119. doi: 10.1007/s12035-018-1363-7.

Kammoun, F. *et al.* (2004) 'Screening of MECP2 coding sequence in patients with phenotypes of decreasing likelihood for Rett syndrome: a cohort of 171 cases', *Journal of medical genetics*, 41(6), pp. e85–e85.

Kang, J., Gocke, C. B. and Yu, H. (2006) 'Phosphorylation-facilitated sumoylation of MEF2C negatively regulates its transcriptional activity', *BMC biochemistry*, 7(1), p. 5.

Kasler, H. G. and Verdin, E. (2007) 'Histone deacetylase 7 functions as a key regulator of genes involved in both positive and negative selection of thymocytes', *Molecular and cellular biology*, 27(14), pp. 5184–5200.

Kato, Y. *et al.* (1997) 'BMK1/ERK5 regulates serum induced early gene expression through transcription factor MEF2C', *The EMBO journal*, 16(23), pp. 7054–7066.

Kawaguchi, Y., Wilson, C. J. and Emson, P. C. (1989) 'Intracellular recording of identified neostriatal patch and matrix spiny cells in a slice preparation preserving cortical inputs.', *Journal of neurophysiology*. American Physiological Society Bethesda, MD , 62(5), pp. 1052–68. doi: 10.1152/jn.1989.62.5.1052.

Kee, N. *et al.* (2002) 'The utility of Ki-67 and BrdU as proliferative markers of adult neurogenesis', *Journal of Neuroscience Methods*, 115(1), pp. 97–105. doi: 10.1016/S0165-0270(02)00007-9.

van Keimpema, M. *et al.* (2014) 'FOXP1 directly represses transcription of proapoptotic genes and cooperates with NF- B to promote survival of human B cells', *Blood*, 124(23), pp. 3431–3440. doi: 10.1182/blood-2014-01-553412.

Kelly, R. *et al.* (2009) 'An Investigation into Young and Aged Rat Brain Volume Differences by Optimized Voxel-Based Morphometry', in *Proceedings 17th Scientific Meeting, International Society for Magnetic Resonance in Medicine*, p. 1085. Available at: http://www.fmrib.ox.ac.uk/fsl (Accessed: 29 September 2018).

Kempermann, G., Song, H. and Gage, F. H. (2015) 'Neurogenesis in the Adult

Hippocampus.', *Cold Spring Harbor perspectives in biology*. Cold Spring Harbor Laboratory Press, 7(9), p. a018812. doi: 10.1101/cshperspect.a018812.

Kessaris, N. *et al.* (2006) 'Competing waves of oligodendrocytes in the forebrain and postnatal elimination of an embryonic lineage', *Nat Neurosci*. Nature Publishing Group, 9(2), pp. 173–179. doi: http://www.nature.com/neuro/journal/v9/n2/suppinfo/nn1620_S1.html.

Kim, J. *et al.* (2002) 'Transcriptional activity of CCAAT/enhancer-binding proteins is controlled by a conserved inhibitory domain that is a target for sumoylation', *Journal of Biological Chemistry*, 277(41), pp. 38037–38044.

Kim, K. K., Adelstein, R. S. and Kawamoto, S. (2009) 'Identification of neuronal nuclei (NeuN) as Fox-3, a new member of the Fox-1 gene family of splicing factors.', *The Journal of biological chemistry*. American Society for Biochemistry and Molecular Biology, 284(45), pp. 31052–61. doi: 10.1074/jbc.M109.052969.

Kolata, S. *et al.* (2010) 'A dopaminergic gene cluster in the prefrontal cortex predicts performance indicative of general intelligence in genetically heterogeneous mice.', *PloS one*. Public Library of Science, 5(11), p. e14036. doi: 10.1371/journal.pone.0014036.

Konstantoulas, C. J., Parmar, M. and Li, M. (2010) 'FoxP1 promotes midbrain identity in embryonic stem cell-derived dopamine neurons by regulating Pitx3', *Journal of Neurochemistry*. Wiley/Blackwell (10.1111), 113(4), pp. 836–847. doi: 10.1111/j.1471-4159.2010.06650.x.

Koob, G. F. *et al.* (2004) 'Neurobiology of drug addiction.', in *Drug abuse: Origins & interventions.* American Psychological Association, pp. 161–190. doi: 10.1037/10341-008.

van der Kooy, D. and Fishell, G. (1987) 'Neuronal birthdate underlies the development of striatal compartments', *Brain Research*. Elsevier, 401(1), pp. 155–161. doi: 10.1016/0006-8993(87)91176-0.

Krushel, L. A., Connolly, J. A. and van der Kooy, D. (1989) 'Pattern formation in the mammalian forebrain: patch neurons from the rat striatum selectively reassociate in vitro', *Developmental Brain Research*. Elsevier, 47(1), pp. 137–142. doi: 10.1016/0165-3806(89)90116-8.

Kunii, Y. *et al.* (2011) 'Altered DARPP-32 expression in the superior temporal gyrus in schizophrenia', *Progress in Neuro-Psychopharmacology and Biological Psychiatry*, 35(4), pp. 1139–1143. doi: 10.1016/j.pnpbp.2011.03.016.

De la Fuente-Fernández, R. *et al.* (2002) 'Dopamine release in human ventral striatum and expectation of reward', *Behavioural Brain Research*, 136(2), pp. 359–363. doi: 10.1016/S0166-4328(02)00130-4.

Lambert de Rouvroit, C. and Goffinet, A. M. (1998) 'The reeler mouse as a model of brain development.', *Advances in anatomy, embryology, and cell biology*, pp. 1–106. doi: 10.1007/978-3-642-72257-8.

Lavdas, A. A. *et al.* (1999) 'The medial ganglionic eminence gives rise to a population of early neurons in the developing cerebral cortex', *Journal of Neuroscience*, 19(18), pp. 7881–7888. doi: 10.1523/jneurosci.19-18-07881.1999.

Lazaro, J.-B., Bailey, P. J. and Lassar, A. B. (2002) 'Cyclin D–cdk4 activity modulates the subnuclear localization and interaction of MEF2 with SRC-family coactivators during skeletal muscle differentiation', *Genes & development*, 16(14), pp. 1792–1805.

Lee, Y. *et al.* (1997) 'Myocyte-specific enhancer factor 2 and thyroid hormone receptor associate and synergistically activate the alpha-cardiac myosin heavy-chain gene', *Molecular and cellular biology*, 17(5), pp. 2745–2755.

Lefebvre, V. *et al.* (2007) 'Control of cell fate and differentiation by Sry-related high-mobility-group box (Sox) transcription factors', *The International Journal of Biochemistry & Cell Biology*. Pergamon, 39(12), pp. 2195–2214. doi: 10.1016/J.BIOCEL.2007.05.019.

Leifer, D., Golden, J. and Kowall, N. W. (1994) 'Myocyte-specific enhancer binding factor 2C expression in human brain development', *Neuroscience*, 63(4), pp. 1067–1079. doi: 10.1016/0306-4522(94)90573-8.

Lemasson, M. *et al.* (2005) 'Neonatal and Adult Neurogenesis Provide Two Distinct Populations of Newborn Neurons to the Mouse Olfactory Bulb', *Journal of Neuroscience*, 25(29), pp. 6816–6825. doi: 10.1523/JNEUROSCI.1114-05.2005.

Levine, N. D. *et al.* (2013) 'Advances in thin tissue Golgi-Cox impregnation: fast, reliable methods for multi-assay analyses in rodent and non-human primate brain.', *Journal of neuroscience methods*. NIH Public Access, 213(2), pp. 214–27. doi: 10.1016/j.jneumeth.2012.12.001.

Li, Hao, Radford, J. C., Ragusa, M. J., Shea, K. L., McKercher, S. R., Zaremba, J. D., Soussou, W., Nie, Z., Kang, Y.-J., Nakanishi, N., *et al.* (2008) 'Transcription factor MEF2C influences neural stem/progenitor cell differentiation and maturation in vivo.', *Proceedings of the National Academy of Sciences of the United States of America*.

National Academy of Sciences, 105(27), pp. 9397–402. doi: 10.1073/pnas.0802876105.

Li, H. *et al.* (2008) 'Transcription factor MEF2C influences neural stem/progenitor cell differentiation and maturation in vivo', *Proceedings of the National Academy of Sciences*, 105(27), pp. 9397–9402. doi: 10.1073/pnas.0802876105.

Li, Hao, Radford, J. C., Ragusa, M. J., Shea, K. L., McKercher, S. R., Zaremba, J. D., Soussou, W., Nie, Z., Kang, Y.-J. and Nakanishi, N. (2008) 'Transcription factor MEF2C influences neural stem/progenitor cell differentiation and maturation in vivo', *Proceedings of the National Academy of Sciences*, 105(27), pp. 9397–9402.

Li, M. *et al.* (2007) 'MECP2 and CDKL5 gene mutation analysis in Chinese patients with Rett syndrome', *Journal of human genetics*, 52(1), pp. 38–47.

Li, X. *et al.* (2015) 'Foxp1 Regulates Cortical Radial Migration and Neuronal Morphogenesis in Developing Cerebral Cortex', *PLOS ONE*. Edited by M. Sato. Public Library of Science, 10(5), p. e0127671. doi: 10.1371/journal.pone.0127671.

Li, Z. *et al.* (2008) 'Myocyte enhancer factor 2C as a neurogenic and antiapoptotic transcription factor in murine embryonic stem cells', *The Journal of neuroscience*, 28(26), pp. 6557–6568.

Lilly, B. *et al.* (1995) 'Requirement of MADS domain transcription factor D-MEF2 for muscle formation in Drosophila', *Science*, 267(5198), pp. 688–693.

Lin, Q. *et al.* (1997) 'Control of mouse cardiac morphogenesis and myogenesis by transcription factor MEF2C', *Science*, 276(5317), pp. 1404–1407.

Lin, Q. *et al.* (1998) 'Requirement of the MADS-box transcription factor MEF2C for vascular development', *Development*, 125(22), pp. 4565–4574.

Liu, K.-Y. *et al.* (2015) 'Disruption of the nuclear membrane by perinuclear inclusions of mutant huntingtin causes cell-cycle re-entry and striatal cell death in mouse and cell models of Huntington's disease', *Human Molecular Genetics*. Oxford University Press, 24(6), pp. 1602–1616. doi: 10.1093/hmg/ddu574.

Lobo, M. K. *et al.* (2006) 'FACS-array profiling of striatal projection neuron subtypes in juvenile and adult mouse brains', *Nature Neuroscience*. Nature Publishing Group, 9(3), pp. 443–452. doi: 10.1038/nn1654.

Lobo, M. K. *et al.* (2007) 'Genetic control of instrumental conditioning by striatopallidal neuron–specific S1P receptor Gpr6', *Nature Neuroscience*. Nature Publishing Group, 10(11), pp. 1395–1397. doi: 10.1038/nn1987.

Lobo, M. K. and Nestler, E. J. (2011) 'The Striatal Balancing Act in Drug Addiction: Distinct Roles of Direct and Indirect Pathway Medium Spiny Neurons', *Frontiers in Neuroanatomy*. Frontiers, 5, p. 41. doi: 10.3389/fnana.2011.00041.

Van Der Loos, H. (1956) '[Combination of two old methods of histological study of the central nervous system].', *Monatsschrift fur Psychiatrie und Neurologie*, 132(5–6), pp. 330–4. Available at: http://www.ncbi.nlm.nih.gov/pubmed/13407627 (Accessed: 31 January 2018).

Louis Sam Titus, A. S. C. *et al.* (2017) 'Reduced Expression of Foxp1 as a Contributing Factor in Huntington's Disease.', *The Journal of neuroscience : the official journal of the Society for Neuroscience*. Society for Neuroscience, 37(27), pp. 6575–6587. doi: 10.1523/JNEUROSCI.3612-16.2017.

Lozano, R. *et al.* (2015) 'A de novo FOXP1 variant in a patient with autism, intellectual disability and severe speech and language impairment', *European Journal of Human Genetics*. Nature Publishing Group, 23(12), pp. 1702–1707. doi: 10.1038/ejhg.2015.66.

Lu, J. *et al.* (2000) 'Signal-dependent activation of the MEF2 transcription factor by dissociation from histone deacetylases', *Proceedings of the National Academy of Sciences*, 97(8), pp. 4070–4075.

Luzzati, F. *et al.* (2014) 'Quiescent neuronal progenitors are activated in the juvenile guinea pig lateral striatum and give rise to transient neurons', *Development*, 141(21), pp. 4065–4075. doi: 10.1242/dev.107987.

Lyons, D. *et al.* (1996) 'Cocaine alters cerebral metabolism within the ventral striatum and limbic cortex of monkeys', *Journal of Neuroscience*, 16(3), pp. 1230–1236. doi: 10.1523/jneurosci.16-03-01230.1996.

Lyons, G E *et al.* (1995) 'Expression of mef2 genes in the mouse central nervous system suggests a role in neuronal maturation', *The Journal of neuroscience*, 15(8), pp. 5727–5738.

Lyons, Gary E, Micales, B. K., Schwarz, J., Martin, J. F., *et al.* (1995) 'Expression of mef2 genes in the mouse central nervous system suggests a role in neuronal maturation', *Journal of Neuroscience*, 15(8), pp. 5727–5738.

Lyons, Gary E, Micales, B. K., Schwarz, J., Martin, F., *et al.* (1995) *Expression of mef2 Genes in the Mouse Central Nervous System Suggests a Role in Neuronal Maturation*, *The Journal of Neuroscience*. Available at: https://www.jneurosci.org/content/jneuro/15/8/5727.full.pdf (Accessed: 7 August 2019).

Magli, A. *et al.* (2010) 'Proline isomerase Pin1 represses terminal differentiation and myocyte enhancer factor 2C function in skeletal muscle cells', *Journal of Biological Chemistry*, 285(45), pp. 34518–34527.

Mallet, N. *et al.* (2005) 'Feedforward inhibition of projection neurons by fast-spiking GABA interneurons in the rat striatum in vivo', *Journal of Neuroscience*, 25(15), pp. 3857–3869. doi: 10.1523/JNEUROSCI.5027-04.2005.

Mao, Z *et al.* (1999) 'Neuronal activity-dependent cell survival mediated by transcription factor MEF2.', *Science (New York, N.Y.)*. American Association for the Advancement of Science, 286(5440), pp. 785–90. doi: 10.1126/SCIENCE.286.5440.785.

Mao, Zixu *et al.* (1999) 'Neuronal activity-dependent cell survival mediated by transcription factor MEF2', *Science*, 286(5440), pp. 785–790.

Mao, Z. and Wiedmann, M. (1999) 'Calcineurin enhances MEF2 DNA binding activity in calcium-dependent survival of cerebellar granule neurons.', *The Journal of biological chemistry*. American Society for Biochemistry and Molecular Biology, 274(43), pp. 31102–7. doi: 10.1074/JBC.274.43.31102.

Mari, F. *et al.* (2005) 'CDKL5 belongs to the same molecular pathway of MeCP2 and it is responsible for the early-onset seizure variant of Rett syndrome', *Human molecular genetics*, 14(14), pp. 1935–1946.

Marin, O. *et al.* (2001) 'Sorting of Striatal and Cortical Interneurons Regulated by Semaphorin-Neuropilin Interactions', *Science*, 293(5531), pp. 872–875. doi: 10.1126/science.1061891.

Martin, J. F., Schwarz, J. J. and Olson, E. N. (1993) 'Myocyte enhancer factor (MEF) 2C: a tissue-restricted member of the MEF-2 family of transcription factors', *Proceedings of the National Academy of Sciences*, 90(11), pp. 5282–5286.

Maxeiner, S. *et al.* (2014) 'The molecular basis of the specificity and cross-reactivity of the NeuN epitope of the neuron-specific splicing regulator, Rbfox3', *Histochemistry and Cell Biology*. Springer Berlin Heidelberg, 141(1), pp. 43–55. doi: 10.1007/s00418-013-1159-9.

Maya-Espinosa, G. *et al.* (2015) 'Mouse Embryonic Stem Cell-Derived Cells Reveal Niches that Support Neuronal Differentiation in the Adult Rat Brain', *STEM CELLS*, 33(2), pp. 491–502. doi: 10.1002/stem.1856.

Mayer, C. *et al.* (2018) 'Developmental diversification of cortical inhibitory interneurons', *Nature*. Nature Publishing Group, 555(7697), pp. 457–462. doi: 10.1038/nature25999.

McKinsey, T. A. *et al.* (2000) 'Signal-dependent nuclear export of a histone deacetylase regulates muscle differentiation', *Nature*, 408(6808), pp. 106–111.

McKinsey, T. A., Zhang, C. L. and Olson, E. N. (2001) 'Control of muscle development by dueling HATs and HDACs', *Current opinion in genetics & development*, 11(5), pp. 497–504.

McKinsey, T. A., Zhang, C. L. and Olson, E. N. (2002) 'MEF2: a calcium-dependent regulator of cell division, differentiation and death', *Trends in biochemical sciences*, 27(1), pp. 40–47.

Meerschaut, I. *et al.* (2017) '*FOXP1* -related intellectual disability syndrome: a recognisable entity', *Journal of Medical Genetics*, 54(9), pp. 613–623. doi: 10.1136/jmedgenet-2017-104579.

Mencarelli, M. A. *et al.* (2010) 'Novel FOXG1 mutations associated with the congenital variant of Rett syndrome', *Journal of medical genetics*, 47(1), pp. 49–53.

Le Meur, N. *et al.* (2010) 'MEF2C haploinsufficiency caused by either microdeletion of the 5q14. 3 region or mutation is responsible for severe mental retardation with stereotypic movements, epilepsy and/or cerebral malformations', *Journal of medical genetics*, 47(1), pp. 22–29.

Meyer-Lindenberg, A. *et al.* (2007) 'Genetic evidence implicating DARPP-32 in human frontostriatal structure, function, and cognition.', *The Journal of clinical investigation*. American Society for Clinical Investigation, 117(3), pp. 672–82. doi: 10.1172/JCI30413.

Meyer, G. *et al.* (1998) 'Different origins and developmental histories of transient neurons in the marginal zone of the fetal and neonatal rat cortex', *Journal of Comparative Neurology*, 397(4), pp. 493–518. doi: 10.1002/(SICI)1096-9861(19980810)397:4<493::AID-CNE4>3.0.CO;2-X.

MINK, J. W. (1996) 'THE BASAL GANGLIA: FOCUSED SELECTION AND INHIBITION OF COMPETING MOTOR PROGRAMS', *Progress in Neurobiology*. Pergamon, 50(4), pp. 381–425. doi: 10.1016/S0301-0082(96)00042-1.

Miska, E. A. *et al.* (1999) 'HDAC4 deacetylase associates with and represses the MEF2 transcription factor', *The EMBO journal*, 18(18), pp. 5099–5107.

Miyachi, S., Hikosaka, O. and Lu, X. (2002) 'Differential activation of monkey striatal neurons in the early and late stages of procedural learning', *Experimental Brain Research*, 146(1), pp. 122–126. doi: 10.1007/s00221-002-1213-7.

Miyoshi, G. *et al.* (2010) 'Genetic fate mapping reveals that the caudal ganglionic

eminence produces a large and diverse population of superficial cortical interneurons', *Journal of Neuroscience*, 30(5), pp. 1582–1594. doi: 10.1523/JNEUROSCI.4515-09.2010.

Moffat, J. J. *et al.* (2015) 'Genes and brain malformations associated with abnormal neuron positioning', *Molecular Brain*. BioMed Central Ltd. doi: 10.1186/s13041-015-0164-4.

Le Moine, C. *et al.* (1990) 'Dopamine receptor gene expression by enkephalin neurons in rat forebrain.', *Proceedings of the National Academy of Sciences of the United States of America*. National Academy of Sciences, 87(1), pp. 230–4. doi: 10.1073/PNAS.87.1.230.

Molkentin, J. D. *et al.* (1995) 'Cooperative activation of muscle gene expression by MEF2 and myogenic bHLH proteins', *Cell*, 83(7), pp. 1125–1136.

Molkentin, J. D. *et al.* (1996) 'MEF2B is a potent transactivator expressed in early myogenic lineages', *Molecular and cellular biology*, 16(7), pp. 3814–3824.

Morrow, E. M. *et al.* (2008) 'Identifying autism loci and genes by tracing recent shared ancestry', *Science*, 321(5886), pp. 218–223.

Mullen, R. J., Buck, C. R. and Smith, A. M. (1992) 'NeuN, a neuronal specific nuclear protein in vertebrates', *Development*, 116(1).

Nestler, E. J., Hope, B. T. and Widnell, K. L. (1993) 'Drug addiction: A model for the molecular basis of neural plasticity', *Neuron*, pp. 995–1006. doi: 10.1016/0896-6273(93)90213-B.

New, L. and Han, J. (1998) 'The p38 MAP kinase pathway and its biological function', *Trends in cardiovascular medicine*, 8(5), pp. 220–228.

Nikouei, K., Muñoz-Manchado, A. B. and Hjerling-Leffler, J. (2016) 'BCL11B/CTIP2 is highly expressed in GABAergic interneurons of the mouse somatosensory cortex', *Journal of Chemical Neuroanatomy*. Elsevier, 71, pp. 1–5. doi: 10.1016/J.JCHEMNEU.2015.12.004.

Nishi, A. *et al.* (1999) 'Requirement for DARPP-32 in mediating effect of dopamine D2 receptor activation.', *The European journal of neuroscience*, 11(7), pp. 2589–92. Available at: http://www.ncbi.nlm.nih.gov/pubmed/10383649 (Accessed: 29 January 2018).

Noctor, S. C. *et al.* (2001) 'Neurons derived from radial glial cells establish radial units in neocortex', *Nature*, 409(6821), pp. 714–720. doi: 10.1038/35055553.

Okamoto, S *et al.* (2000) 'Antiapoptotic role of the p38 mitogen-activated protein kinase-myocyte enhancer factor 2 transcription factor pathway during neuronal differentiation.', *Proceedings of the National Academy of Sciences of the United States of America*. National Academy of Sciences, 97(13), pp. 7561–6. doi: 10.1073/pnas.130502697.

Okamoto, Shu-ichi *et al.* (2000) 'Antiapoptotic role of the p38 mitogen-activated protein kinase–myocyte enhancer factor 2 transcription factor pathway during neuronal differentiation', *Proceedings of the National Academy of Sciences*, 97(13), pp. 7561–7566.

Okamoto, S., Li, Z., Ju, C., Scholzke, M. N., *et al.* (2002) 'Dominant-interfering forms of MEF2 generated by caspase cleavage contribute to NMDA-induced neuronal apoptosis.', *Proceedings of the National Academy of Sciences of the United States of America*. National Academy of Sciences, 99(6), pp. 3974–9. doi: 10.1073/pnas.022036399.

Okamoto, S., Li, Z., Ju, C., Schölzke, M. N., *et al.* (2002) 'Dominant-interfering forms of MEF2 generated by caspase cleavage contribute to NMDA-induced neuronal apoptosis', *Proceedings of the National Academy of Sciences*, 99(6), pp. 3974–3979.

Olsson, M., Björklund, A. and Campbell, K. (1998) 'Early specification of striatal projection neurons and interneuronal subtypes in the lateral and medial ganglionic eminence', *Neuroscience*, 84(3), pp. 867–876. doi: 10.1016/S0306-4522(97)00532-0.

Ouimet, C. C., Langley-Gullion, K. C. and Greengard, P. (1998) 'Quantitative immunocytochemistry of DARPP-32-expressing neurons in the rat caudatoputamen.', *Brain research*, 808(1), pp. 8–12. Available at: http://www.ncbi.nlm.nih.gov/pubmed/9795103 (Accessed: 29 January 2018).

Paciorkowski, A. R. *et al.* (2013) 'MEF2C Haploinsufficiency features consistent hyperkinesis, variable epilepsy, and has a role in dorsal and ventral neuronal developmental pathways', *neurogenetics*, 14(2), pp. 99–111.

Palmesino, E. *et al.* (2010) 'Foxp1 and Lhx1 Coordinate Motor Neuron Migration with Axon Trajectory Choice by Gating Reelin Signalling', *PLoS Biology*. Edited by F. Polleux. Public Library of Science, 8(8), p. e1000446. doi: 10.1371/journal.pbio.1000446.

Palumbo, O. *et al.* (2013) '3p14.1 de novo microdeletion involving the FOXP1 gene in an adult patient with autism, severe speech delay and deficit of motor coordination', *Gene*. Elsevier, 516(1), pp. 107–113. doi: 10.1016/J.GENE.2012.12.073.

Parent, A. and Hazrati, L. N. (1995) ‘Functional anatomy of the basal ganglia. I. The cortico-basal ganglia-thalamo-cortical loop’, *Brain Research Reviews*, pp. 91–127. doi: 10.1016/0165-0173(94)00007-C.

Park, J. Y. *et al.* (2011) ‘Comparative analysis of mRNA isoform expression in cardiac hypertrophy and development reveals multiple post-transcriptional regulatory modules’, *PLoS One*, 6(7), p. e22391.

Parra, M. *et al.* (2005) ‘Protein kinase D1 phosphorylates HDAC7 and induces its nuclear export after T-cell receptor activation’, *Journal of Biological Chemistry*, 280(14), pp. 13762–13770.

Paternoster, V. *et al.* (2018) ‘The importance of data structure in statistical analysis of dendritic spine morphology’, *Journal of Neuroscience Methods*. Elsevier B.V., 296, pp. 93–98. doi: 10.1016/j.jneumeth.2017.12.022.

Pearson, G. *et al.* (2001) ‘Mitogen-activated protein (MAP) kinase pathways: regulation and physiological functions 1’, *Endocrine reviews*, 22(2), pp. 153–183.

Peters, R. (2006) ‘Ageing and the brain.’, *Postgraduate medical journal*. BMJ Publishing Group, 82(964), pp. 84–8. doi: 10.1136/pgmj.2005.036665.

Pfeiffer, B. E. *et al.* (2010) ‘Fragile X mental retardation protein is required for synapse elimination by the activity-dependent transcription factor MEF2’, *Neuron*, 66(2), pp. 191–197.

Philippe, C. *et al.* (2010) ‘Phenotypic variability in Rett syndrome associated with FOXG1 mutations in females’, *Journal of medical genetics*, 47(1), pp. 59–65.

Pickel, V. M. and Chan, J. (1990) ‘Spiny neurons lacking choline acetyltransferase immunoreactivity are major targets of cholinergic and catecholaminergic terminals in rat striatum’, *Journal of Neuroscience Research*, 25(3), pp. 263–280. doi: 10.1002/jnr.490250302.

Pitcher, T. L. *et al.* (2012) ‘Reduced striatal volumes in Parkinson’s disease: a magnetic resonance imaging study’, *Translational Neurodegeneration*. BioMed Central, 1(1), p. 17. doi: 10.1186/2047-9158-1-17.

Pleasure, S. J. *et al.* (2000) ‘Cell migration from the ganglionic eminences is required for the development of hippocampal GABAergic interneurons’, *Neuron*. Cell Press, 28(3), pp. 727–740. doi: 10.1016/S0896-6273(00)00149-5.

Pon, J. R. and Marra, M. A. (2016) ‘MEF2 transcription factors: Developmental regulators and emerging cancer genes’, *Oncotarget*. Impact Journals LLC, 7(3), pp.

2297–2312. doi: 10.18632/oncotarget.6223.

Porter, A. G. and Jänicke, R. U. (1999) 'Emerging roles of caspase-3 in apoptosis', *Cell Death & Differentiation*. Nature Publishing Group, 6(2), pp. 99–104. doi: 10.1038/sj.cdd.4400476.

Potthoff, M. J. and Olson, E. N. (2007) 'MEF2: a central regulator of diverse developmental programs', *Development*, 134(23), pp. 4131–4140.

Poukka, H. *et al.* (2000) 'Covalent modification of the androgen receptor by small ubiquitin-like modifier 1 (SUMO-1)', *Proceedings of the National Academy of Sciences*, 97(26), pp. 14145–14150.

Prange, O. and Murphy, T. H. (1999) 'Correlation of miniature synaptic activity and evoked release probability in cultures of cortical neurons.', *The Journal of neuroscience : the official journal of the Society for Neuroscience*, 19(15), pp. 6427–38. Available at: http://www.ncbi.nlm.nih.gov/pubmed/10414971 (Accessed: 31 January 2018).

Precious, S. V *et al.* (2016) 'FoxP1 marks medium spiny neurons from precursors to maturity and is required for their differentiation.', *Experimental neurology*. Elsevier, 282, pp. 9–18. doi: 10.1016/j.expneurol.2016.05.002.

Preston, R. J., Bishop, G. A. and Kitai, S. T. (1980) 'Medium spiny neuron projection from the rat striatum: an intracellular horseradish peroxidase study.', *Brain research*, 183(2), pp. 253–63. doi: 10.1016/0006-8993(80)90462-x.

Puelles, L. *et al.* (2000) 'Pallial and subpallial derivatives in the embryonic chick and mouse telencephalon, traced by the expression of the genes Dlx-2, Emx-1, Nkx-2.1, Pax-6, and Tbr-1', *The Journal of Comparative Neurology*. Wiley-Blackwell, 424(3), pp. 409–438. doi: 10.1002/1096-9861(20000828)424:3<409::AID-CNE3>3.0.CO;2-7.

Rakic, P. (1972) 'Mode of cell migration to the superficial layers of fetal monkey neocortex', *Journal of Comparative Neurology*, 145(1), pp. 61–83. doi: 10.1002/cne.901450105.

Ranganayakulu, G. *et al.* (1995) 'A series of mutations in the D-MEF2 transcription factor reveal multiple functions in larval and adult myogenesis in Drosophila', *Developmental biology*, 171(1), pp. 169–181.

Redgrave, P., Prescott, T. J. and Gurney, K. (1999) 'The basal ganglia: a vertebrate solution to the selection problem?', *Neuroscience*, 89(4), pp. 1009–1023. doi: 10.1016/S0306-4522(98)00319-4.

Regan, C. P. *et al.* (2002) 'Erk5 null mice display multiple extraembryonic vascular and embryonic cardiovascular defects', *Proceedings of the National Academy of Sciences*, 99(14), pp. 9248–9253.

Rice, M. E. and Cragg, S. J. (2004) 'Nicotine amplifies reward-related dopamine signals in striatum', *Nature Neuroscience*, 7(6), pp. 583–584. doi: 10.1038/nn1244.

Rocha, H. *et al.* (2016) 'MEF2C haploinsufficiency syndrome: Report of a new MEF2C mutation and review', *European Journal of Medical Genetics*. Elsevier Masson, 59(9), pp. 478–482. doi: 10.1016/J.EJMG.2016.05.017.

Rosas, H. D. *et al.* (2001) 'Striatal volume loss in HD as measured by MRI and the influence of CAG repeat.', *Neurology*. Wolters Kluwer Health, Inc. on behalf of the American Academy of Neurology, 57(6), pp. 1025–8. doi: 10.1212/WNL.57.6.1025.

Ross, G. W. *et al.* (2004) 'Parkinsonian signs and substantia nigra neuron density in decendents elders without PD', *Annals of Neurology*. Wiley-Blackwell, 56(4), pp. 532–539. doi: 10.1002/ana.20226.

Ross, S. *et al.* (2002) 'SUMO-1 modification represses Sp3 transcriptional activation and modulates its subnuclear localization', *Molecular cell*, 10(4), pp. 831–842.

Rubenstein, J. L. R. *et al.* (1998) 'REGIONALIZATION OF THE PROSENCEPHALIC NEURAL PLATE', *Annual Review of Neuroscience*. Annual Reviews 4139 El Camino Way, P.O. Box 10139, Palo Alto, CA 94303-0139, USA , 21(1), pp. 445–477. doi: 10.1146/annurev.neuro.21.1.445.

Rudy, B. *et al.* (2011) 'Three groups of interneurons account for nearly 100% of neocortical GABAergic neurons', *Developmental Neurobiology*, 71(1), pp. 45–61. doi: 10.1002/dneu.20853.

Sakai, Y. *et al.* (2013) 'Neuroendocrine phenotypes in a boy with 5q14 deletion syndrome implicate the regulatory roles of myocyte-specific enhancer factor 2C in the postnatal hypothalamus', *European journal of medical genetics*, 56(9), pp. 475–483.

Sandmann, T. *et al.* (2006) 'A temporal map of transcription factor activity: mef2 directly regulates target genes at all stages of muscle development', *Developmental cell*, 10(6), pp. 797–807.

Santelli, E. and Richmond, T. J. (2000) 'Crystal structure of MEF2A core bound to DNA at 1.5 Å resolution', *Journal of molecular biology*, 297(2), pp. 437–449.

Santini, E. *et al.* (2007) 'Critical Involvement of cAMP/DARPP-32 and Extracellular Signal-Regulated Protein Kinase Signaling in L-DOPA-Induced Dyskinesia', *Journal of*

*Neuroscience*, 27(26), pp. 6995–7005. doi: 10.1523/JNEUROSCI.0852-07.2007.

Sapetschnig, A. *et al.* (2002) 'Transcription factor Sp3 is silenced through SUMO modification by PIAS1', *The EMBO journal*, 21(19), pp. 5206–5215.

Scheschonka, A., Tang, Z. and Betz, H. (2007) 'Sumoylation in neurons: nuclear and synaptic roles?', *Trends in neurosciences*, 30(3), pp. 85–91.

Schiffmann, S. N. (1997) 'Reelin mRNA expression during mouse brain development', *European Journal of Neuroscience*, 9(5), pp. 1055–1071. doi: 10.1111/j.1460-9568.1997.tb01456.x.

Schneider, C. A., Rasband, W. S. and Eliceiri, K. W. (2012) 'NIH Image to ImageJ: 25 years of image analysis', *Nature Methods*, pp. 671–675. doi: 10.1038/nmeth.2089.

Schüler, A. *et al.* (2008) 'The MADS transcription factor Mef2c is a pivotal modulator of myeloid cell fate.', *Blood*. American Society of Hematology, 111(9), pp. 4532–41. doi: 10.1182/blood-2007-10-116343.

Schultz, W. (1997) 'Dopamine neurons and their role in reward mechanisms', *Current Opinion in Neurobiology*. Elsevier Ltd, 7(2), pp. 191–197. doi: 10.1016/S0959-4388(97)80007-4.

Schultz, W. (2002) 'Getting Formal with Dopamine and Reward', *Neuron*. Cell Press, 36(2), pp. 241–263. doi: 10.1016/S0896-6273(02)00967-4.

Sekiyama, Y., Suzuki, H. and Tsukahara, T. (2012) 'Functional gene expression analysis of tissue-specific isoforms of Mef2c', *Cellular and molecular neurobiology*, 32(1), pp. 129–139.

Selemon, L. D. and Goldman-Rakic, P. S. (1985) 'Longitudinal topography and interdigitation of corticostriatal projections in the rhesus monkey', *Journal of Neuroscience*, 5(3), pp. 776–794. doi: 10.1523/jneurosci.05-03-00776.1985.

Shalizi, A. *et al.* (2006) 'A calcium-regulated MEF2 sumoylation switch controls postsynaptic differentiation', *Science*, 311(5763), pp. 1012–1017.

Shim, J. S. *et al.* (2015) 'MEF2C-Related 5q14.3 Microdeletion Syndrome Detected by Array CGH: A Case Report.', *Annals of rehabilitation medicine*. Korean Academy of Rehabilitation Medicine, 39(3), pp. 482–7. doi: 10.5535/arm.2015.39.3.482.

Shimamura, K. *et al.* (1995) 'Longitudinal organization of the anterior neural plate and neural tube', *Development*, 121(12), pp. 3923–3933.

Shore, P. and Sharrocks, A. D. (1995) 'The MADS box family of transcription factors',

*European Journal of Biochemistry*, 229(1), pp. 1–13.

Smart, I. H. M. and Sturrock, R. R. (1979) 'Ontogeny of the Neostriatum', in *The Neostriatum*. Elsevier, pp. 127–146. doi: 10.1016/B978-0-08-023174-7.50012-6.

Smith, Y. *et al.* (1998) 'Microcircuitry of the direct and indirect pathways of the basal ganglia', *Neuroscience*. Elsevier Ltd, pp. 353–387. doi: 10.1016/S0306-4522(98)00004-9.

Smith, Y., Shink, E. and Sidibé, M. (1998) 'Neuronal circuitry and synaptic connectivity of the basal ganglia.', *Neurosurgery clinics of North America*, 9(2), pp. 203–22. Available at: http://www.ncbi.nlm.nih.gov/pubmed/9556359 (Accessed: 11 December 2019).

Smrt, R. D. and Zhao, X. (2010) 'Epigenetic regulation of neuronal dendrite and dendritic spine development', *Frontiers of Biology in China*, pp. 304–323. doi: 10.1007/s11515-010-0650-0.

Soler, C., Han, J. and Taylor, M. V. (2012) 'The conserved transcription factor Mef2 has multiple roles in adult Drosophila musculature formation', *Development*, 139(7), pp. 1270–1275. doi: 10.1242/dev.077875.

Sollis, E. *et al.* (2016) 'Identification and functional characterization of *de novo FOXP1* variants provides novel insights into the etiology of neurodevelopmental disorder', *Human Molecular Genetics*. Oxford University Press, 25(3), pp. 546–557. doi: 10.1093/hmg/ddv495.

Somogyi, P., Bolam, J. P. and Smith, A. D. (1981) 'Monosynaptic cortical input and local axon collaterals of identified striatonigral neurons. A light and electron microscopic study using the golgi peroxidase transport degeneration procedure', *Journal of Comparative Neurology*, 195(4), pp. 567–584. doi: 10.1002/cne.901950403.

Song, D. D. and Harlan, R. E. (1994) 'Genesis and migration patterns of neurons forming the patch and matrix compartments of the rat striatum', *Developmental Brain Research*. Elsevier, 83(2), pp. 233–245. doi: 10.1016/0165-3806(94)00144-8.

Stenman, J., Toresson, H. and Campbell, K. (2003) 'Identification of two distinct progenitor populations in the lateral ganglionic eminence: implications for striatal and olfactory bulb neurogenesis.', *The Journal of neuroscience : the official journal of the Society for Neuroscience*. Society for Neuroscience, 23(1), pp. 167–74. doi: 10.1523/JNEUROSCI.23-01-00167.2003.

Sussel, L. *et al.* (1999) 'Loss of Nkx2.1 homeobox gene function results in a ventral to

dorsal molecular respecification within the basal telencephalon: Evidence for a transformation of the pallidum into the striatum', *Development*, 126(15), pp. 3359–3370.

Svenningsson, P. *et al.* (2000) 'Regulation of the phosphorylation of the dopamine- and cAMP-regulated phosphoprotein of 32 kDa in vivo by dopamine D1, dopamine D2, and adenosine A2A receptors.', *Proceedings of the National Academy of Sciences of the United States of America*, 97(4), pp. 1856–60. Available at: http://www.ncbi.nlm.nih.gov/pubmed/10677546 (Accessed: 29 January 2018).

Svenningsson, P. *et al.* (2004) 'DARPP-32: An Integrator of Neurotransmission', *Annual Review of Pharmacology and Toxicology*, 44(1), pp. 269–296. doi: 10.1146/annurev.pharmtox.44.101802.121415.

Svenningsson, P., Nairn, A. C. and Greengard, P. (2005) 'DARPP-32 mediates the actions of multiple drugs of abuse.', *The AAPS journal*. Springer, 7(2), pp. E353-60. doi: 10.1208/aapsj070235.

Svensson, M. (2000) 'Evolution of a family of plant genes with regulatory functions in development; studies on Picea abies and Lycopodium annotinum'.

Takeda, K. and Ichijo, H. (2002) 'Neuronal p38 MAPK signalling: an emerging regulator of cell fate and function in the nervous system', *Genes to Cells*. Blackwell Science Ltd, 7(11), pp. 1099–1111. doi: 10.1046/j.1365-2443.2002.00591.x.

Tamamaki, N., Fujimori, K. E. and Takauji, R. (1997) 'Origin and route of tangentially migrating neurons in the developing neocortical intermediate zone', *Journal of Neuroscience*, 17(21), pp. 8313–8323. doi: 10.1523/jneurosci.17-21-08313.1997.

Tamura, S. *et al.* (2004) 'Foxp1 gene expression in projection neurons of the mouse striatum', *Neuroscience*. Pergamon, 124(2), pp. 261–267. doi: 10.1016/J.NEUROSCIENCE.2003.11.036.

Toresson, H., Potter, S. S. and Campbell, K. (2000) 'Genetic control of dorsal-ventral identity in the telencephalon: opposing roles for Pax6 and Gsh2', *Development*, 127(20).

Torres, K. C. L. *et al.* (2009) 'The leukocytes expressing DARPP-32 are reduced in patients with schizophrenia and bipolar disorder', *Progress in Neuro-Psychopharmacology and Biological Psychiatry*, 33(2), pp. 214–219. doi: 10.1016/j.pnpbp.2008.10.020.

Valjent, E. *et al.* (2009) 'Looking BAC at striatal signaling: cell-specific analysis in new

transgenic mice.', *Trends in neurosciences*. Elsevier, 32(10), pp. 538–47. doi: 10.1016/j.tins.2009.06.005.

Vazquez, L. E. *et al.* (2004) 'SynGAP regulates spine formation', *The Journal of neuroscience*, 24(40), pp. 8862–8872.

Vong, L. H., Ragusa, M. J. and Schwarz, J. J. (2005) 'Generation of conditionalMef2cloxP/loxP mice for temporal- and tissue-specific analyses', *genesis*. Wiley-Blackwell, 43(1), pp. 43–48. doi: 10.1002/gene.20152.

Walaas, S. I. and Greengard, P. (1984) 'DARPP-32, a dopamine- and adenosine 3':5'-monophosphate-regulated phosphoprotein enriched in dopamine-innervated brain regions. I. Regional and cellular distribution in the rat brain.', *The Journal of neuroscience : the official journal of the Society for Neuroscience*. Society for Neuroscience, 4(1), pp. 84–98. doi: 10.1523/JNEUROSCI.04-01-00084.1984.

Wang, D.-Z. *et al.* (2001) 'The Mef2c gene is a direct transcriptional target of myogenic bHLH and MEF2 proteins during skeletal muscle development', *Development*, 128(22), pp. 4623–4633.

Wang, H.-Y. *et al.* (2015) 'RBFOX3/NeuN is Required for Hippocampal Circuit Balance and Function.', *Scientific reports*. Nature Publishing Group, 5, p. 17383. doi: 10.1038/srep17383.

Weaving, L. S. *et al.* (2004) 'Mutations of< i> CDKL5</i> Cause a Severe Neurodevelopmental Disorder with Infantile Spasms and Mental Retardation', *The American Journal of Human Genetics*, 75(6), pp. 1079–1093.

West, A. G., Shore, P. and Sharrocks, A. D. (1997) 'DNA binding by MADS-box transcription factors: a molecular mechanism for differential DNA bending', *Molecular and cellular biology*, 17(5), pp. 2876–2887.

Wichterle, H. *et al.* (1999) 'Young neurons from medial ganglionic eminence disperse in adult and embryonic brain', *Nature Neuroscience*, 2(5), pp. 461–466. doi: 10.1038/8131.

Winden, K. D. *et al.* (2009) 'The organization of the transcriptional network in specific neuronal classes', *Molecular systems biology*, 5(1).

Wise, R. A. and Rompre, P. P. (1989) 'Brain Dopamine and Reward', *Annual Review of Psychology*. Annual Reviews, 40(1), pp. 191–225. doi: 10.1146/annurev.ps.40.020189.001203.

Wonders, C. P. and Anderson, S. A. (2006) 'The origin and specification of cortical

interneurons', *Nature Reviews Neuroscience*, pp. 687–696. doi: 10.1038/nrn1954.

Woronicz, J. D. *et al.* (1995) 'Regulation of the Nur77 orphan steroid receptor in activation-induced apoptosis', *Molecular and cellular biology*, 15(11), pp. 6364–6376.

Xu, Q., Tam, M. and Anderson, S. A. (2008) 'Fate mapping Nkx2.1-lineage cells in the mouse telencephalon', *Journal of Comparative Neurology*, 506(1), pp. 16–29. doi: 10.1002/cne.21529.

Yan, Z. *et al.* (1999) 'Protein phosphatase 1 modulation of neostriatal AMPA channels: regulation by DARPP–32 and spinophilin', *Nature Neuroscience*, 2(1), pp. 13–17. doi: 10.1038/4516.

Yang, C.-C. *et al.* (1998) 'Interaction of myocyte enhancer factor 2 (MEF2) with a mitogen-activated protein kinase, ERK5/BMK1', *Nucleic acids research*, 26(20), pp. 4771–4777.

Yang, S.-H. and Sharrocks, A. D. (2004) 'SUMO promotes HDAC-mediated transcriptional repression', *Molecular cell*, 13(4), pp. 611–617.

Yger, M. and Girault, J.-A. (2011) 'DARPP-32, Jack of All Trades… Master of Which?', *Frontiers in behavioral neuroscience*. Frontiers Media SA, 5, p. 56. doi: 10.3389/fnbeh.2011.00056.

Ying, C. Y. *et al.* (2013) 'MEF2B mutations lead to deregulated expression of the oncogene BCL6 in diffuse large B cell lymphoma', *Nature immunology*, 14(10), pp. 1084–1092.

Youn, H.-D. *et al.* (1999) 'Apoptosis of T cells mediated by Ca2+-induced release of the transcription factor MEF2', *Science*, 286(5440), pp. 790–793.

Youn, H., Chatila, T. A. and Liu, J. O. (2000) 'Integration of calcineurin and MEF2 signals by the coactivator p300 during T cell apoptosis', *The EMBO journal*, 19(16), pp. 4323–4331.

Yung, K. K. L. (1996) 'Synaptic connections between spiny neurons of the direct and indirect pathways in the neostriatum of the rat: Evidence from dopamine receptor and neuropeptide immunostaining', *European Journal of Neuroscience*. Blackwell Publishing Ltd, 8(5), pp. 861–869. doi: 10.1111/j.1460-9568.1996.tb01573.x.

Zahorakova, D. *et al.* (2007) 'Mutation analysis of the MECP2 gene in patients of Slavic origin with Rett syndrome: novel mutations and polymorphisms', *Journal of human genetics*, 52(4), pp. 342–348.

Zald, D. H. *et al.* (2004) 'Journal of Neuroscience', *J. Neurosci.* Society for Neuroscience, 23(1), pp. 303–307. doi: 20026534.

Zhang, C. L. *et al.* (2002) 'Class II histone deacetylases act as signal-responsive repressors of cardiac hypertrophy', *Cell*, 110(4), pp. 479–488.

Zhu, B. and Gulick, T. (2004) 'Phosphorylation and alternative pre-mRNA splicing converge to regulate myocyte enhancer factor 2C activity', *Molecular and cellular biology*, 24(18), pp. 8264–8275.

Zhu, B., Ramachandran, B. and Gulick, T. (2005) 'Alternative pre-mRNA splicing governs expression of a conserved acidic transactivation domain in myocyte enhancer factor 2 factors of striated muscle and brain', *Journal of Biological Chemistry*, 280(31), pp. 28749–28760.

Zuo, Y. *et al.* (2005) 'Development of long-term dendritic spine stability in diverse regions of cerebral cortex', *Neuron*. Cell Press, 46(2), pp. 181–189. doi: 10.1016/j.neuron.2005.04.001.

Zweier, C. *et al.* (2008) 'Further delineation of Pitt–Hopkins syndrome: phenotypic and genotypic description of 16 novel patients', *Journal of medical genetics*, 45(11), pp. 738–744.

Zweier, M. *et al.* (2010) 'Mutations in MEF2C from the 5q14. 3q15 microdeletion syndrome region are a frequent cause of severe mental retardation and diminish MECP2 and CDKL5 expression', *Human mutation*, 31(6), pp. 722–733.

Zweier, M. and Rauch, A. (2012) 'The MEF2C-related and 5q14. 3q15 microdeletion syndrome', *Molecular syndromology*, 2(3–5), pp. 164–170.